THE PETROLOGY OF THE KIELDER SULPHIDE BODIES AND THEIR WALL ROCKS; DISTRICT OF PRIESKA, N. CAPE, SOUTH AFRICA.

by:

RICHARD K. CORTON

This thesis is submitted in fulfilment of the requirements for the degree of MASTER OF SCIENCE.

Department of Geology,
University of Cape Town.

April, 1981.

ABSTRACT

Recently discovered base metal (Zn>Cu>>Pb) massive sulphide deposits in the Northern Cape district of Prieska occur at Kielder 12 kilometres north-west of a similar Zn-Cu deposit, the Copperton mine. Three massive sulphide bodies known as K3, K1 and K6 occur as stratabound massive sulphide lenses within granulite grade quartz-feldspar gneisses, basic granulites and amphibolites. Extensive exploratory core-drilling provided specimens of the massive sulphides, their disseminated pyritic haloes and the enclosing wall rocks in an area of poor outcrop with extensive calcrete and sand cover and, in places, in situ Karoo Super-group Dwyka System varved shales.

Geothermometry and geobarometry using garnet-biotite, garnet-cordierite, garnet-hypersthene, and the FeS content of sphalerites showed a gradual metamorphic gradient from east to west, with the K3 area suffering P-T conditions of 695°C and 6.0 Kbars; the K1 area 686°C and 5.8 Kbars and the K6 area 590°C and 5.6 Kbars. The presence of amphibolites and lower-grade metamorphic mineral assemblages indicate retrograde metamorphism which from geothermometry of cordierite grain edges, occurred at a temperature of 530°C. Metamorphic mineral assemblages correspond to the Regional Hypersthene or Granulite high grade zone. The sulphide textures exhibit typical high grade metamorphic features such as coarse grain size ($\geq$0.85mm), exsolution blebs of chalcopyrite in sphalerite and pyrrhotite in pyrite. Abundant evidence of sulphide/gangue reaction exists with the presence of phlogopite, rutile, gahnite and the alteration of pyrite to magnetite. The pyrrhotite grain size coarsens concomitantly with the increasing metamorphic grade from K6 to K3.

Lithostratigraphic correlation has been aided by the use of immobile trace elements, in particular, Ti, Zr and Y. The northern pyroxene granulites have similar trace elements contents to their stratigraphic equivalents which formed the immediate hanging wall to the K3 mineralization and differ, geochemically, from the southern pyroxene granulites which are not associated with mineralization.

The elements Al, Mn, Co, Ti, Y, Zr, Mg, Fe, P, Ni and Nb were immobile under the metamorphic conditions reached at Kielder.

The relative abundances of major and trace elements and Niggli values of the amphibolites are typical of igneous rocks whereas the pyroxene granulites have a geochemistry typical of pelites, carbonate pelites and in the immobile wall rocks of the proximal massive sulphide, Mg-enriched pelites. The geochemistry of the ortho-amphibolites shows them to have similarities to ocean-island tholeiites.

The three mineralized zones have been identified as exhalative base-metal massive sulphide deposits with the typical simple sulphide mineralogy of pyrite, pyrrhotite, sphalerite, chalcopyrite and galena with a gangue of barite, chlorite, phlogopite, apatite, tourmaline and quartz. The massive sulphide lenses occur within different lithologies with a possible stratigraphic correlation between K3 and K6 horizons although poor outcrop prevents definite correlation. The K6 represents a more distal facies whereas the K3 is a proximal massive sulphide deposit although they may not have had a common vent. The K1 body, the least well-developed mineralization, occurs within slightly older lithologic units. The K3 body exhibits strong vertical mineralogical and metal zoning and associated chlorite alteration zone and has formed above its own hydrothermal exhalative system. The K6 body with its absence of metal zoning, lack of an alteration zone but an associated B.I.F. in the hanging wall represents a distal facies exhalative massive sulphide. The K1 body has intermediate characteristics.

The chloritic/silicification alteration zone formed below the K3 (and the K1) massive sulphide lens at the time of its formation has been metamorphosed to a quartz-cordierite rock.

The manganese content in the wall rocks, as exhibited in the garnet chemistry, is higher in the distal K6 area than the K3 and K1 areas. Narrow manganese haloes (~5 metres wide) surround the massive sulphide lenses.

Mineralogical and metal zoning and the presence of alteration zones in their hanging walls show the steeply dipping K3 and K1 sulphide bodies to be overturned. The K6 sulphide body is steeply dipping but the stratigraphy is not inverted.

The Copperton/Kielder district, when compared with typical massive sulphide districts elsewhere, is shown to have the potential for further base metal discoveries.

"Besides, what we are pleased to call the riches of a mine are riches relatively to a distinction which nature does not recognize".

John Playfair, 1802.

so

"Go, my sons, buy stout shoes, climb the mountains, search the valleys, the deserts, the sea-shores and the deep recesses of the earth. Mark well the various kinds of minerals, note their properties and their mode of origin".

Petrus Severinus, 1571.

CONTENTS

			PAGE
1.	INTRODUCTION		
	1.1	Location	1
	1.2	Aims	1
	1.3	Approach	
		1.3.1. Surface Mapping	2
		1.3.2. Diamond Drilling and Core Logging	3
		1.3.3. Sampling	3
		1.3.4. Petrographic Microscope Examination	4
		1.3.5. X-ray Diffractometry	4
		1.3.6. Geochemistry	5
		1.3.7. Opaque Mineral Etching	5
	1.4	Previous Work	6
2.	STRATIGRAPHY		
	2.1	The K3 Area	
		2.1.1. The K3 Footwall	8
		2.1.2. The K3 Sulphide Unit	9
		2.1.3. The K3 Hanging-wall	10
		2.1.4. The K3 Intrusives	13
	2.2	The K1 Area	
		2.2.1. The K1 Footwall	13
		2.2.2. The K1 Sulphide Unit	14
		2.2.3. The K1 Hanging-wall	15
	2.3	The K6 Area	
		2.3.1. The K6 Footwall	16
		2.3.2. The K6 Sulphide Units	16
		2.3.3. The K6 Hanging-wall	17
	2.4	The Southern Granulite	18
	2.5	The Northern Granulite	18
	2.6	Overall Stratigraphy Summary	19
3.	METAMORPHISM		
	3.1	Geobarometry and Geothermometry	
		3.1.1. Garnet-biotite Geothermometry	21
		3.1.2. Garnet-cordierite Geothermometry/ Barometry	23

3. METAMORPHISM CONT. PAGE

3.1 Geobarometry and Geothermometry Cont.

3.1.3. Garnet-hypersthene Geobarometry 24

3.1.4. Sphalerite Geobarometry 25

3.1.5. Results 27

3.2 Metamorphic Petrology

3.2.1. Metamorphic Mineral Assemblages 28

3.2.2. Parent Lithologies 32

3.2.3. Metamorphic Textures of the Wall Rocks 32

3.2.4. Isochemical Metamorphism 33

3.3 Effects of Metamorphism

3.3.1. Massive Sulphides 34

3.3.1.1. Mobilization 34

3.3.1.2. Mineralogical/Chemical Effects 35

3.3.1.3. Textural Effects 38

3.3.2. Banded Iron Formation 41

4. BULK ROCK GEOCHEMISTRY

4.1 Introduction 45

4.2. Results and Interpretation 47

4.2.1. Identification of Immobile Elements 47

4.2.2. Ortho and Para-basic Metamorphites 48

4.2.3. Tectonic Setting of the Ortho-Amphibolites 49

4.2.4. Stratigraphic Correlation 51

4.3 Discussion 51

5. GENESIS OF THE KIELDER MASSIVE SULPHIDE DEPOSITS

5.1 Characteristic Features of the Mineralization 54

5.1.1. Vertical Mineralogical and Metal Zoning 54

5.1.2. Lateral Mineralogical and Metal Zoning 55

5.1.3. Footwall Alteration Zone 58

5.1.4. Tourmaline Distribution 60

5.1.5. Wall Rocks and their Depositional Setting 61

5.1.6. The Manganese Halo 64

5.1.7. Associated Intrusives 66

5. GENESIS OF THE KIELDER MASSIVE SULPHIDE DEPOSITS PAGE

5.2 Comparison with Exhalative Massive Sulphide Models 68

5.2.1. Stanton's (1972) M

5.2.2. Sangster and Scot

5.2.3. Solomon's (1976) M

5.2.4. Hutchinson's (197

5.2.5. Other Models

5.3 Regional Depositional Sett
Copperton Region

6. SUMMARY

7. ACKNOWLEDGEMENTS

8. REFERENCES

APPENDICES

I Detailed Petrography of the Wall Rocks and Massive Sulphides 97

II Bulk Rock Analytical Methods 139

III Microprobe Analytical Methods and Results 144

IV Chemical Etching Methods 146

V List of Samples and Locations for Thin Section and Geochemistry 148

VI X-Ray Diffraction Methods 152

Page Whole book with Maps.
Name Sam (U.B.C.)
Ext. no.
Maps page
Plates page

The following maps and cross-sections are included in pockets at the back of the thesis:

MAP 1 Geological Map of the K3 Area ✓
MAP 2 Geological Map of the K1 Area ✓
MAP 3 Geological Map of the K6 Area ✓
MAP 4 Regional Geological/Outcrop Map of the Kielder Properties ✓

CROSS-SECTION 1: Geological cross-section along line 54E ✓
CROSS-SECTION 2: Geological " " " " 52E ✓
CROSS-SECTION 3: " " " " " 53E ✓ K3 AREA
CROSS-SECTION 4: " " " " " 55E ✓
CROSS-SECTION 5: " " " " " 56E ✓

CROSS-SECTION 6: Geological Cross-Section AB ✓

CROSS-SECTION 7: " " " CD ✓

CROSS-SECTION 8: " " " EF ✓ K1 AREA

CROSS-SECTION 9: " " " GH ✓

CROSS-SECTION 10: " " " KJ ✓

CROSS-SECTION 11: Geological Cross-Section along line 2S ✓

CROSS-SECTION 12: " " " " " 1S ✓ K6 AREA

CROSS-SECTION 13: " " " " " 3S ✓

CROSS-SECTION 14: " " " " " 4S ✓

CROSS-SECTION 15: " " " " " 00 ✓

CROSS-SECTION 16: " " " " " 2.5S MISSING?

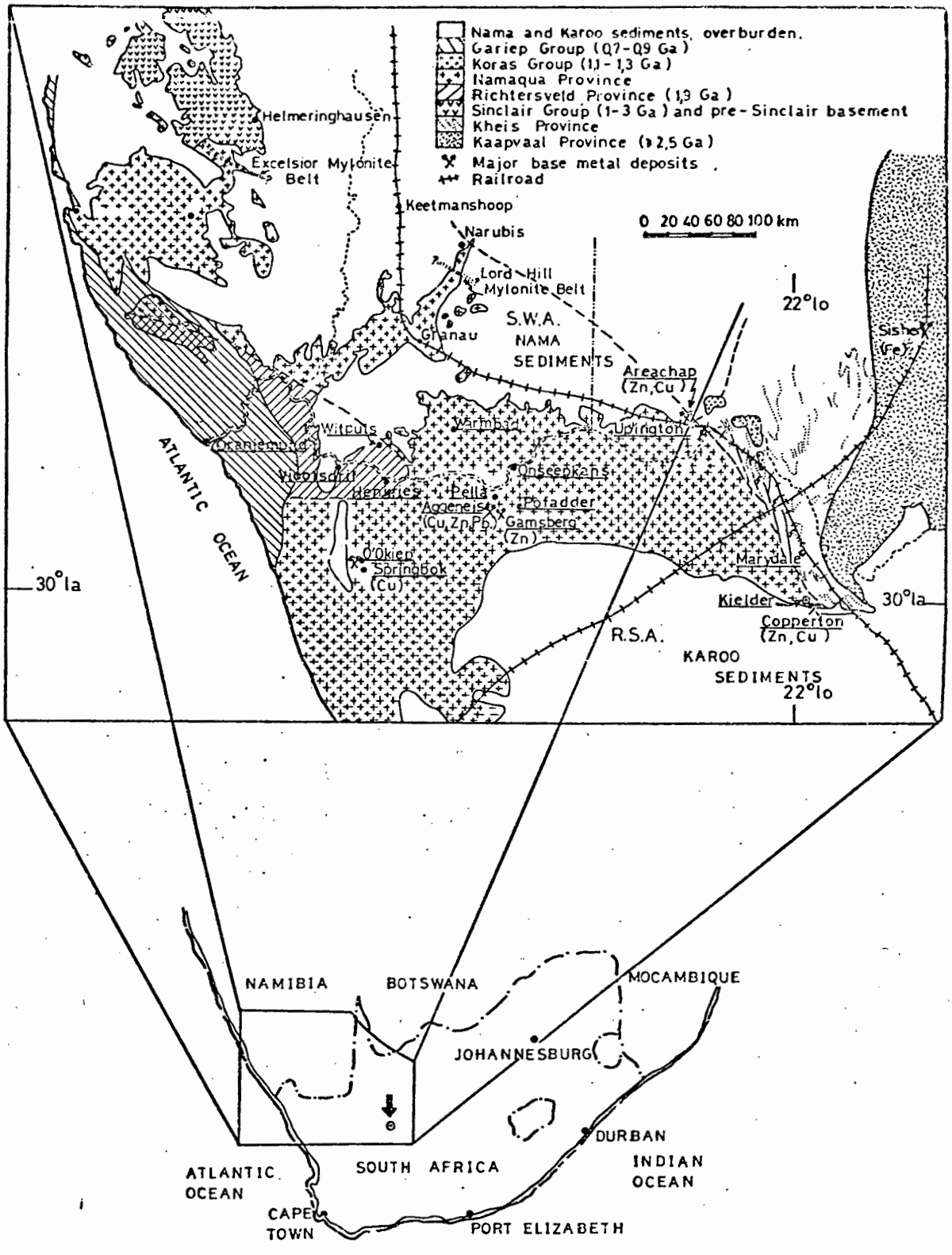

FIGURE 1: LOCALITY PLAN OF KIELDER AND NAMAQUA METAMORPHIC BELT AND OTHER MAJOR BASE METAL DEPOSITS. (MODIFIED AFTER KRÖNER 1976)

1. INTRODUCTION

1.1. Location

The Kielder properties cover 8568 hectares in the district of Prieska, Northern Cape Province and are situated 12 kms to the northwest of the operational (± 8500 tonnes ore per day) zinc-copper mine at Copperton (Fig. 1).
Three massive sulphide bodies known as K3, K1 and K6 occur in the extreme east and central part of Kielder, 2 and 4.5 kms apart respectively (See Map. No. 4).
The peneplained surface corresponds to the Bushmanland surface as defined by Mabbutt (1955) with the elevation varying from 1040 to 1100 metres above sea level. Two drainage systems, flowing to the north-east and south-west respectively, form the lower elevations as broad, sand choked, poorly defined "stream beds". Ubiquitous calcrete is developed to thicknesses of ≥1m and this is covered by ~30cms of red sandy soil (or ≥1.5m in the stream beds). Pebbles and cobbles of Dwyka Tillite derived erratics are scattered over the sandy surface. In situ basal Dwyka varved shales occur below the sand and calcrete in the extreme south-east of the K3 area. There is no surface expression of the Karro Supergroup presence, and was discovered by core drilling which intersected 30m of this yellow shale. Prior to the discovery of the gossan by Newmont South Africa Limited prospectors in 1976, no knowledge of mineralization was known on the properties.
The area is sparsely populated and consists of monotonous, undulating, barren, semi-desert with the only agriculture possible being sheep and goat ranching. Water is obtained from boreholes which yield feeble amounts (100-1000 litres per hour) of brackish water.

1.2. Aims

The aims of the present study are:-

(i) To establish a detailed stratigraphy of the three sulphide bodies and their wall rocks by observation of thin and polished sections of core and surface rock specimens.

(ii) To attempt correlations between the three areas based on the above stratigraphy and trace and major element geochemistry in an area where surface exposure is minimal to nonexistent.

(iii) To determine the pre-metamorphic rock type using trace and major element analyses of the amphibolites and basic granulites.

(iv) To determine the grade of metamorphism and P-T gradients across the properties using various mineral pairs as geothermometers and geobarometers and the mineralogy and textural observations of the thin sections.

(v) To observe the effects of metamorphism on the textures and mineralogy of the sulphide horizons.

(vi) To establish a model for the origin of these base metal deposits and, using the model, to predict the existence, likelihood, and location of further such deposits in the Copperton-Kielder region.

1.3. Approach

1.3.1. Surface Mapping

A surface geological map (See Map No. 4) was completed by the author during the last quarter of 1976 at a scale of 1:10000. Survey grid lines 400m apart were traversed across the properties with two flanking field assistants to find the rare outcrops and any possible gossan float. Aerial photographs were employed but were of limited use because of poor outcrop and lack of vegetation patterns. In many areas the lithology below the ubiquitous calcrete and sand had to be deduced from the cobble sized float. Outcrops were usually less than 1m across and with poorly-foliated gneisses and granulites, measurement of the foliation was very difficult. The map therefore is of limited use but nevertheless does show the regional strike and dip of the stratigraphy and the gossan occurrences.

Detailed plane table mapping was initially done by P.G. Gresse (Newmont company report 1978) of the three gossan areas and these maps were later modified (See Map Nos. 1, 2 and 3) by

the author using information obtained from trenching, pitting, shallow percussion drilling and core drilling. The plane table mapping obviously suffers from the same limitations outlined above.

1.3.2. Diamond-drilling and Core Logging

From April 1977 to July 1979 thirty diamond-drill holes totalling ~7500m of core were completed on the three gossan occurrences and their lateral pyritic extensions. The bulk of the core was logged by the author except for the early drilling which was done by P.G. Gresse (Newmont company geologist) and the later drilling which was logged by various geologists from Prieska Copper Mines Pty. Ltd. However, all the core was relogged and sampled by the author at a later date.

Because the weathering is deep (~100m), and the stratiform sulphide bodies are steeply dipping, inclined drill holes had to be collared to intersect the sulphides below the leached zone; this had the fortunate result of producing extensive intersections of the hanging wall host rocks. The mineralogy, foliation, mineralization, faults and shear zones were logged and this information plotted on cross-sections. All the drill-holes were measured by the author using a "Sperry-Sun Multishot" borehole instrument to determine the exact inclination and "off-section" drift of the holes.

The cross-sections were all redrawn after the detailed petrography was established by microscopic examination and enabled "hole to hole" correlations. (See cross-sections 1 to 16).

1.3.3. Sampling

Specimens of 10-15cm of core were sampled in each drill hole for thin sectioning in strategic places in each drilled area. The locations of these specimens are marked on the cross-sections except where sampling was too intensive. Type specimens for each lithology used for core logging were also thin sectioned.

Larger (± 7 kg.) specimens which were used for whole rock analyses (and thin sectioning) represented some 2 metres of core intersection.
Intersections of sulphide horizons required for economic metal analyses were sampled in lengths up to 1.5m split lengthwise; the half-core being retained for observation and polished thin sections.
Ten kilogram surface specimens were also collected for chemical analysis and thin sections. (The localities are marked on the geological maps 1 to 4).
All samples from both core and surface were fresh and unweathered.
285 samples of core were taken, 80 of which were bulk sampled for analysis and 15 surface bulk samples were collected (See Appendix V).

1.3.4. Petrographic Microscope Examination

All sections were cut normal to the foliation and specimens with more than 1% opaque phases were cut into polished thin sections to enable identification of the opaque minerals.
Mineral proportions were estimated, either using the visual comparison system established by Terry et al. (1955), or by point count analysis.
Any minerals which were difficult to identify or ambiguous were analysed by X-ray diffraction if present in sufficient quantities or by electron microprobe if single grains.
The enigmatic textures of the granulites and gneisses were described according to the terminology established by Moore (1970), which is strictly descriptive and devoid of any genetic connotations.
The detailed petrographic descriptions of each rock unit and photomicrographs are contained in Appendix I.

1.3.5. X-ray Diffractometry

The detailed methods of X-ray diffraction are contained in Appendix VI.
X-ray diffraction was particularly useful in the identification of the clay minerals and chlorites found in the gangue, the

finer grained amphibolites and some of the ambiguous colourless pyroxenes in the wall rocks.
Hexagonal and monoclinic pyrrhotite were distinguished semiquantitatively after Arnold (1962 and 1966) and Graham (1969) and confirmed by the magnetic colloid method after Scott (1974) (See Appendix IV). The presence of the two polymorphs were determined to allow the use of the sphalerite geobarometer and to detect possible zoning (with respect to the pyrrhotite polymorphs) within the mineralized zones.

1.3.6. Geochemistry

The detailed X-ray fluorescence analytical and microprobe methods are contained in Appendices II and III.
It has been attempted to prove that certain elements remain immobile under the conditions of metamorphism attained here. Variation trends, metal ratios, and ternary diagrams involving these elements have been used to distinguish between amphibolites and basic granulites of igneous and sedimentary parentage. Secondly, it is attempted to distinguish between the different stratigraphic units. Thirdly, it is proposed, after the methods suggested by Pearce and Cann (1973) and Winchester and Floyd (1976) to identify the tectonic setting in which the volcanics were formed.
The bulk rock analyses for Cu, Zn, Pb, Ag and Au in the sulphide zones have been used to indicate the metal zonation.
In addition to the qualitative analyses of minerals, chalcopyrite, galena and sphalerite were analysed semiquantitatively by microprobe for silver to find the host when no discrete silver minerals could be identified in the ore.
Quantitative analyses of biotite, garnet, cordierite, orthopyroxene and sphalerite were completed for geothermometry and geobarometry and in the latter case to determine the impurities in the main ore mineral.

1.3.7. Opaque Mineral Etching

The isotropic sulphide minerals were etched to enable the

study of the grain size and internal textures. The results are discussed in section 3.3. and the methods used are outlined in Appendix IV. The metamorphic gradient which is present from the K3/K1 to K6 area provided an excellent opportunity for studying the effects of varying grades of metamorphism on the sulphide grain size and texture.

1.4. Previous Work

These relatively recent sulphide deposit discoveries by Newmont South Africa Ltd., and subsequent core drilling (1977 to 1980) have not been studied in any detail prior to this present research. A company report by P.G. Gresse (1978) included the surface mapping and drilling up to that date and subsequent progress reports have been completed by the author. Some limited petrographic (12 thin section descriptions) work was completed under contract by Prof. J. McIvor of the University of the Witwatersrand. The only published literature dealing specifically with Kielder is a discussion by Gorton (1980) on a paper on metamorphism north of the Kielder area by Botha et.al (1979). The latter authors were cautioned for extrapolating metamorphic isograds across areas of rare outcrop and ignoring the presence of retrograde metamorphism. Botha et.al's preference for regional studies is not always feasible and detailed studies of areas "exposed" by core drilling or mining will always be more definitive.

Recent lead isotope work on the K6 banded iron formation by D. Cornell (pers. comm.) suggests a similar origin to that of the Copperton ore-body. Research on the 47 million tonne Cu-Zn massive sulphide deposit at Copperton has been published by Cornell (1975), Middleton (1976), Wagener(1980) and Koeppel (1980). These provide excellent material for comparison with the Kielder ore bodies and it has become clear that they have similar origins and deformational histories.

The only published regional map of the area (Middleton, 1976), which was based largely on aeromagnetic and other geophysical data supported by aerial and satellite photography, is incorrect.

Subsequent mapping by Neumont South Africa Limited and Prieska Copper Mines has proven the previous idea of a volcanic pile to be fallacious. Wagener (1980) interprets the stratigraphic sequence enclosing the Copperton ore body as being predominantly meta-sediments with dacite in the footwall.

Lead isotope data (Koeppel, 1980) and Rb/Sr data (Cornell, 1975) from the Copperton ore body and wall rocks respectively, suggest an age of 1305m.y. and the lead isotope characteristics indicate a mantle origin. Notwithstanding the isotopic data, the age of the Copperton /Kielder rocks and the entire Namaqua Metamorphic complex remain controversial (Joubert, 1976; Kröner, 1976; Koeppel, 1980).

The relationships between the Marydale banded iron formation and greenstones dated at ≥2990 m.y. (Cornell and Barton, 1979), the Haib Volcanics at 1980 m.y. (Reid 1975), the Bushmanland sequence hosting the Gamsberg and Aggeneys orebodies at 1300 m.y. (Koeppel, 1980), the Kaaien quartzites, and the Namaqua Metamorphic rocks hosting the Prieska and Kielder sulphide deposits remain unresolved.

Pressure/temperature conditions from wall rock geothermometers and barometers are reported for the Copperton ore body as 680-720^{o}C and 4-6 Kbars (Cornell, 1975).

At present, a South African Geodynamics project to produce a strip map across the Kaapvaal-Namaqua metamorphic complex close to the Copperton-Kielder area, is in progress (Scott, W.D. and Cornell, D.H.).

2. STRATIGRAPHY

The details of the impersistent, interfingering nature of the stratigraphy are best observed on the cross-sections (Cross-sections 1 to 16); nevertheless, the macroscopic features of the units are briefly described individually. The detailed mineralogy, textural features and hand specimen description for each unit are in Appendix 1.

2.1. The K3 Area

2.1.1. The K3 Footwall Stratigraphy

The banded biotite-garnet gneiss (Unit 15), and the felsic sillimanite gneiss (Unit 14), form the bulk of the footwall. The mineralogy of Unit 15 is variable and the rock has characteristics intermediate between the diopside plagioclase granulite (Unit 12) and the banded hypersthene granulites (Unit 13). Nevertheless, the unit is macroscopically very distinct. The unit interfingers with other rock types with individual bands varying from 10 to 60m thick.

The overlying felsic sillimanite gneiss (Unit 14) is petrographically identical to its hanging wall equivalent (Unit 5) and macroscopically it is similar in its interfingering nature. It is found as bands varying from 5 - 50m in thickness interbedded with the banded hypersthene granulite biotite garnet gneiss (Unit 13). Except for the central section of K3 (i.e. the well developed massive sulphide), there is a narrow band of Unit 14 (5 - 10m wide) immediately below the sulphide zone.

The banded hypersthene granulite (Unit 13) underlies the diopside plagioclase granulite (Unit 12), varying in thickness from 20 to 30m. In the central K3 area it is persistent, but to the west this rock type is stratigraphically lower in the footwall, is interbedded with felsic sillimanite gneiss, and the thickness here varies from 6 to 12m in three distinct units (see Cross-section 3).

In the eastern end of K3 (Cross-section 5) this unit forms the bulk of the footwall. 130m below the massive sulphide is a 10-15m zone of disseminated pyrite and pyrrhotite within the banded hypersthene granulite.

The immediate footwall unit, the diopside plagioclase granulite (Unit 12), reaches a maximum thickness of 15-20m immediately below the massive sulphide unit. The unit

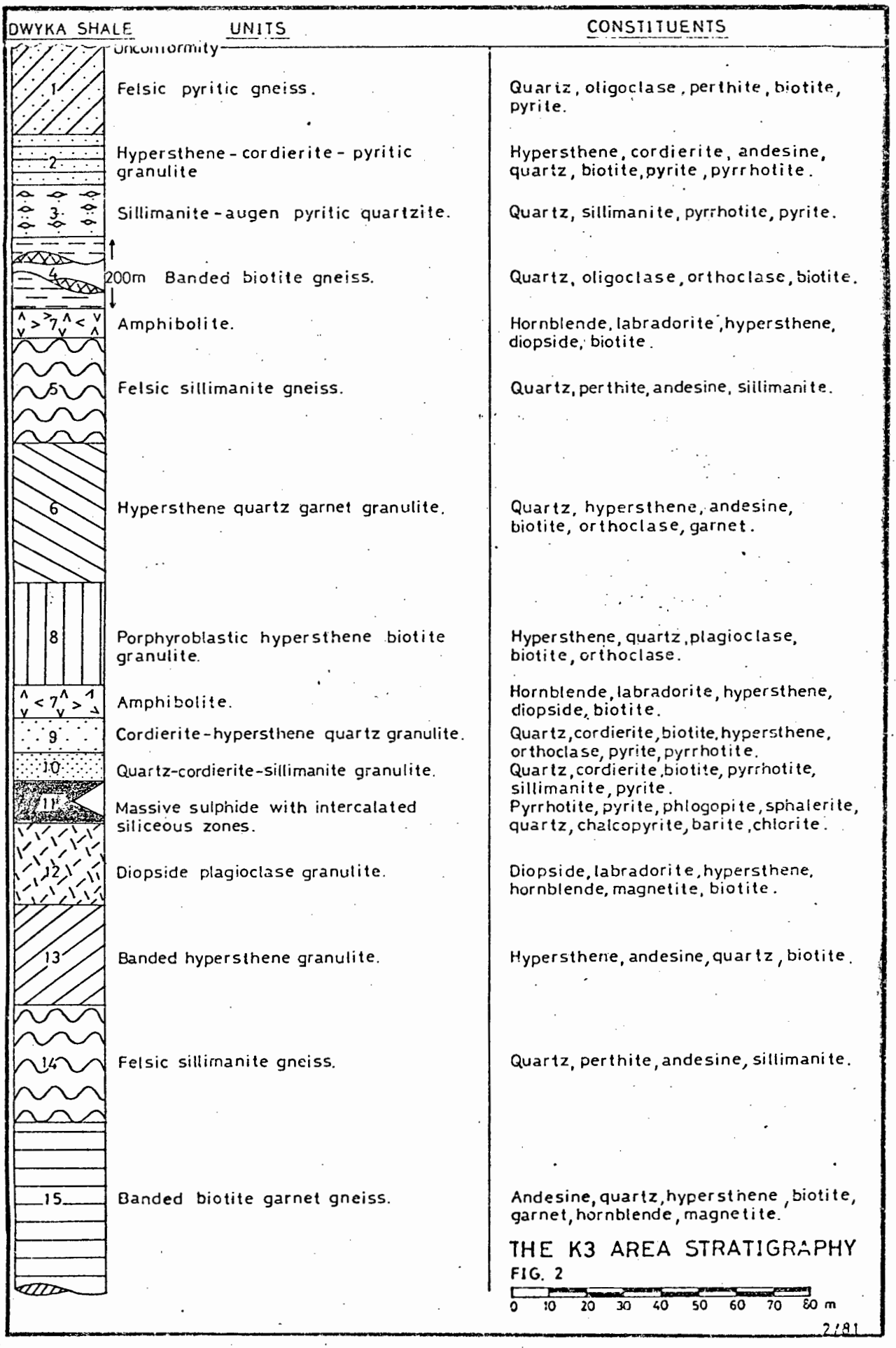
DWYKA SHALE
UNITS
CONSTITUENTS
Unconformity
1
Felsic pyritic gneiss.
Quartz, oligoclase, perthite, biotite, pyrite.
2
Hypersthene - cordierite - pyritic granulite
Hypersthene, cordierite, andesine, quartz, biotite, pyrite, pyrrhotite.
3
Sillimanite - augen pyritic quartzite.
Quartz, sillimanite, pyrrhotite, pyrite.
200m
4
Banded biotite gneiss.
Quartz, oligoclase, orthoclase, biotite.
7
Amphibolite.
Hornblende, labradorite, hypersthene, diopside, biotite.
5
Felsic sillimanite gneiss.
Quartz, perthite, andesine, sillimanite.
6
Hypersthene quartz garnet granulite.
Quartz, hypersthene, andesine, biotite, orthoclase, garnet.
8
Porphyroblastic hypersthene biotite granulite.
Hypersthene, quartz, plagioclase, biotite, orthoclase.
7
Amphibolite.
Hornblende, labradorite, hypersthene, diopside, biotite.
9
Cordierite - hypersthene quartz granulite.
Quartz, cordierite, biotite, hypersthene, orthoclase, pyrite, pyrrhotite.
10
Quartz-cordierite-sillimanite granulite.
Quartz, cordierite, biotite, pyrrhotite, sillimanite, pyrite.
11
Massive sulphide with intercalated siliceous zones.
Pyrrhotite, pyrite, phlogopite, sphalerite, quartz, chalcopyrite, barite, chlorite.
12
Diopside plagioclase granulite.
Diopside, labradorite, hypersthene, hornblende, magnetite, biotite.
13
Banded hypersthene granulite.
Hypersthene, andesine, quartz, biotite.
14
Felsic sillimanite gneiss.
Quartz, perthite, andesine, sillimanite.
15
Banded biotite garnet gneiss.
Andesine, quartz, hypersthene, biotite, garnet, hornblende, magnetite.
THE K3 AREA STRATIGRAPHY
FIG. 2
0 10 20 30 40 50 60 70 80 m
2/81

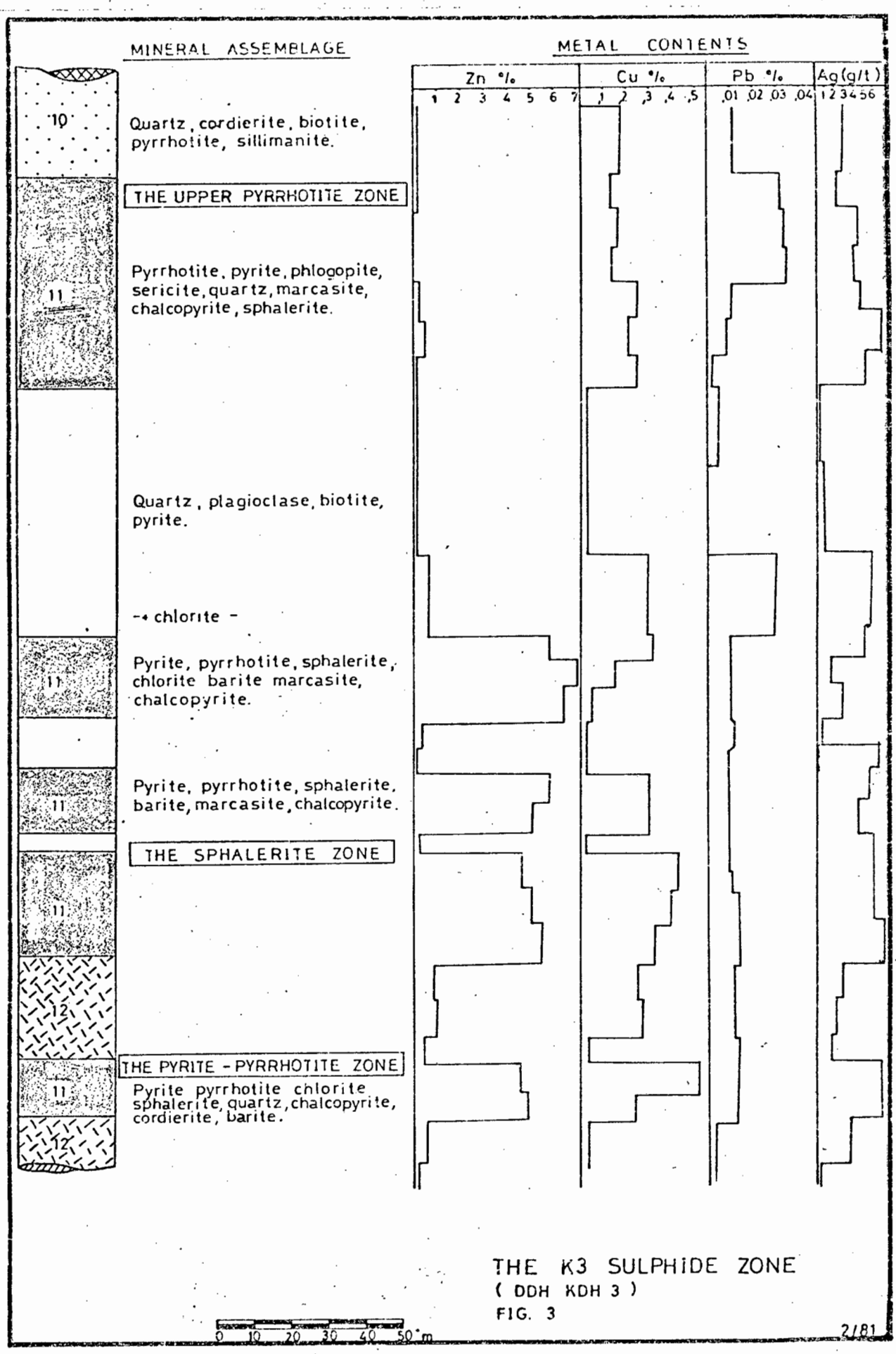

THE K3 SULPHIDE ZONE
(DDH KDH 3)
FIG. 3

2/81

wedges out to the east (and downdip) but reappears as a thin band (~2m) on Section 58E. This thin band is interbedded with the banded hypersthene granulite (Unit 13) 12m below the sulphide zone on Section 56E, and 15m below the ore on Section 54E.

Where the diopside-plagioclase granulite is absent from the vicinity of the ore horizon the sulphides are not massive, but disseminated within a quartz cordierite-sillimanite gneiss. Towards the west of the K3 area this unit is found deeper down in the footwall. On Section 53E the unit occurs as two thin (~3m) bands interlayered with felsic gneiss, and on Section 52E the unit is 22m thick. The contacts with adjacent rocks are sharp and conformable.

2.1.2. The K3 Sulphide Unit

The unit has a maximum thickness of 18m (including the intercalated 5-6m thick siliceous zone) in the central part of the K3 area but thins to <6m along strike and down-dip. There are sharp contacts with the footwall diopside plagioclase granulite (Unit 12) and the hanging wall quartz-cordierite-sillimanite granulite (Unit 10), although the latter displays more disseminated sulphides (mainly pyrite, minor pyrrhotite and chalcopyrite) than the former. Where the ore zone is thickest, an intercalated siliceous zone is present, the contacts between the sulphide and felsic rock being sharp. Along strike to the east and west the massive sulphides become progressively less massive, until the unit is represented by thin lenses (~30cm) of semi-massive pyrite, pyrrhotite, and traces of chalcopyrite within the quartz- cordierite-sillimanite unit (Unit 10). This facies change takes place over ~50m.

The individual zones, with their corresponding metal contents are illustrated in Fig. 5.? K1 zone?

The upper pyrrhotite zone varies in thickness from 0.5 to 5.5m, and is directly below the quartz-cordierite-sillimanite granulite (Unit 10), or as in KDH 4, below an upper siliceous zone lens.

The sphalerite zone varies in thickness from ≤0.5m to 5m thick, and is either a discrete unit separated from the other sulphides by lenses of siliceous rock, or it grades into the

overlying pyrrhotite zone.

The siliceous zone lenses vary in thickness from 10cm to 5m. Although usually free of sulphide it can contain stringers of sulphides near its contacts and throughout the thinner lenses.

The lower pyrite-pyrrhotite zone forms the base of the sulphide unit and its thickness varies from 1m to 3m. The unit usually grades upwards into the sphalerite zone (i.e. in drillhole KDH2), or is in sharp contact with the overlying siliceous zone (i.e. in drillhole KDH3). There is also a similar sulphide unit interbedded within the quartz cordierite sillimanite granulite (Unit 10) in one instance (see drillhole KDH3 Cross-section 1).

The major differences between the three massive sulphide sub-zones are tabulated below:

	TOP			BASE
	Pyrrhotite Zone (≤5.5m)		Sphalerite Zone (≤5m)	Pyrite-Phyrrhotite Zone (Max. ≤5m)
(i)	Py/po	0.15	3.0	2.0
(ii)	Sph/Cpy	1	10	2.5
(iii)	% Sulphide	85%	75-85%	60-75%
(iv)	Ag. (PPM)	3.5	5	6
(v)	Major Gangue Minerals	Phlogopite Sericite Quartz	Chlorite Edenite Barite Quartz Apatite	Chlorite Calcite Cordierite Barite Apatite

X-ray diffraction indicates a predominance (i.e. ~85-90%) of monoclinic pyrrhotite over the hexagonal variety. In places the hexagonal presence is below the detectable value of 10%. Sampling from each sub-unit within the massive sulphides failed to reveal any zoning of pyrrhotite varieties.

2.1.3. The K3 Hanging-wall Stratigraphy

The quartz-cordierite-sillimanite granulite (Unit 10) forms the immediate hanging-wall to the sulphide unit, and varies in thickness from 4 to 16m. The contact with the massive sulphides is sharp. The unit is persistent in areas where semimassive lenses of sulphides are developed instead of massive sulphide units.

There is a variation in the Py/Po ratio and sulphide/oxide ratio along strike within Unit 10. In the central area of K3 where the unit forms a discrete hanging-wall to massive

sulphides, the Py/Po ratic varies from 0.1 - 0.5 with traces of chalcopyrite and minor sphalerite within 4cm of the massive sulphide. Towards the east, Py/Po varies from 2 to 6, and sulphide/oxide (magnetite) ≈10. Towards the west of the central massive sulphide occurrence, Py/Po varies from 10 to 2 and sulphide /oxide ≈1.

The cordierite-hypersthene-quartz granulite (Unit 9) occurs above the thickest development of massive sulphide (i.e. central K3 area) and varies in thickness from 5 to 20m. Where the underlying sulphides thin and become less massive the unit pinches out, or alternatively, the sulphides occur as disseminated pods within this unit.

The porphyroblastic hypersthene biotite granulite (Unit 8) reaches a maximum thickness of 30-35m on Section 54E in the central area of K3. It appears to pinch out to the west (i.e. 15m on Section 53E and 8m on Section 52E) and east (i.e. zero on 55E and 20m on 56E). The unit also interfingers with the overlying hypersthene-quartz-garnet granulite (Unit 6) and underlying hypersthene-cordierite granulite (Unit 9); the contacts with both these units are gradational.

Amphibolite (Unit 7) forms two marker units in the hanging wall. The upper unit is usually 5-10m thick and is developed at the contact between the banded biotite gneiss (Unit 4) and the hypersthene-garnet-quartz granulite (Unit 6). The lower unit is found 10-40m above the ore horizon. Both units are best developed in the western K3 area (Cross-sections 52E and 53E) and lens out towards the east, although the upper unit is more persistent. Both units appear to wedge out rapidly downdip.

Hypersthene-quartz-garnet granulite (Unit 6) occurs as two well defined bodies. The upper body reaches its maximum thickness (55m) on Section 52E in the extreme west of K3. The lower unit is 5m thick on this section. The units interfinger with the felsic sillimanite gneiss (Unit 5) towards the east. Neither unit was encountered on Section 55E but both reappear in the extreme east on Section 56E, where they are 15m and 5m thick. The upper unit is banded (50cm wide bands), with felsic and intermediate layers. Some felsic, coarse bands contain up to 75% quartz with biotite and plagioclase making up the remainder.

The felsic sillimanite gneiss (Unit 5) has a variable thickness yet it is ubiquitous. A similar unit (Unit 14), in the foot-

wall of the sulphide unit has been discussed separately. On Section 54E the unit reaches its maximum thickness of 110m but decreases in thickness down-dip and towards the east, where it becomes interlayered with other units. Towards the west it thins to a unit 30m thick with a subordinate layer (~10m thick) lower down in the sequence. At a depth of 440m on Section 54E the unit increases in thickness (~60m).

Numerous pegmatite lenses and bodies occur within the gneiss; up to 40% of its mass consisting of pegmatite. The contacts between gneiss and pegmatite are gradational. There is a gradual increase in grain size from the gneiss to a massive pegmatite in which the sillimanite content is generally less than in the adjacent sillimanite gneiss. Large amounts of pegmatite lenses were intersected in drillhole KDH 4 (Section 1) within the banded biotite gneiss (Unit 4). These are thought to represent lit-par-lit intrusions of pegmatites emanating from the adjacent interfingering felsic sillimanite gneiss.

The banded biotite gneiss (Unit 4) has a variable thickness (average 200m) but is ubiquitous in the Kielder area. In the eastern end of K3 the unit is interlayered with the felsic sillimanite gneiss, but towards the west the latter unit predominates. On cross-section 54E the interfingering of these units is most pronounced. Pegmatites are found in the banded biotite gneiss on Section 54E.

The sillimanite-augen pyritic quartzite (Unit 3) has a minimum thickness of 15m, but the true thickness is unknown because the lower contact is with the intrusive granodiorite. The hypersthene-cordierite-pyritic granulite (Unit 2) has a thickness of 15m, although it was intersected only on Section 54E. The underlying sillimanite-augen pyritic quartzite (Unit 3) has a sharp contact with this unit.

The true thickness of the felsic pyritic gneiss (Unit 1) is not known as it is unconformably overlain by Dwyka Group shales. The lower contact with hypersthene-cordierite pyritic gneiss is gradational. The minimum thickness is 25m. Near surface the rock is highly weathered to a clayey gneiss.

The upper pyritic units (Units 1, 2 and 3) are assumed to be stratigraphic equivalents of the K1 massive sulphides which occur 2km to the west; poor outcrop prevents positive

correlation (See Map 4). However, geophysical surveys, in particular ground magnetics and resistivity/IP, tend to support a correlation.

2.1.4. The K3 Intrusives

A coarse grained granite (Unit 17) was encountered in only one drill hole (i.e. KDH4 on Section 54E), where it exists below a major fault breccia zone. The breccia zone is 1.5m wide and consists of highly fractured quartz and feldspar (altered to clay minerals) with extensive (≥30%) quartz and calcite veining. The granite body is 15m wide, and its basal contact is sheared. The rock has no preferred orientation of minerals and is a post-tectonic granite.
A granodiorite sill (Unit 18) is best developed on Section 54E, and dips to the north-east.
Consequently, the rock is not encountered on Sections 53E and 52E. A second sill is seen only on Section 54E (as no other section had diamond drill holes in this southern area). The contacts are always sheared and there has been considerable displacement (~100m) along this contact. The upper granodiorite contact is well preserved and sharp and can be observed in a single thin section (RKG 88) over a distance of ~5mm. The contact cross-cuts the foliated diopside granulite and from this it is estimated that the granodiorite sill dips shallowly to the north-east.

2.2. The K1 Area

2.2.1. The K1 Footwall Stratigraphy

Quartz-cordierite-garnet gneiss (Unit 10) forms one of the lower units in this area and is interbedded with the diopside amphibolite (Unit 9) and reaches a maximum thickness of 30m. In the extreme north-east the unit is underlain by a quartz-biotite gneiss (Unit 3) with a gradational contact between them.
Diopside amphibolite (Unit 9) forms the bulk of the footwall, with the thickness varying greatly from ≥100m in the south-west to ≤15m in the north-east. The change in thickness is accompanied by a slight mineralogical change, i.e. a minor amount of quartz is found in the north-eastern unit, whereas it is absent in the south. Towards the base of the unit in the south the diopside content increases from <5% to ~20%. The diopside content in the north (only the upper unit is

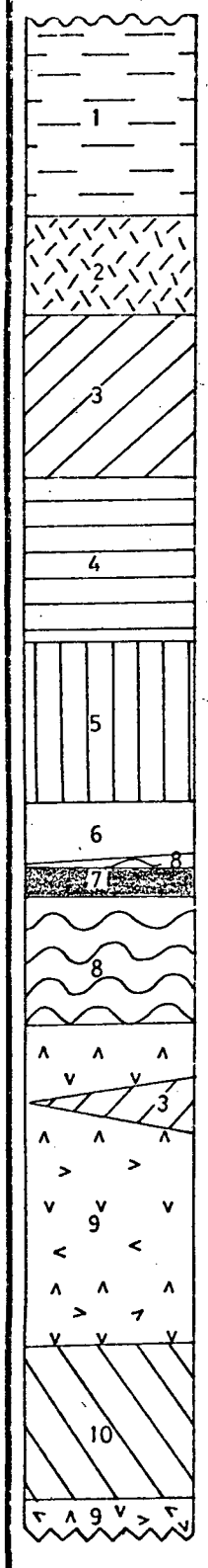

UNIT	CONSTITUENTS
Banded biotite gneiss.	Quartz, plagioclase, orthoclase, biotite.
Amphibole quartz granulite.	Edenite, hornblende, quartz, labradorite, cordierite, garnet, diopside.
Quartz - biotite gneiss.	Quartz, plagioclase, (labradorite) biotite, hypersthene ± garnet
Hypersthene - cordierite - biotite gneiss.	Hypersthene, cordierite, biotite, quartz, plagioclase.
Quartz - plagioclase - garnet gneiss.	Quartz, plagioclase, biotite, garnet.
Quartz - cordierite granulite.	Quartz, cordierite, plagioclase, hypersthene, biotite.
Sulphide zone.	Pyrite, quartz, chalcopyrite, sphalerite, cordierite.
Felsic sillimanite gneiss.	Quartz, plagioclase, orthoclase, biotite, sillimanite.
Diopside amphibolite.	Hornblende, labradorite, diopside, quartz.
Quartz - cordierite - garnet gneiss.	Quartz, cordierite, plagioclase, perthite, garnet, biotite.
Diopside amphibolite.	Hornblende, labradorite, diopside, quartz.

THE K1 AREA STRATIGRAPHY
FIG 4.

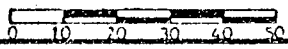

2/81

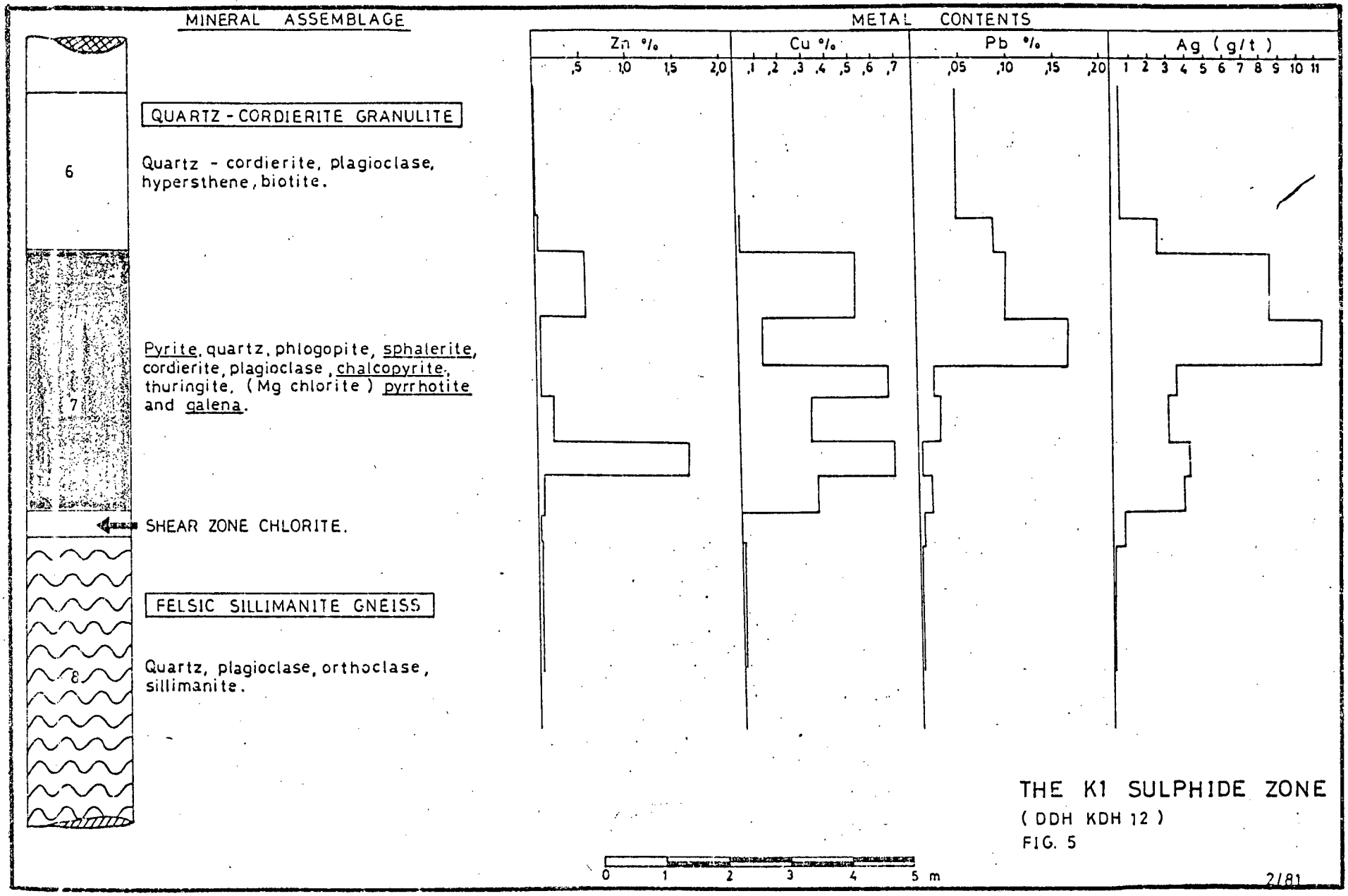

THE K1 SULPHIDE ZONE
(DDH KDH 12)
FIG. 5

2/81

intersected) is only present in minor quantities. The plagioclase composition varies randomly within the unit (particularly in the southern unit) from bytownite ($Ab_{28}An_{72}$) through labradorite to andesine ($Ab_{52}An_{48}$).
Felsic sillimanite gneiss (Unit 8) is similar to the gneiss (Unit 14) found in the K3 area and the intercalated coarse pegmatitic rock is also present, with the same relationships as described before.
A maximum thickness of 30m is attained in the south-west, with thinning to the north and east to a minimum of 4m. In all five (K1) sulphide intersections this unit forms the immediate footwall. In the extreme west this unit is found in the hanging wall of the ore and has a thickness of 2.5m. Minor bands (<8m wide) of this lithology are found lower in the footwall interbedded with the diopside amphibolite and the quartz cordierite garnet gneiss (Units 9 and 10).

2.2.2. The K1 Sulphide Unit

The massive sulphide unit (Unit 7) varies in thickness from 4-5m in the south-west to 1-2m in the north-east. The contact with the underlying felsic sillimanite gneiss is sharp and appears sheared in places.
The thickness of the sulphide unit may be dependent upon the location within the synform (See Cross-sections 6 to 10), with the thickest development expected in the fold closure (as yet unproven).
In the extreme north-east (drill-hole KDH 23, Cross-section 10) the sulphide unit changes its character. There are two thin sub-units (~2m each) interbedded with amphibolite, although the lower has the characteristic sillimanite gneiss as footwall. The sulphides here are similar to those in the south-east, except the total sulphide content is generally lower (≤45%) and minor galena is present.
The possibility that the north and south "limbs" as discussed above could be different stratigraphic units does exist. However, as in the other areas (K6 and K3) the impersistent nature of individual stratigraphic units is typical. Consequently, the thinning of the amphibolite (Unit 9) and the sulphide unit in the north, together with some minor mineralogical differences is not sufficient evidence to postulate separate stratigraphic units. Structural evidence (See Map 2)

exists at surface to indicate a fold closure. Nevertheless, conclusive evidence can only be obtained by coredrill probing down plunge of the fold axis.

2.2.3. The K1 Hanging-wall Stratigraphy

The quartz-cordierite granulite (Unit 6) forms the immediate hanging wall to the sulphide unit, and varies in thickness from 3 to 15m; towards north and north-east the unit is absent. It appears that the thicknesses of this unit and the sulphides vary sympathetically. The contacts with the adjacent units are sharp.

The quartz-plagioclase-garnet gneiss (Unit 5) has an average thickness of 25m, and is fairly consistent in the K1 area (see Cross-sections 6-10). The gradational contact with Unit 3 is manifested in a gradual decrease in garnet content. The contact with the more mafic amphibole-quartz granulite is sharp.

The hypersthene-cordierite-biotite gneiss (Unit 4) is impersistent and is found on the south-west of the K1 only, with a maximum thickness of 25m thinning rapidly to the east and north (See Cross-section 6). The contact with the overlying quartz-biotite gneiss is sharp but it grades into the underlying quartz plagioclase garnet gneiss (Unit 5).

The thickness of the quartz-biotite gneiss (Unit 3) is variable from 15 to 30m.

The amphibole-quartz-granulite (Unit 2) consists of two similar rock types; a more felsic edenite-quartz lithology is interbedded with a mafic amphibolite, the contacts being gradational. The thickness of this unit is variable because of its presence in a fold hinge, the true thickness in the west of K1 is 12-16m.

The unit changes towards the east in that the overall thickness increases ($\leq$30m), it becomes interbedded with quartz-plagioclase-garnet gneiss (Unit 5) and the amphibolite variety predominates over the edenite-quartz granulite which is 4m thick.

The banded biotite gneiss (Unit 1) has not been sufficiently cored by drilling to provide a true thickness, however it has a minimum thickness of 30m. The rock is similar to the banded biotite gneiss of the K3 area.

2.2.4. The K1 Intrusive Rocks

Apart from the numerous pegmatitic lenses within the felsic sillimanite gneiss, minor amounts of thin (< 1m) quartz-orthoclase pegmatites cut the various rock units.

2.3. The K6 Area

2.3.1. The K6 Footwall Stratigraphy

Biotite garnet gneiss (Unit 2) forms the bulk of the footwall (and the hanging wall) of the sulphide unit and all other units are intercalated within it. In the footwall there is at least 80m of this gneiss containing intercalated amphibolite and felsic sillimanite gneiss.
Variations in quartz and plagioclase contents are random and not related to proximity to major amphibolite units, massive sulphides, or any other lithologies. Neither can any systematic mineralogical variation with depth or strike be established.
The amphibole-hypersthene granulite (Unit 6) is more commonly found in the hanging wall, however, minor bands (<15m thick) are found within the biotite garnet gneiss of the footwall.
Minor bands of amphibolite (Unit 4) usually $\leq$ 5m thick occur within the biotite garnet gneiss below the sulphide zones.
Magnetite-Ilmenite porphyritic amphibolite (Unit 9) is found within 10m of the massive sulphide unit, usually in the immediate footwall. It is always intercalated with the biotite garnet gneiss, except where forming the immediate base to the massive sulphides, and has well defined contacts.

2.3.2. The K6 Sulphide Units

The felsic stringer-sulphide unit (Unit 8) is a narrow (<2m), impersistent zone, which underlies the massive sulphides in places; its upper and lower contacts, with garnet gneisses, are always sharp.
The sulphide unit (Unit 7) is composed of two distinct rock types; a massive sulphide zone (sulphide $\geq$65%), and a semi-massive micaceous sulphide zone (~50% sulphides). The overall thickness of the unit varies considerably from 0.3 to 5m, and appears to vary randomly, although a thicker ore shoot may plunge to the south (as yet unproven).
The unit has a sharp contact with the hanging wall gneisses with a narrow halo (<2m) of sulphide minerals extending

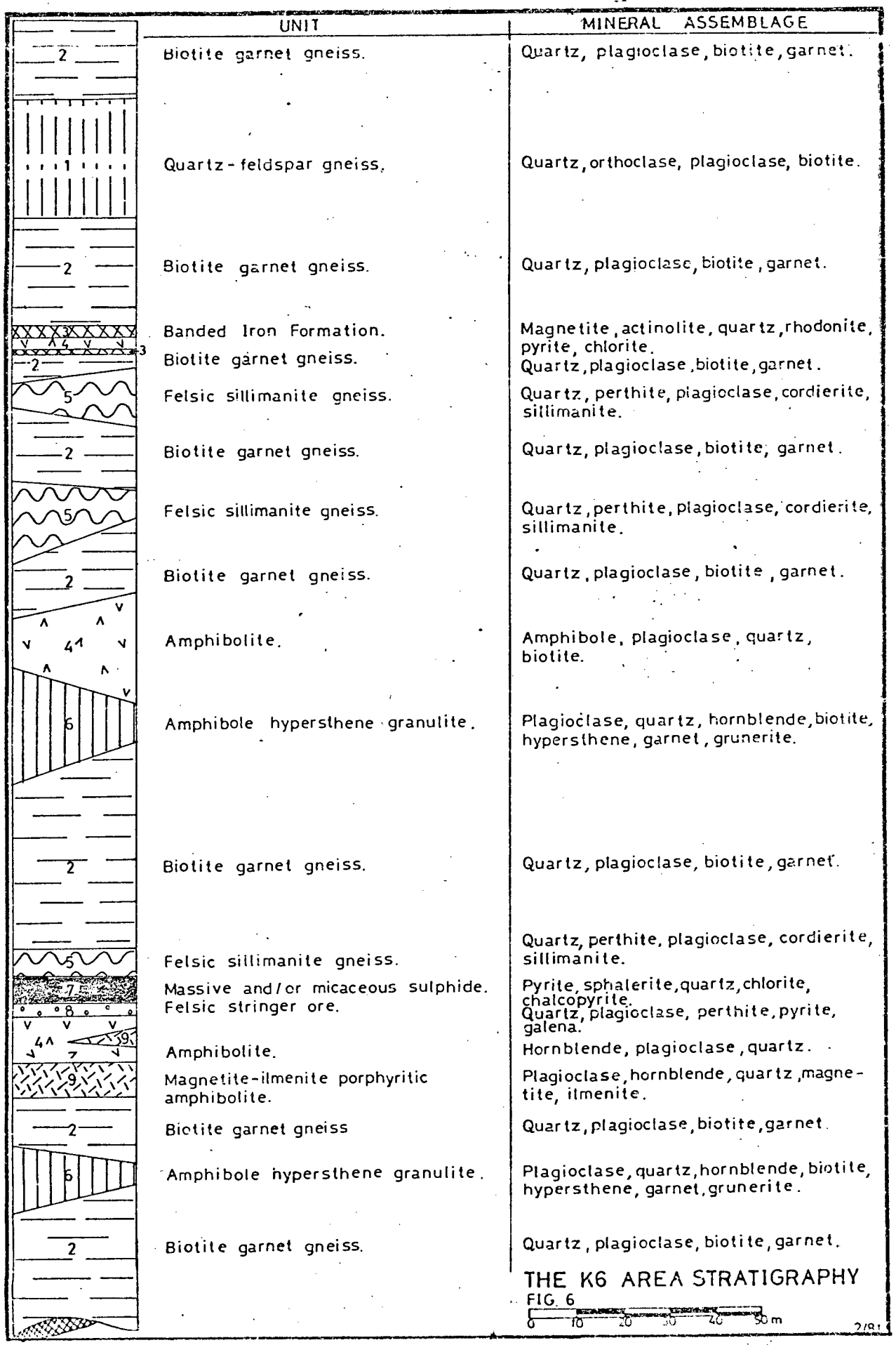
UNIT
MINERAL ASSEMBLAGE
Biotite garnet gneiss.
Quartz, plagioclase, biotite, garnet.
Quartz-feldspar gneiss.
Quartz, orthoclase, plagioclase, biotite.
Biotite garnet gneiss.
Quartz, plagioclase, biotite, garnet.
Banded Iron Formation.
Magnetite, actinolite, quartz, rhodonite, pyrite, chlorite.
Biotite garnet gneiss.
Quartz, plagioclase, biotite, garnet.
Felsic sillimanite gneiss.
Quartz, perthite, plagioclase, cordierite, sillimanite.
Biotite garnet gneiss.
Quartz, plagioclase, biotite, garnet.
Felsic sillimanite gneiss.
Quartz, perthite, plagioclase, cordierite, sillimanite.
Biotite garnet gneiss.
Quartz, plagioclase, biotite, garnet.
Amphibolite.
Amphibole, plagioclase, quartz, biotite.
Amphibole hypersthene granulite.
Plagioclase, quartz, hornblende, biotite, hypersthene, garnet, grunerite.
Biotite garnet gneiss.
Quartz, plagioclase, biotite, garnet.
Felsic sillimanite gneiss.
Quartz, perthite, plagioclase, cordierite, sillimanite.
Massive and/or micaceous sulphide. Felsic stringer ore.
Pyrite, sphalerite, quartz, chlorite, chalcopyrite.
Quartz, plagioclase, perthite, pyrite, galena.
Amphibolite.
Hornblende, plagioclase, quartz.
Magnetite-ilmenite porphyritic amphibolite.
Plagioclase, hornblende, quartz, magnetite, ilmenite.
Biotite garnet gneiss
Quartz, plagioclase, biotite, garnet.
Amphibole hypersthene granulite.
Plagioclase, quartz, hornblende, biotite, hypersthene, garnet, grunerite.
Biotite garnet gneiss.
Quartz, plagioclase, biotite, garnet.
THE K6 AREA STRATIGRAPHY
FIG. 6
0 10 20 30 40 50 m
2/81

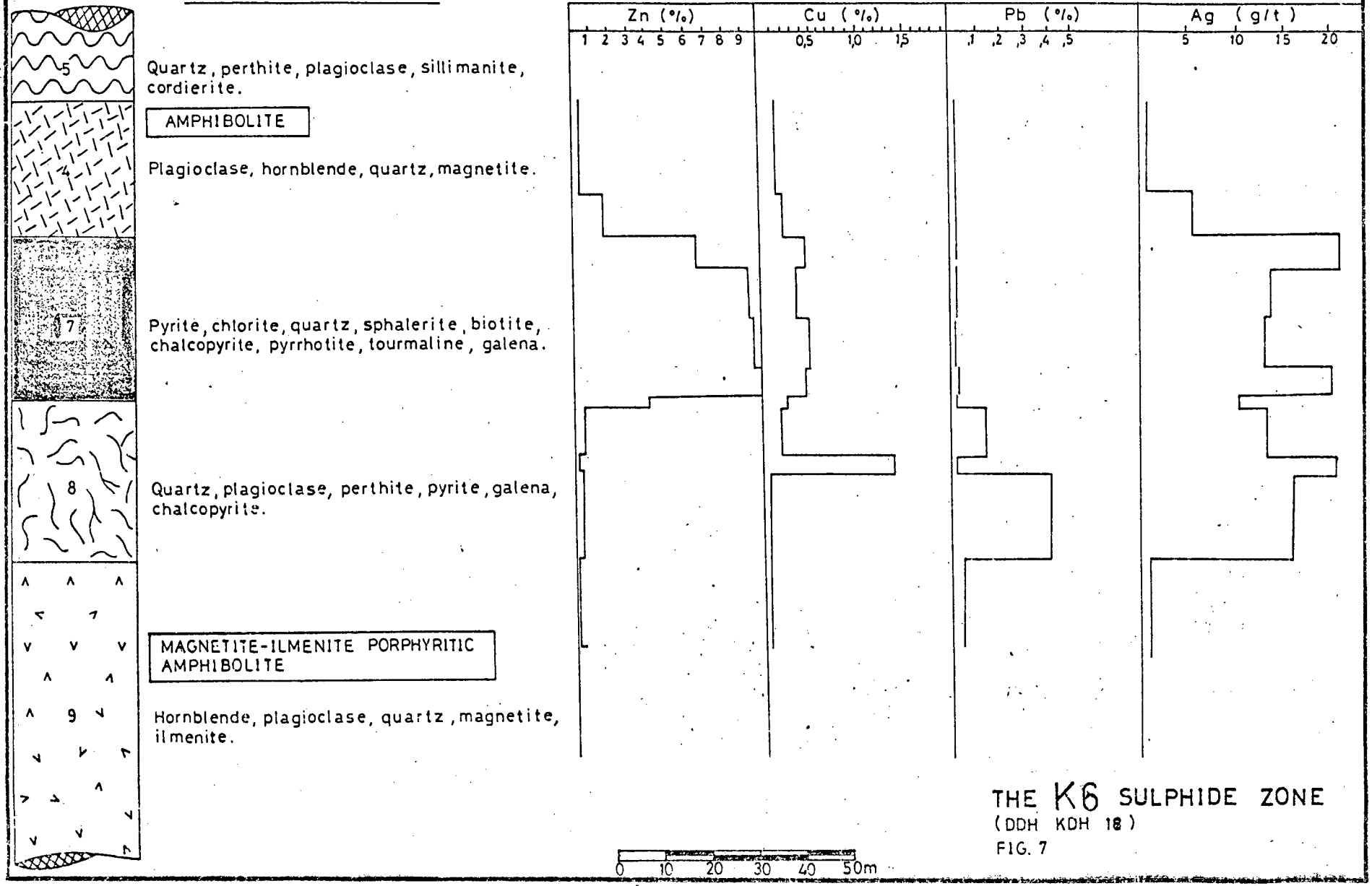

THE K6 SULPHIDE ZONE
(DDH KDH 18)
FIG. 7

upwards; the underlying felsic stringer ore also has sharp contacts with the darker massive sulphide. The contact relationship between the massive and semi-massive varieties is gradational, and usually occur in equal proportions.

2.3.3. The K6 Hanging-wall Stratigraphy

The felsic sillimanite gneiss (Unit 5), mineralogically identical to the units found in K1 and K3, is found as impersistent bands throughout the sequence, varying from <1m to 25m. The thickest development is in the hanging wall in the north of K6, intercalated with the biotite-garnet gneiss (Unit 2).

A narrow (~5m) band of this rock forms the immediate hanging wall to the massive sulphides, in places. The contact is sharp. However, extending ~2m from the sulphide contact the felsic gneiss contains up to 5% disseminated magnetite, pyrrhotite, chalcopyrite and rarely galena.

Biotite garnet gneiss (Unit 2) forms the bulk of the hanging wall and is identical to the gneiss in the footwall. Two major bands exist above the massive sulphide and banded iron formation (60m and 150m respectively).

The amphibole-hypersthene granulite (Unit 6) is impersistent but usually occurs below the amphibolite (Unit 4) horizon, and minor bands occur in immediate hanging and footwall of the massive sulphides (see Cross-section 12). The thickness varies from 3 to 25m. The mineralogy is also variable as can be seen in Appendix 1.

Amphibolite (Unit 4) is found in the hanging-wall within the garnet-biotite gneiss (Unit 2) and at its thickest is 80m in the south but thins rapidly to the north to only 5m (See Cross-sections 14 and 15). The unit is found midway between the banded iron formation (Unit 3) and the massive sulphides (Unit 7).

A narrow band (<2m) usually separates two banded iron formation units (see Fig. 7).

The banded iron formation (Unit 3) occurs as two distinct units within the biotite garnet gneiss. Between the two iron formation bands is amphibolite and minor felsic sillimanite gneiss. Their relationships can be seen on Cross-sections 11, 12, 13, 14 and 16. Both units vary in thickness from 0.1 to 1m, with the upper being consistently thicker at 0.75m. Minor

lenses of B.I.F. (~1 - 2cms) occasionally occur within the intercalated amphibolite.
This unit is persistent throughout the K6 area and serves as a valuable marker horizon consistently 135m above the massive sulphides.
Quartz-feldspar gneiss (Unit 1) exists as intercalated bands (10 - 20m thick) within biotite-garnet gneiss and felsic sillimanite gneiss (Units 2 and 5 respectively). It has gradational contacts with the former gneiss.

2.3.4. The K6 Intrusive Rocks

Acid pegmatites occur throughout the K6 area as narrow (<3m) lenses, usually concordant with the foliation. The felsic sillimanite gneiss, as was the case in the K1 and K3 areas, contains frequent pegmatite lenses.

2.4. The Southern Granulite

Due to lack of exposure and no drilling in this area a minimum thickness of this unit, a pyroxene granulite, can only be obtained. The widest outcrop in the south-east of the property (see Map. No. 4) is approximately 100 metres. The enclosing rock types can only be described as felsic gneisses. However, this unit, by virtue of its resistant nature, does form one of the few marker horizons on the property. It strikes easterly in the south-east portion of the area and wraps around in a regional structure to strike northerly west of the K6 area (see Map. No. 4). Petrographic examination of chip samples along its strike do not reveal facies changes in the mineralogy. To date geochemical and geophysical exploration methods do not indicate sulphide mineralization associated with the pyroxene granulite.

2.5. The Northern Granulite

This unit outcrops between co-ordinates 32 east/ 1 south and 40 east/base line (see Map. No. 4). The minimum thickness of this unit is ~50m and is enclosed by undifferentiated felsic gneiss. These pyroxene granulites appear as strike extensions of the K3 area stratigraphy. Poor exposure, particularly to the west where thick sand obscures all outcrop, prevents positive correlation.

2.6. Overall Stratigraphy Summary

Employing the regional strike trends obtained from the rare outcrops and the detailed stratigraphy which has been provided by the core drilling in the areas of sulphide mineralization, a comparison, and possible correlation, is made between the three areas of mineralization and two areas of pyroxene granulite outcrop.

The wall rock sequences of the three sulphide bodies have only the broadest similarity to each other. The most noticeable features of the K3 mineralization are the presence of porphyroblastic hypersthene granulites in the hanging-wall, lack of significant amphibolite units, and the presence of large granodiorite dykes and sills. In the case of K1 the presence of up to 150m thick amphibolite unit in the footwall, and a more felsic edenite (amphibole) quartz granulite in the hanging-wall, make it unique. In the K6 area a significant (up to 80m thick) amphibolite occurs in the hanging-wall. The stratigraphy is relatively uncomplicated with the predominant wall rock being a biotite-garnet gneiss and 135m stratigraphically above the sulphide zone, there is a thin but persistent banded iron formation.

However, in a broad sense the stratigraphies are similar; the predominant rock type is a banded biotite gneiss with or without garnet, ubiquitous lenses of felsic sillimanite gneiss and, naturally, the presence of massive sulphide lenses.

The stratigraphy of the massive sulphide units can also be compared in this broad sense.

The general widths are comparable, varying from 1 to 8m, the sulphide mineralogy is relatively simple with predominantly pyrite, sphalerite, minor pyrrhotite and very minor chalcopyrite and galena, there are thin impersistent siliceous zones within the sulphide, the gangue usually consists of chlorite and earthy hematite and cordierite-bearing granulites are ubiquitous.

However, each sulphide unit has its unique features. The K3 area is typified by the presence of significant amounts of pyrrhotite (po/py $\approx$1), there is strong mineralogical zoning with a pyrrhotite-rich top and sphalerite-rich base and the sulphide unit is thicker than in the other (K1 and K6)

areas.

The K1 area is typified by a much thinner (1 - 2m wide) zone, the sulphides are less massive in a micaceous gangue, the copper/zinc ratio is higher than that of the K3 area and galena is present in minor quantities. The K6 area is unique, with its felsic siliceous chalcopyrite and galena stringer zone below the massive sulphides, the minor quantities of pyrrhotite in the massive ore, the ubiquitous presence of galena, and the higher precious metal contents of the ore, and the presence of both massive and micaceous types of ore.

These features of the sulphide zones will be discussed at greater depth in Section 5 (see p. 54). From the above summary it can be seen that differences between the sulphide zones and their wall rocks do exist.

Surface mapping indicates that the three sulphide units do occupy different stratigraphic horizons. The pyritic horizons intersected in the hanging-wall of K3 area (see Cross-section No.1) are the strike extensions of the north limb of the K1 sulphide 2 kilometres to the west (see Map No.4).

The northern granulites are possible strike extensions of the granulites associated with the K3 sulphide mineralization. Although the mineralogy is slightly different (less hypersthene and cordierite than the K3 granulites) the major and trace element geochemistry does indicate some affinity. This will be discussed at length in Section 4.2.4. (see page 51).

The banded iron formation, which serves as a marker in the K6 area, is also seen to outcrop at co-ordinates 32 east/13.5 south (see Map No. 4), 4 kms east of K6 and 700m south of the K1 area.

It is therefore tentatively suggested that the sulphide horizons occupy three different stratigraphic levels within the sequence of gneisses, granulites and amphibolites. However, the stratigraphic "distance" between them does not appear to be more than 500m.

3. METAMORPHISM

3.1. Geobarometry and Geothermometry

3.1.1. Garnet-biotite Geothermometry

The iron and magnesium partitioning between almandine garnet and biotite is temperature dependent and independent of the volatile elements present at the time of crystallisation.

Since the earlier work of Albee (1965), Saxena (1969) and Thompson (1976), the garnet-biotite thermometer has been used successfully by various workers (Weaver et.al 1977, Plimer 1976, Mocre, Kartun and Waters 1979 and Ghent et.al 1979).

Ferry and Spear (1979) experimentally calibrated the Fe-Mg partitioning between garnet and biotite and their results produced the following equation:

$$12454-4.662T\ (^{o}K) + 0.057P\ (bars) + 3RT\ln K = 0$$

where $K = \dfrac{X_{Fe}^{gar}}{X_{Mg}^{gar}} \cdot \dfrac{X_{Mg}^{biot}}{X_{Fe}^{biot}}$

These results are used to calculate peak temperatures of metamorphism in the wall rocks of the Kielder sulphide bodies.

Garnet-biotite pairs (from ten core specimens) were analysed by electron microprobe. Traverses across garnet and biotite grains did not reveal zoning. Nevertheless, mineral cores were probed in case some showed retrograde zoning effects. In some instances the biotite edges could be seen to have altered to chlorite. The petrography of the various rock units from which these specimens came are described in Appendix 1. (K3 area - Unit 8, 13; K1 area - Unit 6, 10; K6 area - Unit 2, 5 and 6).

In all cases where this method was employed the biotite formed a major constituent of the thin section (i.e. >10% biotite), and in direct contact with the almandine.

The manganese content of the garnet is variable, containing up to 14.50% MnO, but did not seem to have any marked effect on the K values. Work done by Albee (1965) and Dougan (1974)

suggests a decrease in KD by 0.006 to 0.007 per atom percent of $\frac{Mn}{Mn+Fe+Mo}$ garnet. From the data obtained in this study the effect appears to be the reverse or to have very little effect. The manganese content is therefore not corrected for, when calculating KD here. The results are as follows:

Specimen/Thin Section No.	Footwall or Hanging Wall of Ore Zone	% MnO in Garnet	T °C
AREA K3:			
RKG 10 (Pair 1)	hw (Unit 8)	2.43	711
RKG 10 (Pair 2)	hw (Unit 8)	2.46	709
RKG 111 (Pair 1)	fw (Unit 13)	2.95	686
RKG 111 (Pair 2)	fw (Unit 13)	2.75	678
RKG 71 (Pair 1)	hw (Unit 8)	2.52	689
RKG 71 (Pair 2)	hw (Unit 8)	2.24	702 (n=6)
	$\bar{X}$ = 695°C (S = 13.4)		
AREA K1:			
RKG 179 (Pair 1)	hw (Unit 6)	2.53	634
RKG 179 (Pair 2)	hw (Unit 6)	2.71	687
RKG 190 (Pair 1)	fw (Unit 10)	2.91	706
RKG 190 (Pair 2)	fw (Unit 10)	2.80	693
RKG 209 (Pair 1)	immediate hw (Unit 6)	4.48	711 (n=5)
	$\bar{X}$ = 686°C (S = 30.7)		
AREA K6:			
RKG 217 (Pair 1)	hw (Unit 6)	3.5	587
RKG 217 (Pair 2)	hw (Unit 6)	3.6	558
RKG 288 (Pair 1)	hw (Unit 5)	14.5	588
RKG 298 (Pair 1)	fw (Unit 2)	9.8	585
RKG 298 (Pair 2)	fw (Unit 2)	7.91	557
RKG 255 (Pair 1)	hw (Unit 2)	7.37	632
RKG 255 (Pair 2)	hw (Unit 2)	7.37	627 (n=7)
	$\bar{X}$ = 590°C (S = 29.7°C)		

3.1.2. Garnet-Cordierite Geothermometry/Geobarometry

Iron and magnesium partitioning between garnet and cordierite (assuming equilibrium) is temperature dependent and independent of the volatile elements at the time of crystallisation. The early work on this geothermometer (Currie 1971, Hensen and Green 1971 and Wood 1973) produced contradictory results where the KD (i.e. $KD = \frac{X_{Fe}^{ga}}{X_{Mg}^{ga}} \cdot \frac{X_{Mg}^{cord}}{X_{Fe}^{cord}}$) was found by Currie to increase with temperature, whereas Hensen and Green found the opposite effect. Subsequent work, experimental and theoretical, (Thompson 1976, Hensen and Green 1973 and Holdaway and Lee 1977) has proved conclusively that the KD is inversely proportional to temperature. Subsequent use of this geothermometer has been extensive and successful (Moore et.al 1979, Selverstone 1980, Ghent et.al 1979 and Weaver et.al 1978).

In this study the equation from Holdaway and Lee (op-cit) has been used to calculate the equilibrium temperatures:

$$\ln KD = \frac{3095 + 0.0152\,(P(K\ bars) - 1)}{T\ (^{o}K)} - 1.35$$

(where KD is defined as above)

For the microprobe analyses only the fresh unweathered specimens were chosen and in all cases the garnet-cordierite pairs were in direct contact with each other. Garnet and cordierite are major (i.e. >7%) constituents of the rock. It was found that garnet and cordierite grain centres gave the most consistent results, the cordierite edges gave erratic results and the temperatures calculated from the latter tended to be lower, probably reflecting retrograde metamorphism (at 530-560^{o}C).

Rocks with the appropriate mineralogy, and in particular garnet and cordierite in direct contact, could only be found in the K1 area, in both the hanging and footwall of the ore zone. (For petrography of these rock units see Appendix 1 - Units 6 and 10 respectively).

The temperatures were not corrected for manganese content in the garnet because at 2 - 4% MnO the correction is insignificant.

The results are: K1 Area

Specimen/Thin Section No.	Stratigraphic position w.r.t. ore zone	% MnO in garnet	T°C
RKG 209 (Pair 1)	immediate hw	4.70	596
RKG 209 (Pair 2)	" "	4.80	643
RKG 190 (Pair 1)	footwall	2.80	654 (n=3)
		$\bar{X}$ = 631°C (S = 30.8)	

It is possible to use Hensen and Greens' (1973) garnet-cordierite-sillimanite-quartz geobarometer which gives, in spite of an absence of sillimanite, a maximum pressure value. Hensen and Greens' isopleths were determined for higher temperatures and therefore at 631°C an extrapolated curve gives a maximum pressure of 5.8 Kbars. This figure, in spite of the above limitations, agrees well with other methods.

3.1.3. Garnet-hypersthene Geobarometry

The solubility of Al in orthopyroxene, in equilibrium with garnet, decreases with increasing pressure at constant temperature. B.J. Wood (1974) has experimentally developed a geobarometer using (X_{Al}^{mI} opx) over a range of pressures (8-30 Kbars) and temperatures (800-1250°C). Garnet and hypersthene exists in equilibrium commonly in the K3 and K1 assemblages and rarely in the K6 area. However, the pressure-temperature conditions do not allow the quantitative use of Wood's (op cit) barometer. Nevertheless, the X_{Al}^{mI} for the hypersthene in equilibrium with almandine have been calculated and can give relative pressure conditions. The results are:

K3 Area: X_{Al}^{mI} = 0.280 (mean, n=6 s= 0.034) $(P \approx K1 \gg K6)$

K1 Area: X_{Al}^{mI} = 0.269 (mean, n=5 s= 0.005) $(P \approx K3 \gg K6)$

K6 Area: X_{Al}^{mI} = 0.669 (mean, n=3 s= 0.004) $(P \ll K3 \approx K1)$

The K3 and K1 garnet-hypersthene assemblages have equilibrated at pressures which are in the same range. This agrees with other results (See 3.1.2. and 3.1.4.).

The pressure at K6 appears to be lower than in the other

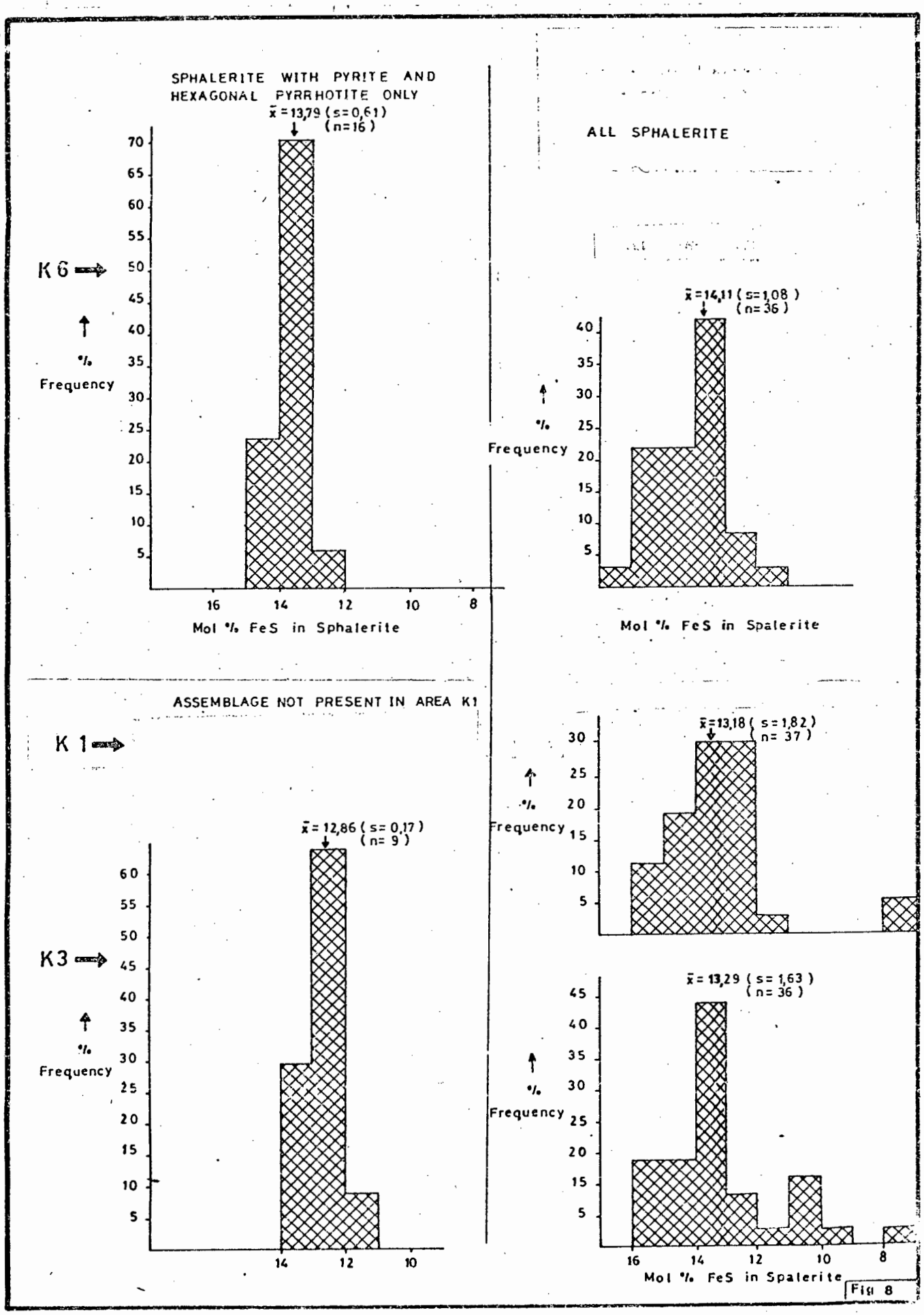
SPHALERITE WITH PYRITE AND HEXAGONAL PYRRHOTITE ONLY
x̄ = 13,79 (s = 0,61)
(n = 16)
K 6
% Frequency
Mol % FeS in Sphalerite
ALL SPHALERITE
x̄ = 14,11 (s = 1,08)
(n = 36)
% Frequency
Mol % FeS in Spalerite
ASSEMBLAGE NOT PRESENT IN AREA K1
K 1
x̄ = 12,86 (s = 0,17)
(n = 9)
K 3
% Frequency
x̄ = 13,18 (s = 1,82)
(n = 37)
% Frequency
x̄ = 13,29 (s = 1,63)
(n = 36)
% Frequency
Mol % FeS in Spalerite

Fig 8

areas (the $X \frac{mI}{Al}$ - pressure relationship is not linear)which is in agreement with results from the sphalerite geobarometer. The presence of hypersthene in the K6 area is rare and the above figures were calculated from one garnet-orthopyroxene pair found in specimen RKG 217.

3.1.4. Sphalerite Geobarometry

The FeS content of sphalerite has been recognized as an indication of pressure and temperature since the pioneering work of Kullerud (1953). Experimental work subsequently (Scott and Barnes 1971, Boorman 1967 and Boorman, Sutherland and Chernystev 1971) has disproved its use as a geothermometer. However, the FeS content of sphalerite is a useful geobarometer. One criterion essential for geobarometry is that sphalerite must have equilibrated with pyrite and hexagonal pyrrhotite. Scott (op cit 1973) and Kissin (1974) showed that the iron content in sphalerite could reequilibrate when hexagonal pyrrhotite inverted to the monoclinic form below 254°C. Consequently, the sphalerite grains chosen for analysis must be in direct contact with hexagonal pyrrhotite and pyrite. This was shown to be effective in the Ruttan Mine, Manitoba (Bristol 1979). This method remains controversial, but it is generally agreed that for metamorphic conditions above lower greenschist facies, where sphalerite and iron sulphide phases have equilibrated, pressures agree with silicate geobarometer minerals in the host rocks. This is confirmed for the Kielder sphalerites.

In two studies of sphalerite geobarometry (Campbell et.al 1968 at the Quemont Mine, Noranda;and Ethier et.al 1976 at the Sullivan Mine, British Columbia) the method was found to disagree with the silicate geobarometers. In both cases the FeS content of sphalerite was highly variable and because of lower greenschist facies metamorphic conditions it is unlikely that equilibrium was reached. In a recent publication (Stumpfl 1980) the author discards the sphalerite geobarometer as unreliable; however, the weight of evidence from other workers does not agree. The method was applied successfully on ores from the Ruttan Mine, Manitoba (Bristol 1979); Bodenais Ore, Bavaria (Boctor

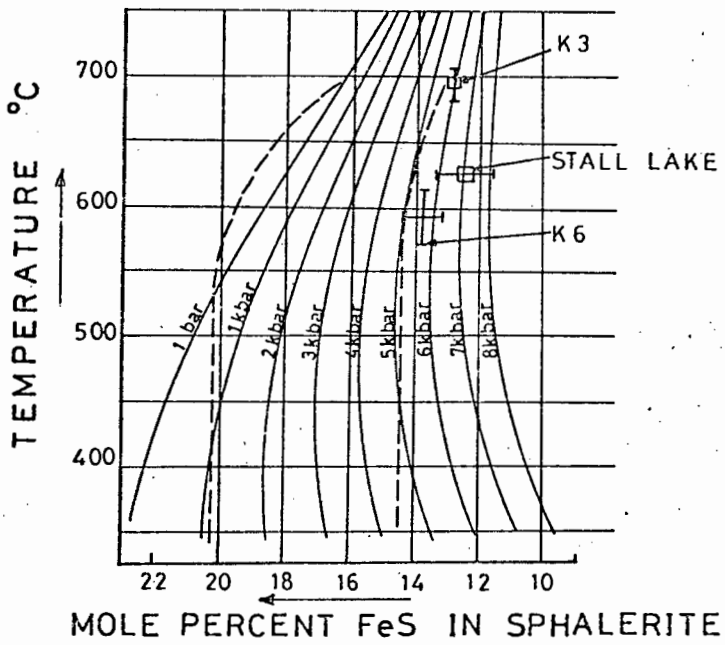

(From: I. Hutcheon 1978.)

FIG 9

1977); Anvil Ore Body, British Columbia (Campbell and Ethier 1974) and in the Balmat-Edwards District, New York (Brown et al. 1978).

The presence of Cadmium, copper and manganese in sphalerite can lead to erroneous results (Brown et al. 1978). However, with contents less than 1% MnO, CdO (as is found in Kielder sphalerites) the geobarometer is not affected. The presence of copper within the sphalerite, and as chalcopyrite exsolution blebs and rims, has an insignificant effect on the pressure determinations (Hutchinson and Scott 1978; Wiggins and Craig 1980).

Hutcheon (1978) has calculated P-T-X relations of the pyrite-pyrrhotite-sphalerite assemblage from pyrite-pyrrhotite equilibrium, molar volumes and activities from sphalerite solution models. These calculated isobars agree well with Bristol's (1974) and Scott's (1973) experimental work. In this study the isobars published by Hutcheon (1978) have been used to calculate the metamorphic pressure.

In the present study, samples of massive sulphide were analysed by X-ray diffraction (methods described Appendix IV) to detect the presence of hexagonal pyrrhotite. Polished sections of these specimens were studied microscopically and the magnetic colloid method as described by Scott (Scott S.D. 1974 Sulfide Mineralogy: Short course notes) was used to identify hexagonal pyrrhotite. Sphalerite grains in direct contact with hexagonal and monoclinic pyrrhotite (usually intimately intergrown) and with pyrite were analysed by microprobe (See Appendix III). The overall sphalerite and pyrrhotite mineralogy is described in Sections 2, 3.3., and Appendix I.

The pyrite-pyrrhotite-sphalerite assemblage appear to be in equilibrium because of intimate intergrowth of sulphides and uniform unzoned sphalerite grains, usually with a variation of $<0.1\%$ Fe within grains.

The results, together with the overall mol.% FeS content of sphalerite compositions are shown on the histograms in Figure 3. The narrow distribution of the mol.% FeS of sphalerite in the limiting assemblage in the K6 and K3 areas

($\bar{X}$ = 13.79 s=0.61 and $\bar{X}$ = 12.86 s= 0.17) contrasts markedly with the broad distribution of the overall mol.% FeS (standard deviations for the K6, K1, K3 areas being 1.08; 1.82; 1.63 respectively).
These results are plotted on the working curve (Fig. 4) established by Hutcheon (op cit), using temperatures given by the garnet-biotite geothermometer. Because of the absence of pyrrhotite in the K1 area, the sphalerite geobarometer was not employed there. It is of interest that if the mean Mol.% FeS in the K1 sphalerites is used, the pressure is approximately equal to the K3 area (this agrees with the silicate indicators) but the range is too large to enable a confident pressure prediction (the range is from 3 to 8.5 Kbars).

3.1.5. Results

Although the garnet-biotite and garnet-cordierite methods disagree by only 50°C in the K1 area, the garnet-biotite geothermometer results are quoted because:

(i) The garnet-biotite pairs are in all three areas in sufficient abundance to allow perfect pairs to be selected; whereas garnet-cordierite pairs are rare and only found in the K1 area.
(ii) There was no zoning in either mineral, this with the petrographic observation suggests an equilibrium assemblage; whereas zoned cordierite introduces uncertainty as to the equilibrium and retrograde effects.
(iii) The results agree with the metamorphic mineral assemblage for the given temperatures and pressures (Winkler 1974).
(iv) Water in the cordierite lattice has an unknown effect on the analyses.

The results are:

AREA K3	AREA K1	AREA K6
682 - 708°C	656 - 716°C	560 - 620°C
(mean 695°C)	(mean 686°C)	(mean 590°C)
5.9 - 6.1 Kbars	5.8 Kbars	4.9 - 6.4 Kbars
(mean 6.0 Kbars)	(maximum)	(mean 5.6 Kbars)

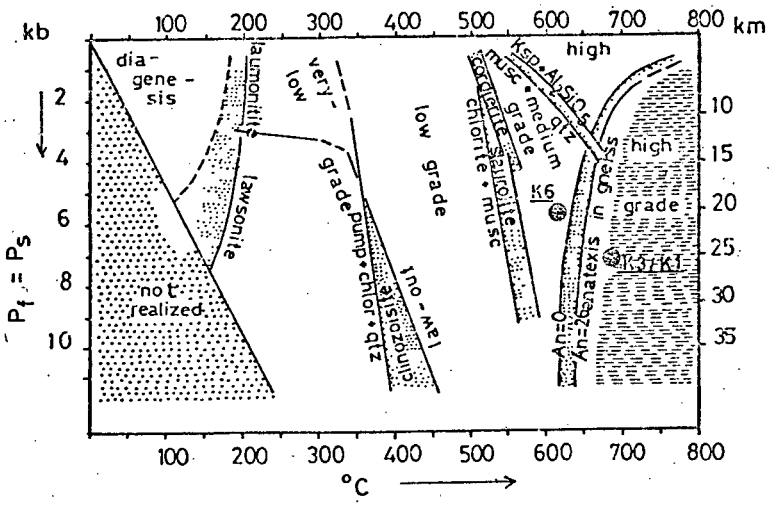

Fig. 10; The four divisions of metamorphic grade: very-low, low, medium, and high grade. Pressure condition for the graphically shown P,T data is that $P_S \approx P_{H_2O}$, showing positions of the Kielder assemblages. (After Winkler, 1976.)

3.2. Metamorphic Petrology

3.2.1. Metamorphic Mineral Assemblages

The mineral assemblages and metamorphic textures (described in detail in Appendix I) of all three areas of mineralization are consistent with the results of the geothermometry and geobarometry and place the grade of metamorphism unequivocally in the Regional Hypersthene or Granolite* High grade zone as defined by Winkler (1974). These assemblages and P-T conditions agree also with the observations of other workers (Ghent et.al 1979, Selverstone 1980 and Mehnert 1972).

The conditions of pressure and temperature of the three areas are plotted on Fig.10. An assumption is made that the load pressure is greater than the water pressure and the anhydrous minerals were formed under medium to high pressures (~6 Kbars). However, as is found in most other granulite terrains the parageneses are complicated by hornblende and biotite in the more "amphibolitic" rocks (Turner, 1968, De Waard 1967, Dougan 1974). The slight decrease in P-T conditions revealed by geothermometry/barometry from east (K3) to west (K6) is reflected in the mineral assemblages.

(i) Abundant hypersthene in the K3 area; rare hypersthene with occasional cummingtonite in the K6 area (the retrogression of hypersthene to cummingtonite; also noted by Himmelberg and Phinney 1967).

(ii) The K6 almandine-garnet has a higher spessartine component than elsewhere.

(iii) The presence of sphene in the K6 area.

The diagnostic granulite minerals with the pertinent characteristics are listed below. These can be seen to match the mineralogical features listed by Winkler (1974, p. 256) in the definition of the Granolite high grade zone.

(i) Alkali feldspar - is typically perthitic with a high percentage of the albite component, plagioclase lamellae making up 40-45% of the mineral.

* The term granulite is used here in preference, because of its more universal usage.

(ii) plagioclase - which is usually andesine and labradorite (occasionally oligoclase) also exhibits exsolution phenomena. However, the lamellae form only 5-10% of the mineral. The more Ca-rich plagioclase is found in the more basic rocks (i.e. amphibolites), indicating that the plagioclase composition is controlled largely by the bulk chemistry of the lithology rather than by P-T conditions.

(iii) orthopyroxene - is nearly always hypersthene, strongly pleochroic with Al_2O_3 varying from 6-12%(See Appendix IV). Bronzite is occasionally intergrown with hypersthene (See Plate D Appendix I).

(iv) clinopyroxene - usually a pale green hedenbergitic variety (low in Fe^{3+}); the Al_2O_3 content, however, is not known.

(v) garnet - usually almandine with the pyrope and grossularite components varying inversely (MgO 1-6%, CaO 1-5%)(See Appendix III). The spessartine component was significantly higher in the K6 area, varying between 3 and 14% MnO (MnO in K3/K1 area was 1-3%). The garnet grains were not significantly zoned, in contrast with Turner's (1968) observations.

(vi) hornblende - is usually green to olive-green and rarely brown. Green hornblende from the K6 area (specimen RKG 298, See Appendix III) proved to be iron-rich. Heinrich (1965) observes that green hornblende is characterized by high SiO_2, low Al_2O_3, Na_2O, K_2O and TiO_2. According to Winkler, however, granulite grade hornblende usually has higher TiO_2, and therefore would be a brown colour.

(vii) biotite - usually rich in Mg and Ti (MgO 8-16% and TiO 1-5% See Appendix III) varies in colour from green to brown. The colour is not characteristic of metamorphic grade and often biotite of different colours occur in the same rock (See Plate AH, Appendix I). The biotite also appears to be of two generations; the first as intergrowths with hypersthene (See Plates A and C, Appendix 1) and the second as skeletal intergrowths with quartz and feldspar.

(viii) Al_2SiO_5 polymorph - is almost invariably sillimanite; however, in one thin section (RKG 53) a single grain of andalusite was observed (confirmed by microprobe analysis).

In addition, hercynite, which is commonly found in metamorphic argillaceous sediments, somewhat richer in iron than those yielding pleonaste (Deer et.al 1966), is a common accessory in most of the Kielder wall rocks. The occurrence of hercynite with iron-rich cordierite (See Plate AJ, Appendix I) is common and is a probable metamorphic product of chlorite rich rocks (at 675°C and 7 Kbars chloritoid breaks down to form iron-rich cordierite + hercynite + vapour, Winkler 1974). Hercynite and magnetite solid solution intergrowths are ubiquitous. Cordierite, a common mineral in the wall rocks of all three mineralized zones, also occurs in the sulphide units and has been shown to be highly magnesian rich, but the cordierite in the wall rock is slightly more iron-rich. This is presumably due to it's recrystallizing with the iron-rich sulphides which have "captured" most of the iron.

A typical wall rock cordierite (150m below the sulphide zone) and a cordierite occurring within the sulphide zone are compared below:

Element	Wall Rock Cordierite (RKG 190)	Sulphide Zone Cordierite (RKG 211)	Scottish Hornfels Cordierite (Deer, Howie and Zussmann)
SiO_2	47.6	47.7	47.69
TiO_2	0.0	0.0	tr
Al_2O_3	33.4	33.1	32.52
FeO	6.4	0.70	8.50
MnO	0.17	0.30	0.04
MgO	8.96	13.57	7.56
CaO	0.0	0.0	0.52
Na_2O	0.14	0.86	0.53
K_2O	0.015	0.21	0.42
H_2O^+	n.d.	n.d.	1.85
TOTAL	96.82	96.44	99.63

The magnesian cordierite found in the sulphides (and their immediate wall rocks) are considered to be metamorphic products of the chlorite alteration zone, typically associated

with massive sulphide deposits of this nature; whereas the relatively iron-rich cordierite is typical of metamorphosed, argillaceous, iron-rich sediments.
The element partitioning between almandine and cordierite has been discussed at length in Section 3.1.2., where it was shown that pressure is a controlling factor in the cordierite-garnet paragenesis. The presence of garnet-cordierite pairs, found only in the K1 area, also reflect the higher MgO/FeO and lower CaO than in the K3 and K6. The garnet chemistry and overall mineralogy also supports this observation, i.e. the K1 pelitic rocks were magnesium rich and lower in calcium.
The tendency to more soda-rich amphiboles (edenite as found in K1 hanging wall and southern and northern granulites) is often found in granulite grade rocks (e.g. Marydale metabasites, Cornell, 1975). The reaction can be seen as follows:

$$NaAlSi_3O_8 + Ca_2(Mg,Fe)_5Si_8O_{22}(OH)_2 \rightleftharpoons NaCa_2(Mg,Fe)_5(Al,Si_7)O_{22}(OH)_2 + 4SiO_2$$

albite — actinolite — edenite — quartz

(after Cornell 1975)

Retrograde metamorphism has overprinted the assemblages, leading to the presence of more hydrous minerals such as hornblende and biotite. The replacement of optically uniform, coarse-grained diopside by hornblende, is common. (See Plates AQ, AR and AS, Appendix I). Although ilmenite and rutile are the common titanium-bearing accessory minerals, sphene, which is rarely found in granulite grade rocks (Turner 1968) has replaced ilmenite in some of the Kielder rocks (See Plate BQ, Appendix I). Zoning in the cordierite grains probably reflects retrograde temperatures of 530-560°C (See Section 3.1.2.). Consequently these retrograde overprints obscure many of the high grade assemblages with virtually ubiquitous hornblende and biotite.
The Kielder hornblendes, which have lower TiO_2 contents than generally reported (Heinrich 1965, Winkler 1974) for granulite grade rocks, also suggest a retrograde origin.

3.2.2. Parent Lithologies

Turner (1968) quotes some typical granulite grade assemblages and their probable parent lithologies; some of these are found at Kielder and are listed below:

Granulite Assemblage	Parent Lithology	Equivalent Kielder Unit
(i) quartz-perthite-plagioclase sillimanite ±(garnet)	aluminous sediment	K1-unit 8 K3-units 5 & 14 K6-unit 5
(ii) quartz-hypersthene-garnet-plagioclase ± (perthite)	sedimentary (arkose) or igneous rocks	K1-unit 3 K3-units 6,8 & 13 K6-unit 6
(iii) plagioclase-hypersthene diopside (quartz ± orthoclase)	noritic igneous rock	K3-unit 12 K6-unit 9

Assemblages quoted by Winkler, 1974, which have formed under granulite grade conditions are listed below:

Granulite Assemblage	Parent Lithology	Equivalent Kielder Unit
In all cases add (Quartz+K-feldspar+ plagioclase+magnetite)		
(i) almandine-cordierite biotite	pelitic rocks and greywacke	K1-units 2,6 & 10
(ii) almandine-biotite-hypersthene	pelitic rocks and greywacke	K3-units 6,15 K1-units 6,10 K6-units 2,6
(iii) cordierite-hypersthene biotite	pelitic rocks and greywacke	K3-units 2,9 K1-units 10,6 & 4

The major and trace element evidence for the igneous and sedimentary parentage of the amphibolite units and some of the granulites will be discussed under Section 4.2.1. Table I incorporates the geochemistry and the foregoing discussion on metamorphic mineral assemblages to give the original lithologies of each area.

3.2.3. Metamorphic Textures of the Wall Rocks

The textures observed in the petrographic study and described in Appendix I are generally very similar across the three areas. However, in the K6 area the presence of mortar texture was observed (See Plates AU and BB, Appendix I), usually accompanied by severely strained quartz grains.

TABLE I. SUGGESTED PARENTAGE OF THE KIELDER METAMORPHITES

AREA K3:

Unit No.	Name	Premetamorphic Lithology
1	Felsic pyritic Gneiss	Pyritic quartzite
2	Hypersthene-cordierite-pyritic granulite	Chlorite alteration zone with disseminated pyrite
3	Sillimanite-augen pyritic gneiss	Disseminated pyrite mineralization in aluminous quartzite
4	Banded biotite gneiss	Arkosic sediment
5 (14)	Felsic Sillimanite gneiss	Quartzite minor aluminous component
6	Hypersthene-quartz garnet granulite	Dacite or pelitic rock
7	Amphibolite	Tholeiitic basalt
8	Porphyroblastic-hypersthene-biotite granulite	Semi-pelitic sediment (supported by geochemical data)
9	Cordierite-hypersthene quartz granulite	Chlorite alteration zone (minor disseminated Py)
10	Quartz-cordierite-sillimanite granulite	Chlorite alteration zone with disseminated sulphide (Py)
11	Massive Sulphide and intercalated siliceous zones	Massive sulphide with chert lenses
12	Diopside plagioclase granulite	Noritic basic igneous rock
13	Banded hypersthene granulite	Pelitic greywacke
15	Banded biotite gneiss	Pelitic greywacke

AREA K1:

1	Banded biotite gneiss	Pelitic greywacke
2	Amphibole quartz granulite	Pelitic rock
3	Quartz-biotite gneiss	Arkosic quartzite (or possibly dacite)
4	Hypersthene cordierite biotite gneiss	Pelite
5	Quartz-plagioclase-garnet gneiss	Greywacke
6	Quartz-cordierite granulite	Chlorite alteration zone
7	Massive Sulphide	Massive sulphide mineralization in strongly chloritized rocks

TABLE I. SUGGESTED PARENTAGE OF THE KIELDER METAMORPHITES

AREA K1 CONTINUED:

Unit No.	Name	Premetamorphic Lithology
8	Felsic Sillimanite gneiss	Quartzite (arkosic) with aluminous component
9	Amphibolite	Tholeiitic basalt
10	Quartz-cordierite-garnet gneiss	Pelite

AREA K6:

1	Quartz-feldspar gneiss	Arkosic meta sediment
2	Biotite-garnet gniss	Greywacke
3	Banded iron formation	Banded iron formation
4	Amphibolite	Tholeiitic basalt
5	Felsic sillimanite gneiss	Arkosic quartzite with some chloritic alteration
6	Amphibole-hypersthene granulite	Pelitic greywacke or dacite
7	Massive sulphide	Massive sulphide
8	Felsic stringer sulphide zone	Cherty rock with disseminated sulphide pyrite and galena, chalcopyrite
9	Magnetite porphyritic amphibolite	Tholeiitic basalt
2	Biotite-garnet gneiss	Greywacke

The broken crystals are often accompanied by chemical degradation to biotite. Examples of shattered garnet are observed in the K6 area (See Plates AV and BE, Appendix I) only. Harker (1939) explained the presence of shattered garnet as a product of revived stress after the mineral had lost its power of rejuvenation because of lowered temperature.

The presence of fine myrmekitic intergrowths of quartz and feldspar is common in the more acidic granulites. Numerous pegmatitic lenses and veins are characteristic of the felsic sillimanite gneiss unit, the contacts are gradational, and in places the felsic gneiss and pegmatite are difficult to distinguish. The partial melting of the more acidic rocks is to be expected at these P-T conditions (Barth, 1962; Chappel and White, 1977; Fershatter, 1977). The aligned platy and acicular minerals, ribbon like grains of quartz, and twinning in the hypersthene (See Plate H, Appendix I) indicate that most of the metamorphic minerals crystallised during a period of deformational stress. However, some stress was present after the main prograde metamorphic event. The weakly foliated amphibolites (retrograde products) and strained quartz grains illustrate this.

3.2.4. Isochemical Metamorphism

Considering the emphasis placed upon trace and major element interpretation to determine the genesis and parentage of these granulites and amphibolites in the following section (See Section 4.2.), it is important to consider the question of isochemical metamorphism. The process of metamorphism forming granulite grade assemblages is essentially one of almost complete dehydration. The presence of hornblende (and biotite) is explained either by water trapped in the system (i.e. isochemical metamorphism) or by retrograde conditions subsequent to the P-T conditions necessary for granulites. From the previous discussion of the chemistry and petrography of the hornblende and other minerals, it is apparent that a lower grade overprint exists on these rocks. Isochemical metamorphism cannot therefore be assumed, although certain elements (See Section 4.2.) may have remained immobile notwithstanding the movement of water, and the more mobile

elements.

3.3. Effects of Metamorphism

3.3.1. Massive Sulphides

The slight metamorphic gradient is not sufficient to account for all the different features of the three sulphide bodies and most are primary characteristics. However some, in particular, sulphide grain sizes and the iron content of sphalerite are due to different P-T conditions.

The behaviour of massive sulphides under metamorphic conditions has been studied extensively (Stanton, 1959; Gilmour, 1965; McDonald, 1967; Vokes, 1971; Sangster, 1972; Mikkola and Vaisanen, 1972; Rockingham and Hutchinson, 1980) and the Kielder bodies provide further excellent examples.

3.3.1.1. Mobilization

The Kielder sulphide horizons have remained essentially stratabound and support Vokes (1971) observations that mobilization of the sulphide elements involve distances of 1 - 3 meters, if any at all. In both cases, where mobilization appears to have occurred, it is difficult to prove that a primary halo was not present prior to metamorphism. In the K3 area disseminated iron sulphides form a halo 15m into the hanging wall granulites. The pyrite and pyrrhotite (Py/Po $\sim$0.10) reach a maximum of 10% (by volume) up to 2m from the ore zone and gradually decrease to 1-2% at 15m from the massive sulphide contact, with a Py/Po ratio of $\sim$2.0. The change in the Py/Po ratio possibly reflects the more mobile nature of the pyrrhotite. Fine chalcopyrite and sphalerite occur in the hanging wall up to 4cm from the massive sulphide contact.

In the K6 area galena occurs as veinlets and fine disseminations (See Plates BN, BON, Appendix I) in the felsic stringer zone (Unit 8, Appendix I). The silver content is not higher in the "mobilised" galena as was observed by Vokes (1971) for massive sulphides in general. Galena is rare in the other wall rocks and it seems probable

TABLE II. SPHALERITE COMPOSITIONS

	AREA K3 (n = 36)	AREA K1 (n = 37)	AREA K6 (n = 36)
Mean % Zn	$\bar{X}$ = 58.39% (S = 1.44)	$\bar{X}$ = 58.88% (S = 1.34)	$\bar{X}$ = 58.33% (S = 0.80)
Mean % Fe	$\bar{X}$ = 7.63% (S = 0.94)	$\bar{X}$ = 7.610% (S = 1.10)	$\bar{X}$ = 8.18% (S = 0.70)
Mean % S	$\bar{X}$ = 33.05% (S = 0.53)	$\bar{X}$ = 32.45% (S = 0.86)	$\bar{X}$ = 32.63% (S = 0.41)
Mean Mol.%FeS	$\bar{X}$ = 13.29% (S = 1.63)	$\bar{X}$ = 13.18% (S = 1.82)	$\bar{X}$ = 14.11% (S = 1.08)
Mol.% FeS in sphalerite with pyrite+monoclinic and hexagonal pyrrhotite	$\bar{X}$ = 12.86% (S = 0.17) (n = 9)	Assemblage not present	$\bar{X}$ = 13.79% (S = 0.61) (n = 16)
Mol.% FeS in sphalerite with pyrite+monoclinic pyrrhotite	$\bar{X}$ = 13.73% (S = 0.41) (n = 8)	Assemblage not present	Assemblage not present
Mol.% FeS in sphalerite with pyrite only	$\bar{X}$ = 13.11% (S = 2.87) (n = 10)	$\bar{X}$ = 12.13% (S = 2.05) (n = 18)	$\bar{X}$ = 15.81% (S = 0.37) (n = 4)
Mol.% FeS in sphalerite with pyrite+chalcopyrite ± minor pyrrhotite	$\bar{X}$ = 13.35% (S = 1.35) (n = 4)	$\bar{X}$ = 14.05% (S = 0.82) (n = 19)	$\bar{X}$ = 14.14% (S = 1.20) (n = 16)

that the felsic stringer zone contained galena prior to metamorphism. Consequently, the veins and disseminations were only mobilised centimetres rather than metres. The chalcopyrite which occurs with the galena has been affected similarly.

3.3.1.2. Mineralogical/Chemical Effects

An important chemical effect that metamorphism has had on the sulphide zones is the variation in the iron content of sphalerite (discussed fully under Section 3.1.4. Sphalerite Geobarometry).

The results of microprobe analyses of 109 sphalerite grains can be seen in Table II. The colour of the sphalerite in transmitted light is dependent upon the iron content and varies from a deep red-brown to pale "biscuity" yellow. However, because it is critical to the colour variation in thin section, thickness precludes any quantitative measurements. The sphalerite colour/iron content relationship has been researched extensively and in only one case (Roedder and Dwornick, 1968) was the relationship reported to behave unsystematically. In one thin section (RKG 99) two types of sphalerite occurred within 0.5mm of each other. A pale yellow sphalerite (4.56% Fe) was in contact with pyrite only, while a deep red sphalerite (8.47% Fe) was in contact with pyrite and monoclinic pyrrhotite. Unless the sphalerite recrystallizes in equilibrium with pyrite and hexagonal pyrrhotite (which buffers the iron) the sphalerite composition does not vary systematically with metamorphic pressure.

Flamelike lamellae of monoclinic pyrrhotite in a grain of hexagonal pyrrhotite is illustrated in Plate L (Appendix I). The reverse (i.e. hexagonal lamellae) is also seen. Because the monoclinic variety is not stable above 260°C and reverts upon cooling to the hexagonal variety, this texture formed during the cooling from higher temperatures. Pyrrhotite polymorph ratios have been used to reveal latent mineralogical zoning (Hutchinson, 1979) in the Tasmanian tin deposits. Using X-ray diffraction methods described by Graham (1969) and Arnold (1966) (See Appendix VI) a similar study was attempted on the Kielder bodies. No zoning (vertical or lateral) of the pyrrhotite polymorphs was observed in the K3 or K6 bodies. However, in the K6

area hexagonal pyrrhotite was more often present than in K3, where the hexagonal/monoclinic ratio appeared to vary randomly.

The desulphurization of pyrite to pyrrhotite, ($FeS_2 \rightarrow Fe_{1-x}S + S$) and magnetite under these P-T conditions is to be expected. The alteration of pyrite to magnetite was observed in the K3 area (See Plate K, Appendix I). However, because of an overprint of marcasite on pyrrhotite (See Plate BG, BL, Appendix I) the pyrite → pyrrhotite reaction could not be readily observed. It is not possible to distinguish between primary and secondary pyrrhotite and assuming that the metamorphic pressure gradient between K6 and K3 was not sufficient to produce significantly different Py/Po ratios, then it is suggested that the K3 area may have had considerable pyrrhotite prior to metamorphism. This will be discussed in Section 5.

Rutile occurs as discrete grains, occasionally with pyrrhotite, within the massive sulphides and the immediate wall rocks which contain ≥2% disseminated sulphide in the K3 and K6 areas. Rutile has been used as an indicator of sulphur fugacity (ilmenite + $\frac{1}{2}S_2$ = pyrrhotite + rutile + $\frac{1}{2}O_2$) and indirectly as an indicator of the width of the sulphide zones (Nesbitt and Kelly, 1980).

The presence of rutile has been detected ≤3m from the massive sulphides, although there is no correlation between the zone thickness and the rutile presence. However, the absence of rutile from K1, the least well developed mineralization, may be significant. The rutile-pyrrhotite zone in the Ducktown massive sulphides has also been reported to be discontinuous (Nesbitt and Kelly, 1980). It is also significant that the ilmenite rich footwall (magnetite-ilmenite porphyritic amphibolite Unit 9) of the K6 massive sulphides does not contain rutile but sphene, which occurs as halos around euhedral magnetite (not the ilmenite/magnetite grains). (See Appendix I). These observations suggest a low sulphur fugacity around the Kielder sulphide zones.

Gahnite, which is found as fine inclusions in sphalerite in the most zinc rich portions of the sulphide zones, is typical of metamorphosed zinc deposits (e.g. Broken Hill, N.S.W.) and has been ascribed as a reaction product of sphalerite and aluminous

silicates.
The presence of phlogopite in the sulphide zones and immediate wall rocks also suggest a reaction between gangue and sulphides during metamorphism. The generation of "new pyrite" (Sangster and Scott, 1976) has been noted in North American ores and in the Kielder sulphides two generations of pyrite have been observed (See Appendix I, Plate BK). In the Ducktown ores Kalliokoski (1965) noted euhedral pyrite in finer grained pyrrhotite and interpreted it as being porphyroblastic growth of pyrite at the expense of pyrrhotite.
Poikiloblastic grains of pyrite occur in the Kielder massive sulphides and enclose other sulphide minerals and gangue. A similar phenomenon was observed in the Geco ore (Suffel, et.al, 1971) and was taken as evidence for the premetamorphic presence of sulphide. An epigenetically introduced sulphide phase would not enclose both primary silicates and "later sulphides".
The sulphides (if massive) are totally oxidized to gossan down to depths of 90-100m as is the case in other massive sulphide bodies below the Bushmanland surface, namely Gamsberg (Rozendaal, 1980) and Copperton (Blain and Andrew 1977).
Partial oxidation is present between 100-150m below surface. Pyrrhotite is altering to marcasite (See Plate BL); sphalerite, pyrite and chalcopyrite to limonite; chalcopyrite has intergrown covellite, and the magnetite euhedra are altering to hematite (See Plate BA).
The process from fresh sulphide to gossan is not studied in detail here because of lack of specimens; the core drilling obviously avoided the zone of weathering. The process is unlikely to be different from that at Copperton which has been adequately dealt with by Blain and Andrew (1977).
Hydration of the silicate minerals has proceeded preferentially around the massive sulphides, presumably because of increased access of meteoric water by the more permeable sulphide/gossan zones. The minerals which are affected are hypersthene (to antigorite, Plate G, F), cordierite (to pinite), biotite (to chlorite) and plagioclase (to clay minerals).

TABLE III. COMPARISON OF THE PYRRHOTITE GRAIN SIZES

SULPHIDE DEPOSIT	METAMORPHIC GRADE	PYRRHOTITE GRAIN SIZE (MM)
Kidd Creek*	lower green-schist	$\bar{X}$ = 0.031 (S = 0.03) (n = 140)
Lake Dufault*	greenschist-amphibolite	$\bar{X}$ = 0.12 (S = 0.063) (n = 500)
Hood River*	lower amphibolite	$\bar{X}$ = 0.12 (S = 0.055) (n = 515)
Geco*	amphibolite	$\bar{X}$ = 0.53 (S = 0.265) (n = 505)
K6	granulite grade (590°C; 5.6 Kbars)	$\bar{X}$ = 0.84 (S = 0.34) (n = 15)
K3	granulite grade (695°C; 6.0 Kbars)	$\bar{X}$ = 1.05 (S = 0.55) (n = 121)

(* Data after Rockingham and Hutchinson (1980)).

3.3.1.3. Textural Effects

The study by Rockingham and Hutchinson (1980) of the textural features of metamorphosed sulphide deposits has provided excellent comparative data for this study. The sulphide grain sizes provided the most reliable textural/metamorphic grade relationship. The other textural features (grain intergrowths, grain boundaries) are not sensitive enough to reflect the P-T variation between K3, K1 and K6. Pyrrhotite, because of its anisotropic nature was the most useful mineral. The grain size was measured by point count analysis, with the largest dimension being measured of grains occurring in a monoclinic area of the thin section (in order to overcome crystalloblastic effects). The sample size therefore was not large (a total of 136 grains) due to the selective nature of the test. The concomitant increase in grain size with metamorphic grade is accompanied by an increase in the variation of grain sizes (See the standard deviation, see Table III).
The other minerals (pyrite, chalcopyrite and sphalerite) were not measured because of difficulty in standardising the etch effects. The grain size, nevertheless, is qualitatively observed to increase from K3 to K6.
At this grade of metamorphism the sulphide minerals have totally recrystallised and no relict primary textures were observed.
Triple junctions in polygonal masses of pyrrhotite were measured and found to be a very uniform 120^{o} (See Plate BM). This was found to be the case for all metamorphosed sulphide deposits of higher rank than greenschist facies (Rockingham and Hutchinson, 1980; Sangster and Scott, 1976).
The exsolution features and intergrowths between the major sulphide minerals are typical of high grade metamorphic facies. Chalcopyrite exsolution blebs in sphalerite are very common (See Appendix I); the exsolution is more marked in zones of higher overall copper content. This effect could also be observed on a microscopic scale where the sphalerite grain abutting chalcopyrite carries a heavier concentration of chalcopyrite (See Plate BG, Appendix I).

This effect has also been noted in the Normetal Mine, Quebec (Cabri et.al, 1974) and is classified as a type of latent zoning effect. This latent zoning is evident in K3 sulphide body but not in the K1 and K6. The chalcopyrite blebs are relatively coarse ($\leq$ 0.04mm), and as in other sulphide deposits of this metamorphic grade are rod like and in places continuous (illustrated in Plates S and BF).

Pyrrhotite exsolution blebs in sphalerite are relatively rare and tend to occur in grains of sphalerite free of chalcopyrite. Rockingham and Hutchinson, (1980), observe a tendency for the pyrrhotite to chalcopyrite (blebs in sphalerite) ratio to increase with metamorphic rank. They postulate that this may be due to more pyrrhotite being available in higher metamorphosed sulphides and, conversely, the minor pyrrhotite blebs in lower grade sphalerites represent primary interstitial pyrrhotite. The three Kielder bodies, all higher rank than those studied by the above authors, contain very few sphalerite grains with pyrrhotite exsolution blebs. The Kielder sphalerites therefore refute the above authors' claim that the Cpy/Po bleb ratio reflects the metamorphic grade. However, it is interesting to note that pyrrhotite blebs occurring in sphalerite occur only in the K3 area, which supports the earlier speculation that the K3 had pre-metamorphic pyrrhotite (See Section 3.3.1.2.)

The distribution and grain shape of chalcopyrite (and pyrrhotite) blebs in sphalerite are controlled by twin planes and grain boundaries (See Plates S, BF, Appendix I) within the host sphalerite.

Other sulphide mineral intergrowths are not as common, although sphalerite in pyrite (Plate N) chalcopyrite in pyrite (Plate BH) are found.

The alteration of pyrite and pyrrhotite to marcasite occurs in the ores closer to surface. The subsequent increase in density causes a pitted surface (Stanton, 1972); the resulting cellular marcasite grains preserve the polygonal grain shape (120^{o}) of the parental pyrrhotite (See Plate BL).

Etching of the polished thin sections reveals strongly twinned sphalerite and galena, again typical of strained sulphide bodies (Ramdohr, 1969).

The apparent order of crystallisation of the chalcopyrite-pyrite-sphalerite varies according to the relative abundances. Where sphalerite forms a minor phase it occurs between the euhedral pyrite and chalcopyrite (See Plates BG, BH and AM). Whereas where chalcopyrite is a minor component it occurs as an intergranular phase between pyrite and sphalerite (See Plates O and Q). This effect has been noted by Stanton (1972) who ascribes it to different interfacial free energy ratios altering the idiomorphism of a particular mineral. This effect neccesitates a great deal of caution when attempting to unravel a paragenetic sequence within a metamorphosed massive sulphide section.

The mineral zoning seen in the sulphide zones cannot be taken (when primary textures have been destroyed) as a simple paragenetic sequence (Large, 1977) as there is overlap in the precipitation of the different layers. Certainly at this grade of metamorphism speculation regarding parageneses on micro-and mesoscopic scales is questionable.

The magnetite-ilmenite exsolution relationship in the footwall of K6 (See Plate BP) is considered by Ramdohr (1969) to be a fairly common high temperature phenomenon.

The durchbewegt "kneaded" texture described by Vokes (1969) and seen elsewhere in metamorphosed sulphide deposits (Geco Mine, Suffel et.al, 1971) is common in the Kielder sulphide deposits. These "balled up" silicate-rich patches are enclosed in coarse grained granoblastic sulphides and tend to have irregular corroded rims (See Plate AL, Appendix I). These silicate balls in the massive sulphide are typically 1-5mm across and generally rounded in shape; usually consist of chlorite (giving a green speckled colour to the ore) or earthy hematite (a red speckled appearance). Larger fragments described by Suffel et.al, 1971, were not seen on Kielder, possibly due to insufficient exposure and drilling. Vokes interprets this texture as being formed by deformation of previously stratiform ores in which the more plastic sulphide acted as a lubricant.

The fragmental sulphide described from numerous other deposits (Heath Steele, New Brunswick; Oswiacki and McAllister, 1979;

Kuroko deposits, Japan, Ito et.al, 1974) and ascribed to primary slumping of unconsolidated sulphide sediment is unlikely to have been preserved here and no textures of this description have been noted.
The effects of deformation on the macroscopic form of the sulphide zones cannot be accurately judged due to insufficient drilling. In the Copperton ore body, rapid pinch and swell of the ore zone is very common (pers. comm. Copperton mine geologists), although the ore remains within one stratigraphic horizon. It is assumed that the Kielder ore bodies are similarly affected(as described by Sangster and Scott, 1976, p. 190).

3.3.2. Banded Iron Formation

In the banded iron formation units of Broken Hill (N.S.W.), the garnet compositions remain remarkably consistent within individual fine (1 - 2mm) beds, but change significantly across the bedding over distances of 5 - 15mm (Stanton and Williams, 1978). These authors postulate that the variations are not a result of metamorphic redistribution of elements because of the strong bedding control. The original chemical compositions of the individual bands have been preserved, notwithstanding that upper amphibolite facies conditions were attained at Broken Hill.
A similar phenomenom has been observed in the K6 banded iron formation. The garnet grains analysed (Table IV) were of a uniform size (0.15mm), were not zoned and had circular clusters of opaque inclusions in their centres (See Plates AW, AX and BAZ).

TABLE IV. GARNET COMPOSITIONS IN B.I.F. (PT/S No.RKG 240 PLATES AW, AX)

	LAYER 1				LAYER 2			
	Grain 1	2	3	4	1	2	3	4
SiO_2	36.27	36.28	36.22	36.35	36.38	36.52	36.26	36.44
Al_2O_3	19.31	19.09	19.19	19.62	19.29	20.07	19.18	20.12
FeO	15.34	15.51	15.68	15.44	15.29	14.63	14.97	15.05
MnO	21.51	21.96	21.63	21.72	21.65	21.50	21.83	22.12
MgO	1.34	1.57	1.50	1.21	1.59	1.43	1.55	1.40
CaO	5.41	4.65	5.19	5.36	5.29	5.44	5.48	4.87
TOTAL	99.22	99.21	99.59	99.72	99.55	99.63	99.55	100.02

TABLE IV. GARNET COMPOSITIONS IN B.I.F. (PT/S No.RKG 240 (CONT.) PLATES AW, AX)

	LAYER 3				LAYER 4			
	Grain 1	2	3	4	1	2	3	
SiO_2	36.74	36.85	36.67	36.95	36.69	36.87	36.72	
Al_2O_3	19.41	18.55	18.92	18.85	19.26	19.91	19.78	
FeO	11.49	13.12	12.07	11.97	15.68	15.17	15.52	
MnO	22.64	21.32	22.27	22.19	21.74	21.92	21.80	
MgO	0.50	0.57	0.55	0.46	1.56	1.23	1.43	
CaO	9.01	9.56	9.47	9.84	3.63	5.73	5.69	
TOTAL	100.00	99.97	99.94	100.29	100.61	100.85	100.93	

The "inbed" variation is illustrated in Fig. 8B, and the across bed variation in garnet composition in Fig. 8A. The Ca and Fe show a greater variation than does the Mn and Mg, probably representing an original fine (1-2mm) bedding. Coarser bedding (0.5m) exists in the B.I.F. unit with quartz rich bands alternating with quartz poor rhodonite bearing bands (See Appendix I).

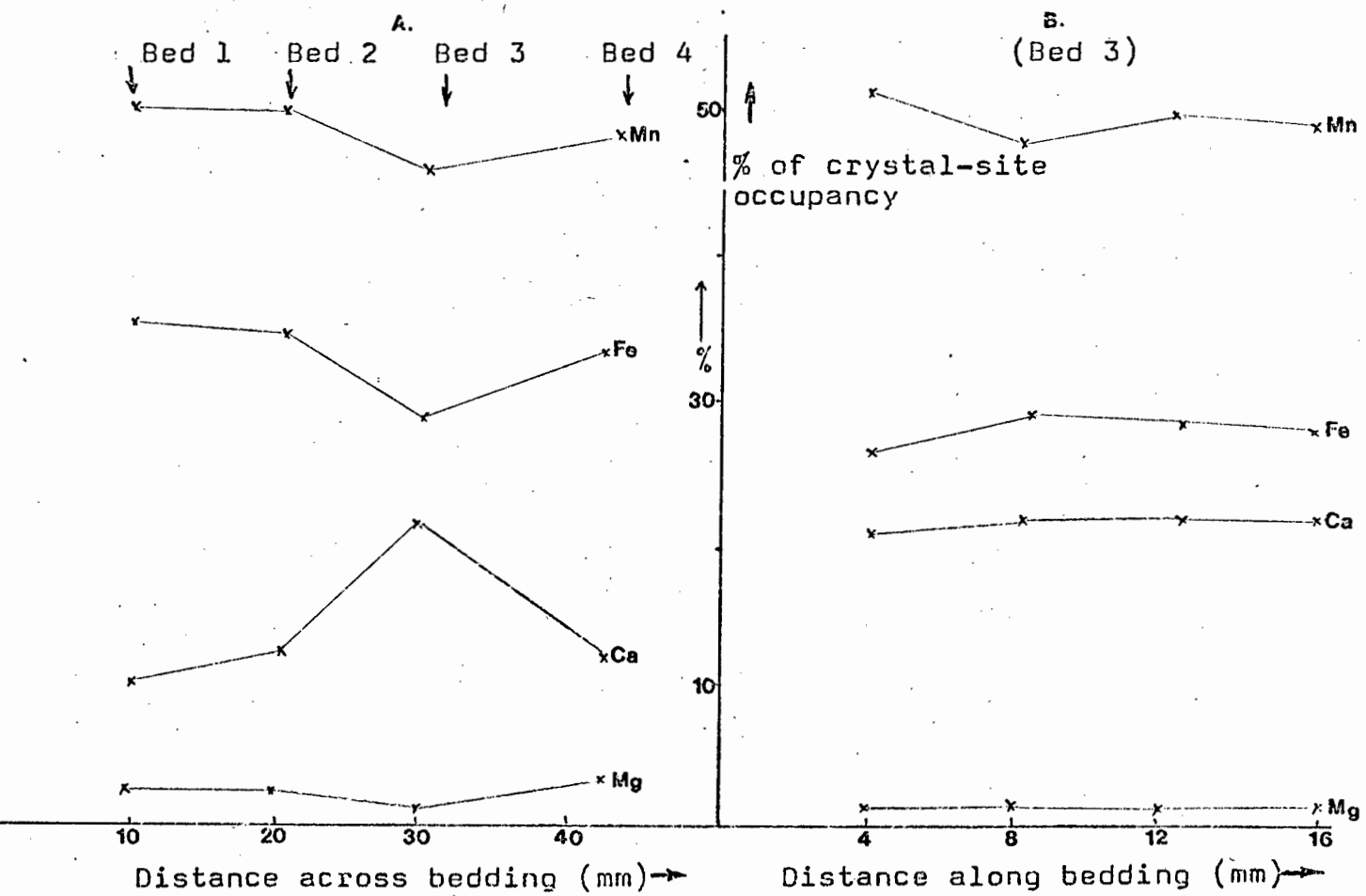

Fig. 11. Garnet analyses across and along bedding.

Within the B.I.F. units (See Plate AX) larger garnet grains (0.4-0.8mm) have a slightly different appearance in that they have no inclusion-packed centre and there is more size variation than for the smaller grains associated with the magnetite. These grains show a variation in composition (CaO 2.67→6.65%; MgO 2.12→3.97%; FeO 17.9→16.34% and Mn 17.45→17.32), although no zoning could be detected. These garnets were not used in the above study because they usually occur in different assemblages, including biotite, and Fe-Mg partitioning effects probably add a further variable. Although Stanton (1972, 1978) states that the "well known" zonal variation of garnet composition with respect to MnO and FeO is common in metamorphic rocks, this was found not to be in the case of Kielder gneisses or B.I.F. Yardley, 1977, established that garnets within metamorphic rocks which have suffered temperatures >700°C have undergone diffusion and any zoning has been obliterated. Retrogression may impart a "zoned" edge to the garnet. This confirms the geothermometry results (See Section 3.1.5.) (This would agree with Stumpfl's (1979) findings that at higher grades of metamorphism zoning in garnets is rare).

The sulphide minerals in the B.I.F. (See Appendix I) exhibit the same textures as in the major sulphide horizons.

The original iron-rich sediment probably consisted of quartz, iron-oxides, rhodocrosite, siderite, manganiferous septechlorite, other clay minerals, minnesotaite, calcite and sulphide (Fe,Cu, Zn) minerals. (cf., Stanton, 1976 at Broken Hill).

The present minerals have been produced from the following reactions; (after Klein 1973, Stanton, 1976)

$$\underset{\text{rhodocrosite}}{MnCO_3} + \underset{\text{quartz}}{SiO_2} \rightleftharpoons \underset{\text{rhodonite}}{MnSiO_3} + CO_2$$

The petrography supports this, with the inverse abundance relationship between rhodonite and quartz and when the former is present it is accompanied by calcite veins.

$$\underset{\text{minnesotaite}}{(Fe, Mg)_3 Si_4 O_{10}(OH)_2} = \underset{\text{actinolite}}{(Fe,Mg)_7Si_8O_{22}(OH)_2} + \underset{\text{quartz}}{4SiO_2} + 4H_2O$$

The amphibole contains significant amounts of MnO.

The garnet was derived in situ from impure manganiferous

chlorite of chamosite type and the biotite from glauconite. It would appear that the garnet composition in particular, and the overall mineral assemblage, have been influenced by the original fine banding in the parent rock and that diffusion of elements has taken place only over minute distances (<5mm).

It is unlikely that this conclusion could be applied to the other mineral assemblages considering the refractory nature of the B.I.F.

4. BULK ROCK GEOCHEMISTRY

4.1. Introduction

Major and trace element compositions of amphibolites and pyroxene granulites were obtained as a further attempt to identify parent lithologies and in the case of igneous varieties, to predict the premetamorphic tectonic setting. Furthermore, trace element geochemistry will be used to evaluate a possible correlation between pyroxene granulites associated and not associated, with mineralization.
Any successful interpretation using geochemistry depends on the degree of element mobility during metamorphism.
A consensus of opinion favours the immobility of certain elements, in particular Ti, Al, P, Mn, Y, Zr, Cr, Co, Ni, Nb, Mg and the rare-earth elements (Dostal and Capedri, 1979; Davies et.al., 1979; Brooks and Coles, 1980).
Past research (Orville, 1969; Armbrustmacher, 1977; Beach and Tarney, 1978) and the present work (See Section 3) suggest that isochemical metamorphism, per se, is seldom attained, particularly at granulite grade conditions.
In addition hydration of granulites during retrograde metamorphism may compound the problem of chemical mobility (Beach, 1974; Plimer, 1975 and Condie et al., 1977).
Concerning this important issue of the chemical mobility, techniques devised by Beswick and Soucie (1978) and Davies et al. (1979) have been evaluated. These authors have used a series of cartesian plots of immobile/mobile element ratios to demonstrate the behaviour of various (both major and trace) elements in a particular rock assemblage which has undergone metamorphism. For example, a plot of Al_2O_3/K_2O versus SiO_2/K_2O for a series of samples from a single amphibolite body should produce a straight line passing through the origin, assuming:

(i) that primary variation is small (i.e. the body is strongly differentiated) and the specimens were from the same parent magma.

(ii) the wide variation in a mobile element (in this case K) used in the ratios is due to metasomatic redistribution, and

(iii) the alternative that supposedly immobile elements were modified by metasomatism in a highly systematic manner is unlikely.

Successful identification of precursors to ortho- and para-amphibolites and basic granulites by comparison of various compositional trends with those displayed by igneous and sedimentary rocks has been claimed by numerous authors (e.g. Van de Kamp, 1969; Geringer, 1979; and Stephenson, 1980) using the techniques of Leake (1964).
Following the identification of basic orthogneisses using the Leake diagrams, these rocks were subsequently evaluated using discriminant diagrams of Pearce and Cann (1973), and others in order to predict the tectonic setting of their igneous precursors. Jensen (1976) used the A(Na_2O + K_2O)-F(Total Fe as Feo)-M(Mgo) plot to distinguish magma types; Winchester and Floyd (1976) used immobile elements (Ti, P, Y, Zr and Nb) to distinguish magma types.
Pearce and Cann (1973) established a set of criteria based on Ti, Zr and Y using $\sim$200 basaltic rocks from known tectonic settings; this method has produced inconsistent results (Cornell, 1975 and Stephenson, 1980) in other areas. Davies et al. (1979) point out the advantages of using a (Zr+Y)-Ti-Cr ternary diagram to classify Archean magma types and plot volcanic rocks from the Yilgarn block, W. Australia, and the Timmins Area, Ontario to develop distinguishing criteria. Pearce, Gorman and Birkett (1977) produced a discriminatory diagram using Fe, Mg and Al contents in 8400 samples of basic and intermediate volcanic rocks from different tectonic settings. They used rocks with 51-56% SiO_2 (recalculated anhydrous) and found that increasing this parameter did not significantly alter the fields. This range of chemical compositions effectively includes all the Kielder ortho-amphibolites with their SiO_2 content (recalculated anhydrous) ranging from 47.9 to 55.3%.
Finally, lithostratigraphic correlations between the southern granulites, northern granulites and those granulites which occur as the immediate wall rocks to the mineralization, are attempted in a similar way to Davies, Grant and Whitehead, 1978.

4.2. Results and Interpretation

Bulk chemical and modal compositions of ten amphibolites and ten pyroxene granulites are contained in Table V. Four analyses of amphibolite from the Copperton mine reported by Geringer (1979) have also been included. Analytical methods are described in Appendix II, together with the calculations used to determine the Niggli Values.

4.2.1. Identification of Immobile Elements

Data for five amphibolite (Unit 9) specimens from K1 were used for the immobile/mobile element diagrams and to calculate correlation coefficients between the various ratios. Inspection of Fig. 12 reveals a good correlation (r= 0.9505) between TiO_2/K_2O and Al_2O_3/K_2O. This relationship is interpreted as showing TiO_2/Al_2O_3 to be constant, with the variation in K_2O being ascribed to metamorphic mobility. A constant TiO_2/Al_2O_3 is furthermore taken to indicate these elements were not affected by metamorphism.
Other plots, not included to save space, have shown that Mn, Y, Fe, Si, Zr, Cr, Ni, P, Co, Nb are relatively immobile, and the appropriate correlation coefficients are listed below. The results agree with the elements regarded as immobile by most recent researchers (e.g. Gray, 1977; Elliot and Harvey, 1980 and Stephenson, 1980).

Ratios	Correlation Coefficient (r)
TiO_2/K_2O vs Al_2O_3/K_2O	.9505
TiO_2/K_2O vs SiO_2/K_2O	.9405
Al_2O_3/K_2O vs SiO_2/K_2O	.9988
MnO/K_2O vs SiO_2/K_2O	.9884
Y/K_2O vs Al_2O_3/K_2O	.7863
Zr/K_2O vs Al_2O_3/K_2O	.8255
Cr/K_2O vs Al_2O_3/K_2O	.3518
Ni/K_2O vs Al_2O_3/K_2O	.6181
MgO/K_2O vs Al_2O_3/K_2O	.9150
Co/K_2O vs Al_2O_3/K_2O	.9780

TABLE V : CHEMICAL ANALYSES - WHOLE ROCK AMPHIBOLITES AND PYROXENE GRANULITES

LOCALITY	K1 AREA							
ROCK TYPE	UNIT 9	UNIT 9	UNIT 9	UNIT 9	UNIT 9	UNIT 2	UNIT 2	UNIT 2
Sample No. / Elements %	RKG 185	RKG 185	RKG 198	RKG 200	RKG 204	RKG 330	RKG 206	RKG 192
SiO_2	47.35	47.28	54.32	46.61	48.61	59.53	53.67	45.68
TiO_2	0.88	1.29	0.83	0.68	1.25	0.35	0.58	0.62
Al_2O_3	14.67	14.45	13.88	13.56	13.06	12.41	14.75	15.69
Fe_2O_3	12.12	14.09	11.77	10.92	13.69	6.75	10.97	13.61
MnO	0.20	0.23	0.20	0.17	0.22	0.22	0.20	0.27
MgO	9.61	7.56	7.31	11.88	8.07	3.66	7.12	8.04
CaO	12.90	12.60	8.06	12.27	9.97	15.59	9.66	11.58
Na_2O	1.52	2.10	1.79	1.26	2.05	0.54	2.65	1.83
K_2O	0.27	0.24	1.03	0.48	0.43	0.33	0.65	1.13
P_2O_5	0.07	0.12	0.09	0.05	0.10	0.10	0.13	0.13
L.O.I.	0.82	0.44	1.04	1.48	0.92	0.54	0.45	1.65
H_2O^-	0.05	0.06	0.08	0.08	0.10	0.13	0.06	0.11
TOTAL	100.44	100.45	100.40	99.45	99.35	100.16	100.90	100.25
NIGGLI VALUES								
al	18.07	18.36	20.85	16.34	16.79	20.57	21.11	26.03
fm	40.56	47.75	51.00	53.59	51.62	30.27	46.44	63.46
c	28.93	29.17	22.05	26.94	24.43	47.10	25.19	3.50
alk	3.44	4.71	6.09	3.13	5.16	2.07	7.25	7.01
mg	0.61	0.51	0.55	0.66	0.53	0.51	0.56	0.54
k	0.11	0.07	0.28	0.20	0.12	0.29	0.14	0.29
al-alk	14.63	13.65	14.76	13.21	13.63	18.50	13.86	19.02
100 Fe/Fe+Mg	59.39	68.38	65.11	51.60	66.78	68.11	64.11	66.25
TRACE ELEMENTS (PPM)								
Co	60	54	43	65	54	19	32	52
Cr	314	85	91	516	146	13	170	51
V	275	381	254	222	357	135	230	354
Cu	32	140	68	80	62	3	69	29
Ni	121	65	44	188	68	14	67	57
Zn	88	86	120	62	205	52	95	139
Y	16	25	23	13	34	33	24	14
Zr	30	49	50	28	57	85	67	22
Pb	2	2	10	6	12	6	7	12
U	1	<1	<1	<1	1	2	2	1
Th	<1	1	2	<1	2	8	4	2
Nb	<1	2	1	<1	2	4	3	1
Sr	145	156	165	138	166	148	318	183
Rb	9	6	56	13	12	8	19	18
Mo	1	2	1	2	1	2	1	1
	MODAL ANALYSES							
Quartz		1.8	14.9		23.2	40.3	30.2	
Plagioclase labradorite bytownite andesine	40.2	35.2	33.7	34.9	19.7	17.7	23.1	40.1
K-feldspar + perthite								
Amphibole hornblende	44.8		48.3	65.1	49.8	24.1 4.0	44.8	39.8
Biotite Green				tr				
Biotite Brown								5.0
Cordierite						9.9		
Carbonate								
Diopside	13.8	19.7			5.3			15.2
Garnet								
Hypersthene								
Sphene						3.1	tr	
Magnetite			1.1		1.9			
Ilmenite								
Apatite							1.9	tr
Pyrite	1.2	tr	2.1		tr	0.9	1.1	
Hercynite								
Lazulite								

TABLE V : CHEMICAL ANALYSES - 'MIGLI ROCK AMPHIBOLITES AND PYROXENE GRANULITES (Cont.)

LOCALITY	K5 AREA				K6 AREA		
ROCK TYPE:	UNIT 6	UNIT 7	UNIT 8	UNIT 12	UNIT 4	UNIT 4	UNIT 9
Sample No. / Elements	RKG 71	RKG 117	RKG 82	RKG [illegible]	RKG 212	RKG 204	RKG 254
SiO_2	66.88	49.88	66.09	46.61	51.16	47.99	50.13
TiO_2	0.53	0.32	0.65	0.41	0.97	1.16	1.70
Al_2O_3	12.75	13.66	12.29	18.57	14.20	14.48	13.41
Fe_2O_3	9.04	11.56	10.37	12.14	13.43	13.29	17.64
MnO	0.23	0.27	0.26	0.20	0.21	0.21	0.27
MgO	6.14	10.69	8.54	5.55	7.05	9.16	6.24
CaO	0.97	11.36	0.44	12.89	9.96	10.54	8.59
Na_2O	1.74	1.94	0.30	2.21	2.09	2.28	1.20
K_2O	1.69	0.16	1.02	0.51	0.35	0.62	0.91
P_2O_5	0.07	0.08	0.13	0.10	0.08	0.08	0.16
L.O.I.	0.75	0.15	0.95	0.93	0.77	1.30	0.85
H_2O-	0.09	0.10	0.05	0.08	0.05	0.10	0.15
TOTAL	100.89	100.15	101.07	100.21	100.32	101.22	101.25
NIGGLI VALUES							
al	27.30	17.06	24.55	24.38	19.84	18.39	18.63
fm	58.92	52.92	70.66	39.28	49.48	51.58	54.99
c	3.78	25.83	1.61	30.83	25.35	24.41	22.17
alk	10.01	4.18	3.17	5.50	5.33	5.62	4.20
mg	0.57	0.64	0.62	0.47	0.51	0.58	0.41
k	0.39	0.05	0.69	0.13	0.10	0.15	0.33
al-alk	17.30	12.88	21.38	18.88	14.51	13.27	14.43
100 Fe/Fe+Mg	63.06	55.64	58.50	71.73	68.71	62.72	76.64
TRACE ELEMENTS (PPM)							
Co	14	50	14	51	53	62	53
Cr	4	655	0	40	55	228	87
V	31	236	30	217	318	317	489
Cu	17	5	12	72	116	141	49
Ni	5	116	5	30	50	101	42
Zn	150	84	245	85	103	82	142
Y	22	8	18	10	27	22	39
Zr	54	10	45	13	50	48	79
Pb	5	2	1	8	6	4	4
U	<1	<1	<1	<1	<1	1	2
Th	4	2	2	2	2	1	2
Nb	3	1	2	<1	3	1	2
Sr	85	186	15	354	187	195	236
Rb	36	2	42	15	9	19	27
Mo	<1	1	<1	1	2	2	2
	MODAL ANALYSES						
Quartz	23.5		26.2		4.8		5.2
Plagioclase							
labradorite		25.2					31.0
bytownite					44.0		
Andesine	20.5		27.1	39.2		49.5	
K-feldspar + perthite	2.7						
Amphibole					51.5	49.5	59.5
hornblende		36.2		16.1			
Biotite Green							
Biotite Brown	19.8		11.1				8.5
Cordierite							
Carbonate							
Diopside		14.9		40.8			
Garnet	7.2						
Hypersthene	24.2	24.1	29.8				
Sphene							
Magnetite	1.9	tr	2.2		tr		4.8
Ilmenite							
Apatite							
Pyrite			4.0	3.9		2.2	1.0
Hercynite	1.2		tr				
Lazulite	tr						

TABLE V : CHEMICAL ANALYSES - WHOLE ROCK AMPHIBOLITES AND PYROXENE GRANULITES (Cont.)

LOCALITY	SOUTHERN GRANULITES			NORTHERN GRANULITES		COPPERTON*			
Sample No. / Elements %	PKG 319	PKG 321	PKG 323	PKG 324	PKG 327	G 79	G 90	G 94	G 96
SiO_2	42.52	68.59	70.26	44.38	47.38	63.63	47.30	52.94	54.55
TiO_2	0.58	0.40	0.43	0.54	0.52	0.53	0.97	1.50	1.50
Al_2O_3	25.31	12.01	13.47	16.74	16.26	14.86	15.65	13.71	13.84
Fe_2O_3	8.28	4.82	4.00	11.67	9.05	7.46	13.18	14.76	17.02
MnO	0.22	0.40	0.09	0.35	0.30	0.11	0.23	0.22	0.27
MgO	1.42	1.08	1.05	3.51	3.74	2.95	7.63	3.95	4.01
CaO	21.39	10.73	5.62	22.39	22.23	3.83	8.77	6.06	6.84
Na_2O	0.40	0.62	2.54	0.37	0.50	2.85	2.12	3.60	2.75
K_2O	0.05	0.38	3.03	0.14	0.20	2.01	0.93	0.46	0.63
P_2O_5	0.18	0.17	0.14	0.12	0.20	0.14	0.09	0.39	0.34
L.O.I.	0.58	1.04	0.45	0.15	0.58	1.85	2.27	1.22	0.70
H_2O-	0.13	0.11	0.11	0.82	0.12	0.56	0.60	0.47	0.29
TOTAL	101.05	100.34	100.60	100.43	101.06	100.04	98.78	98.28	102.55
NIGGLI VALUES									
al	31.85	28.28	35.47	20.26	20.51	32.40	21.60	22.70	21.0
fm	18.24	22.33	20.82	29.45	27.11	37.40	50.3	48.30	52.3
c	49.02	46.01	24.05	49.37	51.06	15.2	22.0	18.3	18.8
alk	0.89	3.38	19.66	0.73	1.32	15.0	6.2	10.6	7.9
mg	0.25	0.29	0.34	0.37	0.44	0.40	0.6	0.4	0.5
k	0.08	0.29	0.44	0.20	0.21	0.30	0.2	0.1	0.1
al-alk	30.96	24.90	15.81	19.53	19.19	17.4	15.4	12.1	13.1
100 Fe/Fe + Mg	87.14	83.77	43.85	79.42	73.74	—	—	—	—
TRACE ELEMENTS (PPM)									
Co	15	10	10	34	24	27	39	36	43
Cr	4	5	5	29	115	14	35	11	43
V	64	44	50	241	169	76	93	184	137
Cu	3	20	6	4	87	ND	ND	ND	ND
Ni	2	4	4	8	200	18	65	17	72
Zn	93	59	52	74	69	ND	ND	ND	ND
Y	35	27	30	11	17	34	25	32	32
Zr	125	73	164	12	34	113	39	59	55
Pb	14	6	23	7	6	ND	ND	ND	ND
U	<1	<1	<1	<1	3	ND	ND	ND	ND
Th	8	5	15	4	2	ND	ND	ND	ND
Nb	7	5	<1	3	<1	1	ND	ND	ND
Sr	402	296	354	318	348	236	169	227	229
Rb	<1	15	15	18	9	58	38	-	5
Mo	3	3	1	1					
	MODAL ANALYSES								
Quartz		34.3	54.6	tr	6.5	10-20	10-20	-	<5
Plagioclase labradorite	59.6	25.7		35.3	35.2				
bytownite andesine			19.9			20-50	10-20	20-50	20-50
K-feldspar + perthite									
Amphibole hornblende	9.9	5.2	9.8		35.0	20-50	5-10	20-50	>5
Biotite. Green						10-20	20-50	-	<5
Brown									
Cordierite				3.1					
Carbonate	2.1			6.9		-	10-20	-	-
Diopside	25.4	24.9	15.7	39.7					
Garnet				15.0	23.5	<5	-	5-10	5-10
Hypersthene		6.9							
Sphene		0.9	1.2						
Magnetite	3.0	2.0							
Ilmenite			tr						
Apatite		tr							
Pyrite									
Hercynite									
Lazulite									

(* After; Geringer G.J. (1979))

SYMBOLS		
	AMPHIBOLITE	GRANULITE
K3 AREA	●	○
K1 AREA	▲	△
K6 AREA	■	□
COPPERTON	◆	◇
SOUTH GRANULITE		X
NORTH GRANULITE		+

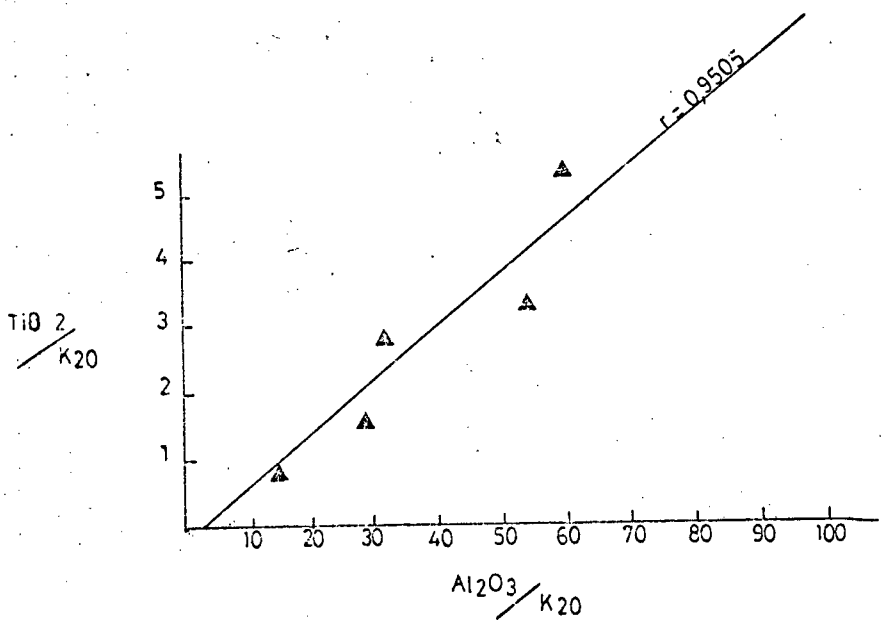

FIG. 12
(AFTER DAVIES etal. 1978)

3/81

Ratios	Correlation Coefficient (r)
Fe_2O_3/K_2O vs Al_2O_3/K_2O	.9823
P_2O_5/K_2O vs Al_2O_3/K_2O	.8762
Nb/K_2O vs Al_2O_3/K_2O	.6575

Since the metamorphic conditions in the K3 and southern and northern granulite areas are similar to those at K1, these elements are inferred to be immobile in those areas as well.
The following discriminant diagrams display data from all the areas on Kielder.

4.2.2. Ortho and Para-Basic Metamorphites

Results obtained from the Leake diagrams are presented below, bearing in mind such limitations as the potential mobility of certain elements. Inspection of Fig. 13, which shows the igneous differentiation trend, pelite field, dolomite field and the field of various pelite-limestone mixtures with respect to the Niggli c and mg, reveals a strong correlation of the amphibolites (K3, K1, K6 and Copperton) with the igneous trend. The northern and southern granulites plot as pelite-limestone mixtures and the K3 hypersthene granulites plot in the pelite field.

Amphibolite data from the Kielder areas of mineralization plot on the igneous trend on Fig. 14, but at the dolomite-pelite tie-line intersection. The granulites tend to be scattered around the igneous trend and pelite-limestone tie-line, so no confident interpretation can be made.
Hypersthene granulites of the K3 area fall on the mg side of the dolomite-pelite tie line, which is interpreted as magnesium metasomatism of the "chlorite alteration" pipe, associated with the footwall of exhalative massive sulphide mineralization.
The inconclusive results from this plot (i.e. Fig. 14) may reflect the probable mobility of Ca and the alkali elements, which will have a profound effect on the Niggli c and Alk values.
Amphibolites show a strong positive correlation between Niggli mg and Cr (Fig. 15) and which is very close to the typical igneous trend.

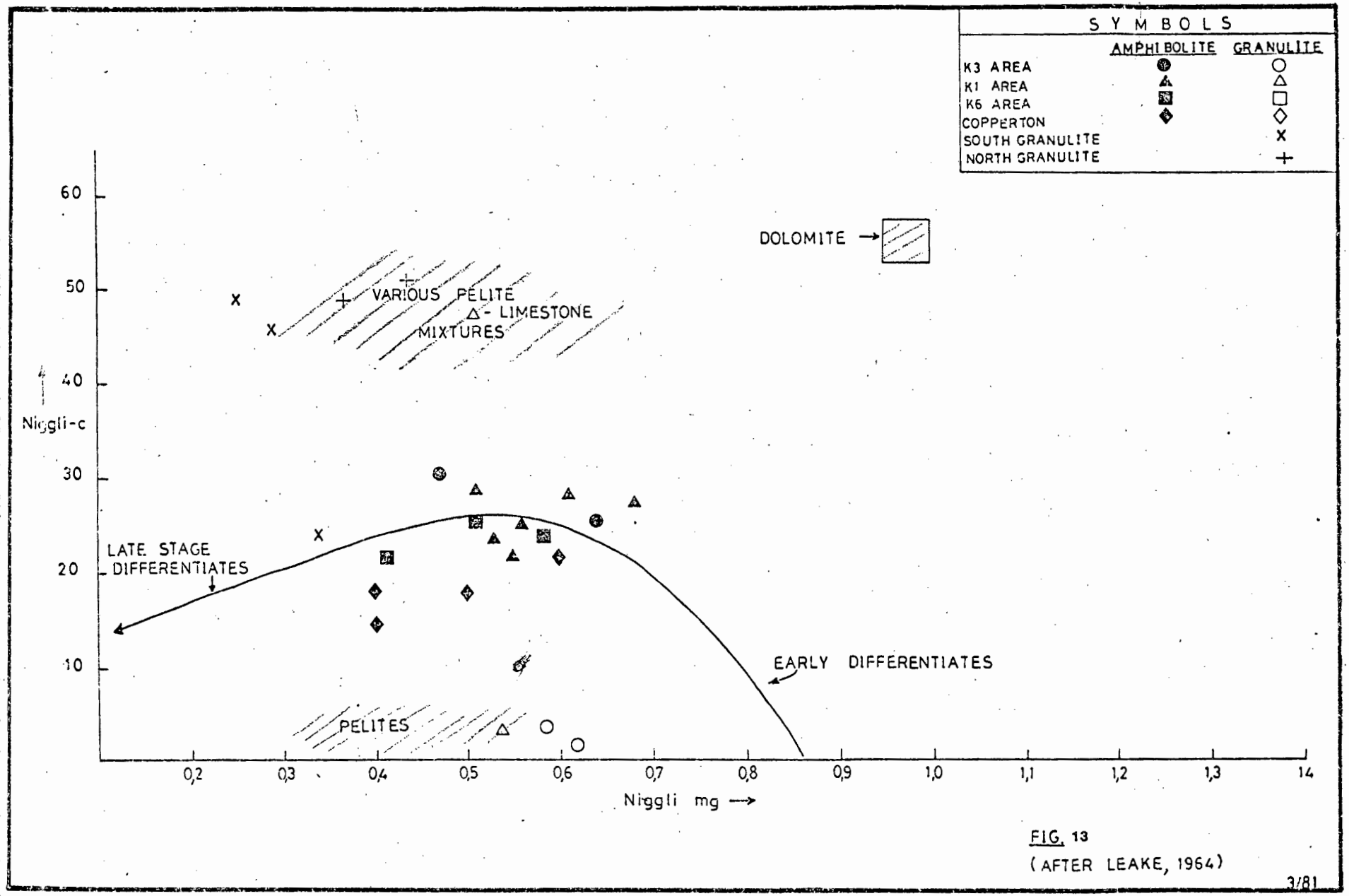

FIG. 13

(AFTER LEAKE, 1964)

3/81

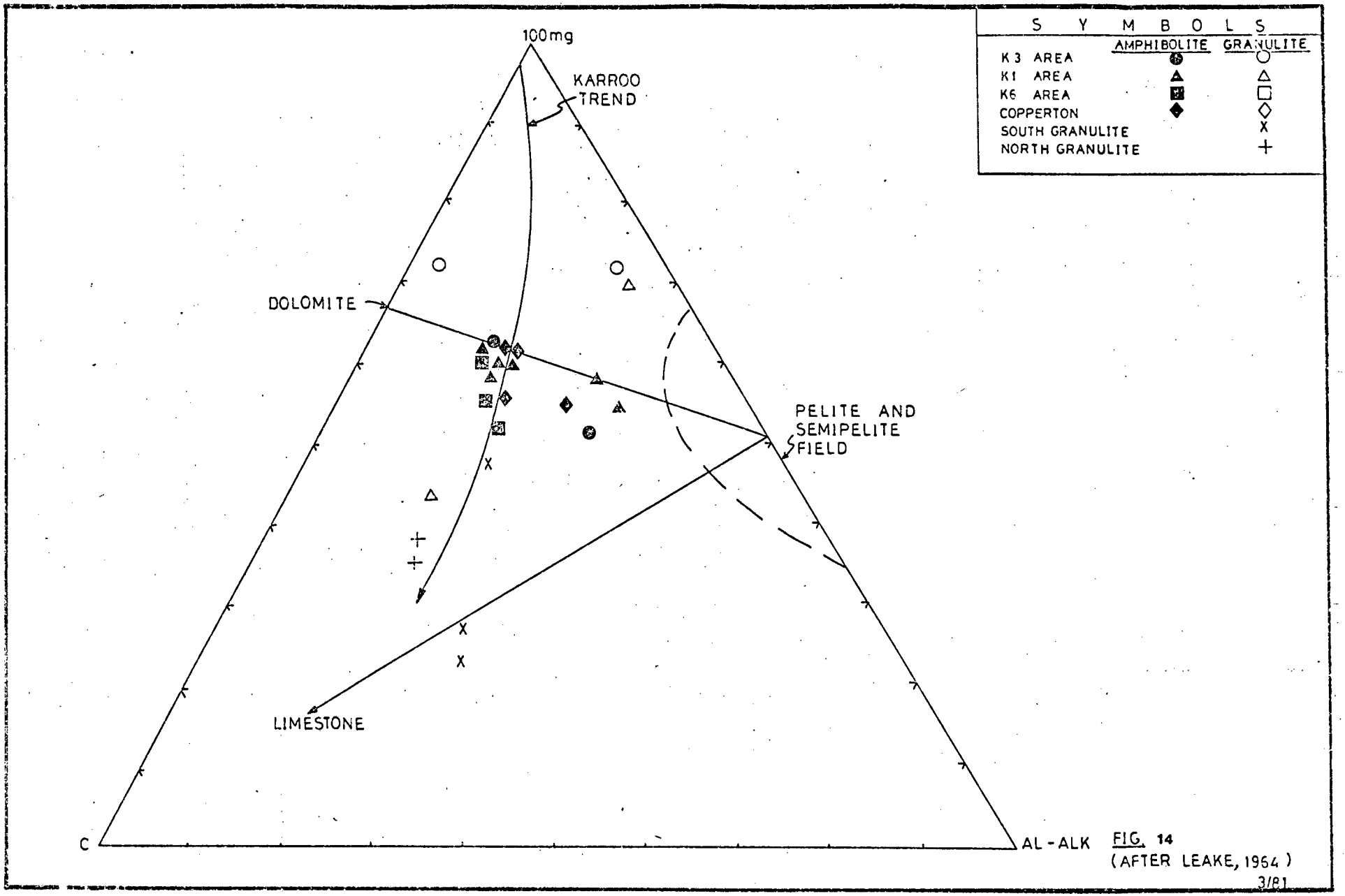

FIG. 14
(AFTER LEAKE, 1964)

3/81

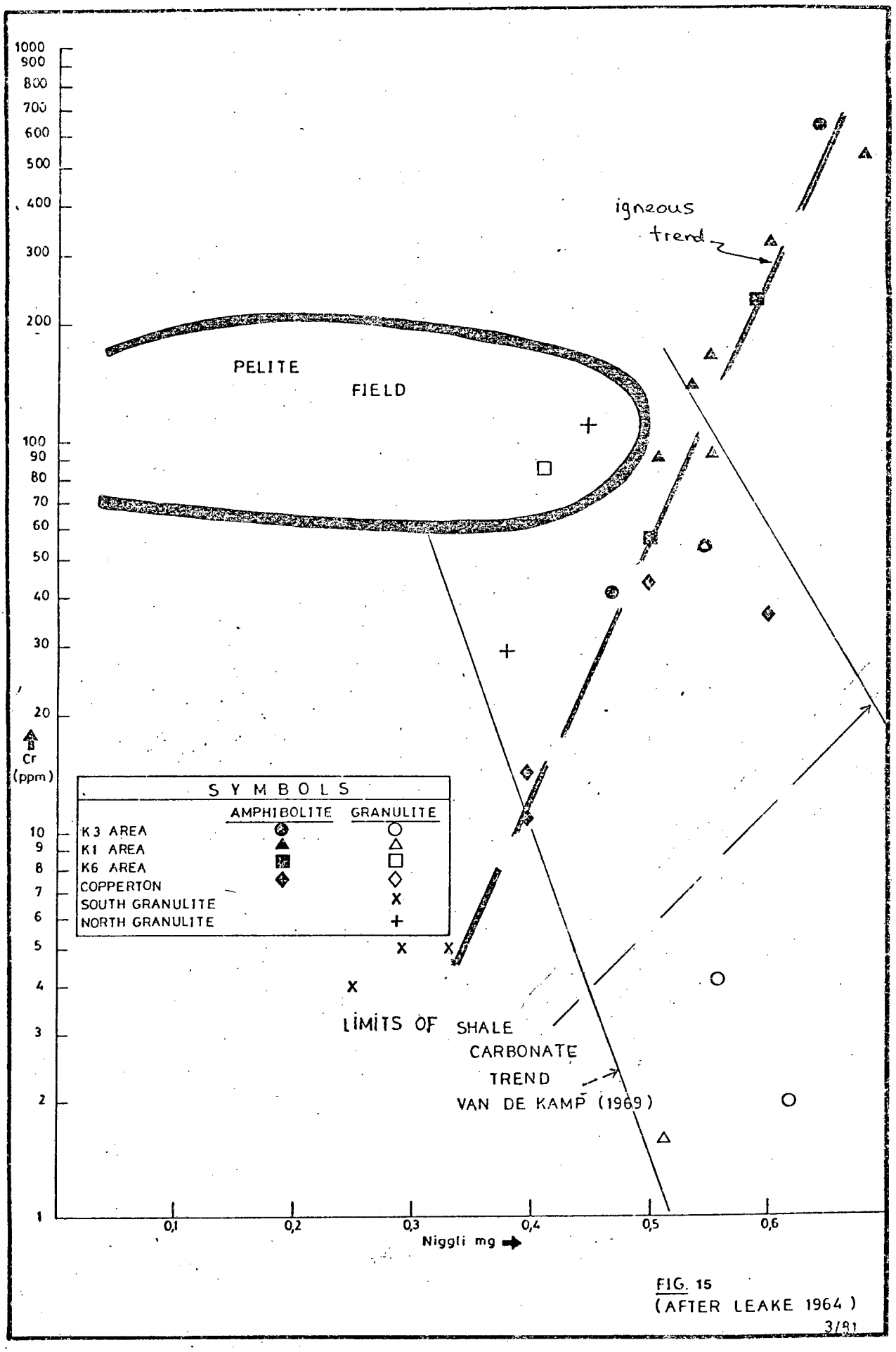

FIG. 15
(AFTER LEAKE 1964)

3/91

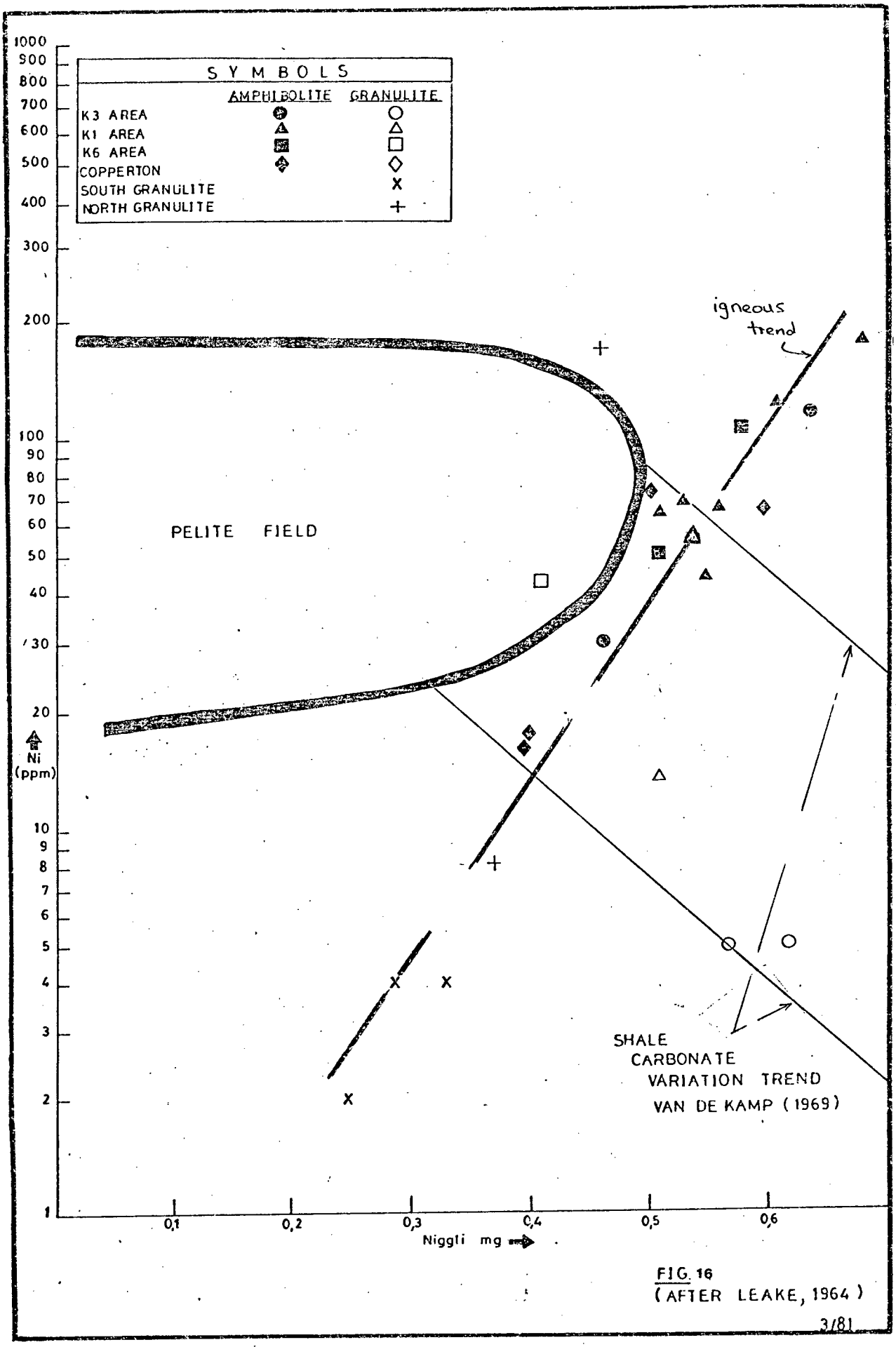

FIG. 16
(AFTER LEAKE, 1964)

3/81

The southern granulites appear to extend the trend to lower mg values.

Other granulites are scattered and further data are required to confirm any affinity with shale-carbonate mixtures. An analagous relationship is shown in the Niggli mg-Ni plot (Fig. 16) with the amphibolites and southern granulites showing an igneous-type trend.

Scrutiny of Figs. 17 and 18, which show the Niggli mg vs Cu and Co respectively, show the southern granulites and northern granulites to be within the pelite field or just beyond, and the other granulites separated with lower Co and Cu contents from the amphibolites.

Further variation diagrams reflecting magmatic differentiation involving elements least affected by metasomatism (i.e. Ni, Cr, Ti and Mg) plotted against 100 x $\frac{Fe}{Fe+Mg}$ (Cornell, 1975) are presented below. Figs. 19 and 20 show the amphibolites to have well defined igneous type compositional trends, while the granulites show very little change in Ti, Mg, Ni and Cr with differentiation.

The K1 amphibolites fall within the basic igneous field in Fig. 21 while the southern granulites correspond to a 80:20 shale-carbonate mixture. The K3 granulites plot in an indeterminant high Fe+Mg+Mn field.

On the basis of the evidence presented above, it is concluded that the amphibolites are meta-igneous rocks and the basic granulites are metasediments.

Parent rock types deduced for all samples analysed are listed in Table VI summarised below.

TABLE VI. BASIC METAMORPHITES AND THEIR PARENT LITHOLOGIES

Name and Rock Unit No.	Present Mineral Assemblage	Parent Rock
Amphibolite, K1 Unit 9	Labradorite, hornblende, diopside and quartz	basic igneous rock
Amphibolite, K3 Units 7, 12	Labradorite, hornblende, diopside and hypersthene	"
Amphibolite, K6 Units 4, 9	Labradorite, hornblende, quartz	"
Amphibolite, Copperton (cf. Geringer 1979)	Andesine, hornblende, quartz, biotite and garnet	"

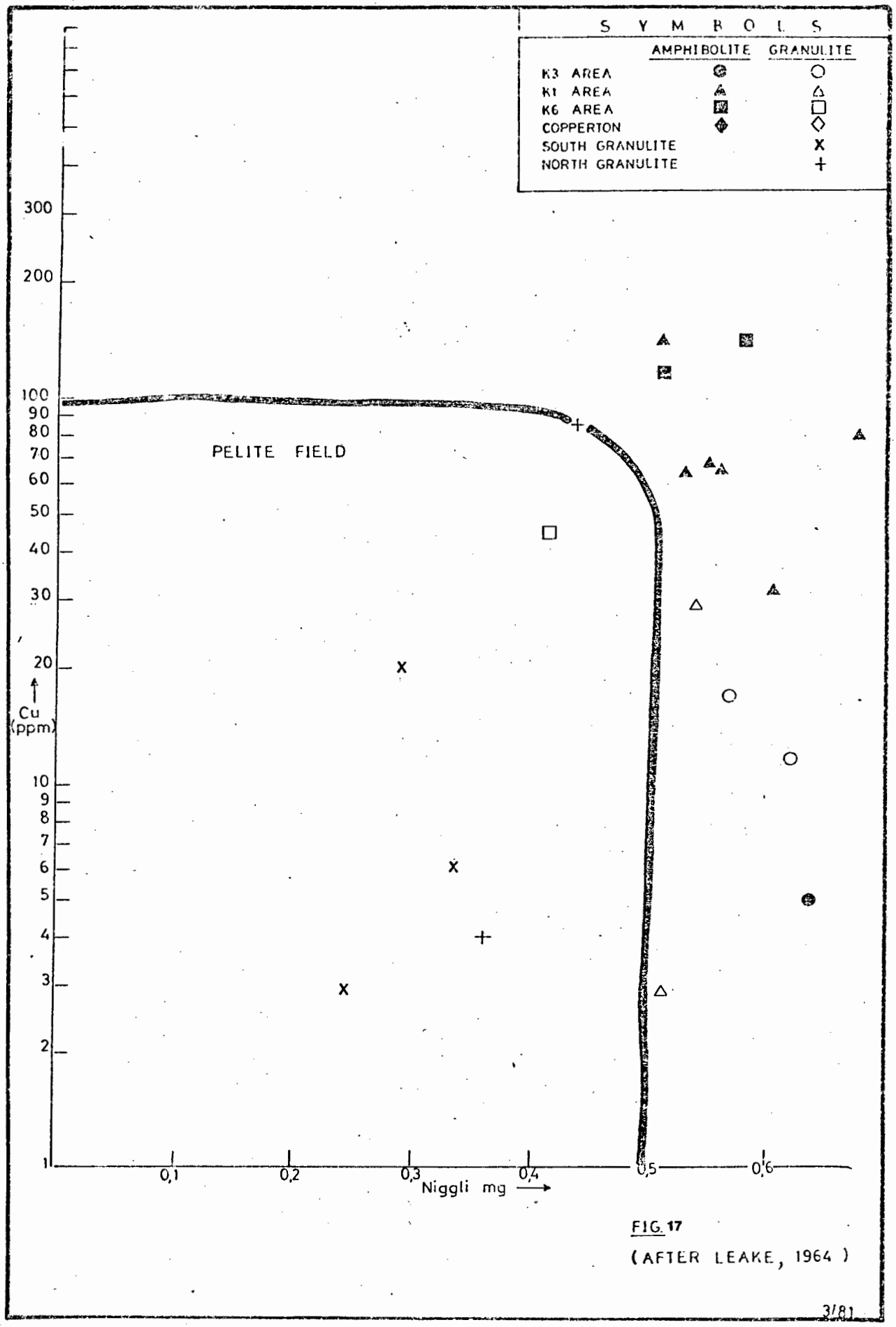

FIG. 17

(AFTER LEAKE, 1964)

3/81

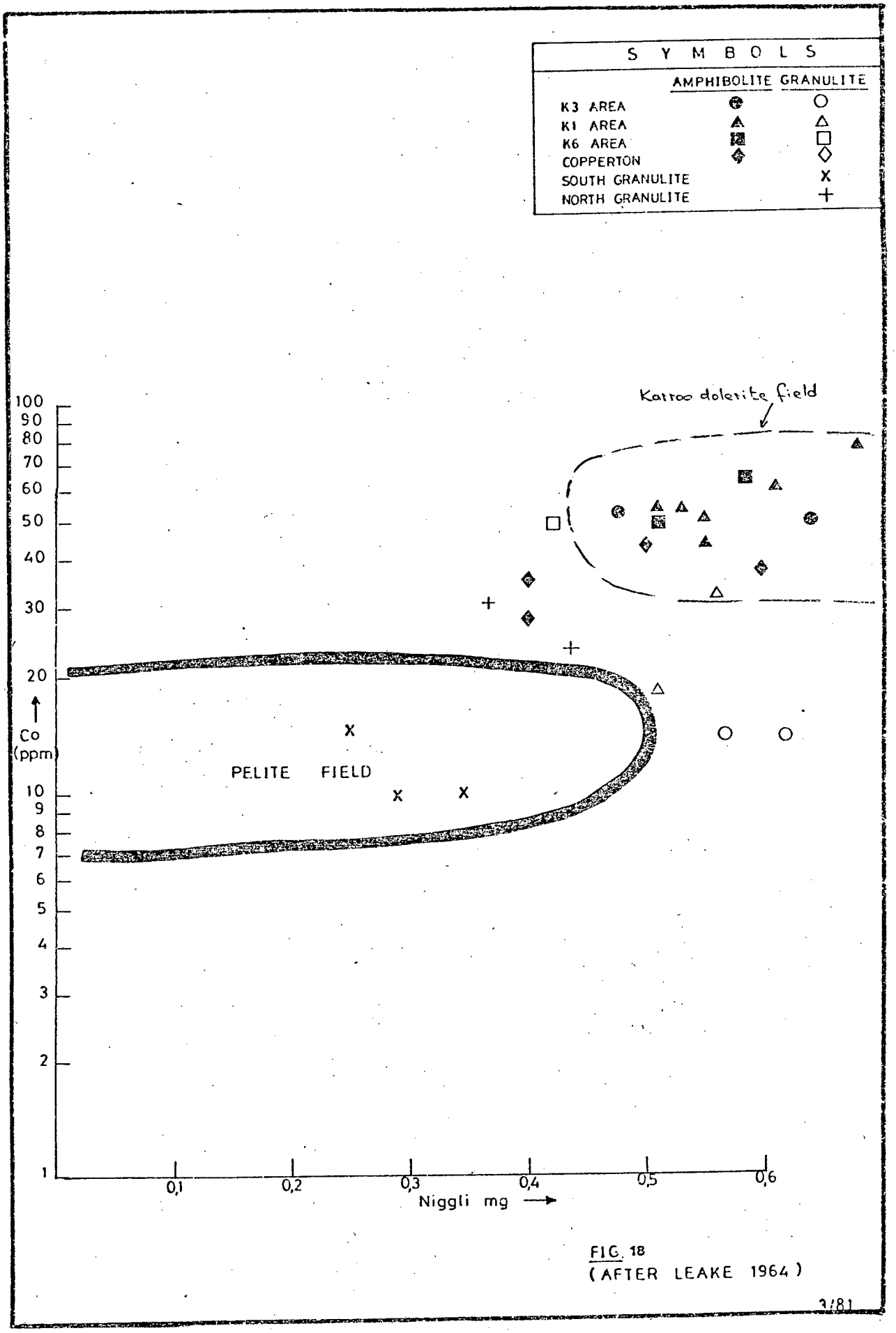

FIG. 18
(AFTER LEAKE 1964)

3/81

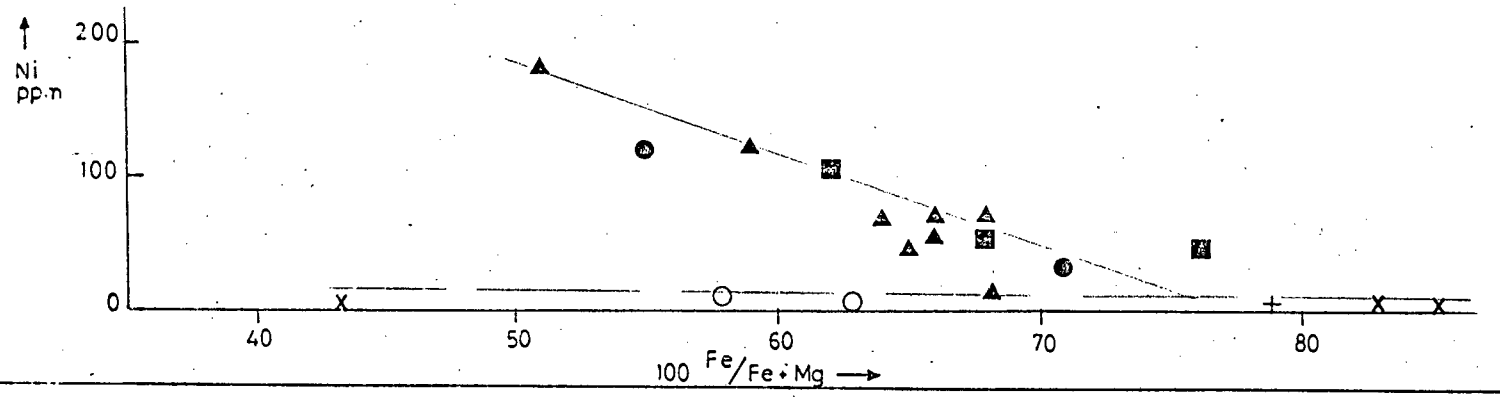

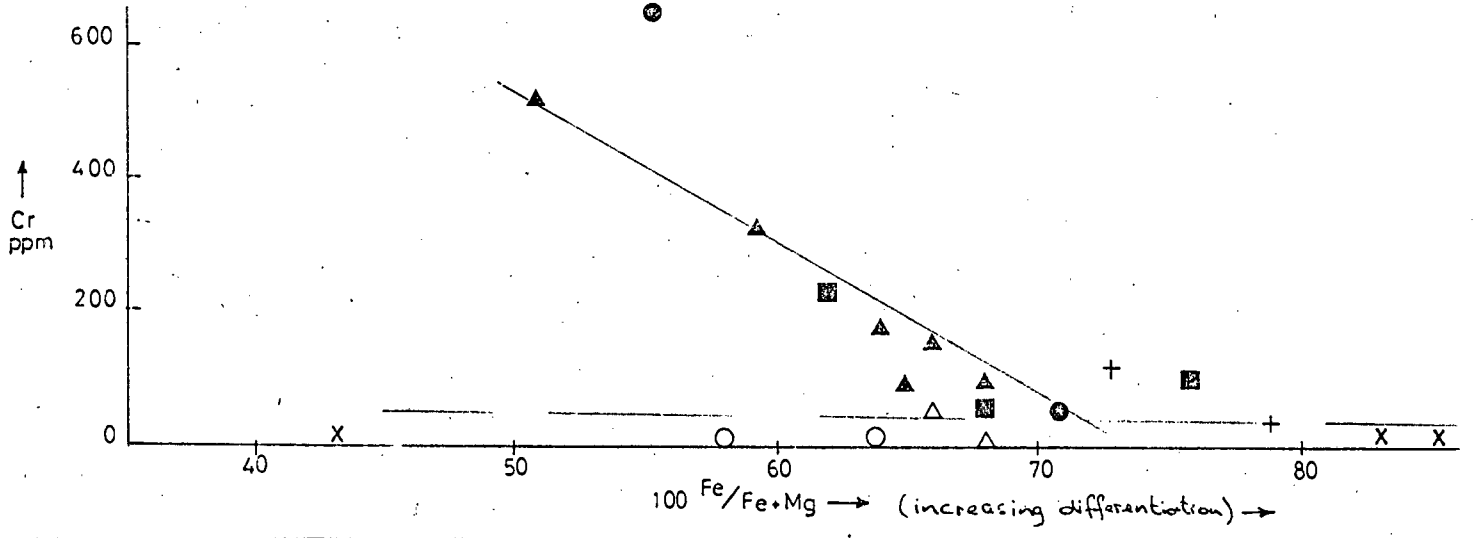

S Y M B O L S	AMPHIBOLITE	GRANULITE
K3 AREA	◉	○
K1 AREA	▲	△
K6 AREA	■	□
COPPERTON	◆	◇
SOUTH GRANULITE		X
NORTH GRANULITE		+

FIG. 19

3/81

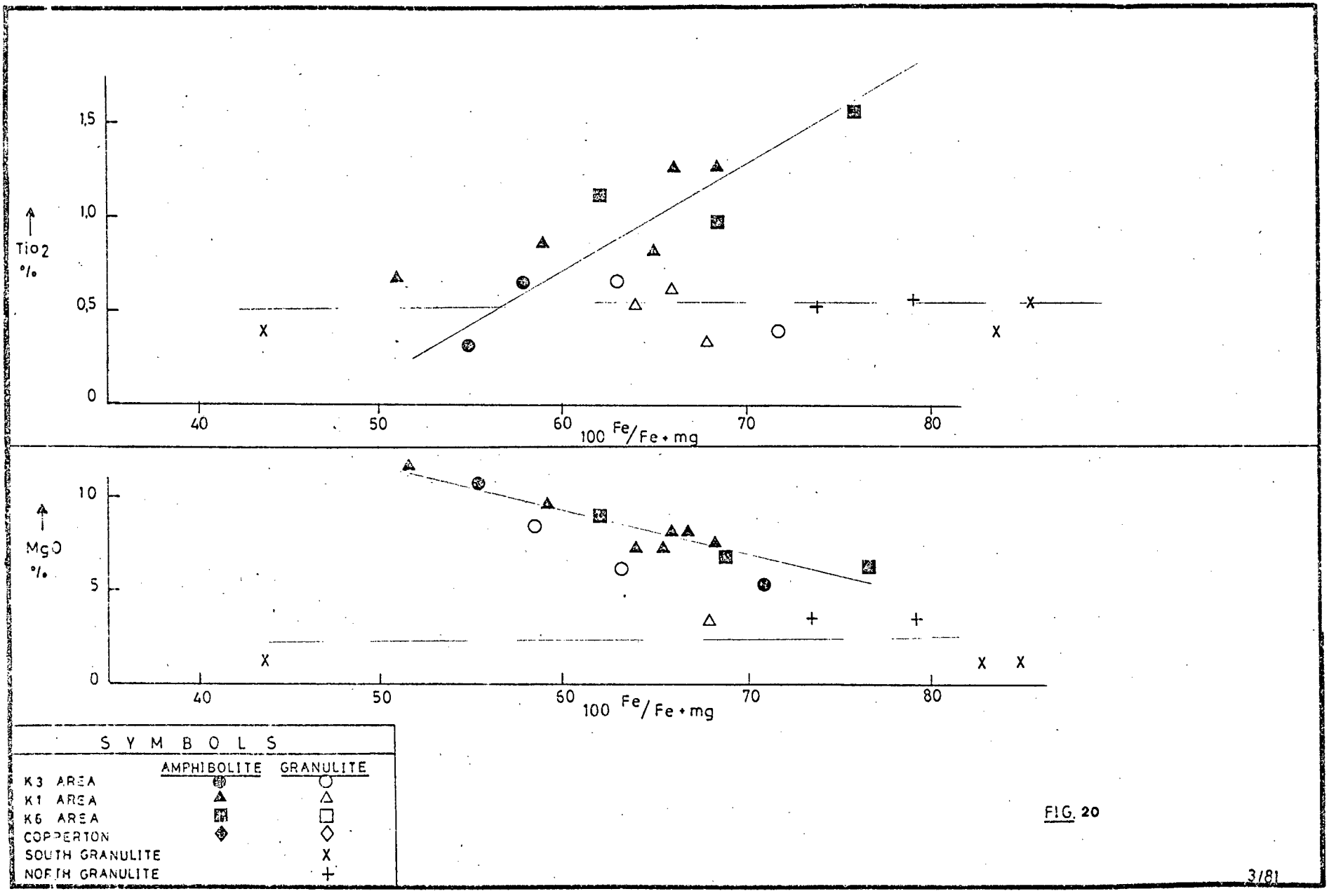
1,5
1,0
0,5
0
TiO2 %
40
50
60
70
80
100 Fe/Fe+mg
10
5
0
MgO %
40
50
60
70
80
100 Fe/Fe+mg
SYMBOLS
AMPHIBOLITE
GRANULITE
K3 AREA
K1 AREA
K6 AREA
COPPERTON
SOUTH GRANULITE
NORTH GRANULITE

FIG. 20

3/81

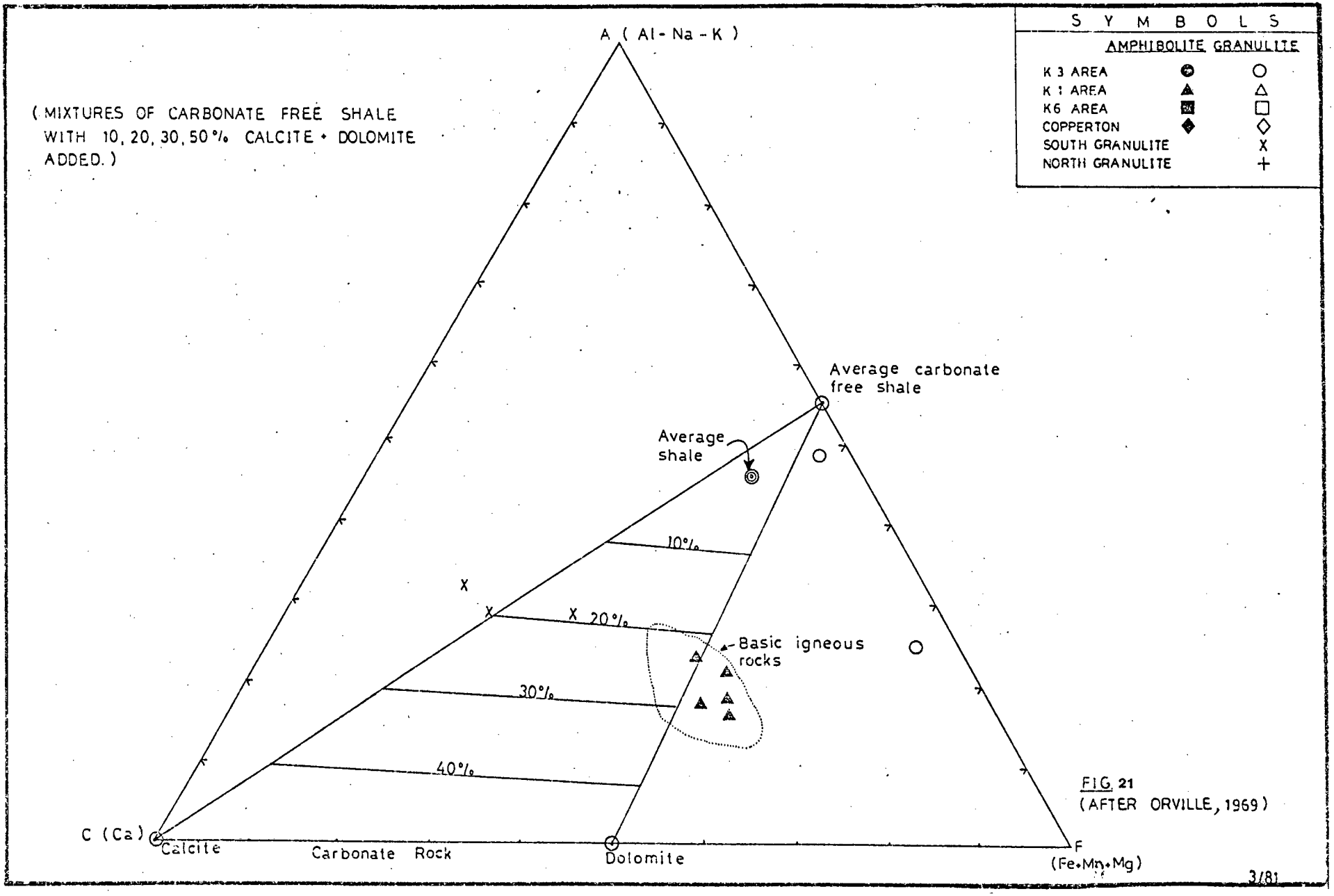

FIG. 21
(AFTER ORVILLE, 1969)

3/81

Name and Rock Unit No.	Present Mineral Assemblage	Parent Rock
Amphibolite-quartz granulite, K1 Unit 2	Labradorite, hornblende, edenite, quartz, diopside and cordierite	marly peliti rock
Hypersthene granulites K3, Units 6, 8	Quartz, andesine, hornblende, hypersthene and garnet	magnesium enriched pelitic rock
Southern Granulite	Labradorite, quartz, hornblende, diopside, hypersthene, carbonate	carbonate pelites
Northern Granulites	Labradorite, hornblende, cordierite, garnet, diopside carbonate ± quartz	marly pelite

4.2.3. Tectonic Setting of the Ortho-amphibolites

Tholeiitic affinities of most of the amphibolites are illustrated on the AFM plot in Fig. 22. Tholeiitic affinities are confirmed for the Kielder ortho-amphibolites on the diagrams using Zr, P, Ti shown in Figs. 23 and 24.

Amphibolites plotted on Figs. 25 and 26 fall within or very close to the low-K tholeiite field, and in the case of Fig. 26, there is some suggestion of oceanic affinities.

Inspection of the Davies (1978) YTC diagram (See Fig. 27) shows the ortho-amphibolites to correspond to an Archean tholeiite trend, although two samples plot close to the Cr apex and suggest an affinity with the Archean magnesian trend, a feature not supported by actual Mg contents. The granulites ("para-amphibolites") show considerable scatter.

The discriminant diagram of Pearce et al. 1977 shows the Kiedler ortho-amphibolites to plot within the ocean island field (See Fig. 28).

To summarise, it is concluded that the Kielder ortho-amphibolites are derived from low potash tholeiites with ocean island affinities.

An interesting feature of Figs. 22, 23, 24, 25, 26, 27 and in particular 28, is that the four samples of Copperton amphibolite display erratic behaviour and no confident interpretation could be attempted using them alone.

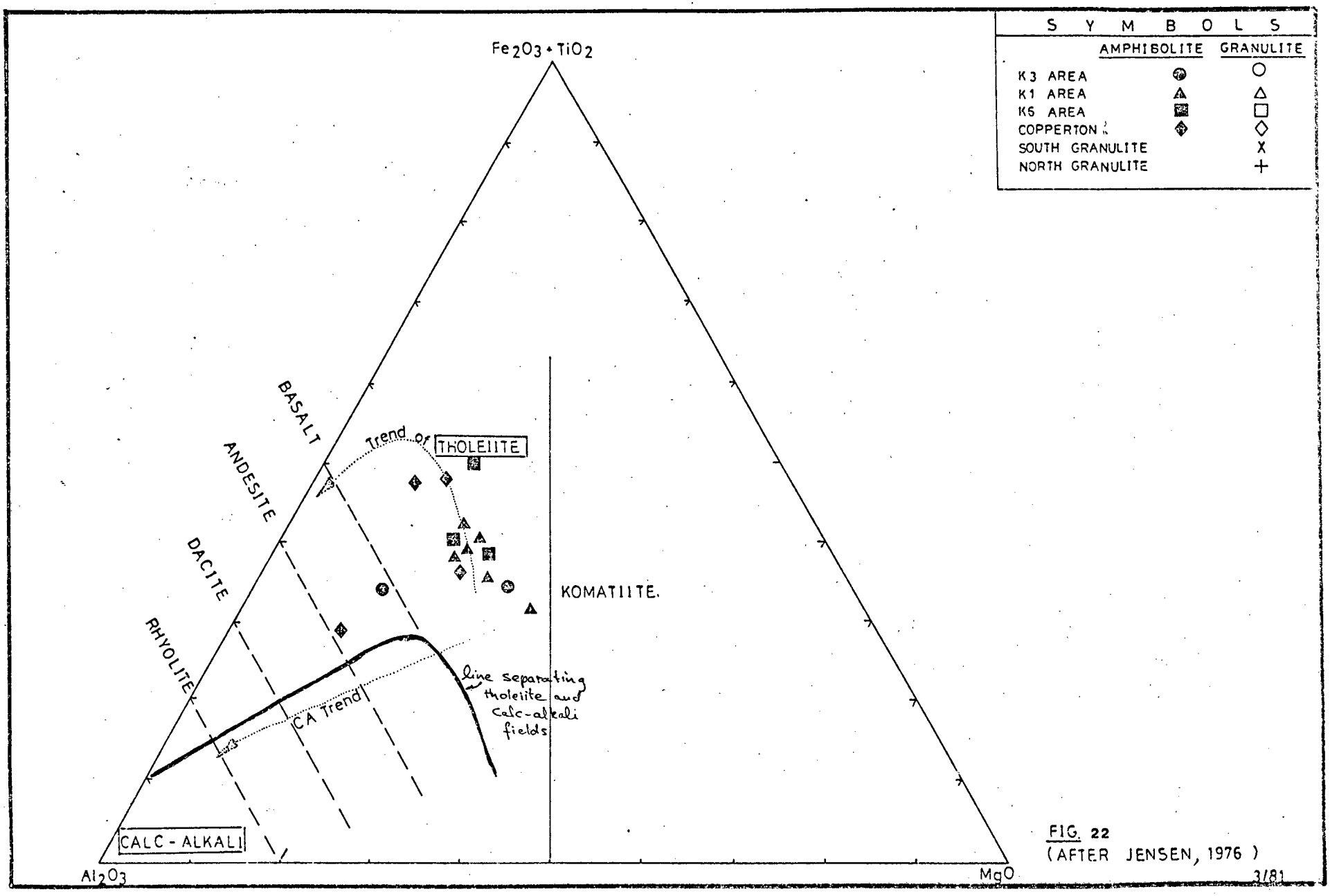

FIG. 22
(AFTER JENSEN, 1976)

3/81

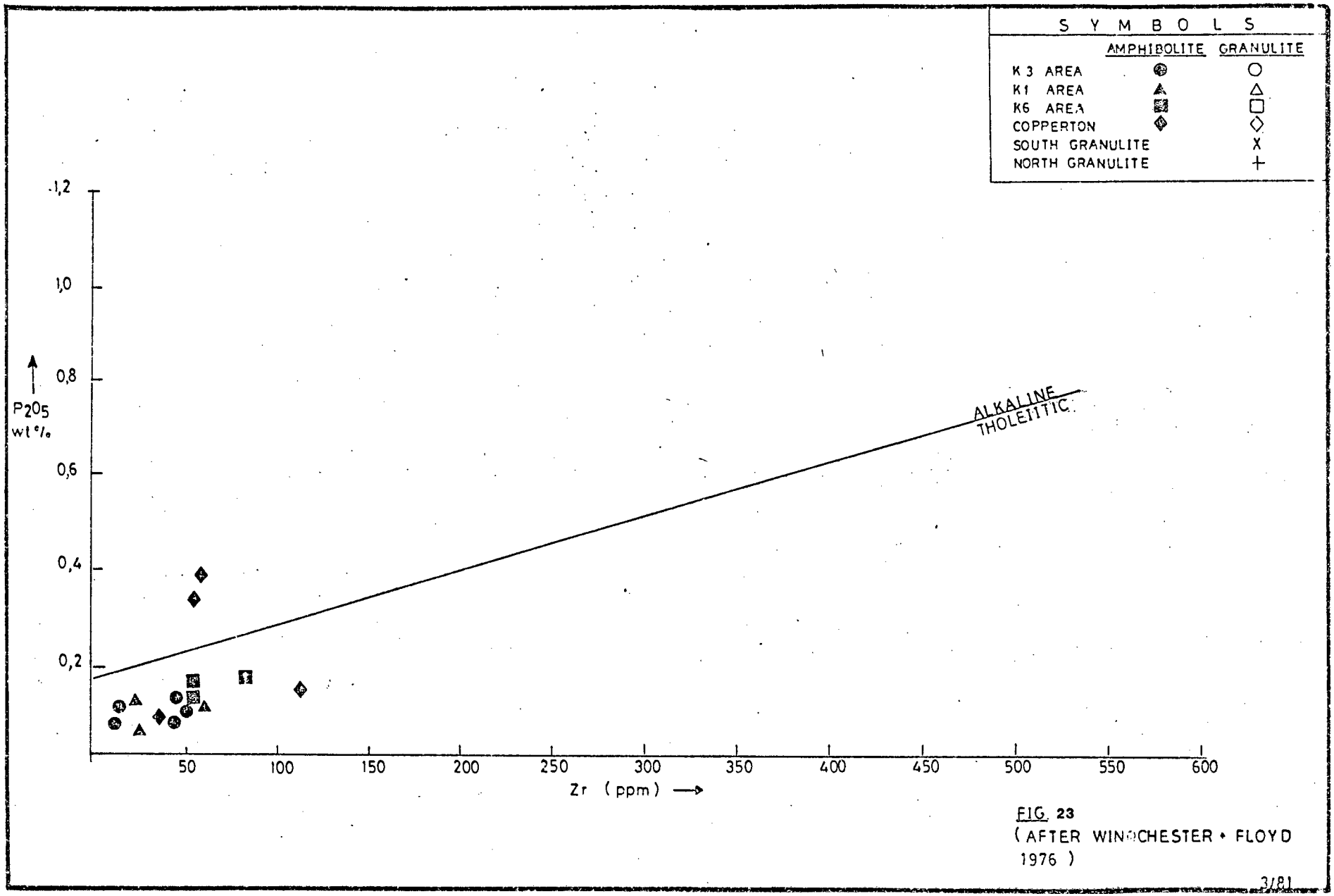

FIG. 23
(AFTER WINCHESTER + FLOYD 1976)

3/81

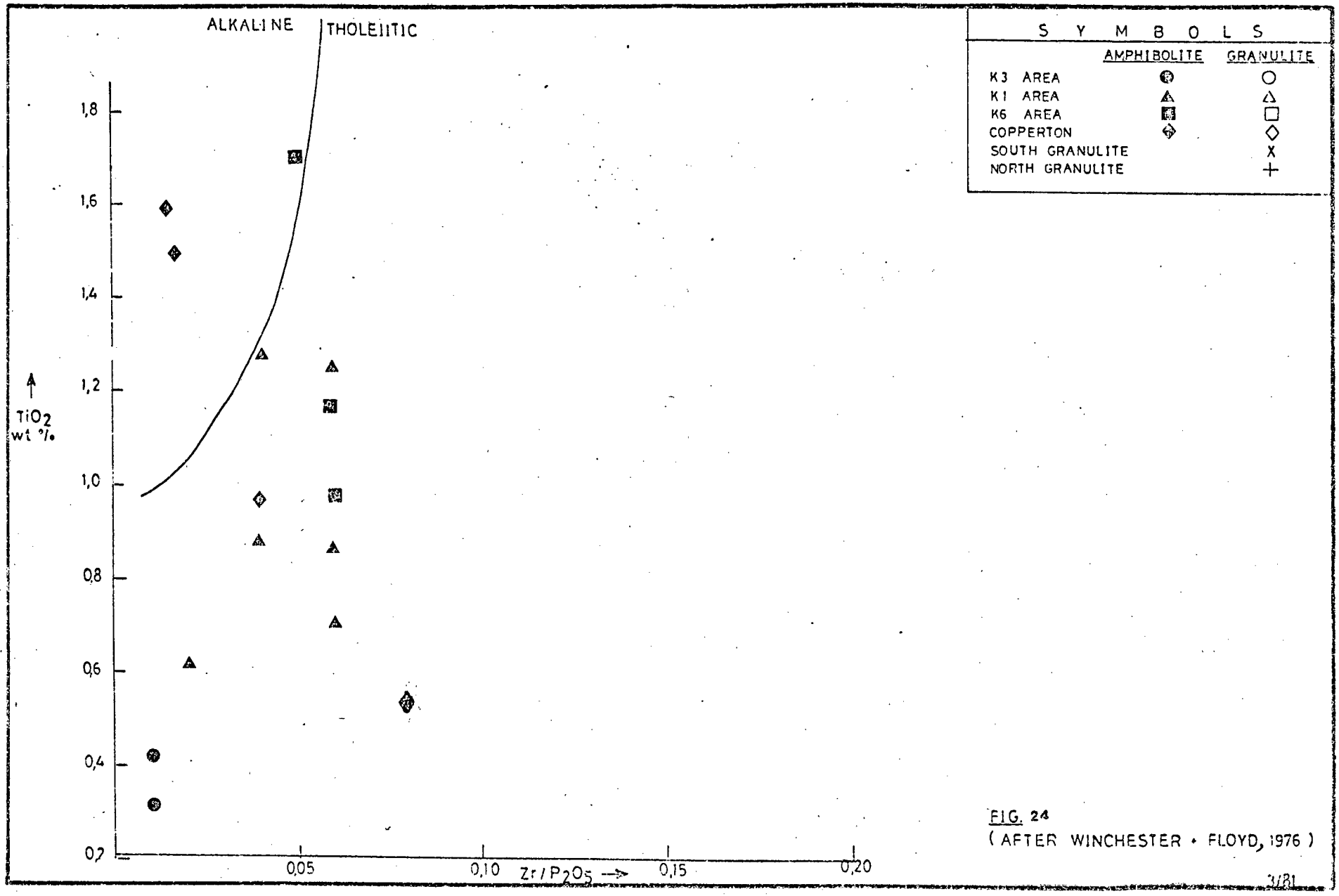

FIG. 24
(AFTER WINCHESTER + FLOYD, 1976)

3/81

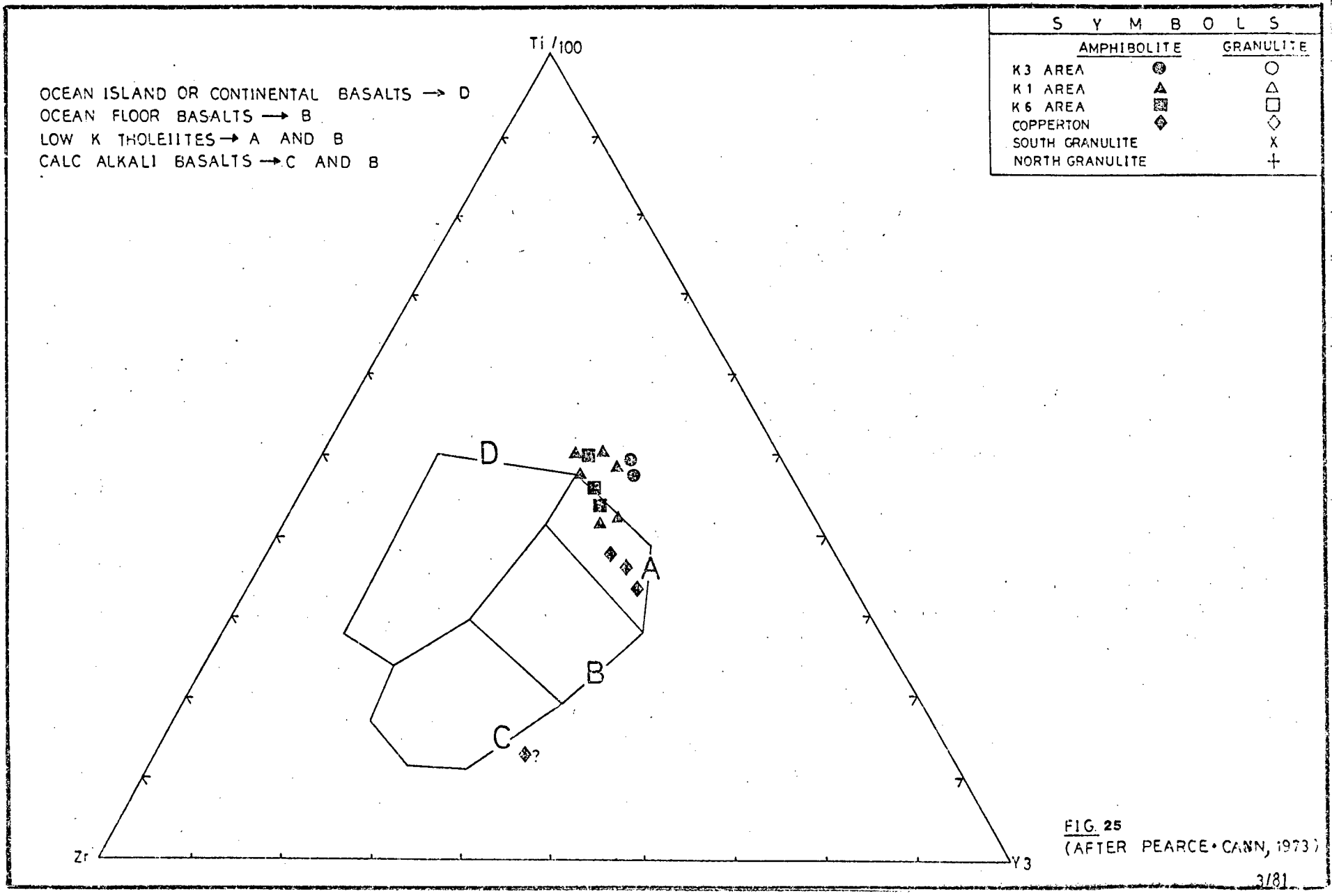

FIG. 25
(AFTER PEARCE • CANN, 1973)

3/81

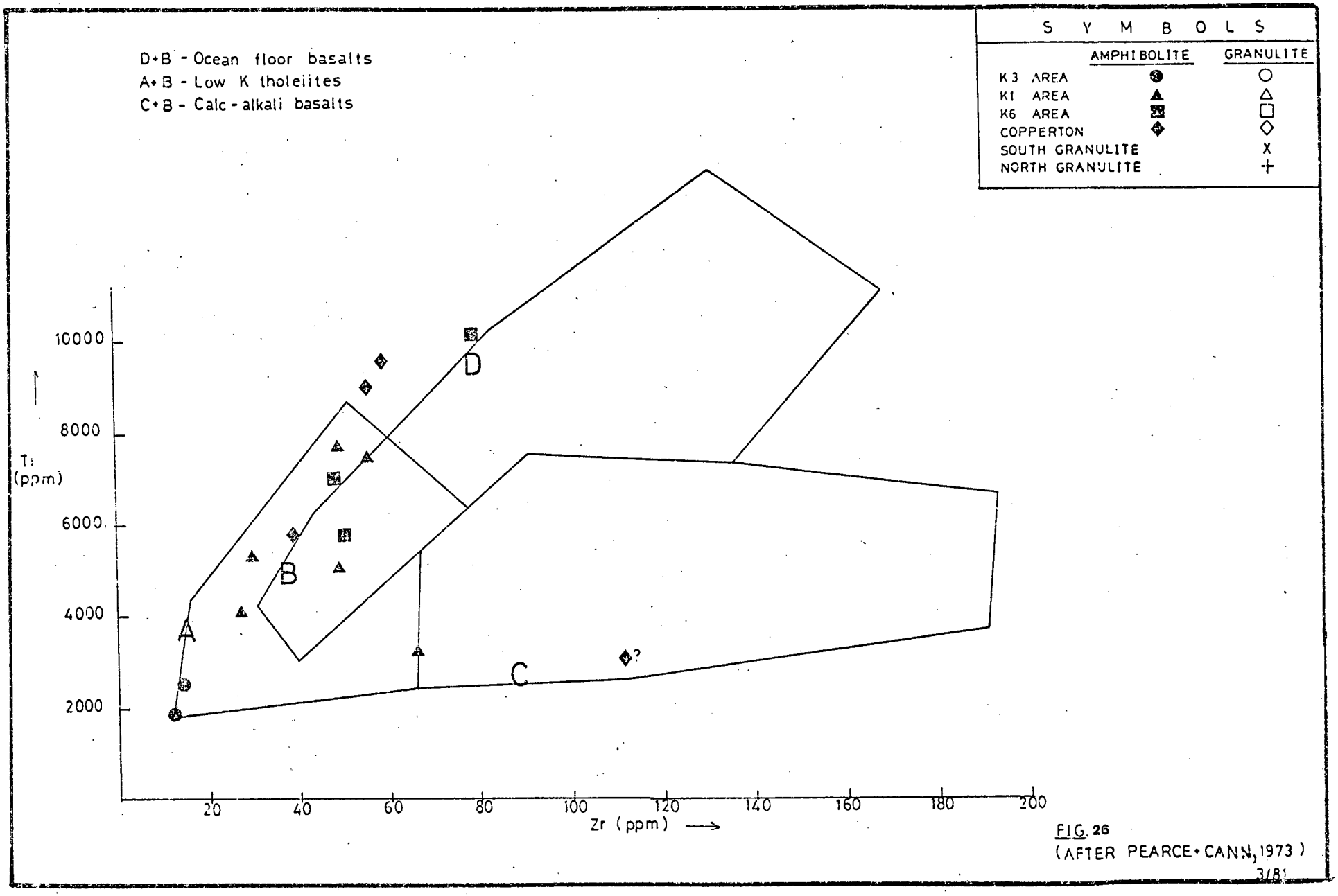

FIG. 26
(AFTER PEARCE+CANN, 1973)

3/81

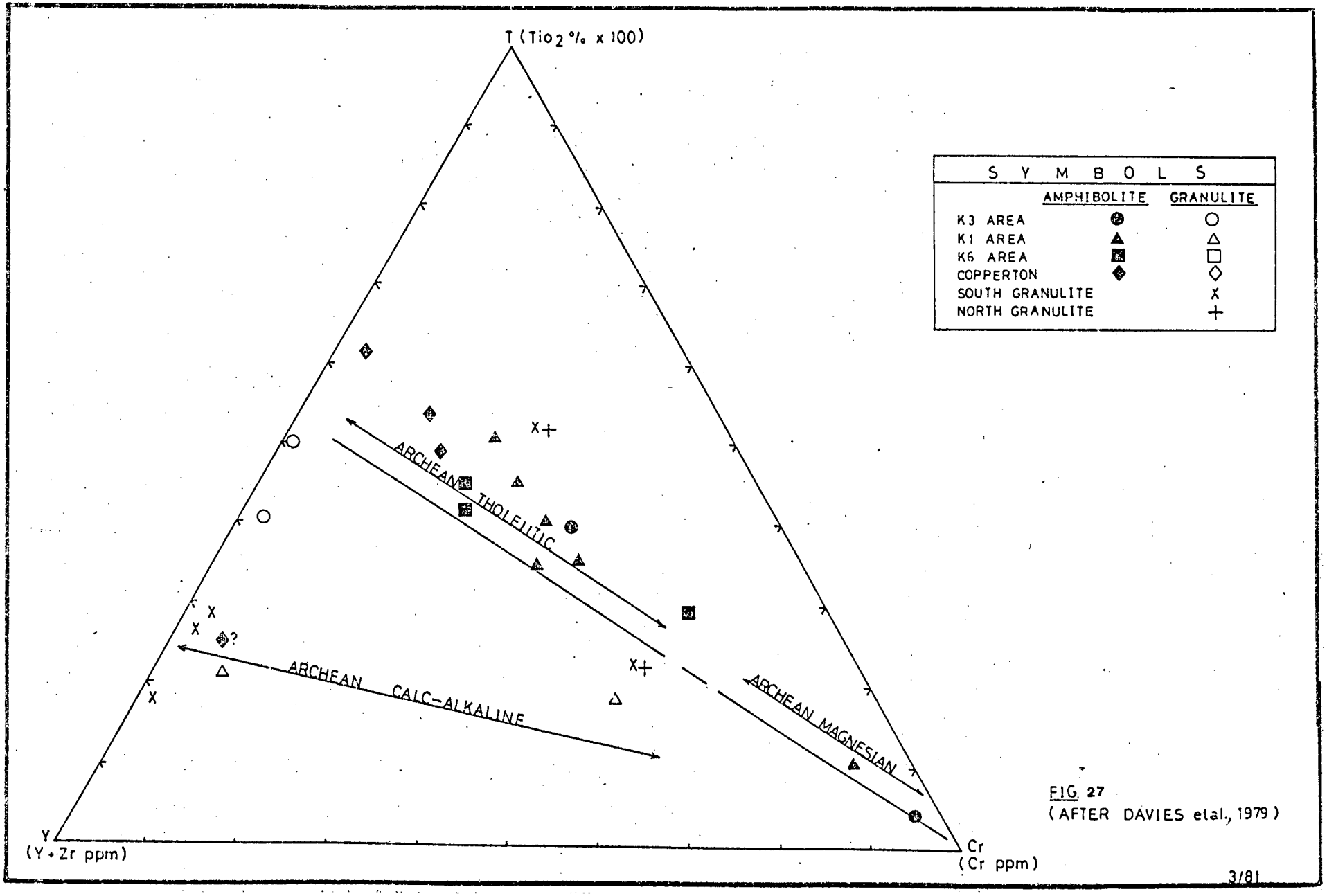

FIG. 27
(AFTER DAVIES etal., 1979)

3/81

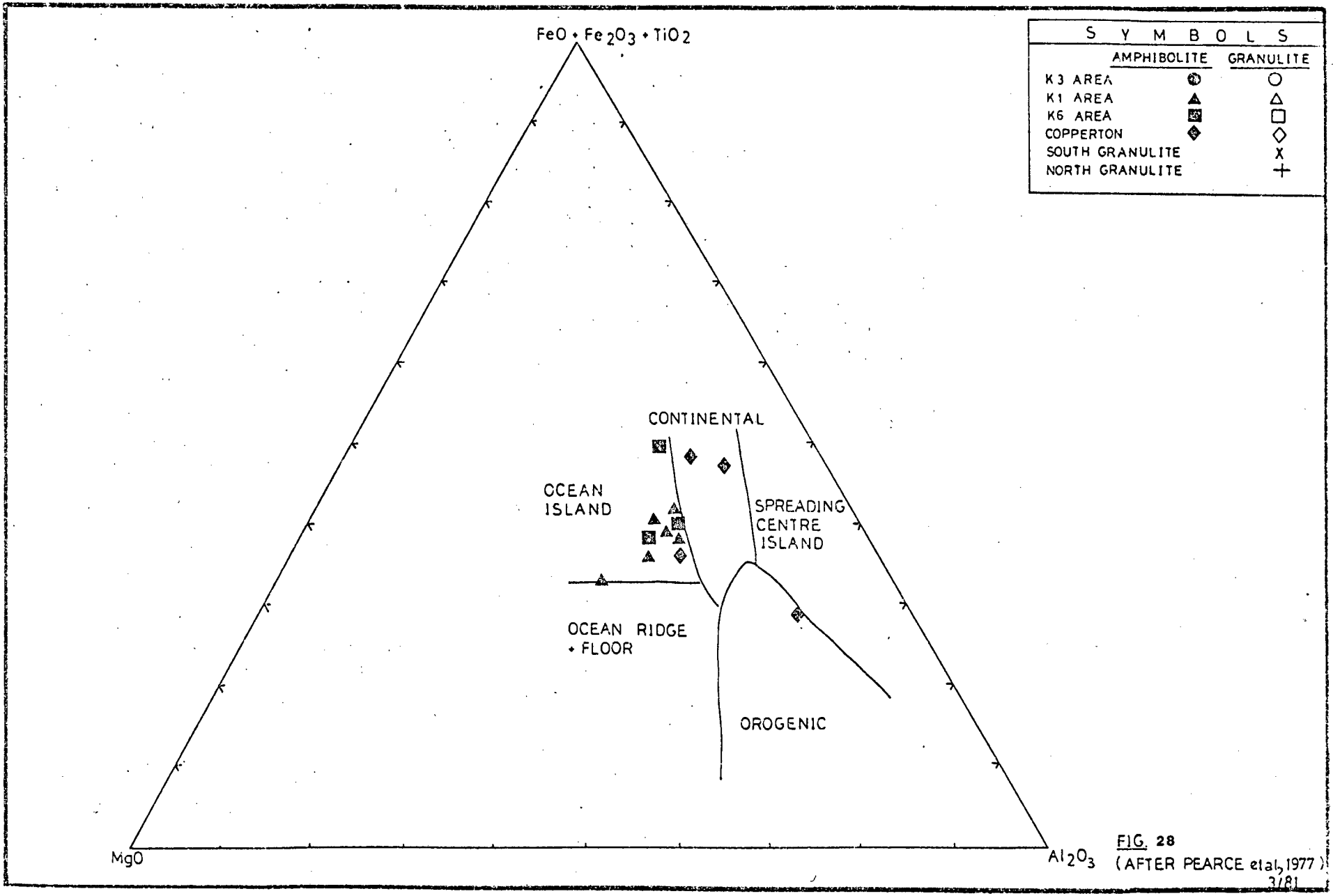

FIG. 28
(AFTER PEARCE et al, 1977)
3/81

4.2.4. Stratigraphic Correlation

Discriminant diagrams of Davies et al. (1978) are illustrated in Figures 29 to 32 with the Kielder basic metamorphites shown. The southern granulites are consistently separated from the northern granulites which cluster with the amphibolites and granulites occurring with sulphide mineralization. While the TiO_2 vs Cr plot illustrated in Fig. 32 separates the ortho and para-amphibolites, no distinction within the latter group is achieved.

4.3. Discussion

Arguments against using chemical trends to distinguish para and ortho-amphibolites have been put forward by Orville (1969), who suggest that amphibolites could be:

(i) meta-igneous rock; produced by recrystallisation of a basic igneous sill, dyke or flow.
(ii) metasediment; by recrystallisation of marl or carbonate shale with a change only in the volatiles.
(iii) metasomatic rock; by recrystallisation of some parent material combined with addition and/or subtractions of, significant non-volatiles.

Orville (1969) points out that any amphibolite (i.e. hornblende-plagioclase rock) will plot in the igneous field because the plot of pure hornblende overlaps with the igneous field. The results will show that the K1 amphibolites which are diopside-plagioclase-hornblende-edenite rocks, plot in the igneous field and do not correspond to the hornblende field. Most of the amphibolites studied by Orville (1969) are thin layered varieties occurring with calc-silicates, marbles and gneisses, whereas the K1 and K6 amphibolites are wide (up to 100m) bodies, with gradual variations in mineralogical composition, if any at all, with no banding present.
Evidence for metasomatic origin of amphibolites is listed by Orville (1969) as

(i) systematic compositional relationship between interlayered marble, calc-silicate, amphibolite and pelitic schist.
(ii) calc-silicate layers within amphibolite.

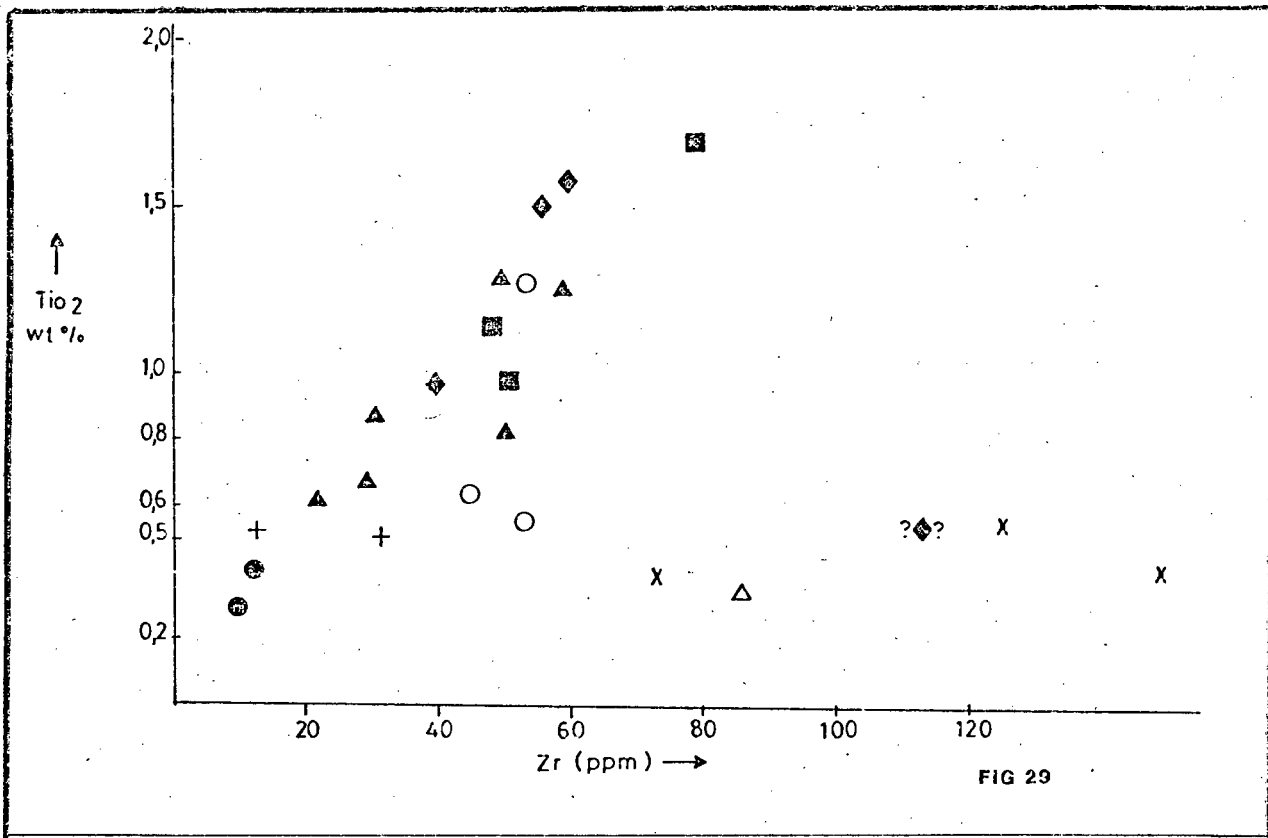

FIG 29

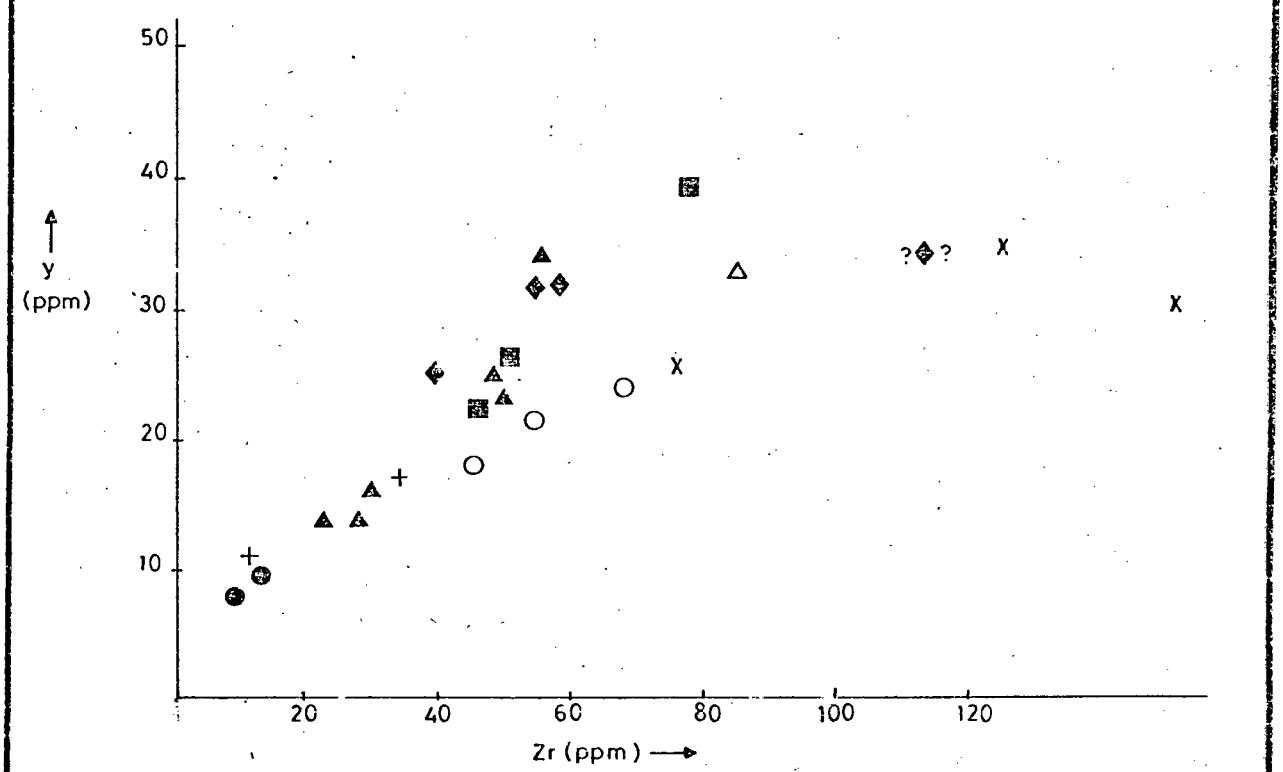

S Y M B O L S	AMPHIBOLITE	GRANULITE
K3 AREA	●	○
K1 AREA	▲	△
K6 AREA	■	□
COPPERTON	◆	◇
SOUTH GRANULITE		X
NORTH GRANULITE		+

FIG. 30
(AFTER DAVIES et al., 1978)

3/81

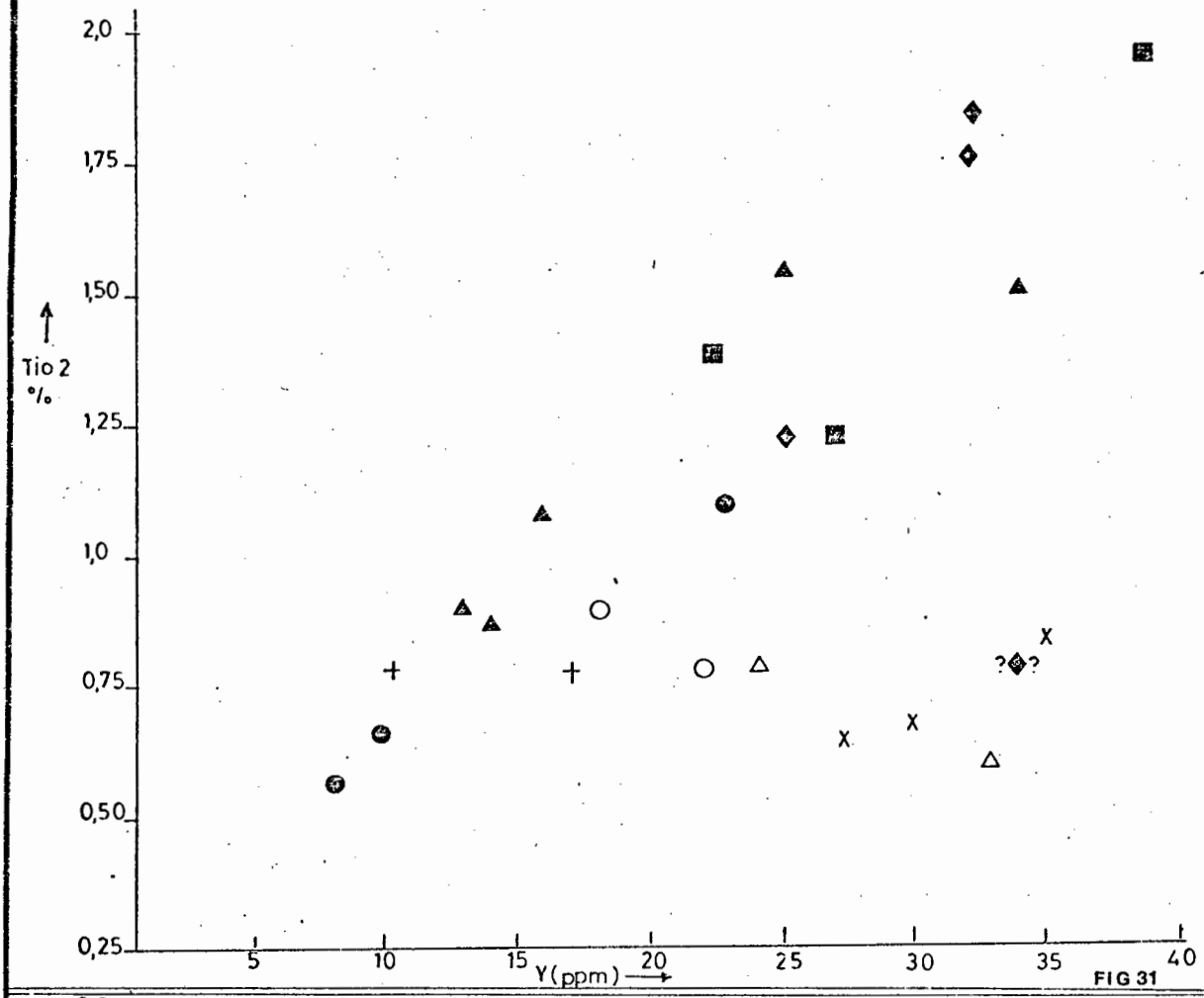

FIG 31

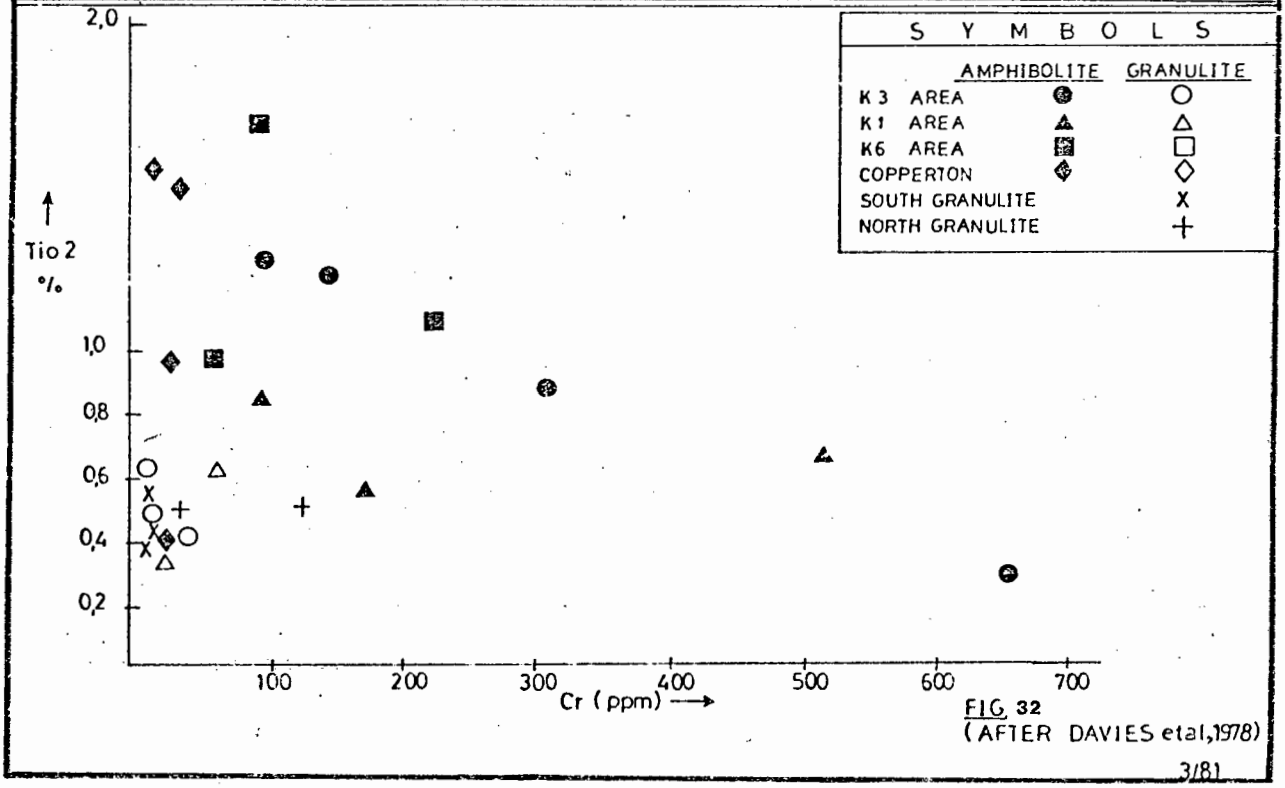

FIG. 32
(AFTER DAVIES etal, 1978)

3/81

(iii) increase in Ca content of the country rock adjacent to the amphibolite.

(iv) decrease in total Mg and Fe adjacent to the amphibolite.

Because none of these features are observed, in fact the opposite is the case with (iii) and (iv) (See Section 3.2.1.), a metasomatic origin for the amphibolites is rejected.

The amphibolites identified to be of igneous origin are interpreted as basaltic flows.
Their chemistry shows a similarity to ocean island tholeiites. Since the K1 amphibolite body is a relatively homogeneous mass, the specimens are likely to satisfy the assumption that they are comagmatic. However, if the K6 and Copperton amphibolites are included, the correlation coefficient is only slightly reduced, suggesting a common parent magma for all the basic igneous rocks in the Copperton-Kielder district.
There appears to be some basic differences between Archean "greenstones" and Cenozoic data on which the tectonic fields of Pearce, Gorman and Birkett (1977) (See Fig. 28) were based, apart from the tendency for the older rocks to have suffered more 'alteration'. They conclude that modern day island arcs are not comparable to those systems which formed the Archean greenstone belts. Bearing in mind the association of these amphibolites with stratabound massive sulphides, and horizons of banded iron formation, a case for an oceanic setting is considerably strengthened. The suggestion of Geringer (1979) that the Namaqua metamorphic complex is divisible into an Eastern domain (which includes the Copperton-Kielder area) of calc-alkaline type magmatism and a Central domain of continental type tholeiitic magmatism (which includes the Gamsberg-Aggeneys deposits), is not supported by the data presented here. Geringer's Eastern Domain has been shown in this study to contain a well defined intra-marine volcano-sedimentary succession, and evidence for a continental margin andesitic province is entirely lacking.
The lithostratigraphic correlation of the K3 hanging wall granulites with the Northern granulites confirms the earlier conclusion in Section 2.6 that these are stratigraphic equivalents. It is therefore postulated that the stratigraphic horizons hosting massive sulphide mineralization in the K3

area continue to the west in the area of the base line (See Map No. 4, from 32E to 40E) into an area of sand cover. Further sampling and analyses would be required to establish stratigraphic suitability for associated mineralization of the other outcropping pyroxene granulites (i.e. at 40E/11N, 26E/11N and 45/14E; See Map No. 4).

The southern granulites are chemically distinct from the Northern granulites and sulphide associated granulite horizons, which also confirms conclusions reached in Section 2.6.

The controversy regarding the presence of a fold closure or two separate sulphide horizons in the K1 area (See Section 2.2.2.) may be solved using this approach; ideally, more analyses are required, but the north and south intersections of the K1 Unit 9 amphibolite cannot be distinguished geochemically, suggesting that they represent a single horizon repeated in the sequence by folding.

5. GENESIS OF THE KIELDER MASSIVE SULPHIDE DEPOSITS

The primary depositional features used in the interpretation of the genesis of the Kielder deposits have been partially obscured by the high grade metamorphism; as in the cases of Copperton (Middleton, 1976; Wagener, 1980), Broken Hill, N.S.W. (Stanton, 1972) and the Scandinavian deposits (Vokes, 1976). In spite of the steeply-dipping and complex nature of the regional structure (not discussed in detail for lack of data) the stratigraphic "way-up" was determined using metal and mineralogical zoning within the massive sulphides and recognition of an alteration zone.

Some caution is necessary in the classification of these deposits based on metal ratios and associated wall rocks because these parameters may vary on regional and global scales. The regional variation of metal ratios has been documented by Stanton (1972) and the variation in the host rock association outlined by Hutchinson (1979) and Sangster (1979).

All the classification schemes and genetic models for massive base metal sulphide deposits are based on occurrences in North America, Japan, Europe and Australia. Nevertheless, it will be seen in the following sections that the Kielder deposits can be classified as exhalative stratabound massive sulphides, as defined by Large, (1977), Plimer (1978) and Sangster (1979).

5.1. Characteristic Features of the Mineralization

5.1.1. Vertical Mineralogical and Metal Zoning

The K3 massive sulphide unit (See Fig. 3, Section 2.1) has a pyrrhotite-rich top, barite toward the bottom and a zinc-rich base. Lead is vaguely concentrated toward the top and silver appears to vary randomly throughout the sulphide unit. Copper, although present in minor quantities, shows an increase (from 0.2% to 0.5%) toward the base of the sulphide zone. Within the K1 massive sulphide mineralogical zoning has not been detected but the zinc tends to increase toward the base; the lead and silver contents are higher in the top of the unit (See Fig. 5, Section 2.2.). The massive sulphide of the K6

area lacks any mineralogical or metal zoning but the felsic stringer zone with galena and chalcopyrite (both rich in silver) underlies the massive sulphide.
The usual zoning pattern in exhalative massive sulphides according to Large (1977) and Sangster (1979) is:

(i) Primary pyrrhotite is usually found in the footwall and base of the massive sulphide.
(ii) Magnetite is found in the footwall rocks usually with chalcopyrite.
(iii) Galena is usually found towards the top of massive sulphide.
(iv) Barite and sphalerite are concentrated toward the top of the massive sulphide lens.

Assuming this zoning is universal, the K3 stratigraphy is inverted and this is supported by the presence of an alteration zone presently overlying the massive sulphide (i.e. hanging wall Unit 9). The subtle metal zoning in the K1 sulphides also suggests inversion of the stratigraphy and is similarly supported by evidence of an alteration zone in the hanging wall, whereas in K6 the felsic stringer zone below the massive sulphide and the B.I.F. in the hanging wall rocks suggest a normal stratigraphic sequence. Large (1977) states that, except for the cupreous pyrite type deposits, no reverse zonation has been reported in exhalative massive sulphides. The metal/mineralogical zoning was used to establish the stratigraphic "way-up" in the Geco deposit (Suffel, et al. 1971).

5.1.2. Lateral Mineralogical and Metal Zoning

Lateral metal zoning within the massive sulphide units of Kielder is not observed. In the case of the K3 massive sulphide lens the Cu/Zn ratio varies randomly from .06 to .10. The absolute abundances of the individual sulphide species do not appear to vary laterally within any of the three occurrences. The massive sulphide lens in the K3 area changes laterally in all directions into disseminated iron sulphides within a quartz-cordierite rock (Unit 10, Appendix I) which also contains occasional massive sulphide pods varying in thickness from 10cm to 1.0 metre. This

disseminated halo shows marked mineralogical zoning; the Py/Po ratio increases from 2 to 10 and from 2 to 6 away from the edge of the massive sulphide to the west and east respectively. The decrease in the pyrrhotite content is accompanied by an increase in the magnetite content from a pyrrhotite/magnetite ratio of 10 near the massive sulphide to ~1 more than 50m from the ore zone.
The vertical (i.e. perpendicular to bedding) mineralogical/metal zoning (See Section 5.1.1.) and the lateral zoning producing the concentric mineralogical halo described above has been explained by Large (1977). These effects are caused by the mixing of the hydrothermal solutions, which supply the metals and sulphur, with sea water as they move out onto the sea floor with a consequent decrease in temperature and simultaneous increase in pH, fO_2 and ΣS. The envisaged temperature contours surrounding the "hydrothermal system" and the resulting mineralogical zoning (vertical and lateral) are shown in Fig. 33.

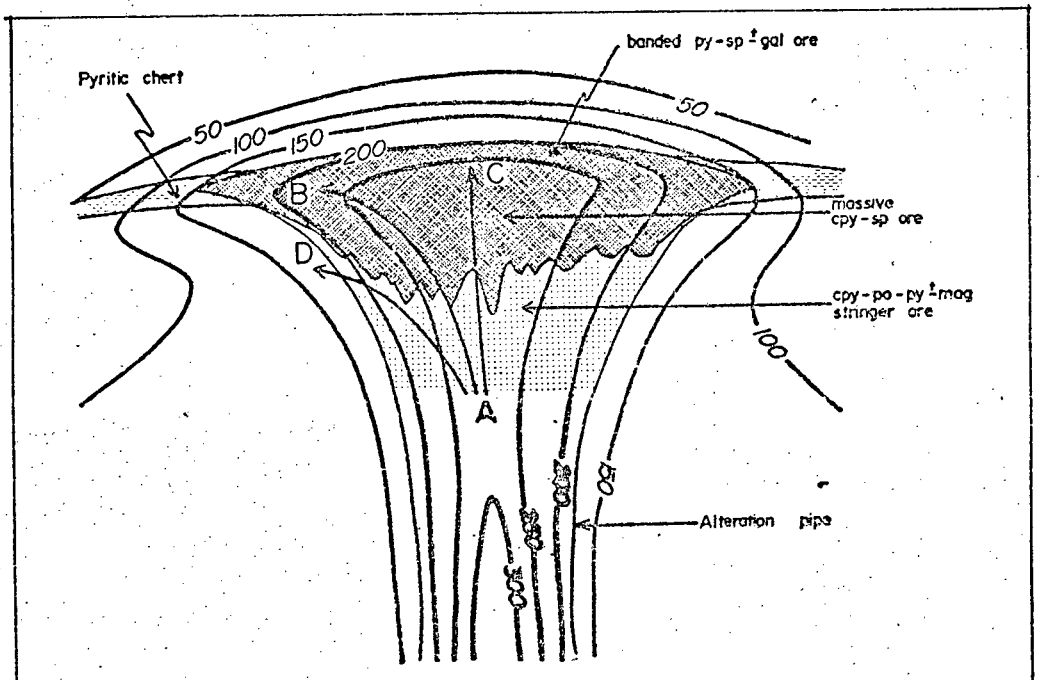

FIG. 33. Idealized temperature regime during the formation of a proximal massive sulfide deposit. Contours in degrees Centigrade.
(after, Large 1977)

The distal (~2 km) facies equivalents of the K1 mineralization (i.e. Units 1, 2 and 3 in Appendix I) found in the upper units

of the K3 area contain up to 12% pyrite and pyrrhotite with no accompanying base or precious metal mineralization. These distal extensions differ from the disseminated sulphide halo closer to the massive sulphides in the following ways:

	<150m from massive sulphide	≥2 kms from massive sulphide
(i)	Py/Po ~2 (up to 10 nearer the ore)	~ 1
(ii)	sillimanite content ~15-25%	~ 0-20%
(iii)	cordierite 15-40%	0-25%
(iv)	occasional massive sulphide pods	fine-grained evenly distributed pyrite and pyrrhotite

The "within deposit" variation in the Py/Po ratio was discussed in Section 5.1.1., but the regional variation in the pyrrhotite presence remains to be explained. There is an almost total absence of pyrrhotite from K1 and only sporadic minor pyrrhotite in the K6 massive sulphide. The traces of pyrrhotite in the K1 and K6 usually occur as fine blebs within coarser pyrite grains. This phenomenon together with the marked pyrrhotite zoning seen in K3 show that primary pyrrhotite was present in the premetamorphic massive sulphides. The pyrrhotite has not been produced solely from the metamorphism of pyrite. It has been suggested (Gehrish, 1975; Plimer and Finlow-Bates, 1978) that primary pyrrhotite records the depositional history, pyrrhotite forming in deeper water more distal from the exhalative centre supplying the metals. On the other hand, Large (1977), supported by evidence in the New Brunswick deposits (Jambor 1979), uses the presence of pyrrhotite as an indicator of proximal deposits (See Section 5.1.5.), based on the mineral-solution equilibria in the Fe-S-O system. There is convincing evidence (See Section 5.1.5.) that the K3 and K1 are proximal deposits as opposed to the K6 which has the characteristics of more distal deposition.

Therefore from the evidence provided by pyrrhotite, the K3 and K1 proximal deposits appear to differ in the depth of water during exhalation, the K3 forming in deeper water than the K1 massive sulphides.

The commonly occurring feature(Plimer and Finlow-Bates, 1978)

of barite occurring with pyrite-rich deposits which supposedly reflects the relative abundance of sulphur in the system was not found in the Kielder deposits. Barite occurs in significant quantities (3% $BaSO_4$, Sphalerite/Barite ~3) in the K3 massive sulphide which contains the larger amount of pyrrhotite (Py/Pc ratio in K3 < K6 << K1). A higher ratio of hexagonal pyrrhotite to monoclinic pyrrhotite polymorphs occurs in the K6 area which also has a higher pyrite content than at K3. This relationship has been noted elsewhere by Plimer (1978).

5.1.3. The "Footwall" Alteration Zone*

In the Kielder deposits the siliceous, Mg-rich cordierite-bearing rock (K3 area; Units 9 and 10 and K1 area Unit 6, See Appendix I) is interpreted to be the metamorphosed equivalent of the chlorite alteration zone normally found adjacent to massive sulphide deposits (Sangster, 1972 and Large, 1977). These rocks can roughly be compared to the dalmatianite of the Noranda Area. Sangster has noted that the exhalative massive sulphides developed in sedimentary sequences are usually underlain by zones of silicification, and less often a zone of magnesium enrichment (more often associated with volcanic hosted sulphides).

Sillimanite-bearing rocks occur persistently as footwall (in the K3 and K1 areas) and hanging wall (K6 area) units. This felsic sillimanite gneiss is basically indistinguishable from its equivalents elsewhere in the sequence. Stanton (1972) attributed the aluminous material found in the footwall of Broken Hill deposit (N.S.W.) to be formerly hydrothermal kaolinite. In the K6 area minor cordierite is found in the footwall and hanging wall rocks; the felsic stringer zone and felsic sillimanite gneiss, respectively. Although rare, some cases of chlorite alteration have been reported to occur above the massive sulphide horizon (e.g. Amulet'A', Quebec, Sangster, 1972). The cordierite-rich zones stratigraphically below the massive sulphide in the K3 area contain disseminated pyrite and pyrrhotite with little Cu-Pb-Zn mineralization although the Cu/Zn ratio is higher than in the massive sulphide unit. In the

* The term '"footwall" alteration zone' is used here following Sangster's (1972) terminology whereby it refers to the alteration zone underlying the massive sulphides at the time of their formation and does not imply the alteration zone to be physically below the massive sulphide in the present configuration.

K1 area the quartz-cordierite rich rock (Unit 6, See Fig. 4. Section 2.2.) contains only disseminated pyrite and pyrrhotite. The present shape of the alteration zone in the K3 area is not known exactly because of the wide spacing of the drill holes, but it varies in thickness concomitantly with the massive sulphide unit thickness. In drillhole KDH 3 (See Cross-Section 1, 54E) the thickest intersection of sulphide was overlain (n.b. stratigraphically below) by the thickest intersection (~15m) of "footwall" alteration zone (Unit 9). Up-dip, in drillhole KDH 2, the alteration zone is much thinner (~6m) and down-dip in drillhole KDH 5 it has pinched out. The alteration zone therefore overlies the massive sulphides asymmetrically. The possibility that the alteration zone has a funnel shape pointing upward (i.e. inverted Fig. 34 (A)) between drillholes KDH 3 and KDH 4 is considered unlikely in view of the extent of deformation of the country rock and sheared massive sulphide/wall rock contacts. The KDH 4 sulphide intersection has been cut off by a fault zone (See Section 54E) and the central section of the K3 massive sulphide lens remains somewhat unknown.

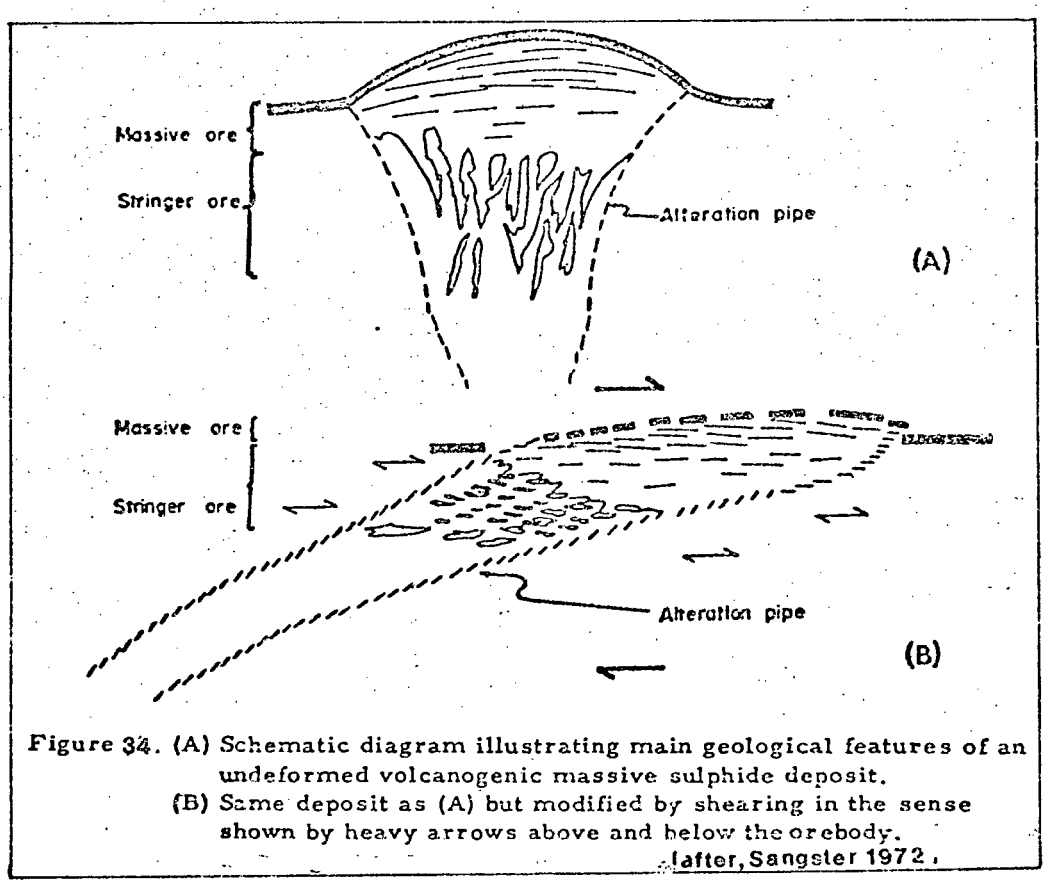

Figure 34. (A) Schematic diagram illustrating main geological features of an undeformed volcanogenic massive sulphide deposit.
(B) Same deposit as (A) but modified by shearing in the sense shown by heavy arrows above and below the orebody.
(after, Sangster 1972.)

The hypothetical cross-section proposed by Sangster (1972, 1979)

to explain the asymmetrical sheared alteration pipes underlying many of the Canadian deposits and the Cobar deposit in New South Wales is considered partially applicable here (See Fig. 34 (B)). The K3 geometry is probably intermediate between (A) and (B) in Fig. 34.
The paucity of drilling in the K1 area prevents similar interpretation of the geometry of the alteration zone in this area. The distal K6 massive sulphide does not have a "footwall" alteration zone.

5.1.4. Tourmaline Distribution

Tourmaline (dravite) is found in minor quantities within the cordierite-rich alteration zone (Unit 9) in the K3 area but not in the massive sulphide. In the K1 and K6 areas zoned tourmaline (with a schorl-rich core) is found within the massive sulphides. A metamorphic origin for the zonation does not explain the distribution in the K3 and K1/K6 areas.

In an explanation of the tourmaline footwall-alteration pipe at the Sullivan Mine B.C., Sangster (1972) envisaged the hydrothermal solutions, rich in Na, Ca, Al, Fe, Mg and Bo to have precipitated tourmaline below the ore horizon but upon reaching the cooler environment above and within the sulphide horizon the solutions would precipitate albite and chlorite with boron being lost to the sea-water. This explanation fits the facts as observed in the K3 area. However in the more distal K6 (and possibly K1) where the massive sulphides may have been transported in a type of turbidity current the presence of zoned tourmaline may be explained differently. The tourmaline, as part of the massive sulphide gel, continued to crystallize as the mass slid down the slope under changing temperature (and pH and Eh) conditions, thereby becoming zoned with an iron-poor rim.
This process of turbidity currents was envisaged by Jambor (1979) in the genesis of the New Brunswick "distal allocthanous massive sulphides" which were deposited "distant from the hydrothermal conduits". The abundant textural evidence of transportation of particulate sulphides in the New Brunswick ores would not have survived the Kielder metamorphism.

5.1.5. Wall Rocks and their Depositional Environment

The following diagrammatic representation (Fig. 35) of the wall rocks expressed as pre-metamorphic equivalents is based on interpretations discussed in Sections 3.2.2. and 4.2.1. The correct stratigraphic sequence or "way-up" is deduced from the mineralogical and metal zoning and "footwall" alteration zones discussed in Sections 5.1.1. and 5.1.2.

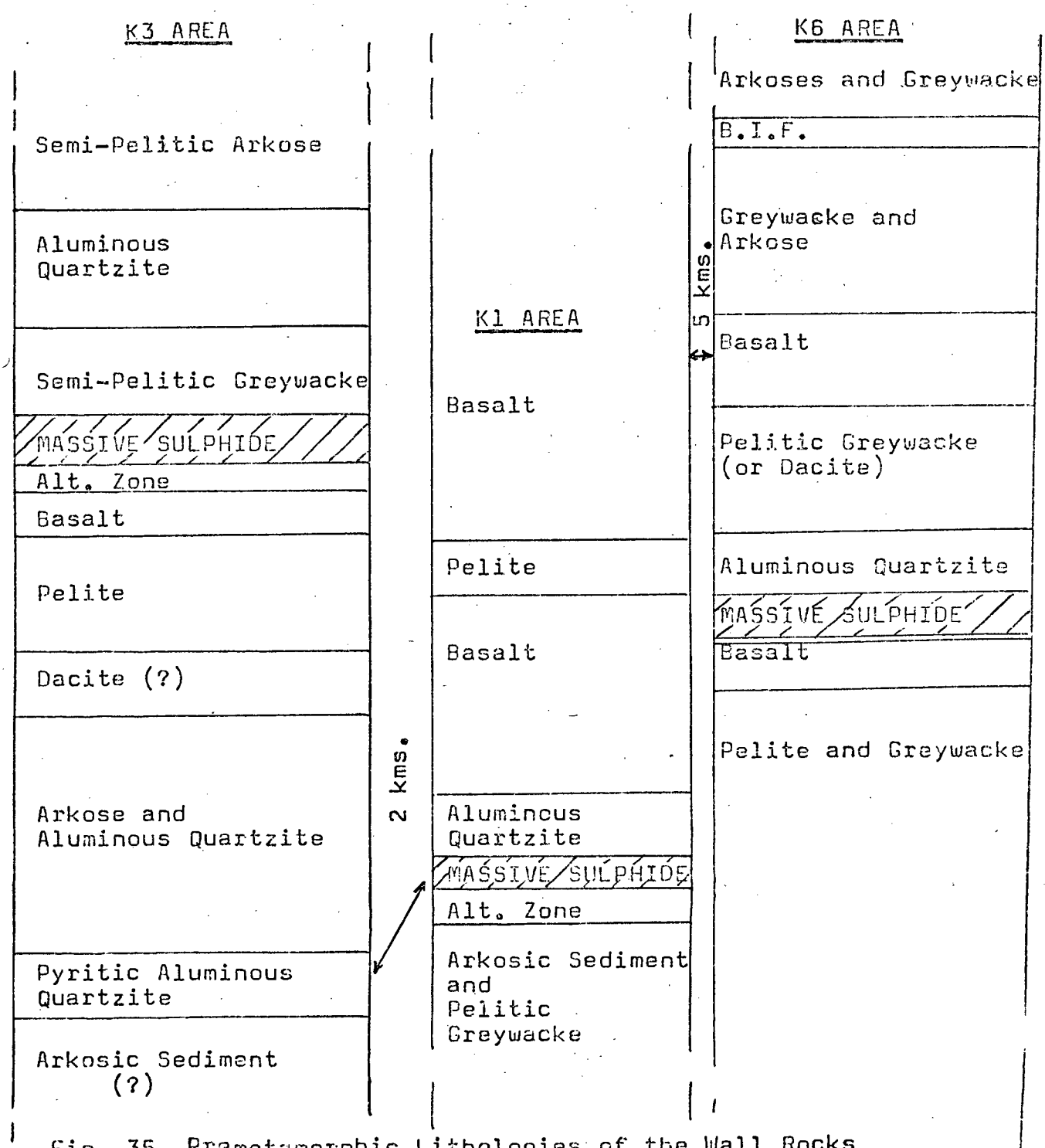

Fig. 35. Premetamorphic Lithologies of the Wall Rocks

The transitional host rocks between the felsic/intermediate volcanic Noranda-type mineralization and the entirely sedimentary association of the Sullivan deposit are described by Sangster and Scott (1976) as typically being volcanic sediments, sedimented volcanics, slightly reworked tuffs and tuffwackes. At the grade of metamorphism attained at Kielder the recognition of these "sediments" by trace or major element geochemistry would be difficult. However, in the Kielder wall rocks the geochemical data have indicated probable igneous rocks (amphibolites) and sedimentary rocks (hypersthene granulites). Other rock types such as the B.I.F. and felsic sillimanite gneiss are assumed to be sedimentary from their mineralogy. A spectrum of intermediate rock types exists in the Kielder wall rocks which is likely to have a similar origin to those described above as volcanic sediments (Sangster and Scott, 1976).
It is important to note in the more recent publications (Sangster, 1979; Hutchinson,1979; Jambor, 1979) that the application of exhalative massive sulphide genetic theory is applied across the entire spectrum of volcanic to sedimentary host rocks (e.g. Sullivan Mine, Cobar Mine, Tasmanian tin and base metal deposits).
The position of massive sulphide mineralization within the Kielder sequence of pelites, greywacke, arkose, quartzite and basalt appears unrelated to any stratigraphic marker indicating an hiatus or change in depositional style. The K3 sulphide is underlain by a narrow basalt horizon, the K1 sulphide is overlain by a significant thickness of basalt and the K6 has a thin basaltic base and a unit of basalt in the hanging wall of variable thickness. A correlation between the K1 and K6 basalts is possible based on geochemical similarity and outcrop evidence. The mineralization appears then to "migrate" laterally and vertically within the host sequence and to be controlled by the position of the exhalative centre, which is not restricted in time and/or space, and to be independent of the basalt outpourings.
Large (1977) used the following scheme to classify the distal and proximal types of exhalative deposits:

Criteria Used	Proximal Ores	Distal Ores
1. Metal Content	Cu-rich (with Au); Zn may be present in economic quantities Pb generally low (K3 and K1)	Pb-Zn rich.Cu poor. (K6)
2. Alteration	Underlain by a distinct alteration zone (pipe) (K3 and K1)	No distinct foot-wall alteration (K6)
3. Iron Sulphides and Oxides	Pyrite and Pyrrhotite dominant, Sulphides, Magnetite in footwall (K3)	Pyrite dominant, (K1?). Pyrrhotite absent, Magnetite may be in hanging wall (K6)
4. Form	Pipe like or mushroom shaped, generally massive and cross cutting. Banding only in hang-ing wall.	Well banded, strati-form and blanket shaped (K6?)
5. Zoning	Good zoning, Cu toward footwall. Zn/Cu increases upward. (K3)	General lack of zoning. (K6)

Massive sulphide deposits formed in more distal environments are likely to be less "massive" (Jambor, 1979), the less dense K6 and K1 massive sulphide units can therefore be taken as further evidence of their distal nature.
The diagrammatic representation shown in Fig. 36 summarises the depositional environment envisaged for the K3, K1 and K6 massive sulphide units.

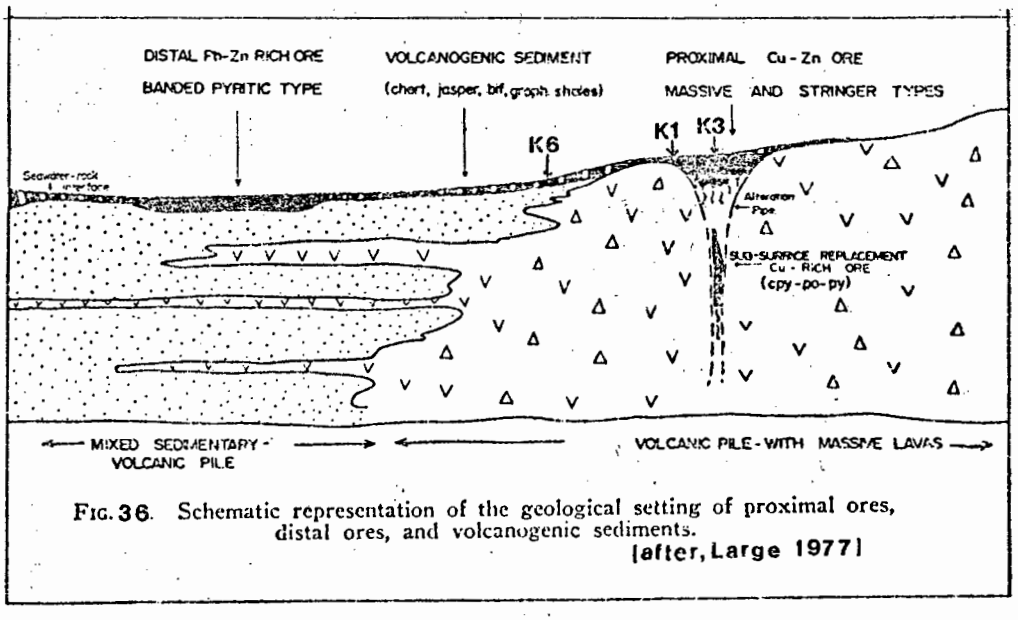

FIG. 36. Schematic representation of the geological setting of proximal ores, distal ores, and volcanogenic sediments.
(after, Large 1977)

The K6 is placed between the proximal and distal types because of its intermediate characteristics. Jambor, (1979) envisages a complete spectrum between Large's (1977) two end members and this type of gradational change appears to be present between the Kielder deposits. Conflicting evidence exists for the relative depth of water during deposition of the three massive sulphide bodies.
The deeper water deposition from the K3 to the K6 area shown in Fig. 36 is supported by the higher copper content of the latter area (K3 Cu $\leq$0.45%, K6 Cu $\leq$1.5%) in that the greater pressure of the deeper water prevents boiling of the hydrothermal solutions and resulting precipitation of chalcopyrite in the hydrothermal feeder zone (Large, 1977; Plimer and Finlow-Bates, 1978).
The evidence provided by pyrrhotite (See Section 5.1.2.), using Plimer's (1978) postulation that pyrrhotite is formed in deeper waters, does not fit the picture presented here. However it should be noted that Fig. 36 represents a diagrammatic comparison between the areas of mineralization and does not imply that the three bodies formed from the same exhalative vent. In fact it has already been shown that the zones are not stratigraphically equivalent. Consequently the K3 massive sulphides may well have formed in deeper water as opposed to K1 and K6.

5.1.6. The Manganese Halo

The higher manganese content of the K6 wall rocks (See Appendix III) as reflected in the MnO content of the garnet is in accordance with the distal nature of K6 massive sulphide environment. The ability of a manganese halo to 'survive' the granulite conditions attained at Kielder can be deduced from the Sections 3.3. and 4.2. and has been shown to exist around other metamorphosed massive sulphide deposits (e.g. Gamsberg, N. Cape; Stumpfl, 1979, Broken Hill, N.S.W.; Plimer 1977).
There is a symmetrical manganese-rich halo surrounding the K1 ore body (See Fig. 37 and Table VII).

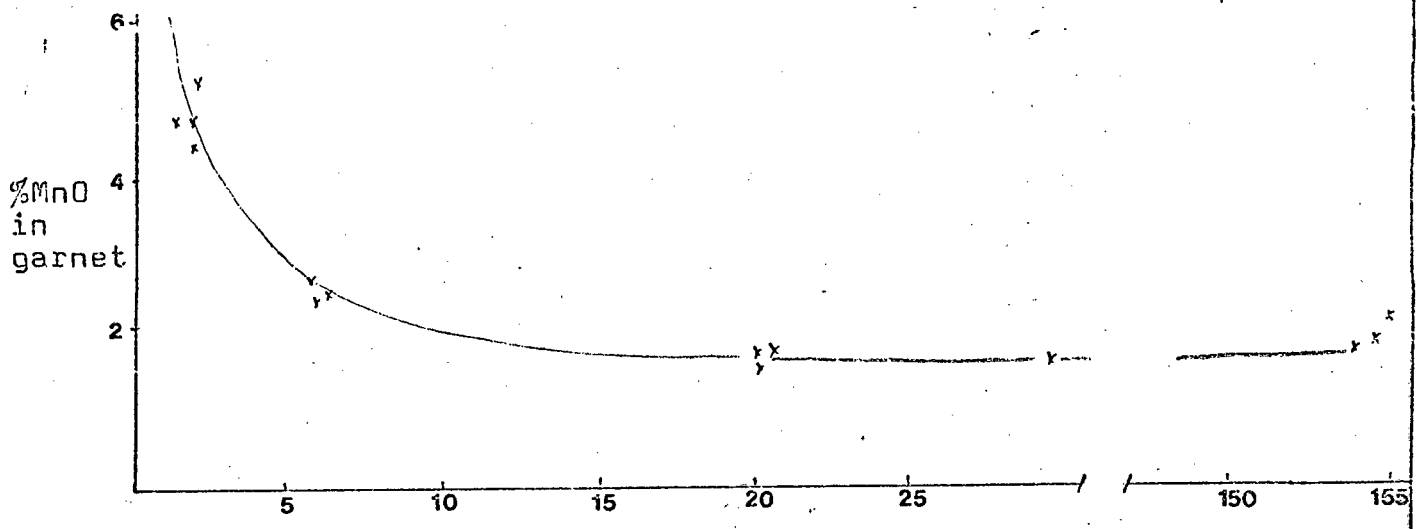

Fig. 37 Variation in the manganese content in garnets approaching the K1 massive sulphide unit.

Insufficient data exist for the K3 and K6 areas but a similar situation is suggested. The halo is restricted to within 5m of the massive sulphide, is narrower than that found at Gamsberg or Broken Hill, N.S.W., and probably reflects the smaller size of the Kielder bodies.

TABLE VII. The Manganese Content of the Wall Rock Garnets.

AREA K3			AREA K1			AREA K6		
Sample No. (RKG)	% MnO	Distance* from ore (m)	Sample No. (RKG)	% MnO	Distance* from ore (m)	Sample No. (RKG)	% MnO	Dist.* from ore (m)
111	2.95	+15	190	2.87	+160	288	14.49	-4
111	2.75	+15	190	2.82	+160	288	14.16	-4
71	2.30	-33	190	2.81	+160	288	13.08	-4
71	2.34	-33	190	2.91	+160	255	7.36	+1
71	2.14	-33	190	2.95	+160	255	7.43	+1
71	2.51	-33	190	2.84	+160	298	9.82	+25
71	2.24	-33	209	4.69	-2	298	7.91	+25
10	2.43	-50	209	4.80	-2	298	9.24	+25
10	2.46	-50	209	4.41	-2	217	3.37	-27
			209	5.16	-2	217	3.42	-27
			209	4.48	-2	217	3.53	-27
			199	1.78	+20			
			199	1.75	+20			
			179	2.53	-6			
			179	2.71	-6			

*(- refers to distance into hanging wall)

*(+ refers to distance into footwall.)

The manganese halo as an exploration tool (as suggested by Stumpfl, 1979) should be used with caution in view of:
(i) its narrowness (i.e. <5m wide)
(ii) the trend of distal deposits to be more Mn-rich.

5.1.7. Associated Intrusives

The granodiorite bodies which cross-cut the stratigraphy in the K3 area (See Cross-section 1, 54E) are definitely intrusive (See Section 2.1.4.). The poorly-foliated texture suggests a late-tectonic intrusion or possibly a pretectonic intrusion which because of its mineralogy did not become strongly-foliated. These intrusives are only present in the proximal K3 area.
The presence of granitic to basic intrusions has been loosely linked, genetically, with massive sulphide mineralization (e.g. Geco deposit; Suffel et al. 1971 and the Sullivan deposit, pers. comm. mine geologists). Sangster and Scott (1976) state "Within many regions of massive sulphide deposits it is not uncommon to find major intrusions of ultramafics, gabbro, diorite, granodiorite and even granite. Felsic intrusions are usually found as large stocks at or near the centre of the volcanic pile. As such they may represent part of the magmatic hearth which originally spawned volcanism and later moved upward to intrude its own daughter products". The presence of more ultrabasic-tending amphibolite (with disseminated pyrite and pyrrhotite and nickel contents≈1000-1500ppm) are known to occur in the extreme North-east of the Kielder area, 1000-1200 meters below the massive sulphide mineralization. These may correspond to the ultra-basic sills which are postulated in the model proposed by Suffel et al. (1971), for the Manitouwadge massive sulphide deposits.

5.2. COMPARISON WITH EXHALATIVE MASSIVE SULPHIDE MODELS

5.2.1. Stanton's (1972) Model

In Stanton's (1959, 1972) descriptions of this ore type the following features typified massive sulphide deposits:
(i) Form: usually lensoid with the two larger dimensions

approximately the same with the lesser dimension an order of magnitude smaller.
The shape of K3 (insufficient drilling on K6 and K1 prevent a shape prediction) fits these dimensions (i.e. 200 x 250 x 15m). The more irregularly shaped rods, plates and boudinaged bodies described at Broken Hill (Stanton, 1972), Scandinavian deposits (Vokes, 1976) and Copperton (pers. comm. Wagener) were not identified at Kielder. However these may be detected if more detailed drilling were completed. Stanton (1972) noted a frequently-occurring phenomenon of semi-continuous en echelon arrangement of sulphide bodies as a particular facies "migrates laterally up the sequence".
The en echelon arrangement of K3, K1 and K6 massive sulphide lenses has been described in Section 2.6. and 5.1.5.

(ii) Setting: a broad association of massive sulphides with volcanic and sedimentary rocks of marine origin. This feature fits the Kielder setting and has been discussed in Section 4.

(iii) Metal Constitution: the following subdivisions were established:

a) Fe
b) Fe-Cu
c) Fe-Cu-Zn
d) Fe-Cu-Zn-Pb

The K1 and K3 correspond to c) and K6 possibly to d).

(iv) Mineralogical Constitution: is typically simple with the common sulphides being pyrite, pyrrhotite, sphalerite, galena and chalcopyrite with minor marcasite, arsenopyrite, tetrahedrite, bismuth minerals and the non-sulphide minerals are magnetite, carbonate, barite, apatite and fluorite.

Except for arsenopyrite, tetrahedrite and fluorite the Kielder sulphides contain the typical suite as listed above. The trend for increasing mineralogical complexity with metamorphic grade (McDonald, 1967 and Stanton 1972) has not been found in the Kielder deposits which agrees with Sangster's (1972) findings in other deposits.
In the Kielder deposits no cassiterite or discrete silver minerals were detected and in the silver-bearing portions of

the ore zones semi-quantitative microprobe analysis showed galena to hold silver in solid solution and chalcopyrite to occasionally contain minute blebs (~10 microns) of silver.

5.2.2. Sangster and Scott's (1976) Model

This model empirically divides the massive sulphides into three groups based on host rock association without any genetic implication. The host rock associations are:

(i) predominantly volcanic rocks
(ii) predominantly sedimentary rocks
(iii) mixed volcanic and sedimentary lithologies

This simple classification scheme is based upon the exhalative concept with a common genesis for all three types, and that the differences in the lithology (of the footwall rocks) cause relatively minor "second order perturbations" on the resulting massive sulphide deposit. The Kielder deposits are classified in this system as type (iii).

5.2.3. Solomon's (1976) Model

This system is based on the volcanic rock type in the footwall with further subdivisions into metal ratio types. The classification scheme is shown on Fig. 38, and the Kielder deposits fall into the Zn-Cu type. Here a mafic sedimentary association is rare (at least in Solomon's sample of 50 deposits) but nevertheless does occur. The tholeiitic basalts of oceanic origin

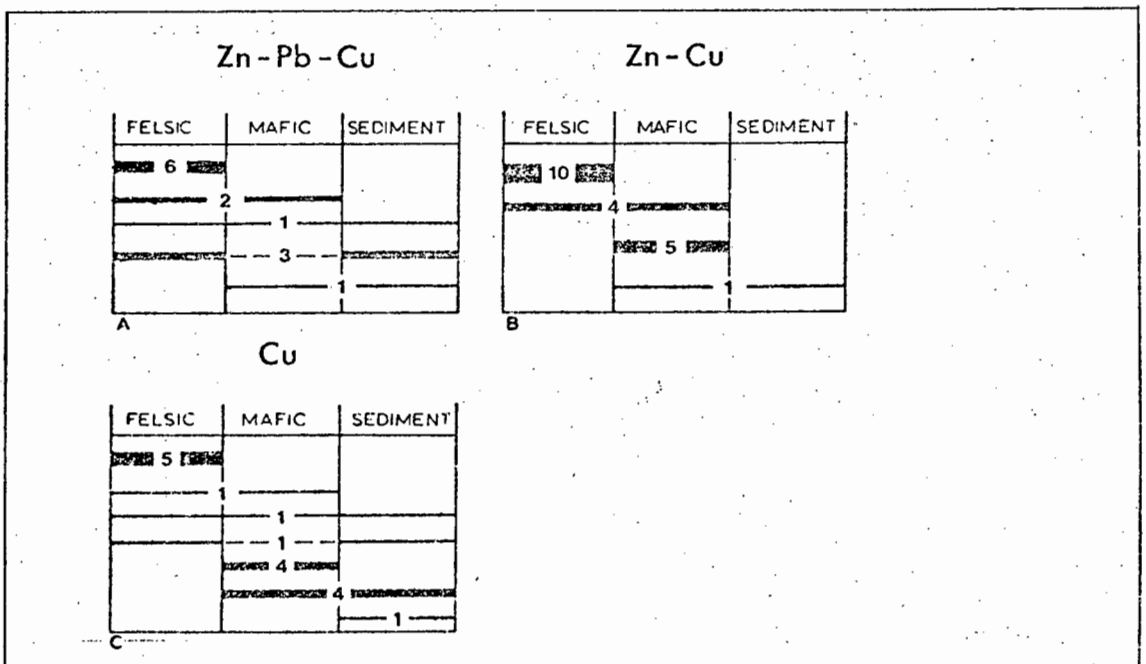

Fig.38 Diagram to illustrate the nature of the footwall rocks to massive sulphides, from a study of 50 deposits: [after: Solomon, 1976]

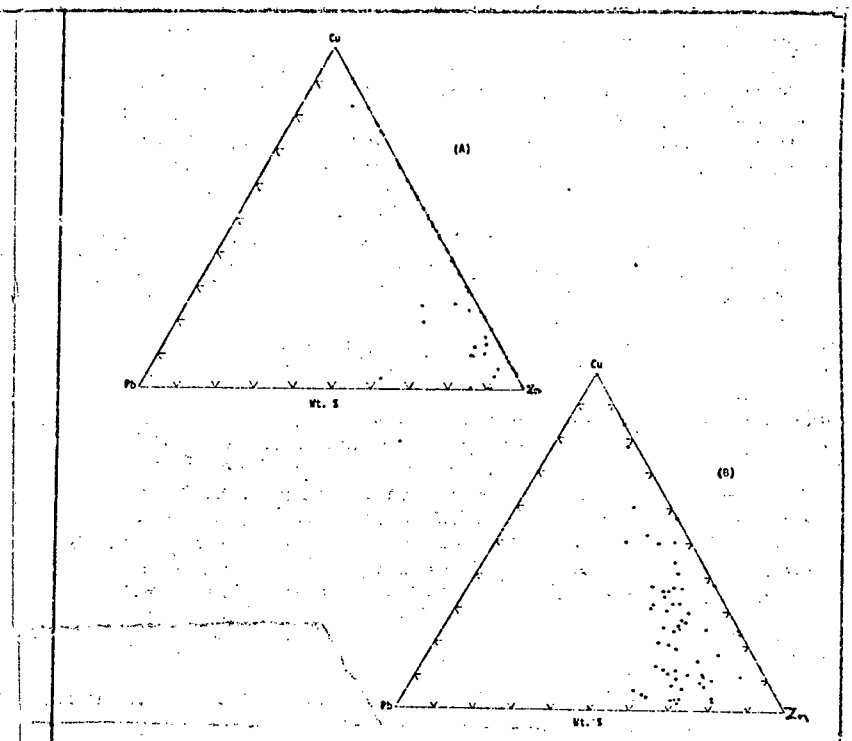

Weight ratios of Cu, Pb and Zn in: A. North American Precambrian massive sulfide deposits in volcanic or volcano-sedimentary host rocks; B. Canadian and Japanese Phanerozoic massive sulfide deposits in volcanic or volcano-sedimentary rocks;

(After Sangster and Scott, 1976).

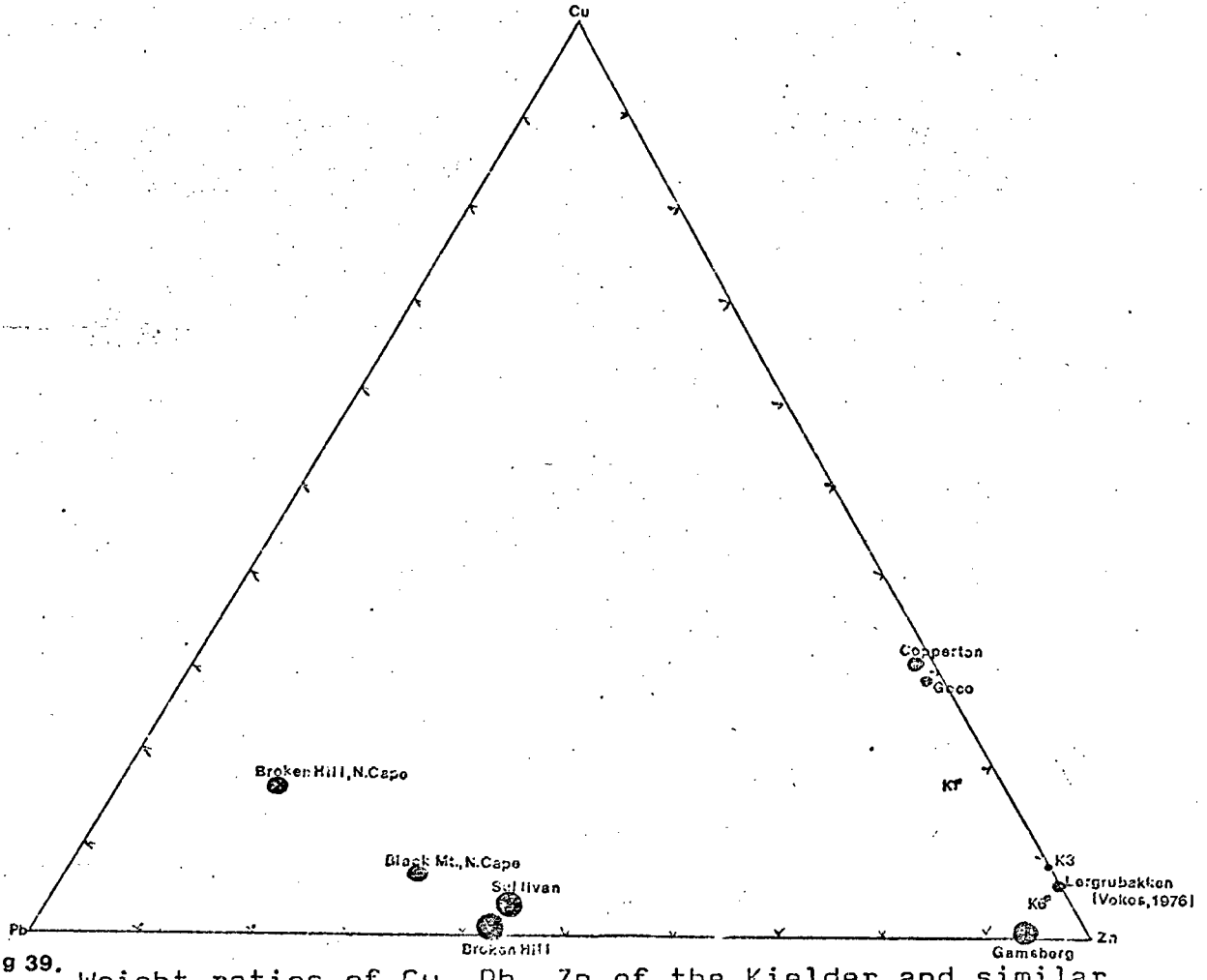

Fig 39. Weight ratios of Cu, Pb, Zn of the Kielder and similar deposits. The size of the dots indicate the relative size of the ore bodies.

of the Kielder wall rocks (Section 4.2.2.) agree with Solomons composition for the associated basic rock.

Solomon postulated that the tholeiitic basaltic magmatism associated with Cu-Zn massive sulphides and clastic sedimentary types (Besshi Type) which are found in the arc "front" of the Kuroko deposits proper may be a forerunner to the Kuroko-type ore-forming event.
The Kielder deposits are plotted on a Cu-Pb-Zn ternary diagram with other deposits to show their composition with respect to previously described bodies. (See Fig. 39).

5.2.4. Hutchinson (1973, 1978)

Hutchinson (1973) defined volcanogenic massive sulphide deposits as: "stratabound, lenticular bodies of massive pyritic mineralization containing variable amounts of chalcopyrite, sphalerite and galena in layered volcanic rocks".
He subdivided the group into three varieties based on their elemental and mineralogical composition, relative and absolute ages, and their host rock association.
The three subdivisions are:

Type 1. Pyrite-sphalerite-chalcopyrite in mafic to felsic volcanic rocks, found in Archean greenstone belts.

Type 2. Pyrite-galena-sphalerite-chalcopyrite in more felsic calc-alkaline volcanics in Proterozoic sequences.

Type 3. Pyrite-chalcopyrite in mafic ophiolites of Phanerozoic age.

Hutchinson (1973) explained the differences between the three types in terms of evolution of the earth's crustal tectonism. The earliest type (Type 1) formed under primitive "proto-crustal" conditions, with the associated volcanics forming from a thick undifferentiated mantle. This produced the thick mafic platform with felsic domes around which the massive sulphides formed. In the Proterozoic when eruptive volcanism became more rare with increasing crustal thickness, epiclastic sedimentation became more extensive. However in deeper

basins (eugeosynclines, rift controlled basins) volcanism from the differentiated mantle produced tholeiitic and basaltic lavas. Locally, in shallower shelves flanking these basins more felsic eruptive centres developed, around which massive sulphides were deposited. The third type, (cupreous-pyrite) developed in Phanerozoic time under plate tectonic activity similar to the present day.

The reappearance of types 1 and 2 in later time is explained by Hutchinson as a "recreation of the Archean type proto-crust" in the vicinity of subduction zones producing felsic domes on basic platforms. In the later "regenerated type 1 deposit" the associated precious metal appears to be gold and not silver and gold.

In later publications (Hutchinson, 1978) expanded on the presence of "massive sulphides" (as described above) existing with predominantly sedimentary sequences in which volcanic rocks are not essential. The exhalative sedimentary massive sulphide concept and terminology were pioneered by Oftedahl (1958) and Ridler (1971). The massive sulphide is envisaged to have been deposited as a gel-like precipitate on the sea floor from heated exhaled metalliferous brines which were probably produced from convection of sea water in sub-seafloor rocks (sediments and/or lavas). The exhalative fumaroles are observed in the present day in the Pacific Galápagos rift (Corliss, 1979) and Red Sea (Degens and Ross, 1969).

In view of this simplified model of the origin of exhalative massive sulphides it can be seen that the divisions between sedimentary and volcanic "types" is arbitrary and a whole spectrum of host rocks may be present. The Kielder deposits, which are compared with a list of characteristics for massive base metal sulphide deposits (Table VIII) (from Hutchinson, 1978) appear to have an intermediate position.

The age of the Kielder host rocks is controversial (See Section 1.4.) with isotopic data indicating ages of 1300 m.y.. The Kielder deposits are not considered to be part of a "regenerated Archean tectonic condition" because of the large size of the related Copperton deposit (47 million tonnes) and the high Ag/Au ratio of both Copperton and Kielder.

TABLE VIII.

CHARACTERISTICS OF MASSIVE BASE METAL SULPHIDE DEPOSITS (AFTER HUTCHINSON, 1973)

	IN(META) SEDIMENTARY ROCKS	IN(META) VOLCANIC ROCKS	THE K3 AREA*	THE K1 AREA*	THE K6 AREA
FORM	LENTICULAR "MASSIVE" BODIES STRATABOUND AND STRATIFORM	LENTICULAR "MASSIVE" BODIES STRATABOUND	LENTICULAR STRATABOUND	LENTICULAR STRATABOUND	LENTICULAR STRATABOUND
METALS -BASE -PRECIOUS	Zn AND Pb Ag	Cu ± Zn ± Pb Ag AND Au	Zn ≫ Cu TRACE Ag	Zn>Cu≫Pb TRACE Ag	Zn>Cu>Pb MINOR Ag
ASSOCIATED ROCKS -VOLCANIC -SEDIMENTARY	MINOR OR NONE MAJOR: THICK SEQUENCES -ARGILLITES, TURBIDITES PREDOMINANT -"IRON FORMATIONS" PRESENT	MAJOR: THICK SEQUENCES MINOR, BUT PRESENT -VOLCANOCLASTIC, "IRON FORMATIONS" RELATIVELY MORE ABUNDANT	MINOR OR NONE MAJOR: ARGILLITES, PELITIC GRAYWACKS NO B.I.F.	BASALTIC HANGING WALL WITH PREDOMINANTLY PELITIC FOOTWALL	BASALTS IN PELITIC AND ARKOSIC GRAYWACKS
STRATAGRAPHIC RELATIONSHIPS TOP ↑ BASE	IRON FORMATIONS MASSIVE BODY SULFIDE-IMPREGNATED ALTERATION "PIPE"	IRON FORMATIONS MASSIVE BODY SULFIDE-IMPREG-NATED ALTERATION "PIPE"	MASSIVE SULPHIDE BARREN ALTERATION PIPE	MASSIVE SULPHIDE BARREN ALTERATION PIPE	B.I.F. MASSIVE SULPHIDE NO ALTERA-TION
MINERAL ZONING TOP ↑ BASE	PYRITIC TOP MASSIVE SPH-GALENA ORE MASSIVE PYRRHOTITE DISSEM. PYRRHOTITE (SULLIVAN)	PYRITIC TOP MASSIVE SPH OR SPH-GAL ORE MASSIVE CHALCOPYRITE ORE DISSEM. CHALCO-PYRITE ORE	PYRITIC TOP SPHALERITE ORE PYRRHOTITE BASE	POOR ZONING POSSIBLE Zn RICH BASE	POOR ZONING
PRIMARY TEXTURES	VERY REGULAR BANDING, BEDDING SEDIMENTARY STRUCTURES COMMON BRECCIATION PRESENT	IRREGULAR BANDING TO MASSIVE SEDIMENTARY STRUCTURES PRESENT BRECCIATION COMMON	NOT RECOGNIZED	NOT RECOGNIZED	NOT RECOG-NIZED
LATER METAMORPHISM	WIDELY VARIABLE FOLDING, RECRYSTALLI-ZATION ETC. CF. SULLIVAN, BROKEN HILL.	WIDELY VARIABLE FOLDING, RECRYSTALLIZATION ETC. CF. KIDD CREEK, GECO.	GRANULITE FACIES	GRANULITE FACIES	GRANU-LITE FACIES
AGE	LATER PROTEROZOIC CIRCA 1.8 B.Y. (?) BROKEN HILL (1.8 B.Y.) SULLIVAN (1.3 B.Y.) FARO-DYNASTY(CAMBRIAN?)	ARCHEAN, EARLY PROTEROZOIC, PHANEROZOIC NORANDA, TIMMINS, ETC. (2.5 B.Y.) VERMILION, ERRINGTON (1.8 B.Y.) UNITED VERDE, ETC. (1.8 B.Y.) MT. ISA, "LOWER PROTEROZOIC" (?) NEW BRUNSWICK (ORDOVICIAN) W. SHASTA (DEVONIAN) E. SHASTA (TRIASSIC) CYPRUS(CRETACEOUS) JAPAN (TERTIARY)	CONTRO-VERSIAL 1300 M.Y. (?)	CONTRO-VERSIAL 1300 M.Y. (?)	CONTRO-VERSIAL 1300 M.Y. (?)

(* THE K1 AND K3 HAVE AN OVERTURNED STRATIGRAPHY)

The Copperton/Kielder deposits correspond to the Sullivan and Broken Hill (N.S.W.) deposits in their wall rock associations and their isotopic ages. These deposits (Sullivan, Broken Hill and Kielder/Copperton) fit into an era (0.7→1.8 b.y.) significantly free of volcanic hosted massive sulphide deposits (Hutchinson, 1973).

5.2.5. Other Models

The above classifications and theories on the genesis are complemented by Large's (1977) review and further subdivision, based on mineral solution equilibria, in which the exhalative massive sulphide deposits were classified in terms of their proximity (or distality) to the exhalative centre. Large envisaged a massive sulphide deposit as proximal when it overlies an alteration pipe represented by chlorite alteration (Mg metasomatism), silicification and pyrite/pyrrhotite and chalcopyrite stringer mineralization. Frequently deposits, particularly of Hutchinson's type 2 (i.e. Py-ga-sph-cpy in volcanic terrains), have no underlying alteration pipe and these were interpreted by Large as chemical precipitates in shallow depressions in the sea floor far away from the exhalative vent, and in this group he included layered and isolated ore bodies in mixed sedimentary-volcanic sequences.

Large (1977) stressed that the terms distal and proximal should refer to the exhalative centre and not necessarily a volcanic centre. Plimer (1979) argued that the terms should be used relative to a volcanic centre because it is easier to recognize. The Kielder deposits would support Large's classification because although the K3 body has the least amount of volcanism associated with the mineralization, it has all the features of a proximal deposit; whereas K6 has meta-basaltic rocks in both hanging and footwall and yet appears to be a more distal type.

Large (1977) also pointed out that the Kuroko deposits have considerable barite and gypsum (no pyrrhotite or magnetite) compared with the Archean ores, possibly due to increased oxygen fugacity in the later environment. The Kielder deposits have minor barite within the massive sulphide units and primary

pyrrhotite and magnetite are present. No massive barite horizons have been discovered along strike from the massive sulphide horizons on Kielder as was found in the Gamsberg deposit (Rozendaal, 1980).

5.3. REGIONAL DEPOSITIONAL SETTING OF THE KIELDER/COPPERTON REGION

The Copperton ore-body, like the K3 sulphide deposit, is probably a proximal exhalative massive sulphide using the same lines of evidence used for the Kielder deposits (i.e. metal and mineralogical zoning, alteration zones etc.). These proximal deposits were probably formed from separate exhalative vents. In addition the presence of primary pyrrhotite at Copperton also indicates that, like the K3 sulphide, the sulphides were deposited at shallower depths than K1.

The interpretation by Wagener (1980) of the Copperton foot-wall intermediate gneisses to be dacites based on the bulk chemistry and mineralogy is considered inconclusive at granulite grade conditions, particularly when the common lithologies associated with exhalative massive sulphides are described as volcanic sediments, tuffwackes, etc., (See Section 5.1.5.). Like the Kielder stratigraphy, Copperton has definite igneous (tholeiitic basalts) and sedimentary lithologies and a whole spectrum of intermediate types.

The deposition of the sediments (arkose, greywackes, tuffwackes, tuffs, quartzites and pelites) continued at a steady pace interspersed with tholeiitic basalt and possibly dacite (Wagener, 1980) extrusions with only brief pauses of deposition at the time of hydrothermal exhalations. These were not spatially related to volcanism, but perhaps to zones of greater permeability enabling the rise of the brines.

The resulting pods and lenses of massive sulphide and pyritic lateral extensions were not all formed simultaneously but rather at different times during continuing host rock deposition in the succession, giving the observed lateral and vertical distribution.

More important perhaps is to take cognizance of the proximal/distal features and the indicated water depth of each deposit and construct a regional picture from that. Unfortunately any regional interpretation is obscured by the complex structure which is little understood. Nevertheless it appears that the K3 and Copperton deposits developed over their own exhalative plumes (i.e. proximal deposits) on an oceanic ridge. Towards the south-west of this south-east striking ridge on the flanks of the ridge are formed the Annex (Middleton, 1976) and K1 ore bodies, and further away to the north-west the distal K6 sulphides and associated B.I.F. were deposited.

Whether the tholeiitic basalt volcanism initiated an island arc type felsic volcanism as in the Kuroko deposits (Solomon, 1976 ; Horikoshi, 1975 is not known and remains speculation for lack of further regional study.

The Kielder/Copperton region has five known (published) massive sulphide deposits with the Copperton ore body being the largest (at 47 million tonnes; 1.7% Cu; 3.8% Zn) and four sub-economic smaller deposits with unpublished tonnages and grades (K3, K1, K6 and the Annex ore body). These five deposits cover an area with a minimum diameter of 20kms. In a quantitative study of eight provinces in Canada and Japan (Sangster, 1980),the size, metal content and number of deposits within each province were measured and led to the establishment of a statistical model for a classical volcanogenic massive sulphide province. The statistical review revealed that:

(i) each district has an average diameter of 32 kms
(ii) the districts contain 4 to 20 deposits each, with an average of 12 deposits
(iii) the average total base metal content per district is 4.6 million tonnes with a coefficient of variation of 32%.
(iv) ranked in order of size the largest deposit in each district contains, on average, 67% of the total metal and the second largest about 13%. The remaining deposits range downward in decreasing proportions.

The Copperton/Kielder region's statistics compared to the above points are:

(i) a minimum diameter of 20 kms, although the shape in the original study is a complicating factor.
(ii) the number of published deposits to date is 5.
(iii) the average total metal content has not been published for the district but the Copperton deposit contains approximately 2.5 million tonnes metal.
(iv) the tonnages and grades of the smaller deposits have not been published.

Since Sangster's (1980) model is based on felsic/intermediate volcanic associated mineralization some caution should be used in extrapolating to the sedimentary/volcanic hosted Kielder/Copperton deposits. Nevertheless considering the similar exhalative genesis for both types it may well be applicable.

6. SUMMARY

Mineralogical geothermometry and geobarometry indicated that the Kielder massive sulphides and their wall rocks have undergone granulite grade metamorphism. There is a gradient in the P-T conditions of metamorphism between the three areas;

K3 Area : 695°C and 6.0 kbars
K1 Area : 686°C and 5.8 kbars
K6 Area : 590°C and 5.6 kbars

These figures indicate a depth of burial for the K3/K1 area to be approximately 25 kms and in the K6 area to be 20 kms, and the metamorphic conditions straddle the "anatexis in gneiss" line (See Fig. 10). The numerous pegmatites and partial melting textures in the more felsic gneisses, in particular the felsic sillimanite gneiss, are obvious consequences of these high grade P-T conditions. The sphalerite geobarometer if used correctly (i.e. buffered by direct contact with pyrite and hexagonal pyrrhotite grains) gives reliable results which agree with the silicate geobarometers. Retrograde metamorphism, reflected in the zoned cordierite grains and uralitized pyroxene granulites, occurred at lower temperature conditions of 530-560°C. The precursor lithologies of the Kielder wallrocks as suggested by the metamorphic mineral assemblages are similar to the predictions of the bulk rock geochemical data, (i.e. tholeiitic basalt, pelites, pelitic greywackes and Mg enriched pelite).

The range in sulphide grain sizes, in particular the pyrrhotite, reflects the decreasing metamorphic gradient from the K3 to the K6 sulphide bodies. The mean grain size of the sulphides at this grade of metamorphism is relatively coarse (i.e. $\geq$0.85mm). The textural effects of the metamorphism on the sulphide minerals has been shown to be very typical (i.e. the coarse grain size, the uniform 120° triple-junction points, the chalcopyrite exsolution blebs in sphalerite etc.). The Kielder deposits do not show the tendency postulated for higher rank deposits by Rockingham and Hutchinson (1980) to have more abundant pyrrhotite blebs within pyrite. However where pyrrhotite (although rare)

does occur as blebs in pyrite it is in the KZ area where other evidence suggests a pre-metamorphic presence of pyrrhotite. The durchbewegt ('kneaded') texture described by Vokes (1968) is typical in the more silicate-rich Kielder massive sulphides. The sulphide horizons have remained essentially stratabound and the mobilization of the metals involves maximum distances of 1 - 3 metres. Pyrrhotite shows slightly greater mobilization than pyrite and sphalerite. The effect of the metamorphism on sphalerite with respect to its iron content is the basis of the geobarometer and behaves in a systematic manner (i.e. the greater the pressure during recrystallization the lesser the iron content in the sphalerite lattice), (See Figs. 8 and 9). Evidence of reaction between sulphide and gangue minerals during metamorphism is abundant (e.g. pyrite altering to pyrrhotite and magnetite; the ubiquitous presence of rutile which is a product of the reaction between ilmenite and sulphur; the presence of gahnite probably as a result of reaction between sphalerite and aluminous silicates; and phlogopite, another product of silicate/sulphur reaction).

The metamorphic effect on the banded iron formation showed results similar to those displayed by the Broken Hill (N.S.W.) B.I.F. as reported by Stanton and Williams (1978). The within layer and across layer analyses of garnet grains by microprobe show a strong bedding control on the garnet chemistry which has not been homogenized by metasomatic redistribution. The diffusion of elements has taken place only over minute distances (<5mm).

Certain elements (i.e. Al, Mn, Co, Ti, Y, Zr, Mg, Fe, P and Nb) which are generally regarded as immobile under conditions of upper amphibolite grade metamorphism have been shown in this study, using the methods of Beswick and Soucie (1978) and Davies et al. (1979) (See Page 45) to be immobile within the Kielder metamorphites notwithstanding the Granulite grade of metamorphism. Using an empirical method of chemical comparison of immobile elements devised by Davies et al. (1978), basic granulites which are associated with massive sulphides are distinguished from granulites that are apparently not associated with mineralization.

The plots of TiO_2 vs Zr; Y vs Zr and TiO_2 vs Y show significantly different fields for the northern granulites (stratigraphic equivalents of hanging wall meta-pelites) and the southern granulites (which, so far as is known, are not associated with any massive sulphide mineralization).

These discriminant plots may provide a useful, quick and cheap method of distinguishing between basic granulites which are possible host rocks for mineralization. However, like any geochemical exploration method, very careful orientation studies are essential in any new area.

Major and trace element bulk rock geochemistry of the wall-rock amphibolites and basic granulites has indicated the presence of metamorphosed basic igneous rocks, marly pelitic rocks, pelites and in the immediate wall rocks of K3, magnesium enriched pelitic rocks. The mineralogy and metamorphic petrology suggest that other lithologies such as the felsic sillimanite gneiss, quartz-feldspar gneiss and certainly the banded iron formation to be metamorphites with sedimentary parentage. However a range of other lithologies such as the amphibole-hypersthene granulite, some of the quartz-biotite gneisses and the hypersthene-quartz garnet granulite may be interpreted as dacitic or intermediate igneous rocks. In the light of what Sangster and Scott (1976) describe as volcanic sediments (tuff-wackes etc.) typically associated with massive sulphide deposits, it seems unlikely, that at the granulite grade of metamorphism attained at Kielder, it would be easy or even possible to distinguish meta-sediments from meta-lavas of an intermediate composition. Following the latest ideas in the formation of exhalative massive sulphides (Sangster, 1979; Hutchinson, 1979), the wall rocks are not critical to their formation, as massive sulphides typically form in a whole range of host rock associations.

The Kielder base metal sulphide deposits have been shown to be of the stratabound exhalative massive sulphide type. The relatively simple sulphide mineralogy of pyrite, pyrrhotite, sphalerite, chalcopyrite and galena with gangue minerals of barite, chlorite, quartz, apatite and phlogopite is typical of exhalative massive sulphide depcsits, as is the vertical

mineralogical and metal zoning in the K3 and K1 sulphide lenses. Pyrrhotite is concentrated in the stratigraphic base with sphalerite and barite in the massive sulphide stratigraphic top. The K3 and K1 massive sulphide lenses are proximal after Large's (1977) classification criteria. The chlorite/silicification zone which formed below the massive sulphides at the time of their formation has been metamorphosed to a quartz-cordierite rock. Minor amounts of tourmaline are found within the alteration zone of the K3 massive sulphide (cf. Sullivan ore body, British Columbia). Some features of the K6 massive sulphide, namely the absence of an underlying quartz-cordierite alteration zone, and the presence of zoned tourmaline grains are interpreted as evidence of their distal origin. The sulphides, with the tourmaline could have been transported downslope as an unconsolidated particulate mass to be deposited in a shallow depression on the sea-floor distal from the exhalative source.

All three sulphide lenses and their enclosing wall rocks are steeply dipping and the vertical (i.e. perpendicular to bedding) metal/mineralogical zoning and the presence of alteration zones in the hanging wall of the K3 and K1 massive sulphide lenses indicate that these two bodies are overturned. There are no indications that the K6 body is overturned, in fact the evidence suggests a "correct stratigraphic sequence".

The form of the massive sulphide lenses and the associated quartz-cordierite alteration, in the case of K3, has the typical deformed asymmetric shape (See Fig. 34, B. p. 59) which exists in many of the Canadian deposits and the Cobar deposit, New South Wales (Sangster, 1979).

Lateral zoning is not apparent within the massive sulphide pods. However if the classical internal metal zoning were developed with a Cu/Zn ratio higher in the immediate centre of the proximal massive sulphide lens (i.e. directly overlying the exhalative centre, without shearing present) the higher Cu/Zn ratio would be, in the case of the K3 area, located somewhere between drill-holes KDH3 and 4. Due to paucity of drillholes and a fault zone intersecting the KDH4 sulphide intersection, detailed information is lacking in this area.

Lateral mineralogical zoning is well developed immediately beyond the massive sulphide pods in the disseminated pyritic fringes. The pyrite/pyrrhotite ratio increases rapidly away from the edge of the massive sulphide but remains relatively constant further than 100 metres from the massive sulphides. The increasing Py/Po ratio is accompanied by an increase in the magnetite content. The vertical and lateral zoning patterns and the alteration zones are similar to the classical patterns produced by an exhalative hydrothermal system envisaged by Large (1977).

Surface mapping aided by pitting/trenching, drilling and geophysics (magnetics and IP-resistivity) shows that the three sulphide bodies K3, K1 and K6 may occupy different horizons arranged en echelon within the stratigraphic sequence. Poor outcrop prevents detailed structural interpretation, nevertheless the approximate stratigraphic "distance" between them is a maximum of 500m. The eastern pyritic extension of the K1 massive sulphides occurs 300 metres stratigraphically below the K3 massive sulphide pod. The K1 and K3 massive lenses themselves lie ~2000 metres apart. The K6 massive sulphide which is situated 5 kms and 7 kms from the K1 and K3 area respectively, may occur stratigraphically above the K1 mineralization. The relationship between the K3 and K6 is not known but it is possible that the K3 and K6 are stratigraphic equivalents, (or nearly so); with K6 and its associated banded iron formation being the distal facies of the proximal K3 mineralization. The poorly-developed K1 mineralization, which in many respects is intermediate between proximal and distal in its characteristics, is situated between the K6 and K3 deposits, and formed at an earlier time when the exhalative hydrothermal system was still to reach its maximum development.

The presence of basalt increases persistently from east to west. In the K3 area (i.e. extreme east) minor amounts of basalt are found within the hanging and footwall rocks; in the K1 area, basalt is the major constituent of all the younger formations, and in the extreme west (i.e. K6 area) basalt is found in footwall and hanging wall rocks as a major constituent.

The depth of sea-water at the time of hydrothermal exhalations as indicated by the mineralogy and metal ratios is not clear. The two lines of evidence are contradictory. Large (1977) showed higher Cu/Zn ratios in massive sulphides to be indicative of deeper water (i.e. higher pressure) environment. However for Kielder where all the deposits formed from separate exhalative vents (in spite of possible stratigraphic correlations between K3 and K6 they are 7kms apart), it may not be valid to compare metal ratios for deposits which may have formed from fluids of differing chemistry. The postulation of Plimer and Finlow-Bates (1978) that pyrrhotite is an indicator of more distal deposits found in deeper water may equally be questioned here. The distal K6 deposit has insignificant pyrrhotite.

Anhaeusser (1980) emphasised the difference between the Canadian Archean greenstone belt made up of basalt, andesite and felsite (ratio of 6:3:1) and the southern African greenstone belts (i.e. Barberton and Zimbabwe)which are composed of ultramafics, basalt and felsites (ratio of 7:20:1). He concluded that "the metallogenic potential for massive sulphide occurrences in southern Africa is poor". The basic: felsic ratio in the Namaqua metamorphic complex is not known and because of the difficulty in recognizing meta-intermediate igneous rocks may always be in doubt. However the author considers the conclusion of Anhaeusser to be invalid. Massive base metal (Cu-Zn) sulphide deposits are relatively rare in southern Africa but since 1968 massive sulphide deposits of various sizes have been discovered in the Namaqua Metamorphic Complex, including the Kielder deposits in 1976/1977. By way of contrast the Noranda-Rouyn area has been a mining camp since the early part of the 20th century and new deposits have been discovered relatively recently.

Base metal deposits in the Namaqua metamorphic complex may not be as rare as generally thought considering the extreme exploration difficulties, not the least of which is the deep weathering which precludes many of the conventional geophysical tools. The twelve years since the discovery of exhalative type massive sulphide deposits in the Namaqua metamorphic complex is a

relatively short period in terms of exploration in mining districts.

Hutchinson (1979) with reference to the massive sulphide base metal and tin deposits of Tasmania stated, " the geologic setting of these deposits in trough deposited sedimentary and mafic volcanic rocks, suggests another favourable environment for massive sulphide exploration which is quite different from the domal felsic volcanic environment so heavily favoured currently in North America". The author concludes here, that in a similar way the Kielder/ Copperton region, as for any other metallogenic province, should have its own model of host rocks, metal contents and ratios and modes of genesis on which further exploration is carried out.

In comparing an average exhalative base metal massive sulphide domain (Sangster, 1980) with the Kielder/Copperton district it is concluded that potential for further deposits within this limited area is good.

7. ACKNOWLEDGEMENTS

I am indebted to Newmont South Africa Limited and Anglo-Transvaal Consolidated Investments Limited who permitted the study and the use of material and core specimens gathered while in the employ of the former. Without the considerable financial and logistical support of Newmont South Africa this research would not have been possible. I am particularly grateful for the motivation and personal encouragement provided by Vivian Vellet of Newmont. Also I can never express enough thanks to the geologists and field men of Newmont; in particular Pieter Gresse, Geoff Grantham and Syd Fraser for the fine work which contributed to the research. I must single out Nan Kühn and Slakkie Seleane without whose perseverance and 'eagle eyes' the gossan and the Kielder deposits would have remained hidden.

I am also indebted to Newmont South Africa and Newmont Mining Corporation for financing and arranging visits to the Canadian massive sulphide mines and provinces such as the Sullivan Mine; the Noranda Camp; the Kidd Creek Mine and Timmins Camp and the New Brunswick deposits.

My thanks also to Colin Patterson, my supervisor, for the many hours spent reading the earlier scribbled draughts and final manuscripts, correcting and providing positive criticism and suggestions. I must also thank Dave Waters and Dave Reid for critically reviewing the sections on metamorphism and geochemistry respectively, and Peter Walker for proof-reading the final manuscript. I also acknowledge the support given me by members of the Geochemistry Department in particular James Willis and Andy Duncan for the XRF analytical procedures and Dick Rickard for the guidance on the microprobe. Also to John Moore for the help on some analytical aspects and the discussions on North-western Cape geology.

Also my thanks go to the Newmont draughtpersons, Ronel Channer and Brenda Hall for colouring and draughting seemingly endless maps, diagrams and graphs.

Finally, to my wife, Nelleke, whom I can never repay for providing so magnificently for the family on a restricted budget. Also for typing all the early drafts and the final manuscript. The work speaks for itself.

8. REFERENCES

Albee, A.L., 1965, Distribution of Fe, Mg and Mn between Garnet and Biotite in Natural Mineral Assemblages: J. Geol., v. 73, p. 155-164.

Anhaeusser, C.R., 1980, The Relation of Mineral Deposits to Early Crustal Evolution: University of the Witwatersrand, E.G.R.U., Info. Circular No. 149.

Armbrustmacher, T.J., and Simons, F.S., 1977, Geochemistry of the Amphibolites from the Central Beartooth Mountains, Montana-Wyoming: J. Res., U.S. Geol. Surv., v. 5, part 1, p. 53-60.

Arnold, R.G., 1962, Equilibrium Relationships between Pyrrhotite and Pyrite from 325-743°C: Econ. Geol., v. 57, p. 72-90.

—— 1966, Mixtures of Hexagonal and Monoclinic Pyrrhotite and the Measurement of the Metal Content of Pyrrhotite by X-ray diffraction: Am. Mineralogist, v. 51, p. 1221-1227.

Ayres, D.E., 1979, The Mineralogy and Chemical Composition of the Woodlawn Massive Sulphide Ore Body: Jour. Geol. Soc. of Australia, v. 26, p. 155-168.

Bachinsky, D.J., 1976, Metamorphism of Cupriferous Iron Sulphide Deposits, Notre Dame Bay, Newfoundland: Econ. Geol., v. 71, p. 443-452.

Bailey, E.H., and Stevens, R., 1960, Selective Staining of K-Feldspars and Plagioclase on Rock Slabs and Thin Sections: Am. Mineral., v. 45, p. 1020-1025.

Baragar, W., and Goodwin, A., 1969, Andesites and Archean Volcanism of the Canadian Shield: in McBirney A.R. ed., Proceedings of the Andesite Conference Oregon dept. Geology and Mineral Industries, Bull. 65, p. 121-142.

Barth, T.F.W., 1962, Theoretical Petrology, J. Wiley, New York.

—— 1968, Additional Data for the Two Feldspar Geothermometer: Lithos, v. 1, p. 305-306.

Barley, M.E., Dunlop, J., and Glover, J., 1979, Sedimentary Evidence for an Archean Shallow Water Volcanic Sedimentary Facies Eastern Pilbara Block, W. Australia: Earth Planet. Sci. Lett., v. 43, p. 74.

Barton, P.B., and Toulmin, P., 1966, Phase Relations involving Sphalerite in the Fe-Zn-S System: Econ. Geol., v. 61, p.815-849.

Barton, E.S., and Cornell, D.H., 1979, Age of the Marydale Group Banded Iron Formation by the Pb-Pb Method: (Abs) Abstracts of the 18th Geokongress 79 of the Geological Society of South Africa.

Beach, A., 1974, Amphibolization of Scourian Granulites: Scott. J. Geol., v. 10, p. 35-43.

—— and Tarney, J., 1978, Major and Trace Element Patterns Established During Retrogressive Metamorphism of Granulite Facies Metamorphism, Scotland: Precamb. Res., v. 7, p. 325-348.

Beeson, R., 1978, The Geochemistry of Meta-Igneous Rocks from the Amphibolite Facies Terraine of South Norway: Nor. Geol. Tidsk., v. 58, p. 1-15.

Bench, A., and Albee, A., 1968, Empirical Correction Factors for the Electron Microanalyses of Silicates and Oxides: J. Geol., v. 76, p. 382-403.

Berglund, S., and Ekström, T., 1974, Sphalerite Composition in Relation to the Stress Distribution of a Boudinage: Lithos., v. 7, p. 1-6.

Beswick, A., and Soucie, G., 1978, A Correction Procedure for Metasomatism in an Archean Greenstone Belt: Precamb. Res., v. 6, p. 235-248.

Bickle, M. and Pearce, J., 1975, Oceanic Mafic Rocks in the Eastern Alps: Contrib. Mineral. Petrol., v. 49, p. 177-189.

Blain, C.F., and Andrew, R.L., 1977, Sulphide Weathering and Evaluation of Gossans in Mineral Exploration: Min. Sci. Enging., v. 19, No. 3, p. 742.

Bloss, F.D., 1961, An Introduction to the Methods of Optical Crystallography: Pub. Holt, Rinehart and Winston.

Boctor, N.Z., 1978, Evaluation of Sphalerite Geobarometry, Bodenais Ore, Bavaria: Carnegie. Inst. Washington Yearbook 77.

Boorman, R., Sutherland, J., and Chernyshev, L., 1971, New Data on the Sphalerite-Pyrrhotite-Pyrite Solvus: Econ. Geol., v. 66, p. 670-673.

Boorman, R., 1967, Subsolidus Studies in the ZnS-FeS-FeS_2 System: Econ. Geol., v. 62, p. 614-631.

Botha, B.J.V., Grobler, N., and Smit, C., 1977, Major Structural Features of the Area between the Langeberg Range and Kenhardt, Northern Cape Province: Trans. Geol. Soc. S. Afri., v. 80, p. 101-109.

Bristol, C.C., 1979, Application of Sphalerite Geobarometry to Ores from Ruttan Mine: Econ. Geol., v. 74, p. 1496.

Bristow, J.W., 1980, The Geochronology and Geochemistry of Karro Volcanics in the Lebombo and Adjacent Areas: Unpublished Ph.D. Thesis, U.C.T.

Brookes, E., and Coles, D., 1980, Use of Immobile Trace Elements to Determine Original Tectonic Setting of Eruption of metabasalts Sierra Nevada, California: Geol. Soc. Am. Bull., v. 51, p. 665-671.

Brown, P.E., Essene, E.J., and Kelly, W.C., 1978, Sphalerite Geobarometry in the Balmat-Edwards District, New York: Am. Mineralogist, v. 63, p. 250-257.

Cabri, L.J., McLean, W.H., and Scott, S.D., 1974, Comments on "Metamorphism at Normetal Mine, N.W. Quebec".: C.I.M. Bull., v. 67, p. 158-159.

Cann, J.R., 1970, Rb, Sr, Y, Zr and Nb in Some Ocean Floor Basaltic Rocks: Earth. Planet. Sci. Lett., v. 10, p. 7-11.

Coates, C., Clark, L., Buchan, R., and Brumner J., 1970, The Geology of the Cu-Zn Deposits of Stall Lake Mines, Snow Lake, N. Manitoba: Econ. Geol. v. 65, p. 970-984.

Campbell, F.A., and Williams, K.L., 1968, Composition of Sphalerite from Quemont Mine, Quebec: Econ. Geol., v. 63, p. 824-831.

Campbell, F.A., and Ethier, V., 1974, Sulphur Isotopes, Iron Content of Sphalerites and Ore Textures in the Anvil Ore Body, Canada: Econ. Geol., v. 69, p. 482-493.

Campbell, F.A., Ethier, V.G., and Krouse, H.R., 1980, The Massive Sulphide Zone: Sullivan Ore Body: Econ. Geol., v. 75, p. 916-926.

Condie, K.C., 1967, Geochemistry of Early Precambrian Greywackes from Wyoming: Geochem. et Cosmo. Acta, v. 31, p. 2135-2149.

Condie, K.C., Viljoen, M., and Kable, E., 1977, Effects of Alteration on Element Distribution in Archean Tholeiites from the Barberton Greenstone Belt, South Africa: Contrib. Mineral. Petrol., v. 64, p. 75-89.

Corliss, J.B. et al, 1979, Submarine Thermal Springs on the Galápagos Rift: Science, v. 203, p. 1073-1083.

Constantinou, G., and Govett, G., 1973, Geology, Geochemistry and Genesis of the Cyprus Sulphide Deposits: Econ. Geol., v. 68, p. 843-858.

Cornell, D.H., 1975, Petrology of the Marydale Metabasites: unpub. Ph.D. thesis, Univ. Cambridge, U.K.

Currie, K.L., 1971, The Reaction 3 Cordierite = 2 Garnet + 4 Sillimanite + 5 Quartz as a Geological Thermometer in the Opinicon Lake Region, Ontario: Contrib. Mineral. and Petrol., v. 33, p. 215-226.

Davies, J.F., Grant, R., and Whitehead, R., 1979, Immobile Trace Element and Archean Volcanic Stratigraphy in the Timmins Mining Area, Ontario: Can. J. Earth. Sci., v. 16, p. 305-311.

Davies, J.F., and Whitehead, R.E.S., 1979, Further Immobile Element data from Altered Volcanic Rocks, Timmins Mining Area, Ontario: Can. J. Earth. Sci., v. 17, p. 419-423.

De Waard, D., 1967, The Occurrence of Garnet in Granulite Facies Terraine of the Aditondock Highlands and Elsewhere, a reply: J. of Petrol., v. 8, part 2, p. 210-232.

Deer, W.A., Howie, R.A., and Zussmann, J., 1966, An Introduction to the Rock Forming Minerals: Longman Goup, London, p. 528.

Degens, E.T., and Ross, D.A. (ed), 1969, Hot Brines and Recent Heavy Metal Deposits of the Red Sea: Springer, New York, p. 600.

Dougan, T.W., 1974, Cordierite Gneisses and Associated Lithologies of the Guri Area, N.W. Guyana Shield Venezuela: Contrib. Mineral. and Petrol., v. 46, p. 169-188.

Dostal, J., 1974, The Origin of Garnet-Cordierite-Sillimanite Bearing Rocks from Chandos Township, Ontario: Contrib. Mineral. Petrol., v. 49, p. 163-175.

Dostal, J., and Capedri, R., 1979, Rare-Earth Elements in High Grade Metamorphic Rocks from the Western Alps: Lithos., v. 12, p. 41-49.

Drury, S., 1974, Chemical Changes during Retrogressive Metamorphism of Lewisian Granulite Facies Rocks from Coll and Tiree: Scott. Jour. Geol., v. 10, p. 237-256.

Eckelmann, F.D., 1978, Paragneiss-Orthogneiss Distinction among Charnockites ... Based on Zircon Morphology Data: Geol. Soc. Am. Abstr. Prgms: v. 10, p. 41.

Edmond, J., Measures, C., and Corliss, J., 1979, On the Formation of Metal Rich Deposits at Ridge Crests: Earth. Planet. Sci. Lett., v. 46, p. 19.

Edwards, A.B., 1954, Textures of the Ore Minerals and their Significance: A.I.M.M., Melbourne, p. 241.

Elliot, R., 1973, The Chemistry of Gabbro/Amphibolite Transitions in South Norway: Contrib. Mineral. Petrol., v. 38, p. 71-79.

Elliot, R., and Harvey, P.K., 1980, Trace Element Geochemistry of the Amphibolites of the Holleindalen Greenstone Group, Norway: Norsk. Geologist. Tidsk., v. 60, p. 195-200.

Ethier, V.G., Campbell, F.A., Both , R., and Krouse, H., 1976, Geological Setting of the Sullivan Ore Body and Estimates of Temperatures and Pressures of Metamorphism: Econ. Geol., v. 71, p. 1570-1588.

Exxon Mineral Co., (Staff), 1978, The Discovery, Geology and Mineralogy of the Crandon Precambrian Massive Sulphide: Geol. Soc. Am. Abstr. Prgms., v. 9.

Ferry, J.M. and Spear, F.S., 1978, Experimental Calibration of the Partitioning of Fe and Mg Between Biotite and Garnet: Contrib. Mineral. Petrol., v. 66, p. 113-117.

Fershatter, G.B., 1977, Isochemical Migmatization and Genesis of Quartz-Feldspar Rocks of the Taratash Metamorphic Complex: Geochem. Int., v. 14, p. 63-72.

Finnemore, S.H., 1978, The Geochemistry and Origin of the Matchless Amphibolite Belt, Windhoek, S.W.A.; in: Mineralization in Metamorphic Terrains ed. W. Verwoerd: Geol. Soc. of S. Africa Special Publication No. 4.

Floyd, P., and Winchester, J., 1975, Magma Type and Tectonic Setting Discrimination using Immobile Elements: Earth. Planet. Sci. Lett., v. 10, p. 211-218.

Geringer, G.J., 1979, The Origin and Tectonic Setting of Amphibolites in part of the Namaqua Metamorphic Belt, South Africa: Trans. Geol. Soc. of S.A., v. 82, p. 287-304.

Ghent, E.D., 1976, Plagioclase-Garnet-Al_2SiO_5-Quartz; A Potential Geobarometer-Geothermometer? Am. Mineral., v. 61, p. 710-714.

Ghent, E.D., Robbins, D., and Stout, M., 1979, Geothermometry, Barometry and Fluid Compositions of Metamorphosed Calc-silicates and Pelites, Mica Creek, British Columbia: Am. Mineral., v. 64, p. 874-885.

Gilmour, P., 1971, Stratabound Massive Pyritic Sulphide Deposits, a Review: Econ. Geol., v. 66, p. 1239-1244.

Gilligan, L.B., Felton, E., and Ogers, F., 1979, The Regional Setting of the Woodlawn Deposit: Jour. of Geol. Soc. Australia, v. 26, p. 135-140.

Gorton, R.K., 1980, A Discussion on "Metamorphic Zonation in the Matsap, Kheis and Namaqua Domains" by Botha, B., et al. (1979): Trans. Geol. Soc. of South Africa, v. 83, p. 113.

Graf, J.L., 1977, Rare-Earth Elements as Hydrothermal Tracers during the Formation of Massive Sulphide Deposits in Volcanic Rocks: Econ. Geol., v. 72, p. 527-548.

Graham, A.R., 1969, Quantitative Determination of Hexagonal and Monoclinic Pyrrhotites by X-ray Diffraction: Can. Mineralogist, v. 10, p. 2-24.

Gray, C.M., 1977, The Geochemistry of Central Australian Granulites in Relation to Chemical and Isotopic effects of Granulite Facies Metamorphism: Contrib. Mineral. Petrol., v. 65, p. 79-89.

Groves, D., Barret, F., and McQueen, K., 1979, The Relative Roles of Magmatic Segregation, Volcanic Exhalation and Regional Metamorphism in the Generation of Volcanic Associated Nickel Ores of West Australia: Can. Mineral., v. 17, No. 2, p. 319-336.

Guidotti, C.V., 1970, The Mineralogy and Petrology of the Transition from the Lower to Upper Sillimanite Zone in the Oquossac Area, Maine: Jour. Petrology, v. 11, p. 277-336.

Harker, A., 1939, Metamorphism. 2nd Edition. Chapman and Hall, London, p. 362.

Hay, D.E., 1979, Mineralogical Investigations related to the Origin of Massive Sulphide Deposits; Ohio: J. Sci., v. 79, p. 32 (Abstr.).

Heier and Thoresen, 1971, Geochemistry of High Grade Metamorphic Rocks, Lofoten-Versteralan, Norway: Geochim. et Cosmo. Acta., v. 35, p. 89-99.

Heinrich, E.W., 1965, Microscopic Identification of Minerals, McGraw Hill, New York, p. 414.

Hensen, B.J. and Green, D.H., 1973, Synthesis of Experimental Data and Geological Implications: Contrib. Mineral. Petrol., v. 38, p. 151-166.

—— 1977, Cordierite-Garnet Bearing Assemblages as Geothermometers and Barometers in Granulite Facies Terrains: Tectonophysics, v. 43, p. 73-88.

Hewins, R.H., 1975, Pyroxene Geothermometry of Some Granulite Facies Rocks: Contr. Mineral. Petrol., v. 50, p. 205-209.

Himmelberg, G., and Phinney, W., 1967, Granulite-Facies Metamorphism Granite Falls - Montevideo Area: J. Of Petrol., v. 8, p. 325-348.

Hodgson, C.J., 1974, The Geology and Geological Development of the Broken Hill Lode in the Broken Hill Consolidated Mine, Australia: J. Geol. Soc. of Australia, v. 21, p. 413-430.

Holdaway, M., and Lee, S.M., 1977, Fe-Mg Cordierite Stability in High Grade Pelitic Rocks based on Experimental Theoretical and Natural Observations: Contrib. Mineral. Petrol., v. 63, p. 175-198.

Holland, J.G., and Lambert, R.S., 1974, Yttrium Geochemistry applied to Petrogenesis using Ca/Y relationships in Minerals and Rocks: Geochim. et Cosmo. Acta., v. 38.

Hutchinson, M.N., and Scott, S.D., 1978, Effect of Copper on the Sphalerite Geobarometer: Geol. Soc. Am. Abstr. Prgms., v. 10, No. 7, p. 426.

Hutchinson, R.W., 1973, Volcanogenic Sulfide Deposits and their Metallogenic Significance: Econ. Geol., v. 68, p. 1223-1246.

—— 1978, Geological and Geochemical Evolution of Massive Sulphide Deposits: Univ. of Witwatersrand, Post Graduate Course in Economic Geology, No. 10.

—— 1979, Evidence of Exhalative Origin for Tasmanian Tin Deposits: Can. Inst. Mining Bull., August 1979, p. 90-104.

Hutcheon, I., 1978, Calculation of Metamorphic Pressure using the Sphalerite-Pyrrhotite-Pyrite Equilibrium: Am. Minerals, v. 63, p. 87-95.

Irvine, T.N., and Baragar, W.R., 1971, A Guide to Chemical Classification of Common Volcanic Rocks: Can. J. Earth. Sci., v. 8, p. 523-548.

Ito, T., Takahashi, T., and Omori, Y., 1974, Submarine Volcanic Sedimentary Features of the Matsumine Kuroko Deposits: Min. Geol. Spec. Issue, No. 6, p. 53-66.

Jambor, J.L., 1979, Mineralogical Evaluation of Proximal-Distal Features in New Brunswick Massive Sulphide Deposits: Can. Mineralogist, v. 17, p. 649-664.

Janecky, D., 1978, Metalliferous Deposits of the Troodoos Ophiolite: EOS, v. 59, No. 12, p. 1221.

Jensen, L., 1976, A New Cation Plot for Classifying Subalkalic Volcanic Rocks: Ontario. Div. Mines, MP 66.

Joubert, P., 1974, The Gneisses of Namaqualand and their Deformation: Trans. Geol. Soc. S. Africa, v. 77, p. 339-345.

—— 1976, The Relationship between the Namaqualand Metamorphic Complex and the Kheis Group: S. Afr. Jour. Sci., v. 72, p. 312-314.

Kalliokoski, J., 1965, Metamorphic Features of North American Massive Sulphide Deposits: Econ. Geol., v. 60, p. 485-505.

Kapp, R.O., 1957, The Presentation of Technical Information; The Macmillan Company, New York.

Kean, B., and Strong, D., 1975, Geochemical Evolution of an Ordovician Island arc System of the Central Newfoundland Appalochians: Am. J. Sci., v. 275, p. 97-118.

Kerr, A., 1979, The Retrogressive Breakdown of Orthopyroxene in Granulite Facies Rocks, Sutherland, U.K.: Mineral. Mag., v. 43, p. 443-445.

Kerr, D.F., 1959, Optical Mineralogy, 3rd Edition, McGraw Hill, New York, p. 442.

Kimberley, M.M., 1979, Geochemical Distinctions among Environmental Types of Iron Formation: Chem. Geol., v. 25, part 3, p. 185-212.

Kissin, S.A., and Scott, S.D., 1972, Phase Relations of Intermediate Pyrrhotites (Abstr.): Econ. Geol., v. 67, p. 1007.

Klein, C., 1973, Changes in Mineral Assemblages with Metamorphism of some banded Pre-Cambrian Iron Formation: Econ. Geol., v. 68, p. 1075-1088.

Knorring, O., and Kennedy, W., 1958, The Mineral Paragenesis and Metamorphic Status of Garnet-Hornblende-Pyroxene-Scapolite Gneiss: Min. Mag., v. 31, p. 846.

Knuckey, J., Comba, C., and Riverin, G., 1979, The Millenbach Deposit - an Update: Geol. Soc. Am. Abstr. Prgms., v. 10, No. 7, p. 436.

Koeppel, V., 1980, Lead Isotope Studies of Stratiform Ore Deposits of the Namaqualand, N.W. Cape Province, South Africa and their Implication on the Age of the Bushmanland Sequence: in Proceedings of the fifth IAGOD Symposium Vol. I, Editor: J.D. Ridge, p. 195-207.

Kröner, A., 1976, The Namaqua Mobile Belt within the Framework of Precambrian Crustal Evolution in Southern Africa; in: Verwoerd W.J. Mineralization in Metamorphic Terraines: Geological Society of South Africa, Spec. Pub. No. 4.

Kullerud, G., 1953, The FeS-ZnS System, A Geological Thermometer: Norsk. Geol. Tidsskr., v. 32, p. 61-147.

Kuno, H., 1950, Petrology of the Hakoe Volcanoe and Adjacent Area: Bull. Geol. Soc. Am., v. 61, p. 957-1020.

Large, D., 1979, Proximal and Distal Stratabound Ore Deposits, - a Discussion of the Paper by I. Plimer: Mineral. Deposita, v. 14, p. 123-4.

Large, R.R., 1977, Chemical Evolution and Zonation of Massive Sulphide Deposits in Volcanic Terraines: Econ. Geol.,v. 72, p. 549-572.

—— and Both, R.A., 1980, The Volcanogenic Sulphide Ores at Mt. Chalmers, Eastern Queensland: Econ. Geol., v. 75, p. 992-1009.

Lambert, I.B., and Sato, T., 1974, The Kuroko and Associated Ore Deposits of Japan: A Review of their Features and Metallogenesis: Econ. Geol., v. 69, p. 1215-1236.

Latvalahti, U., 1979, Cu-Zn-Pb Ores in the Aijala-Orijarvi Area S.W. Finland: Econ. Geol., v. 74, p. 1035-1059.

Leake, B.E., 1964, The Chemical Distinction between Ortho and Para-Amphibolites: Journal. Pet., v. 5, Part 2, p. 238-254.

Mabbutt, J., 1955, Erosion Surfaces in Namaqualand and the Ages of Surface Deposits in S.W. Kalahari: Tran. Geol. Soc. S. Africa, v. 58, p. 13-30.

Mallio, W., and Gheith, M., 1972, Textural and Chemical Evidence Bearing on Sulphide-Silicate Reactions in Metasediments: Mineral. Deposita., v. 7, p. 13-17.

Menzies, M., Blanchard, D., and Jacobs, J., 1977, Rare-Earth and Trace Element Geochemistry of Metabasalts of the Point Sal Ophiolite, California: Earth. Planet. Sci. Lett., v. 37, No. 2, p. 203-215.

McLimans, R.K., Barnes, H., and Ohlnoto, H., 1980, Sphalerite Stratigraphy in the Upper Mississippi Valley Zinc-Lead Dist.I; S.W. Wisconsin: Econ. Geol., v. 75, p. 351-361.

MacDonald, J.A., 1967, Metamorphism and its effects on Sulphide Assemblages: Mineral Deposita, v. 2, p. 200-230.

Mehnert, K.R., 1972, Neues Jahrb. Mineral. Monatash., 1972. p. 139-150.

Middleton, R.C., 1976, The Geology of Prieska Copper Mines Ltd. : Econ. Geol., v. 71, p. 328-350.

Moore, A.C., 1970, Descriptive Terminology for the Textures of Rocks in Granulite Facies Terraines: Lithos. v. 3, p. 123-127.

—— Kartun, K.G., and Waters, D.J., 1979, Metamorphic History of the Aureole Associated with the Tantalite Valley Complex, Namibia: Trans. Geol. Soc. S. Africa, v. 82, p. 67-80.

Moore, J.M., 1977, The Geology of the Namiesberg, N. Cape: Precambrian Research Unit, University of C.T., Bull. No. 20.

—— 1980, Paleo-Environmental Implications of the Origin of Sillimanite Rich Rocks in the N.W. Cape, South Africa and their Relation to the Sulphide Deposits in the Area; in: Ed. J.D. Ridge, Proceedings of the Fifth IAGOD Symposium, v. 1, p. 209.

Moorehouse, S.J., 1979, The Maine Amphibolite Suites of Central and Northern Sutherland, Scotland: Mineral. Mag., v. 43, p. 211-225.

Muecke, R., and Sarkar, P., 1977, Rare-Earth Elements Mobility during Amphibolite Facies Metamorphism of White Rock Meta-volcanics, Nova Scotia: Geol. Soc. Am. Abstr. Prgms.,v. 9, No. 3, p. 303.

Mueller, R.F., 1967, Mobility of the Elements in Metamorphism: J. Geol., v. 75, p. 565-582.

Myashiro, A., 1974, Volcanic Rock Series in Island Arcs: Am. J. Sci., v. 274, p. 321-355.

—— 1975, Classification, Characteristics and Origin of Ophio-lites: J. Geol., v. 83, p. 249-282.

Nesbitt, B.E., and Kelly, W.C., 1980, Metamorphic Zonation of Sulphides, Oxides and Graphite in and around the Orebodies at Ducktown, Tennesee: Econ. Geol., v. 75, p. 1010-1021.

Norrish, K., and Hutton, J.T., 1969, An Accurate X-ray Spectrographic Method for Analysis of a wide range of Geological Samples: Geochim. Cosmochim. Acta., v. 33, p. 431.

Oftedahl, C.A., 1958, A Theory of Exhalative-Sedimentary Ores: Geologiska Föreningen Stockholm Fördhandlinger, v. 80, p.1-19.

Onions, R.K., and Pankhurst, R.J., 1978, Early Archean Rocks and Geochemical Evolution of the Earths Crust: Earth Planet. Sci. Lett., v. 38, p. 211-236.

Orville, P.M., 1969, A Model for Metamorphic Diffrentiation Origin of Thin Layered Amphibolites: Am. J. of Sci., v. 267, p. 64-86.

Ostwald, J., and England, B., 1979, The Relationship between Euhedral and Framboidal Pyrite in Base Metal Sulphide Ores: Mineralog. Mag., v. 43.

Owsiacki, L., and McAllistar, A.L., 1979, Fragmental Massive Sulphides at the Heath Steele Mine, New Brunswick: C.I.M. Bull., Nov. 1979, p. 93-100.

Pearce, T.H., Gorman, B.E., Birkett, T.C., 1977, The Relationship between Major Element Chemistry and Tectonic Environment of Basic and Intermediate Rocks: Earth.Planet. Sci. Lett., v. 36, p. 121-132.

—— 1968, A Contribution to the Theory of Variation Diagrams: Contrib. Mineral. Petrol., v. 19, p. 142-157.

Pearce, J.A. and Cann, J.R., 1973, Tectonic Setting of Basic Volcanic Rocks Determined using Trace Element Analysis: Earth. Planet. Sci. Lett., v. 19, p. 290-300.

—— 1975, Basalt Geochemistry used to Investigate Past Tectonic Environments on Cyprus: Tectonophysics, v. 25, p. 41-68.

Peterson, M., and Lambert, I., 1979, Mineralogical and Chemical Zonation around the Woodlawn Cu, Pb, Zn Ore Deposit, N.S.W., Australia: J. Geol. Soc. Australia, v. 26, p. 169-186.

Plimer, I.R., 1975, A Metamorphigenic Alteration Zone around the Stratiform Broken Hill Ore Deposits, Australia: Geochem. Journal, v. 9, p. 211.

—— 1975, The Geochemistry of Amphibolite Retrogression at Broken Hill, Australia: N. Jb. Miner. Mh. H., v. 10, p. 471-481.

—— 1976, Garnet-Biotite Relationships in High Grade Metamorphic Rocks at Broken Hill, Australia: Geol. Mag., v. 113, p. 263-270.

—— and Elliot, S.M., 1979, The Use of Rb/Sr Ratios as a Guide to Mineralization: Jour. Geochem. Expl., v. 12, p. 21.

—— 1978, Proximal and Distal Stratabound Ore Deposits: Mineral. Deposita, v. 13, p. 345.

—— and Finlow-Bates, T., 1978, Relationship Between Primary Iron Sulphide Species, Sulfur Source, Depth of Formations and Age of Submarine Exhalative Sulphide Deposits: Min. Deposita., v. 13, p. 399-410.

Ramdohr, P., 1969, The Ore Minerals and their Intergrowths: Pergamon Press, Oxford, p. 1137.

Reid, D.L., 1977, Geochemistry of Precambrian Igneous Rocks in the Lower Orange River Section: Precamb. Res. Unit, Bull. 22, Univ. of C.T.

Reynolds, D.G. et al., 1976, Volcanogenic Copper Zinc Deposits in the Pilbara and Yilgarn Archean Blocks; in Economic Geology of Australia, PNG, Australasian I.M.M..

Richardson, S., Gilbert, M., and Bell, P., 1969, Experimental Determination of the Kyanite-andalusite and Andalusite-Sillimanite Triple Point: Am. J. Sci., v. 267, p. 259-272.

Rickard, D.T., Zweifel, H., 1975, Genesis of Precambrian Sulphide Ores, Skellefte District, Sweden: Econ. Geol., v. 70, p. 255-274.

Robinson, D., and Leake, B., 1975, Sedimentary and Igneous Trends in AFM Diagrams: Geol. Mag., v. 112, p. 305-307.

Rockingham, C.J., and Hutchinson, R.W., 1980, Metamorphic Textures in Archean Copper-Zinc Massive Sulphide Deposits: Canadian Inst. Mining Bull., April 1980, p. 104-112.

Roedder, E., and Dwornick, E.J., 1968, Sphalerite Colour Banding Lack of Correlation with Iron Content, Pine Point North-West Territories, Canada: Am. Mineralogist, v. 53, p. 1523-1529.

Ross, A., and Keays, R., 1979, Precious Metals in Volcanogenic Type Ni Sulphide Deposits in W. Australia: Can.Mineral. v. 17, p. 417.

Rozendaal, A., 1980, The Gamsberg Zinc Deposit, South Africa, A Banded Stratiform Base Metal Deposit: in Ed. J.D. Ridge, Proc. of the fifth IAGOD Symposium, v. 1, p. 615-633.

Ridler, R.H., 1971, Analysis of Archean Volcanic Basins in the Canadian Shield using the Exhalite Concept (Abs.): Can. Mining Metall. Bull., v. 64, No. 714, p. 20.

Sangster, D.F., 1972, Precambrian Volcanogenic Massive Sulphide Deposits in Canada: a Review; Geol. Surv. of Canada Paper 72-22.

Sangster, D.F., and Scott, S.D., 1976, Precambrian, Strata-bound Massive Cu-Zn-Pb Sulphide Ores of North America: in:Wolf: Handbook of Stratabound and Stratiform Ore Deposits, v. 6, Chap. 5.

——1979, Evidence of an Exhalative Origin for Deposits of the Coba District, New South Wales: B.M.R. Journal of Australian Geology, v. 4, p. 15-24.

——1980, Quantitative Characteristics of Volcanogenic Massive Sulphide Deposits: C.I.M. Bull., Feb. 1980.

Sawkins, F.J., 1976, Metal Deposits Related to Intracontinental Hotspot and Rifting Environments: J. Geol., v. 84, p. 653-671.

Saxena, S.K., 1969, Silicate Solid Solution and Geothermometry, Distribution of Fe and Mg Between Co-existing Garnet and Biotite: Contrib. Mineral. Petrol., v. 22, p. 259-267.

Schwarz, E., and Harris, D., 1970, Phases in Natural Pyrrhotite and the Effect of Heating on their Magnetic Properties and Composition: Jour. of Geomagnetism and Geolectricity, v. 22, p. 463-470.

Scott, S.D., and Barnes, H.L., 1971, Sphalerite Geothermometry and Geobarometry: Econ. Geol.,v. 66, p. 653-669.

—— 1973, Experimental Calibration of the Sphalerite Geobarometer: Econ. Geol., v. 68, p. 466-474.

—— 1974, Experimental Methods in Sulphide Synthesis; in ed. P.H. Ribbe Sulphide Mineralogy; Mineralogical Soc. of Am., Short Course Notes, v. 1.

Scott, S.D., 1976, Application of the Sphalerite Geobarometer to Regionally Metamorphosed Terraines: Am. Mineralogist, v. 61, p. 661-670.

Schulz, K.J., 1979, Geochemical Evidence for Multiple Sources for Archean Basalt Volcanism: Geol. Soc. Am. Abstr. Prgms., v. 10, No. 7, p. 487.

Selverstone, J., 1980, Cordierite Bearing Granulites from the Coast Ranges, B.C.; P-T Conditions of Metamorphism: Can. Mineral., v. 18, p. 119-130.

Senior, A., and Leake, B., 1978, Regional Metasomatism and Geochemistry of Dalradian Metasediments of Connemarra, W. Ireland: J. Of Petrol., v. 19, p. 585-625.

Shaw, D.M., 1972, The Origin of the Apsley Gneiss, Ontario: Can. Jour. Earth Sci., v. 9, p. 18-35.

Shadlun, T., 1971, Metamorphic Textures and Structures of Sulphide Ores: in: Y. Takeuchi (ed) IAGOD, vol. 1970, p. 241-250.

Shee, S.R., 1978, The Mineral Chemistry of Xenoliths from the Orapa Kimbalite Pipe, Botswana: Unpubl. M.Sc. Thesis, Univ. of Cape Town.

Shegelski, R.J., 1979, A Geochemical Model for Archean B.I.F. in the Sturgeon-Savant Greenstone: Geol. Soc. Am. Abstr. Prgm., v. 10, No. 7, p. 491.

Sherman, T.A., 1966, Modern Technical Writing, Second Edition: Prentice Hall, New Jersey.

Sighinolfi, G.P., 1971, Investigations into Deep Crustal Levels: Fractionating Effects and Geochemical Trends related to High Grade Metamorphism: Geochim. et Cosmo. Acta., v. 35, p. 1005-1021.

Skinner, B.J.,White, D.E., Rose, H.J., and Mays, R.E., 1967, Sulphides Associated with the Salton Sea Geothermal Brine: Econ. Geol., v. 62, p. 316-330.

Smith, J.W., and Burns, M.S.,Stable Isotope Studies of the Origins of Mineralization at Mt. Isa: Mineral. Deposita., v. 13, p. 369.

Smith, R.E., 1968, Redistribution of Major Elements in the Alteration of some Basic Lavas during Burial Metamorphism: J. of Petrol., v. 9, p. 191-219.

Solomon, M., 1976, "Volcanic" Massive Sulphide Deposits and their Host Rocks, a Review and an Explanation in: (Wolf (ed)) Handbook of Stratabound and Strataform Ore Deposits, v. 6, Chap. 2.

Spooner, E., and Fyfe, W., 1973, Sub-seafloor Metamorphism, Heat and Mass Transfer: Contrib. Mineral. Petrol., v. 42, p. 287-304.

Speakman, J., Chornoby, P., Holmes, G., and Bernard, C., 1978, Geology of the Ruttan Deposit: Geol. Soc. Am. Abstr. Prgms., v. 10, p. 496.

Spry, A., 1969, Metamorphic Textures: Publ. Pergamon. Press.

Stanton, R.L., 1972, A Preliminary Account of Chemical Relationships between Sulphide Lode and B.I.F. at Broken Hill, N.S.W.: Econ. Geol., v. 67, p. 1128-1145.

—— 1972, Ore Petrology: McGraw Hill, New York.

—— 1959, Mineralogical Features and Possible Mode of Emplacement of the Brunswick Mining and Smelting Ore Bodies, N.B. Canada: C.I.M. Bull., v. 52, p. 631-643.

—— 1976, Broken Hill, Australia, Banded Iron Formation, Parts 1 to 4: Transactions (Sect. B.) I.M.M., v. 85.

—— and Williams, K., 1978, Garnet Composition at Broken Hill, N.S.W., as Indicators of Metamorphic Processes: J. of Petrol., v. 19, No. 3, p. 514-529.

Stamatelopoulou, K., and McLean, 1977, the Geochemistry of Possible Metavolcanic Rocks and their Relationship to Mineralization at Montauban Les Mines, Quebec: Can. Jour. Earth Sci., v. 14, p. 2440-2452.

Stephenson, N.C.N., 1980, Precambrian Amphibolites and Basic Granulites of the South Coast of Western Australia: Jour. Geol. Soc. Australia, v. 27, p. 91-104.

Stormer, J., 1975, A Practical Two Feldspar Geothermometer: Am. Mineral., v. 60, p. 667-674.

—— and Whitney, J., 1977, The Distribution of $NaAlSi_3O_8$ Between Coexisting Microcline and Plagioclase: Am. Mineral., v. 62, p. 687-691.

Stumpfl, E.F., 1979, Manganese Haloes Surrounding Metamorphic Stratabound Base Metal Deposits: Mineral. Deposita., v. 14, p. 207-217.

—— 1980, A Discussion of the Paper "Manganese Haloes...": Mineral. Deposita., v. 15, p. 237.

Sullivan, C.J., 1979, Intracratonic Basins and Ore Deposits: C.I.M. Bull., v. 72, p. 75-80.

Suen, C.J., et al., 1979, Bay of Island Ophiolite Suite, Newfoundland, Petrological and Geochemical Characteristics with Emphasis on Rare-Earth Elements: Earth. Planet. Sci. Lett., v. 45, p. 337.

Suffel, G.G., Hutchinson, R., and Ridler, R., 1971, Metamorphism of Massive Sulphides at Manitouwadge, Ontario, Canada: in: Y. Takeuchi (ed.) IAGOD, v. 1970, p. 235-240.

Taylor, S.R., 1965, The Application of Trace Element Data to Problems in Petrology: Physics and Chem. of Earth, v. 6, p. 133-213.

Taylor, L. A., 1971, Oxidation of Pyrrhotite and Formation of Anomalous Pyrrhotite: Carnegie Inst. Washington Yearbook 70, p. 287-289.

Terry, R.D. and Chilingar, G.V., 1955, Summary of "Concerning Some Additional Aids in Studying Sedimentary Formations": Jour. Sed. Pet., v. 25, p. 229-234.

Thompson, A.B., 1976, Mineral Relations in Pelitic Rocks, Calculation of Some P-T-X (Fe-Mg).

Thornber, J., 1980, Supergene Alteration of Sulphides versus Laboratory Studies on the Dispersion of Ni, Cu, Co and Fe: Chem. Geol., v. 26, p. 135-149.

Uytenbogaardt, W., 1951, Tables for Microscopic Identification of Ore Minerals: Pub. Princeton Univ. Press.

Vajner, V., 1974, The Tectonic Development of the Namaqua Mobile Belt and its Foreland in Parts of the Northern Cape: Precamb. Research Unit, Univ. of Cape Town, Bull. 14.

—— 1974, The Doringberg Fault and its Relation to the Post-Waterberg Deformation: Trans. Geol. Soc. S. Africa, v. 77, p. 295.

Van de Kamp, C., 1968, Geochemistry and Origin of Metasediments in the Haliburton-Madoc area, S.E. Ontario: Can. J. Earth. Sci., v. 5, p. 1337-1372.

—— 1969, Origin of Amphibolites in the Beartooth Mountains New Data and Interpretations: Bull. Geol. Soc. America, v. 80, p. 1127-1136.

—— and Leake, B., and Senior, A., 1976, The Petrography and Geochemistry of some Californian Arkoses with Application to Identifying Gneissesof Meta-sedimentary Origin: Jour. Geol., v. 84, p. 195-212.

Van Reenen, D., and Du Toit, M.C., 1978, The Reaction Garnet and Quartz = Cordierite + Hypersthene in Granulites of the Limpopo Metamorphic Complex in Northern Transvaal; in: Mineralization in Metamorphic Terraines ed. W.J. Verwoerd, Geol. Soc. of S. Africa, Spec. Publ. 4.

Vogel, T.A., and Widmayer, R., 1979, Feldspar Geothermometry of the Hell Canyon Pluton, Boulder Batholith Montana: Contrib. Mineral. Petrol., v. 71, p. 151.

Vokes, F.M., 1969, A Review of the Metamorphism of Sulphide Deposits: Earth Sci. Rev., v. 5, p. 99-143.

—— 1971, Some Aspects of Regional Metamorphic Mobilization of Pre-existing Sulphide Deposits: Mineral. Deposita., v. 6 p. 122-129.

—— 1976, Caledonian Massive Sulphide Deposits in Scandinavia: A Comparitive Review; in: (Wolf (ed)) Handbook of Stratabound and Stratiform Ore Deposits, v. 6.

Wagener, J.H.F., 1980, The Prieska Zinc-Copper Deposit, Cape Province, South Africa:ed. J.D. Ridge, Proc. of the fifth IAGOD Symposium, v. 1, p. 635.

Weaver, B.L., 1977, Madras Granulites - Geochemistry and P-T Conditions of Crystallization: in Archean Geochemistry ed. Windley and Naquvi: Proc. of Symp. on Archean Geochemistry, 1977.

White, A., and Chappell, B., 1977, Ultrametamorphism and Granitoid Genesis: Tectonophysics, v. 43, p. 7-22.

Whitehead, R.E., 1973, Environment of Stratiform Sulphide Deposits, Variation in Mn/Fe Ratio in Host Rocks at Heath Steele Mine: Mineral. Deposita., v. 8, p. 148-160.

Whitehead, R., and Goodfellow, W., 1978, Geochemistry of Volcanic Rocks from the Tetagouche Group, Bathurst, N.B., Canada: Can. J. Earth. Sci., v. 15, p. 207-219.

Wiggins, L.B., and Craig, J.R., 1980, Reconnaissance of the Cu, Fe, Zn-S System; Sphalerite Phase Relationships: Econ. Geol.,v. 75, p. 742-751.

Willis, J.W., Ahrens, L.H., Danchin, R.V., Erlank, A.J., Gurney, J., Hofmeyr, P.K., McCarthy, T.S., and Orren, M.J., 1971, Some Interelement Relationships between Lunar Rocks and Fines and Strong Meteorites, in: Proceed. Second Lunar Sci. Conf., ed. Levinson, A.A., M.I.T. Press, 1123-1138.

Willis, J., Erlank, A., Gurney, J., Theil, R., and Ahrens, L.H., 1972, Major, Minor and Trace Element Data for some Apollo 11, 12, 14 and 15 samples, in: Proceed. Third Lunar Sci. Conf., ed. Heyman, L.D., M.I.T. Press, 1269-1273.

Wilson, M.D., and Sedeora, S., 1979, An Improved Thin Section Stain for Potash Feldspar: J. of Sed. Pet., v. 49, No. 2, p. 637.

Wilson , H., Andrews, P., Moxham, R., and Ramlal, K., 1965, Archean Volcanism in the Canadian Shield: Can. Jour. Earth Sci., v. 2, p. 161-175.

Williams, K.L., 1967, Electron Microprobe Microanalysis of Sphalerite: Am. Mineralogist, v. 52, p. 475-491.

Winchester, J.A., 1976, Different Mionian Amphibolite Suites in Northern Ross-shire: Scott. J. Geol., v. 12, p. 187-204.

—— and Floyd, P., 1976, Geochemical Magma Type Discrimination Application to Altered and Metamorphosed Basic Igneous Rock: Earth Planet. Sci. Lett., v. 28, p. 459-469.

Winkler, H.G.F., 1976, Petrogenesis of Metamorphic Rocks; Springer-Verlag. New York. p. 334.

Wood, B.J., and Banno, S., 1973, Garnet-Opx and Opx-Cpx Relationships in Simple and Complex Systems: Contrib. Min. Petrol., v. 42, p. 109-124.

—— 1974, The Solubility of Alumina in Orthopyroxene Co-existing with Garnet: Contrib. Mineral. Petrol., v. 46, p. 1-15.

Yardley, B., 1977, An Empirical Study of Diffusion in Garnet: Am. Mineralogist, v. 62, p. 793-796.

APPENDIX I

Detailed Petrography of the Wall Rocks and Massive Sulphides

The textures of the thin sections have been described using the terminology defined by Moore, 1970, and approved by Winkler, 1974, (See Fig. a).

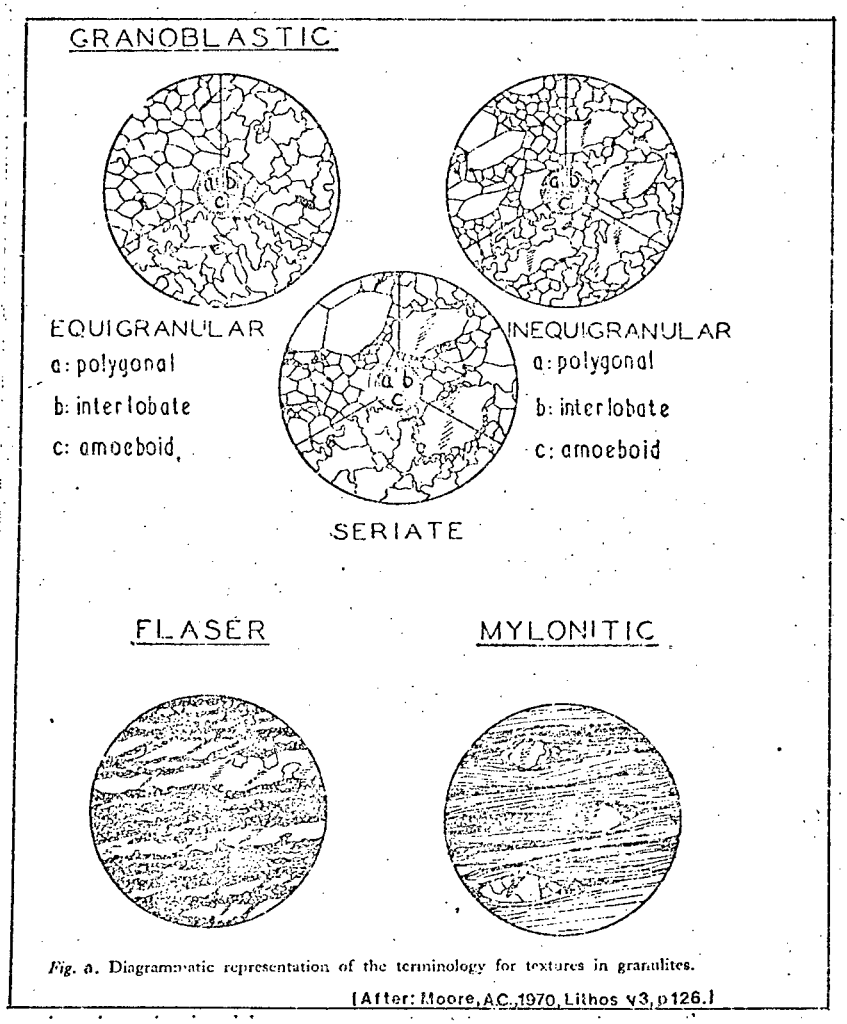

Fig. a. Diagrammatic representation of the terminology for textures in granulites.
(After: Moore, A.C., 1970, Lithos v3, p126.)

The mineral proportions for each rock unit are quoted as a range of values, giving an indication of the uniformity, and the statistical parameter of mode to give the most commonly occurring mineralogical proportions.

On the photomicrograph plates the symbols used for the optical conditions are:

r = reflected light
xn = crossed nicols
r ~ xn = reflected light with partially crossed nicols
⟵⟶ = bar scale represents 0.10mm

The letters used to denote minerals are:

q - quartz
b - biotite
pl - plagioclase
h - hornblende
g - garnet
s - sillimanite
ac - actinolite
hy - hypersthene
d - diopside
se - sphene
rh - rhodonite
cl - chlorite
br - bronzite
a - apatite
ant - antigorite
hc - hercynite
kf - potash feldspar (perthite)
t - tourmaline
c - cordierite
gr - grunerite

p - pyrite
po - pyrrhotite
cp - chalcopyrite
sp - sphalerite
ma - marcasite
ga - galena
mt - magnetite
hm - hematite
il - ilmenite
tb - tellurbismuth

AREA K3

Unit 1. Felsic Pyritic Gneiss

A fine grained micaceous felsic pyritic gneiss was intersected only on section 54E (Fig. 1) and consists of:

	RANGE	MODE
quartz	50-55%	50%
plagioclase-oligoclase ($Ab_{70}An_{30}$)	10-15%	15%
orthoclase/perthite	1-15%	15%
biotite (altering to chlorite)	5-10%	10%
sericite	5%	5%
pyrite	5%	5%

The texture is platy granoblastic seriate amoeboid. The orthoclase, present as perthite, forms porphyroblasts (up to 2mm) with amoeboid grain boundaries. The ground-mass is composed of a platy (ribbon-like quartz grains) mosaic of quartz, plagioclase and biotite. The grains are mostly amoeboid in outline and vary in size from 0.25 to 1mm. Biotite is intergrown with sericite and both are strongly altered to chlorite. The quartz grains exhibit undulose extinction.

Pyrite is present as discrete subhedral to euhedral (0.5mm) grains interstitial to the silicates.

Unit 2. Hypersthene-cordierite-pyritic Granulite

In hand specimen the rock is intermediate to felsic; usually fine grained and poorly foliated. The rock typically has up to 10% disseminated grains and stringers of pyrite and pyrrhotite.
The rock consists of:

	RANGE	MODE
hypersthene	15-50%	25%
cordierite	0-25%	25%
plagioclase-andesine ($Ab_{64}An_{36}$)	10-30%	20%
quartz	10-30%	15%
biotite	5-15%	5%
pyrite/pyrrhotite (py/po≈1)	2-10%	5%
magnetite	2-5%	4%
diopside	0-25%	0%
hornblende	0-20%	0%
orthoclase	0-2%	0%
apatite	tr	tr

The microscopic texture is granoblastic seriate to inequigranular, with the grains having interlobate boundaries. Large, irregularly-shaped grains of hypersthene poikiloblastically enclose quartz, feldspar and pyrite. The biotite is associated with the hypersthene and both are at least partially replaced by chlorite. The groundmass is of variable grain size but generally ≤ 0.75mm and consists of an interlobate mosaic of quartz, plagioclase and sometimes diopside. The hornblende, where present, has replaced the pyroxenes. The cordierite forms anhedral rounded grains (~ 0.5mm) with amoeboid edges usually altered to pinite. The quartz and plagioclase in the ground-mass often exhibit a fine grained myrmekitic intergrowth. The pyrite and pyrrhotite are concentrated in layers (3-6mm wide) in which sulphide concentration is up to 15% - the interlayered zones (also ~6mm) are free of sulphide. The pyrite and pyrrhotite typically form anhedral, irregular, stringer-type composite grains between the coarser gangue minerals. These composite grains vary from 0.1 to 0.5mm in size.

Unit 3. Sillimanite-augen Pyritic Quartzite

In hand specimen the rock is felsic and well foliated with conspicuous sillimanite augen and disseminated pyrite and pyrrhotite.

The rock consists of:

	RANGE	MODE
quartz	60-70%	65%
sillimanite	15-25%	16%
pyrrhotite	6-7%	7%
pyrite	3-6%	5%
limonite	5%	5%
sericite	0-2%	2%
biotite	tr	tr
plagioclase (composition?)	tr	tr
rutile	tr	tr
sphalerite	tr	tr

The rock has a fine grained ($\sim$ 0.5mm) granoblastic platy polygonal inequigranular texture. The ground-mass is composed essentially of a fine grained equigranular platy polygonal mosaic. The sillimanite augen (up to 4-5mm in length), are composed of minute (sub-microscopic in places) sillimanite prisms. The sillimanite is generally associated with the sericite which usually appears as an alteration product.

The sulphides occur as small elongate aggregates of pyrite and pyrrhotite parallel to the foliation. There are traces of anhedral sphalerite within the pyrite/pyrrhotite aggregates. The pyrite tends to be euhedral within the pyrrhotite (anhedral). Very fine (0.1mm) rounded sub-hedral grains of rutile occur within the quartz mosaic and sillimanite layers.

Unit 4. Banded Biotite Gneiss

In hand specimen the rock is a fine grained equigranular banded gneiss which is characterised by fine ($\sim$1mm) impersistent bands of darker minerals (mainly biotite) in a felsic ground-mass.

The rock is composed of the following minerals:

	RANGE	MODE
quartz	30-60%	60%
plagioclase-oligoclase ($Ab_{70}An_{30}$)	5-20%	20%

	RANGE	MODE
orthoclase	5-20%	10%
biotite	10-20%	10%
hypersthene	0-15%	0%
magnetite	tr-1%	tr
pyrite	tr	tr
bustamite/rhodonite	tr	tr
zircon	tr	tr

The gneiss is fine grained (~ 0.5mm) granoblastic inequigranular interlobate. The quartz and orthoclase form porphyroblasts up to 1.5mm in size. The ground-mass is made up of quartz, plagioclase and biotite, with occasional grains of hypersthene tending to poikiloblasticity. The pyrite and magnetite are extremely fine grained (~ 0.1mm), anhedral and are disseminated throughout the rock. The zircon occurs mainly within the biotite grains causing pleochroic halos. The biotite and hypersthene are intergrown and define the foliation. Plate A shows the relationship of quartz, biotite and hypersthene. The biotite is green to green-brown in colour and is altered to chlorite at the edges. The hypersthene is usually faintly pleochroic with some alteration (to antigorite?) along fractures and grain edges.

Unit 5. Felsic Sillimanite Gneiss (Upper Unit)

In hand specimen the rock is typically pink, pale-pink to white, or occasionally a very pale green, with no dark minerals present, and varies from a fine grained weakly foliated granulite (defined by sillimanite), to a coarse grained sillimanite gneiss.

The rock is made up of the following minerals:

	RANGE	MODE
quartz	50-70%	55%
perthite	10-25%	20%
andesine plagioclase ($Ab_{65}An_{35}$)	5-20%	20%
sillimanite	1-10%	4%
biotite	tr-2%	tr
muscovite	tr-2%	tr
magnetite	tr	0
pyrite	tr	0

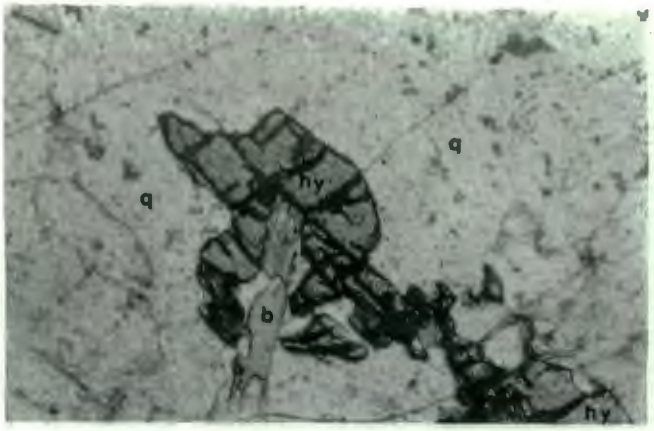

A

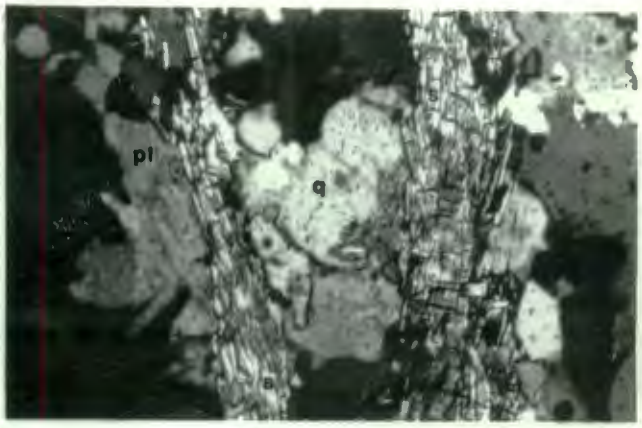

B xn

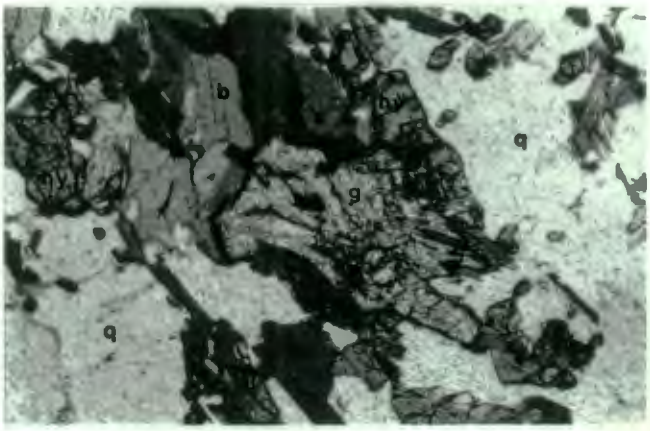

C

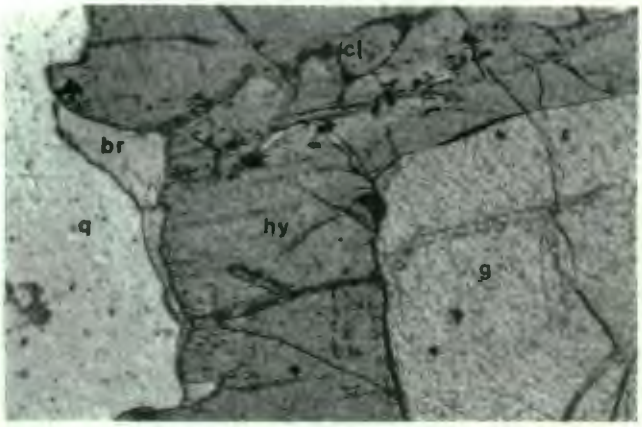

D

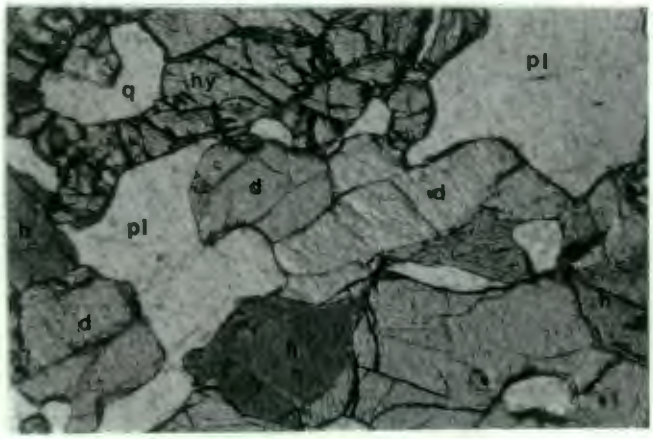

E xn

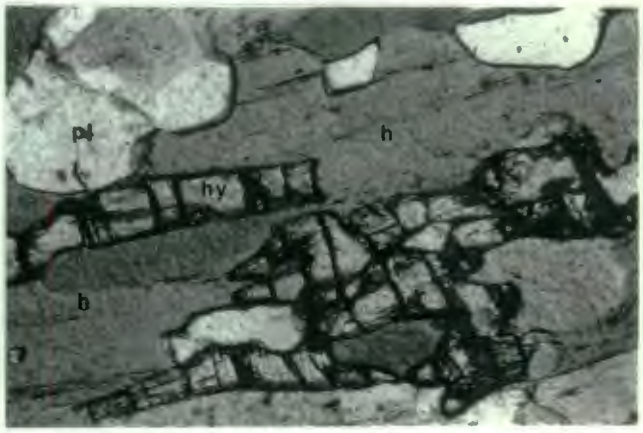

F

G

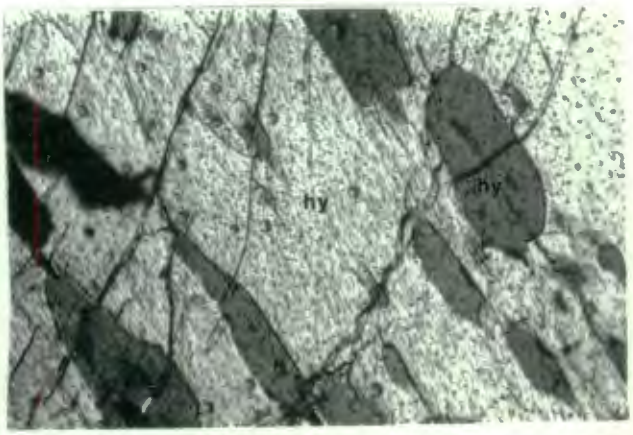

H xn

The microscopic texture is fine grained seriate interlobate with the quartz and perthite tending to be porphyroblastic. These (irregular anhedral shaped) porphyroblasts are ~2mm in grain size. The ground-mass consists of a fine grained (0.3mm) mosaic of plagioclase and quartz. The size of the perthite porphyroblasts increases (up to 6mm) and becomes more amoeboid in outline towards the pegmatitic gneiss. There is usually some granophyric intergrowth between quartz and feldspar. The sillimanite exhibits a preferred orientation and forms lenses up to 6mm long composed of individual sillimanite prismatic grains (0.1 - 0.2mm long). (See Plate B).
The muscovite and green biotite are fine grained (<0.5mm) and disseminated throughout the rock. The anhedral pyrite seems to be intergranular and is probably a later introduced phase associated with secondary quartz crystallisation.

Unit 6. Hypersthene-quartz-garnet Granulite

In hand specimen the rock is a medium grained porphyroblastic intermediate/mafic granulite with a vague foliation. The larger the porphyroblasts of garnet and/or hypersthene the less the foliation is discernible, and conversely, the foliation increases with the quartz content. The most distinctive feature of the rock is the presence of large garnet porphyroblasts.
The rock is composed of the following minerals:
(The quartzose coarse bands are not included).

	RANGE	MODE
quartz	0-35%	33%
hypersthene	20-50%	25%
plagioclase-andesine ($Ab_{65}An_{35}$)	15-30%	20%
biotite	5-15%	10%
orthoclase (perthite)	5-15%	5%
garnet (almandine?)	5-10%	5%
magnetite	1-2%	1%
bronzite	0-3%	0%
hercynite	tr-1%	tr
pyrite	tr-1%	tr
apatite	tr	tr

The microscopic texture is medium grained granoblastic intergranular interlobate/polygonal. The larger grains (2-6mm) of hypersthene are porphyroblastic or rarely poikiloblastic. Porphyroblastic garnet, is often intergrown with the hypersthene (See Plates C and D) and usually the latter rims the almandine. There appear to be two generations of biotite. The first is developed as overgrowths on the hypersthene (See Plate C); the second forms skeletal intergrowths with quartz and feldspar. In both instances the biotite is brown. Bronzite occurs at the edges of hypersthene grains (See Plate D) in one instance. The ground-mass is composed of interlobate (approaching polygonal) fine grained (~0.5mm) quartz, andesine and orthoclase. The quartz also occurs as larger poikiloblastic (at times ribbon-like) grains and as granophyric intergrowth with feldspar.

Magnetite and hercynite invariably occur together (if hercynite is present) as irregular interstitial grains within the polygonal ground-mass.

Unit 7. Amphibolite

In hand specimen the rock is medium grained mafic to intermediate with a poorly developed foliation. It grades into a foliated hypersthene granulite.

The mineralogy is as follows:

	RANGE	MODE
hornblende	25-65%	35%
plagioclase-labradorite ($Ab_{35}An_{65}$)	20-45%	34%
hypersthene	0-25%	20%
diopside	0-15%	10%
biotite	0-2%	1%
muscovite	0-15%	0%
magnetite	tr	tr
apatite	tr	tr

The microscopic texture is granoblastic to nematoblastic (depending on the abundance of hornblende and micas), inequigranular interlobate to polygonal. The amphibole, usually a bright-green variety of hornblende, forms the

larger (~2mm) grains and tends to be poikiloblastic. The amphibole and pyroxenes are intergrown, the amphibole having formed by retrogression, i.e. the hornblende replaced both clinopyroxene and orthopyroxene (See Plates E and F). The orthopyroxene altered along fractures and cleavages to serpentine (antigorite?) (See Plate F). The labradorite forms a fine grained (~0.5mm) polygonal ground-mass, and minor plagioclase is enclosed in the poikiloblastic dark minerals.

On Section 56E, in the extreme east of the K3 area, the amphibolite contains no pyroxenes, the amphibole is altered to clinochlore (chlorite), and muscovite composes up to 15% of the rock. The plagioclase is severely saussuritzed. X-ray diffraction has identified kaolinite-type clays in addition to clinochlore and muscovite.

Unit 8. Porphyroblastic Hypersthene-biotite Granulite

In hand specimen it is a medium to coarse grained intermediate granulite, usually poorly foliated. The hypersthene typically forms coarse porphyroblastic grains, which in the more mafic varieties coalesce into massive hypersthene. The mineralogy is as follows:

	RANGE	MODE
hypersthene	15-30%	30%
quartz	26-60%	30%
plagioclase	0-25%	20%
biotite	10%	10%
orthoclase	5-10%	9%
magnetite	0-3%	1%
pyrite/pyrrhotite	0-2%	0%
hercynite ($60\%\ Al_2O_3$; $32\%\ Fe_2O_3$; $8\%\ MgO$)	tr-2%	tr
apatite	tr	tr

The rock has a granoblastic inequigranular interlobate to amoeboid texture. The porphyroblastic to poikiloblastic hypersthene grains (up to 4mm in size) dominate the texture. These typically have irregular to amoeboid grain boundaries. The hypersthene can also form smaller (1.5mm) subhedral grains. Hypersthene is usually altered to antigorite in cleavage fractures and grain boundaries (See Plate G). This effect

increases markedly near the massive sulphides (within 5-7m). The orthoclase and quartz form larger anhedral porphyroblasts with the quartz tending to ribbon texture. The ground-mass consists of an interlobate fine grained (~1mm) mosaic of quartz and plagioclase. The biotite is invariably associated with the hypersthene. Pyrite and pyrrhotite occur as small, irregular, interstitial, composite grains (0.1-0.2mm) and as fine, rounded grains within quartz and feldspar. Hercynite and magnetite are always associated and occur as finely disseminated intergranular grains.

Unit 9. Cordierite-hypersthene-quartz Granulite

In hand specimen this unit is difficult to distinguish from the porphyroblastic hypersthene biotite granulite (Unit 8), particularly if felsic. The rock is usually fine grained with little or no foliation visible - the rock is intermediate, with the cordierite giving a pale bluish tinge.
The rock is composed of:

	RANGE	MODE
quartz	15-35%	35%
cordierite	5-30%	35%
biotite	5-15%	15%
hypersthene	0-30%	5%
orthoclase	0-30%	5%
pyrite	tr-7%	3%
pyrrhotite	tr-7%	3%
magnetite	tr-10%	2%
plagioclase	0-2%	0%
tourmaline	0-2%	0%
sphalerite	tr	0%
hercynite	tr-1%	tr
chalcopyrite	tr-0.5%	tr
hematite	0-2%	tr

The rock has a granoblastic seriate amoeboid texture. The cordierite forms rounded grains with irregular amoeboid edges, and tends to be poikiloblastic. This mineral has usually altered to pinite at grain edges and fractures. Pyrite seems to be associated with cordierite alteration and is found as an intergranular phase within the pinite. The hypersthene forms large (2-4mm) porphyroblasts, enclosing quartz and feldspar grains. The hypersthene exhibits twinning

(See Plate H) which is usually a sign of recrystallisation under deformation. The biotite is always associated with hypersthene. The quartz and feldspar form an interlobate/ amoeboid mosaic ground-mass and also exhibit a granophyric intergrowth. Rare tourmaline is found within the ground-mass as subhedral grains. Magnetite and hercynite are always associated and occur as small (<0.5mm) intergranular anhedral grains. There is a gradual increase in the abundance of disseminated sulphides (up to 15% within 1m of the massive ore) towards the massive sulphides. The contact however is sharp from 15% sulphide, (disseminated) to >75% massive sulphide over a distance of ≤2cm.

When the sulphide content increases to ~15%, the sulphides form irregular intergranular clots and veins within the silicate grains. There is a vague decrease in the pyrite/ pyrrhotite ratio from 2, 15m from the massive sulphide, to 0.1, 1m from the ore.

The pyrite, pyrrhotite and magnetite usually occur as discrete fine grains (<0.5mm). However, composite grains of pyrrhotite-magnetite-hematite-sphalerite, pyrrhotite-pyrite, pyrrhotite-pyrite-chalcopyrite-magnetite can occur. (See Plates I, J, K).

The pyrite (and more rarely the pyrrhotite) have haloes of magnetite (See Plate K).

Unit 10. The Quartz-cordierite-sillimanite Granulite

In hand specimen the rock is a fine to medium grained felsic equigranular non-foliated granulite which has a distinct blueish-grey colour if the cordierite content is high. Disseminated pyrite and pyrrhotite are always present and there is an increase in sulphide abundance, and the Po/Py ratio, towards the massive sulphide contact.

Sphalerite and chalcopyrite are present ≤10cm from the ore.

The rock is composed of:

	RANGE	MODE
cordierite	15-40%	35%
quartz	20-50%	35%
biotite-phlogopite	5-15%	10%
pyrrhotite	0-20%	8%
sillimanite	0-20%	5%
pyrite	0-20%	5%
magnetite	0-4%	2%

I r

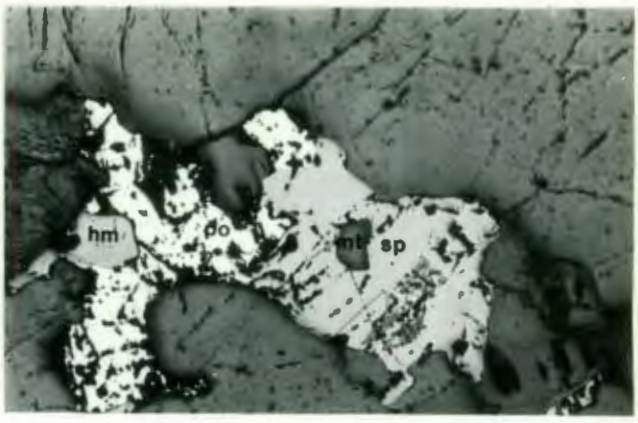

J r

K r

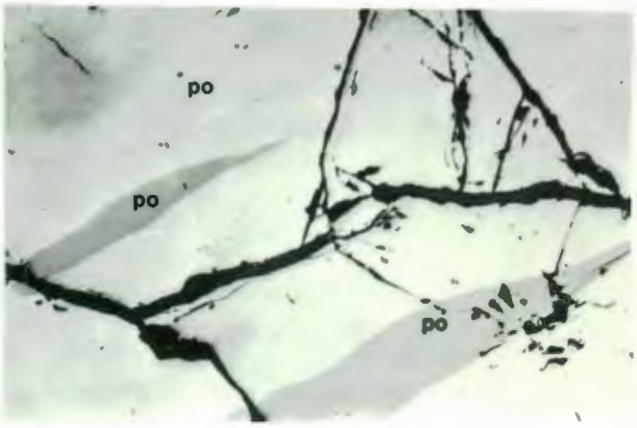

L r - xn

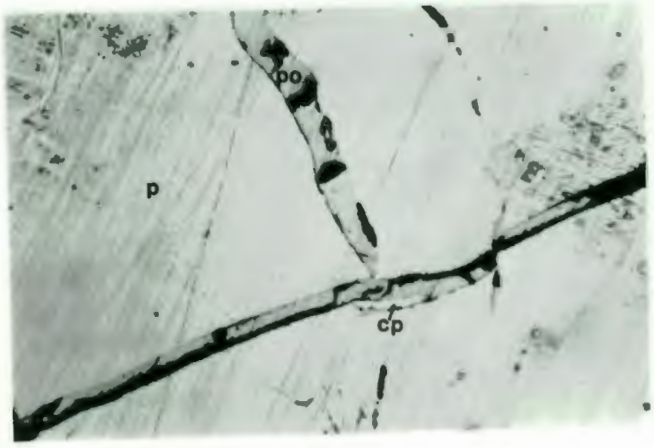

M r

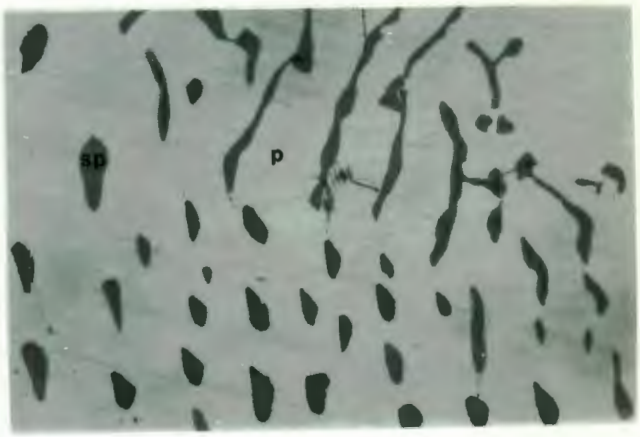

N r

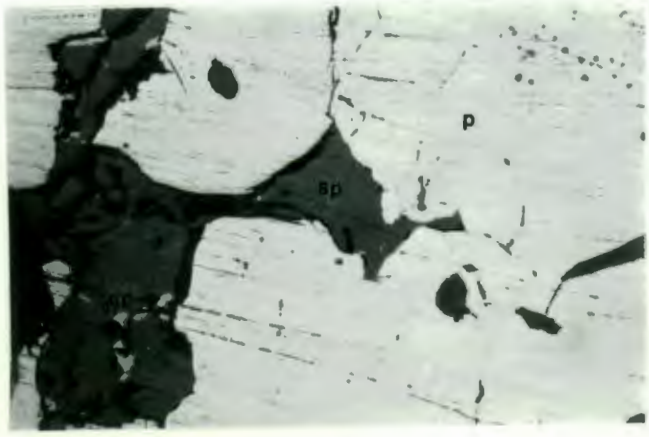

O r

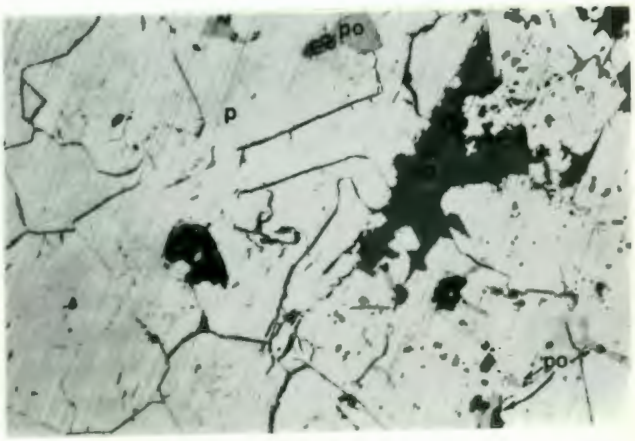

P r

Where the sulphide/oxide ratio is low, composite grains of pyrite, magnetite and pyrrhotite are found; all three minerals can also occur as discrete grains. The opaque minerals are always as interstitial grains between the mosaic of quartz and cordierite. Skeletal pyrite grains have partially replaced cordierite.
Within 4cm of the massive sulphide the rock contains up to 4% sphalerite and 1% chalcopyrite within composite grains of pyrite and pyrrhotite. The chalcopyrite forms interstitial coatings between silicate and sulphide grains and fine blebs within sphalerite.

Unit 11. The Massive Sulphide Unit and Intercalated Siliceous Zones

In hand specimen the rock consists of coarse grained pyrrhotite-pyrite-sphalerite with finely disseminated barite, calcite and chalcopyrite. The gangue consists of chlorite, red earthy hematite and biotite. X-ray diffraction has shown the green "clayey chlorite" to consist of chlorite, amesite (both magnesian chlorites) and minor quartz. There is no foliation visible, although coarse mineralogical and chemical zoning is present. Because of the marked mineralogical zoning the petrographic descriptions will be dealt with under four sub-headings:

a) The Upper Pyrrhotite Zone
b) The Sphalerite Zone
c) The Siliceous Zone
d) The lower Pyrrhotite-Pyrite Zone

a) The Upper Pyrrhotite Zone

The rock is composed of:

	RANGE	MODE
pyrrhotite	70-80%	75%
pyrite	8-20%	10%
phlogopite	0-10%	5%
sericite	0-20%	5%
quartz	0-5%	1%
marcasite	0-4%	1%
chalcopyrite	tr-2%	tr
sphalerite	tr	tr
calcite	tr	tr

The pyrrhotite occurs as large (> 2cm) irregular masses, which are composed of a coarse polygonal mosaic of grains (>3mm).

Pyrite occurs within the pyrrhotite mosaic either as

(i) amoeboid blebs within the individual pyrrhotite grains; this is usually a composite of pyrite and marcasite; or

(ii) euhedral interstitial grains forming a mosaic with pyrrhotite.

Pyrrhotite exhibits lamellae of optically differentiated pyrrhotite (See Plate L). The pyrrhotite is usually clear of inclusions of gangue, whereas pyrite typically has numerous quartz and calcite inclusions.

Chalcopyrite occurs in veins and as an interstitial phase between pyrrhotite and gangue minerals, or as subrounded blebs (with occasional sphalerite blebs) within pyrrhotite. In specimens where pyrite content is high, composite veins of chalcopyrite and pyrrhotite cross the larger pyrite grains (See Plate M).

b) The Sphalerite Zone

The rock is composed of the following minerals:

	RANGE	MODE
pyrite	5-80%	65%
pyrrhotite	tr-70%	25%
sphalerite	1-30%	10%
chlorite	tr-15%	3%
barite	tr-20%	3%
marcasite	0-5%	2%
chalcopyrite	tr-5%	1%
sericite	tr	0%
edenite	0-5%	0%
orthoclase	0-2%	0%
gahnite	0-tr	0%
hypersthene	0-3%	0%
phlogopite	0-15%	0%
plagioclase	0-5%	0%
calcite	tr-10%	tr
biotite	0-10%	tr
quartz	tr-5%	tr

The pyrite/pyrrhotite ratio is highly variable, the sphalerite content is more consistent, and the minor mineral contents are also highly variable.

The pyrite occurs as irregular anhedral grains and as large (4-5mm) euhedral grains. The pyrite is usually composed of polygonal mosaic, although not always discernable unless defined by interstitial blebs of pyrrhotite or sphalerite (See Plate N). The pyrite mass also contains large interstitial grains of sphalerite, chalcopyrite and pyrrhotite (See Plates O and P).

The pyrrhotite has inclusions of amoeboid marcasite and euhedral pyrite (See Plates Q and R).

Frequently chalcopyrite occurs at the contact between pyrrhotite and gangue minerals. Polygonal mosaics of pyrite, pyrrhotite, quartz, barite and sphalerite, the grain size being 1-2mm, can occur.

Chalcopyrite (in addition to occurring as above) is ubiquitously present as exsolution blebs in the larger (1-3mm) sphalerite grains. The grains can be very fine (almost submicroscopic - see Plate O) or relatively coarse (0.01 - 0.03mm) (See Plate S).

The chalcopyrite also forms veinlets cutting all the sulphide minerals but not the gangue minerals.

Irrespective of the form of the chalcopyrite, the grains never exceed 0.05mm.

Sphalerite has also recrystallised into a polygonal mosaic (and like pyrite) made visible by the interstitial grains of chalcopyrite. (See Plate S).

Sphalerite also has blebs of pyrrhotite within the larger grains.

The barite which varies sympathetically with the sphalerite, occurs as 1mm polygonal grains within the sulphide mosaic. It is sometimes associated with sericite and edenite.

Calcite is present as veinlets cutting sulphides and gangue.

Gahnite which is rare is found as fine grained ($\leq$ 0.1mm) euhedral grains within sphalerite.

The silicates, (quartz, hypersthene, orthoclase, plagioclase, biotite and phlogopite) occur as rare interstitial grains usually in the less massive (<65% sulphide) sulphides.

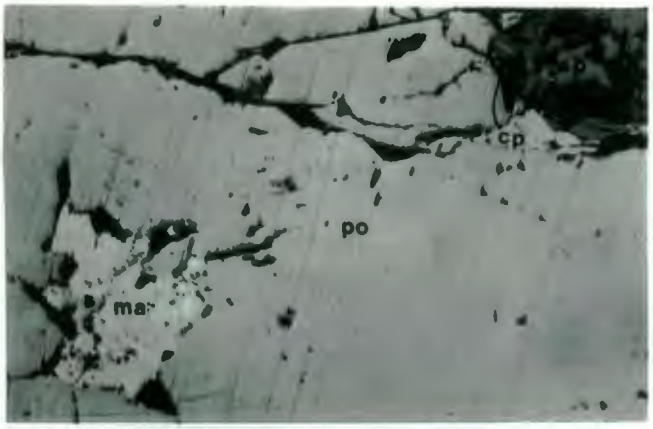

Q r

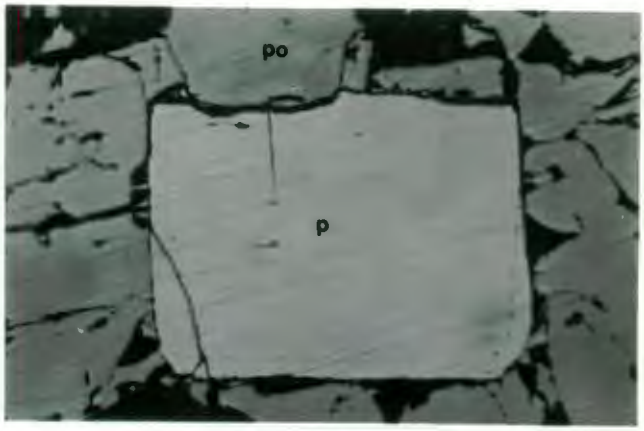

R r

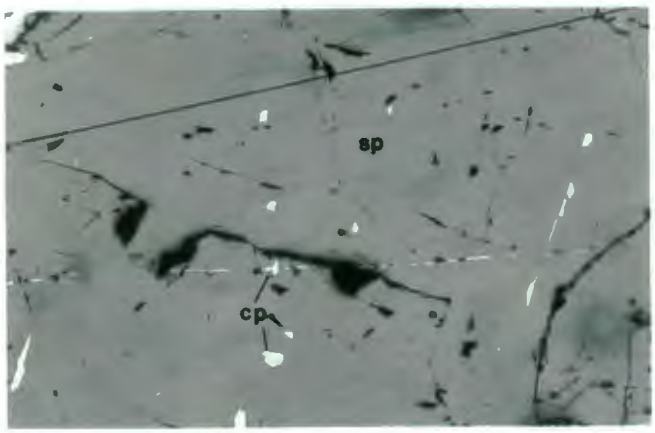

S r

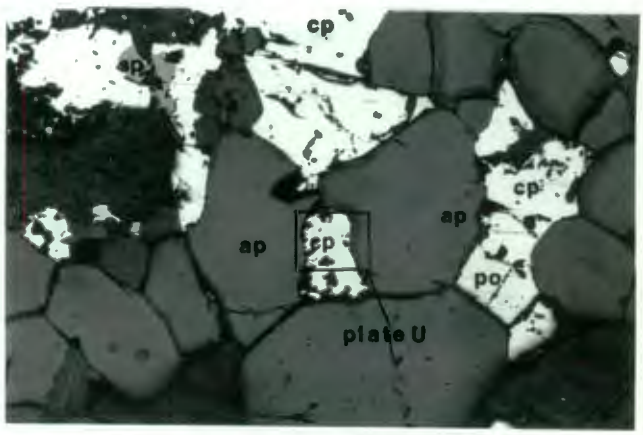

T r

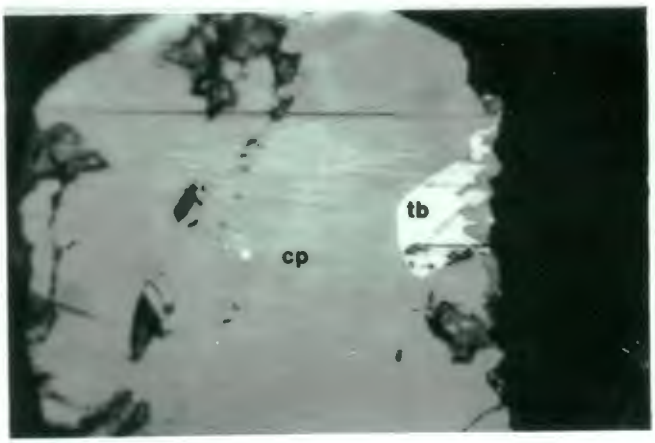

U r

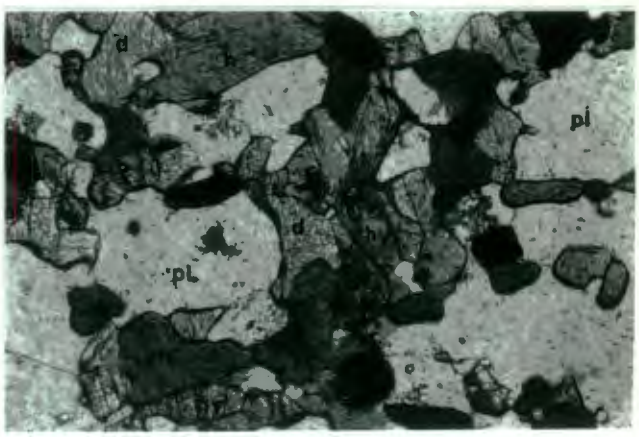

V

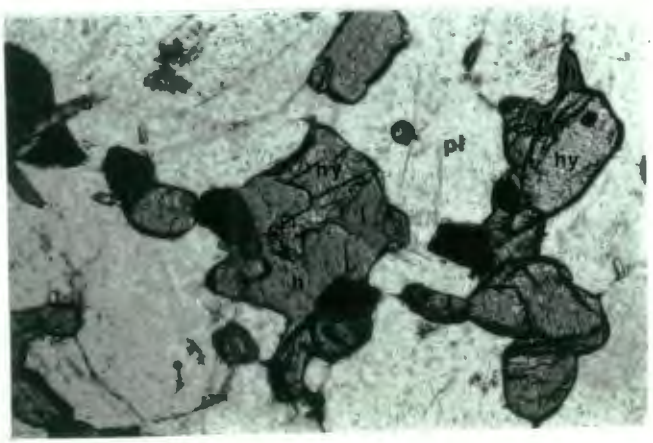

W

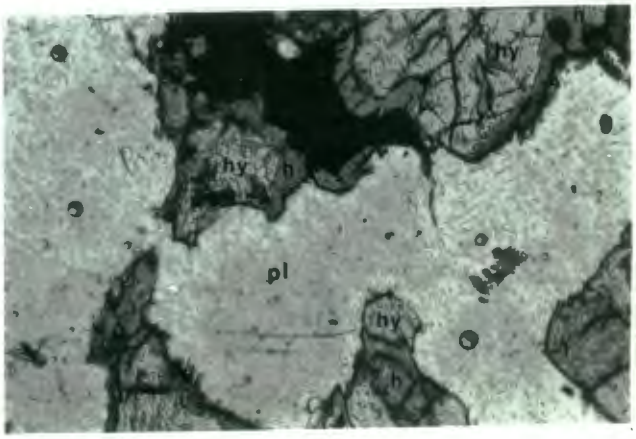

X

c) The Siliceous Zone

The rock is composed of:

	RANGE	MODE
quartz	50-70%	65%
plagioclase-andesine ($Ab_{60}An_{40}$)	0-30%	20%
biotite (altered to chlorite)	5-10%	5%
pyrite.	0-5%	4%
sericite	2-25%	2%
pyrrhotite	0-5%	2%
calcite	0.18%	tr
chalcopyrite	tr	tr
sphalerite	tr	tr
andalusite	tr	tr

The texture varies from granoblastic seriate to equigranular, with amoeboid grain outlines. The quartz forms a fine grained (~1mm) mosaic with plagioclase, both minerals can however occur as larger porphyroblasts (~3mm across). In some instances the quartz forms ribbon-like grains (in which case sericite accentuates the foliation. Usually the rock shows no foliation).

The plagioclase is at least partially sericitized. Fine interstitial flakes of biotite are usually altered to chlorite. Sulphides are present as fine ($\leq$ 0.1mm), subrounded or slightly elongated, grains parallel to the foliation. The grains are composites of pyrite, pyrrhotite, chalcopyrite and rarely sphalerite.

Calcite forms veinlets which cross-cut sulphide and silicate minerals.

d) The Lower Pyrite-Pyrrhotite Zone

The rock is composed of the following:

	RANGE	MODE
pyrite	10-75%	50%
pyrrhotite	10-50%	20%
chlorite	1-20%	8%
sphalerite	tr-25%	5%
quartz	1-20%	5%
calcite	tr-5%	4%
chalcopyrite	tr-5%	2%

	RANGE	MODE
cordierite	0-18%	2%
apatite	0-5%	2%
barite	tr-5%	1%
cubanite	tr	0%
zircon	tr	tr
plagioclase	0-4%	tr
phlogopite	tr-20%	tr
tellurbismuth	tr	tr

The sulphide textures and relationships are identical to the sphalerite zone.

Apatite forms a polygonal mosaic (See Plate T) within the massive sulphide. There is some interstitial sulphide, and phlogopite, within the mosaic.

Cordierite, found only in the semi-massive sulphide units (i.e. <50% total sulphides) forms anhedral subrounded (0.75mm) grains with amoeboid edges against quartz and phlogopite. The cordierite contains some sulphide inclusions. The chalcopyrite contains rare blebs of tellurbismuth (positively identified by microprobe) and fine (~10microns) silver rich specks (See Plates T and U).

12. Diopside-Plagioclase Granulite

In hand specimen the rock is a fine grained mafic granulite with disseminated pyrite and magnetite. Foliation is only weakly developed.

The rock is composed of:

	RANGE	MODE
diopside	20-45%	40%
plagioclase-labradorite ($Ab_{50}An_{50}$)	35-45%	35%
hornblende	0-20%	15%
hypersthene	0-15%	5%
magnetite	2-5%	5%
biotite	0-10%	3%
quartz	0-5%	0%
pyrite	tr-2%	tr
apatite	tr	tr
zircon	tr	tr

The rock has a granoblastic equigranular interlobate/polygonal texture. (See Plates V and W).

Hypersthene is finer grained, more subhedral, and more altered than the diopside. The two pyroxenes occur both discretely and intergrown (See Plate V).
The diopside can be porphyroblastic.
The pyroxenes are invariably intergrown with hornblende, and in some instances the margins of pyroxenes have altered to amphibole (See Plates X and Y). There is no systematic variation in the degree of uralitization either with depth, strike or proximity to massive sulphides. The uralitization of pyroxenes appears to have proceeded preferentially around inclusions of pyrite (See Plate X).
The sulphide phases (mainly pyrite, minor pyrrhotite) are interstitial, and occur within cleavages and fractures of the pyroxenes and amphiboles. Magnetite occurs as euhedral primary grains and is concentrated along plagioclase cleavages.
Within 2m of the contact between diopside granulite and granodiorite the hornblende/pyroxene intergrowths are rimmed by an alteration halo of chlorite (See Plate Z), and the plagioclase is also strongly saussuritized.

Unit 13. Banded Hypersthene Granulite

In hand specimen the rock is banded, medium to coarse grained and in places approaches a feldspathic amphibolite.
The rock consists of:

	RANGE	MODE
quartz	10-30%	30%
hypersthene	25-45%	25%
plagioclase-andesine ($Ab_{52}An_{48}$ to $Ab_{65}An_{35}$)	25%	25%
biotite	12-25%	15%
magnetite	tr-3%	3%
hornblende	0-10%	0%
cordierite	tr-5%	tr

The minerals form a coarse grained, granoblastic, inequigranular, interlobate texture. The hypersthene is poikiloblastic (~3mm grains) and encloses plagioclase. Quartz forms larger (up to 6.5mm) anhedral poikiloblasts enclosing hypersthene and plagioclase. The plagioclase together with smaller grains of hypersthene and quartz (~0.75mm) form an interlobate mosaic. The brown pleochroic biotite

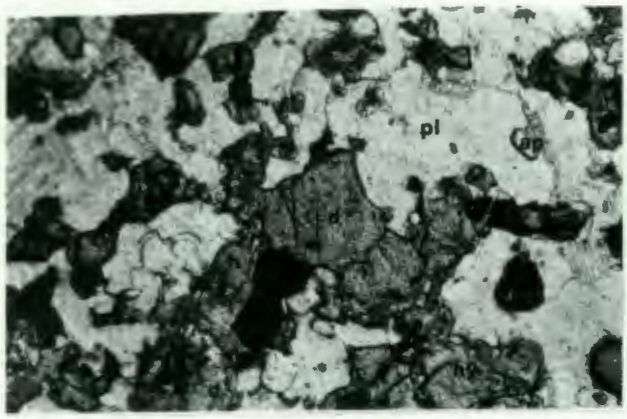

Y

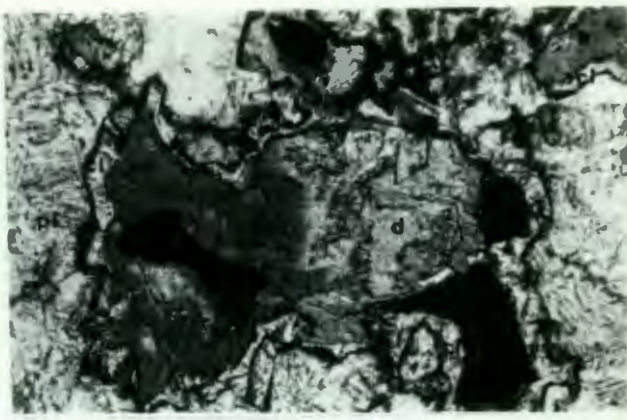

Z

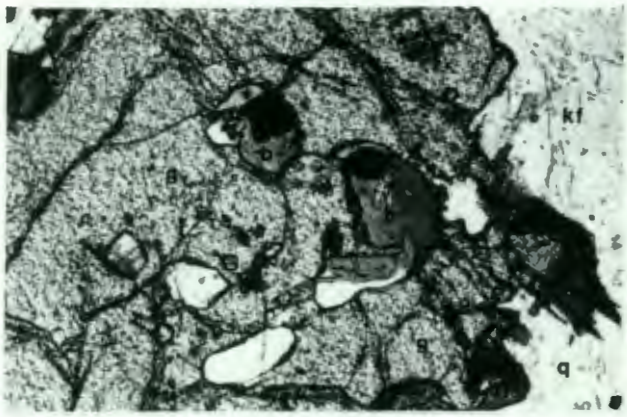

AA

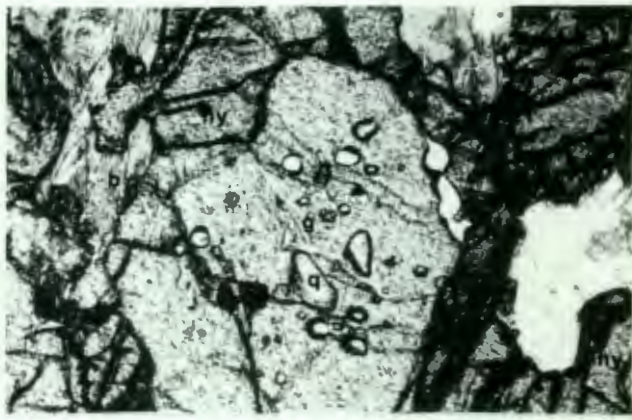

AC

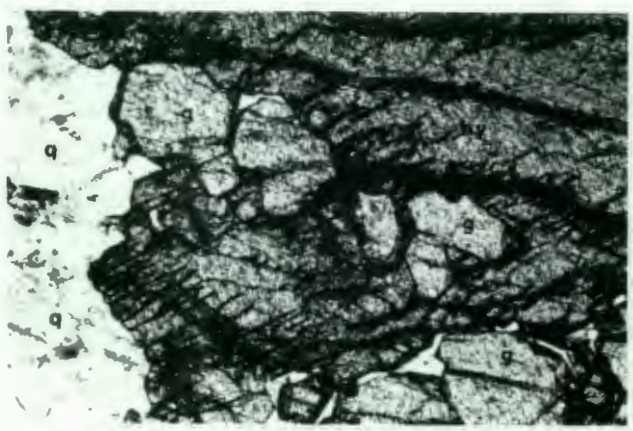

AB

AD

AE

xn

occurs as overgrowths on the hypersthene whereas the less pleochroic, olive-green biotite is intergrown with the plagioclase ground-mass.
The sulphides (~ 5% pyrite, ~5% pyrrhotite, trace chalcopyrite) occur as small, interstitial, ($\leq$ 0.5mm) composite grains. When the total sulphide content reaches about 10% the grains merge to form irregular stringers.

Unit 14. Felsic Sillimanite Gneiss (Footwall)

This unit is mesoscopically and microscopically identical to the one found in the hanging wall (Unit 5).

Unit 15. Banded Biotite-Garnet Gneiss

In hand specimen the rock is a banded inequigranular medium grained intermediate rock.
The mineralogy is as follows:

	RANGE	MODE
quartz	10-50%	35%
plagioclase-andesine ($Ab_{65-70}An_{35-30}$)	10-35%	20%
hypersthene	1-35%	20%
biotite	tr-20%	10%
garnet (almandine)	0-20%	5%
magnetite	2-5%	4%
hornblende	0-35%	3%
diopside	0-20%	0%
orthoclase	0-3%	0%
hercynite	tr-1%	tr
apatite	tr	tr

The rock has a granoblastic inequigranular or seriate, interlobate to amoeboid texture.
The garnet forms large (2.5-5mm) poikiloblasts enclosing quartz and feldspar. Garnet also encloses grains of biotite which usually coexist with quartz and/or plagioclase (See Plate AA). The garnet has irregular amoeboid embayed edges.
Hypersthene, which is partially altered to antigorite, poikiloblastically encloses garnet grains (See Plates AB and AC). The hypersthene is usually intergrown with biotite.
The quartz forms a platy texture with ribbon-like grains up to 4mm long. The ground-mass consists of plagioclase

(antiperthite, fine lamellae of orthoclase) and quartz either as a polygonal fine grained (0.75mm) mosaic or an amoeboid mosaic.
The ribbon-like quartz with the biotite define the foliation, while the garnet and hypersthene have grown across the foliation.
The magnetite, which forms finely disseminated anhedral irregular grains (0.1 - 0.5mm), or rarely euhedral grains, is always intergrown with hercynite.
The hornblende has a sieve texture in which it encloses minute quartz grains (See Plate AD) and is intergrown with biotite.

Unit 16. Coarse-Grained Granite

The granite is coarse-grained white to pink and pegmatitic. The rock consists of:

perthite	40%
quartz	35%
plagioclase-oligoclase ($Ab_{72}An_{28}$)	25%

The texture is coarse-grained inequigranular interlobate. The orthoclase forms large subhedral porphyroblasts (~12mm), with coarse lamellae of exsolved albite (See Plate AE). The perthite porphyroblasts have quartz inclusions (rounded) and veinlets which seem to have acted as "cores" around which the albite exsolved preferentially (See Plate AE). The ground-mass consists of an interlobate mosaic of fine grained (~0.5mm) quartz and plagioclase. Quartz also forms anhedral (~5mm) porphyroblasts.

Unit 17. Granodiorite

In hand specimen the granodiorite is a fine grained intermediate rock with a vague foliation. The characteristic feature of this rock unit is its homogeneity (both in hand specimen and macroscopically). The feldspar gives the rock a typical grey and pink speckled hue.
The rock is composed of:

	RANGE	MODE
quartz	35-45%	35%
plagioclase-andesine ($Ab_{65}An_{35}$)	25-35%	25%

	RANGE	MODE
microcline	10-25%	15%
biotite	10%	10%
muscovite	0-5%	0%
magnetite	tr-2%	tr
pyrite	tr	tr
calcite	tr	tr

The rock has an inequigranular interlobate texture with the microcline tending to be porphyroblastic. The groundmass consists of a fine grained (0.75 - 1.0mm) mosaic of anhedral quartz, plagioclase and microcline. The grain boundaries are irregular and there is ubiquitous granophyric intergrowth. Biotite is generally finer grained ($\sim$0.4mm) and forms irregular grains. Zircon inclusions in biotite are common. The magnetite is fine-grained ($\ll$0.5mm), anhedral and interstitial, and occurs with biotite. The plagioclase is rarely zoned with the cores being more calcic (highly saussuritized).

The granodiorite, near its contact with the country rock, shows evidence of shearing, with a foliation defined by biotite orientation. The quartz content is increased in the granodiorite towards the edges (up to 70% in thin section RKG 89) and the microcline is developed as coarse (5mm) twinned porphyroblasts. This assemblage seems to represent an acid phase of the granodiorite.

AREA K1

Unit 1. Banded Biotite Gneiss

This unit has not been extensively sampled by diamond drilling and its detailed petrography is not known. The unit where intersected was always highly weathered. In this state it appears similar to the banded biotite gneiss found in the K3 area. The impersistent fine bands of biotite in the felsic ground-mass characterise the rock.
The unit has a minimum thickness of 30m.

Unit 2. Amphibole-Quartz-Granulite

In hand specimen the rock is an intermediate, fine grained, non-foliated, granular rock. This unit is unique in that it outcrops relatively commonly, forming rounded black boulders and cobbles. The ubiquitous presence of desert varnish on the surface gives a mafic appearance to the rock. The fresh rock is usually green, but if the garnet content is high the rock is a dark orange.
Parallel alignment of elongate quartz grains gives the rock a distinct lineation in places.
Two varieties of this amphibole-rich unit are recognized:
(i) The edenite-quartz granulite is composed of the following:-

	RANGE	MODE
quartz	30-40%	34%
edenite	25-45%	30%
plagioclase-labradorite ($Ab_{45}An_{55}$)	18-23%	20%
cordierite	0-10%	5%
garnet (orange)	0-5%	4%
hornblende	0-4%	4%
sphene	1-3%	2%
pyrite	1%	1%
apatite	tr-1%	tr

The texture varies from platy granoblastic in the more siliceous varieties to isotropic granoblastic where there is less quartz, otherwise the texture is inequigranular and interlobate. In the platy rock quartz forms ribbon-like composite grains up to 6mm long. Edenite and the

rarer hornblende and garnet form larger (2-5mm) porphyroblastic grains, which are anhedral and can enclose quartz and feldspar. The cordierite and plagioclase form smaller (1-1.5mm) poikiloblastic grains. Sphene is always intergrown with edenite. Pyrite forms irregular intergranular (<0.75mm) grains.

(ii) The amphibolite contains:-

	RANGE	MODE
hornblende	30-40%	40%
plagioclase-labradorite ($Ab_{45}An_{55}$)	25-40%	35%
diopside	5-15%	15%
biotite (brown)	5-10%	5%
garnet (orange)	0-10%	5%
apatite	tr	tr

The texture is granoblastic inequigranular interlobate. The green hornblende predominates with large (~5mm) composite grains poikiloblastically enclosing plagioclase (~0.75mm). The plagioclase, diopside and smaller amphibole grains form a finer grained (0.5-0.75mm) mosaic. The amphibole appears to be forming at the expense of the diopside and biotite after amphibole. The garnet is present as large "lacy" poikiloblasts.

Unit 3. Quartz-Biotite Gneiss

In hand specimen this is a fine grained felsic laminated gneiss, with garnet forming occasional large porphyroblasts. The rock is composed of the following minerals:

	RANGE	MODE
quartz	45-65%	50%
plagioclase-labradorite ($Ab_{45}An_{55}$)	10-45%	35%
biotite (green)	5-15%	15%
hypersthene	0-10%	0%
pyrite	0-2%	tr
magnetite	0-1%	tr

The texture is granoblastic inequigranular interlobate. The quartz forms larger (≥1.5mm) ribbon-like grains which exhibit strongly undulose extinction. The plagioclase, quartz and hypersthene form a fine grained (0.5mm) interlobate mosaic. Myrmekitic intergrowths of quartz and

plagioclase are present. The hypersthene has replaced biotite and forms a sieve texture with rounded quartz grains (See Plate AF).
Magnetite forms discrete disseminated subhedral grains, and the pyrite grains are irregular and intergranular. The magnetite shows skeletal intergrowth with biotite and quartz (See Plate AG).

Unit 4. Hypersthene-Cordierite-Biotite Gneiss

In hand specimen the rock is banded medium-grained intermediate gneiss with laminae of greenish biotite and porphyroblasts of hypersthene.
The rock consists of:

	RANGE	MODE
hypersthene	5-30%	25%
cordierite	15-25%	25%
biotite (green-brown)	20%	20%
quartz	10-30%	15%
orthoclase	5%	5%
plagioclase (composition?)	10-25%	10%
magnetite	tr	tr

The texture is granoblastic seriate amoeboid. The hypersthene occurs as larger (2.5mm) poikiloblasts and as smaller grains within the amoeboid mosaic (0.5 to 1.0mm) of cordierite, biotite and plagioclase. The quartz and orthoclase are porphyroblastic (3mm across) with amoeboid and interlobate grain boundaries respectively. Biotite and hypersthene are invariably associated and together define the foliation. In some coarse bands (5cm) the quartz content increases at the expense of hypersthene and biotite.

Unit 5. Quartz-Plagioclase-Garnet Gneiss

In hand specimen the rock is similar to unit 3 as a fine grained felsic laminated gneiss except that garnet is ubiquitous and becomes, in places, a major constituent.
The mineralogy is as follows:

	RANGE	MODE
quartz	45-50%	45%
plagioclase-andesine (Ab 50-70 An 50-30)	25-30%	30%

AF

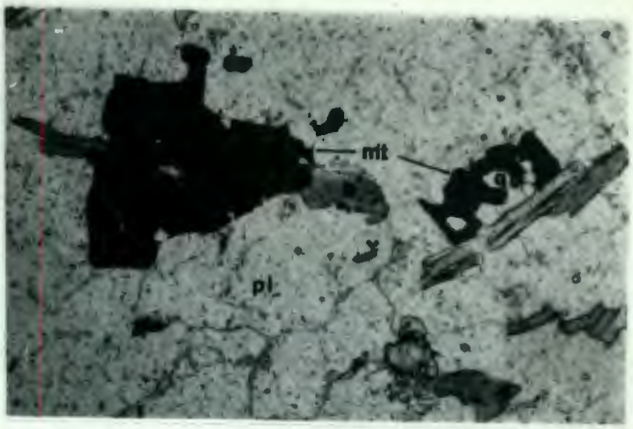

AG

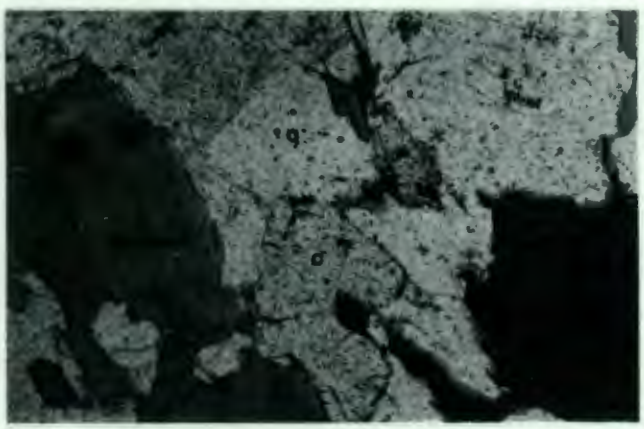

AH

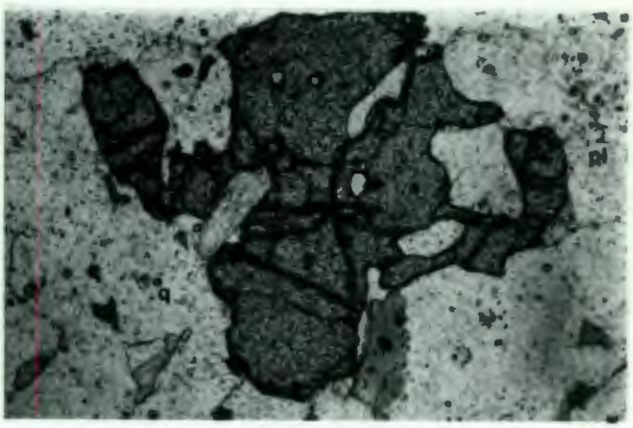

AI

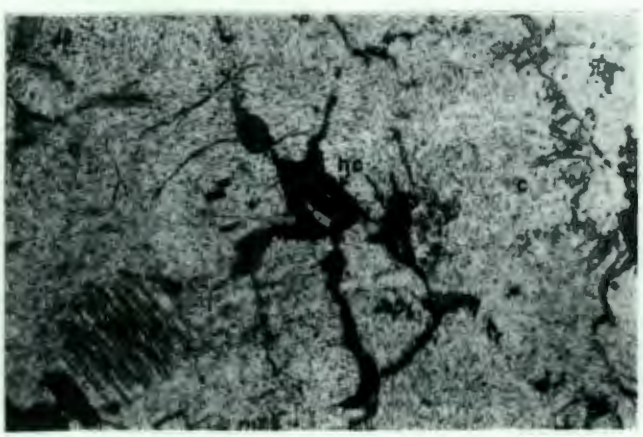

AJ

AK

xn

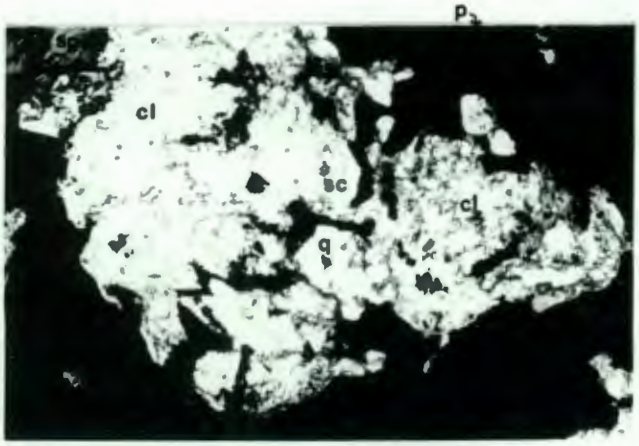

AL

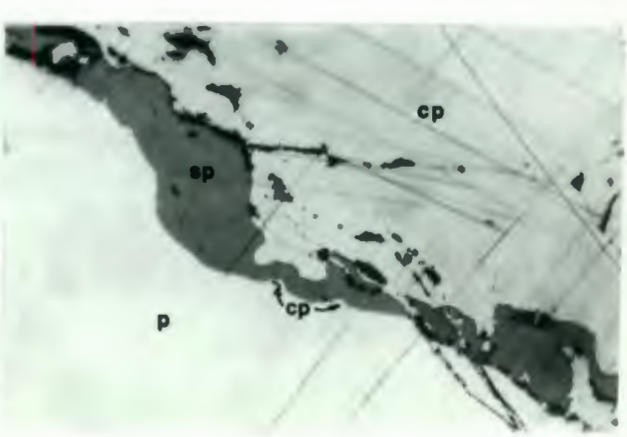

AM

r

	RANGE	MODE
biotite (brown and green-brown)	10-15%	15%
garnet (almandine)	10-15%	12%
magnetite	tr	tr
pyrite	tr	tr

The texture is granoblastic inequigranular to seriate and amoeboid. The garnet forms rounded (2.5mm) poikiloblastic grains that have a lacy or "exploded" texture (See Plate AI). The quartz forms large (≤4mm) amoeboid porphyroblasts and also forms part of the fine grained (≤0.4mm) mosaic with plagioclase (which is strongly 'sericitized') and biotite. The biotite, which is variable in colour (See Plate AH) tends to form wispy fine grains defining the foliation.

Unit 6. Quartz-Cordierite Granulite

In hand specimen this is a fine grained, felsic, greyish-blue granulite with a vague foliation defined by biotite. The rock is composed of the following:

	RANGE	MODE
quartz	35-65%	40%
cordierite	10-20%	20%
plagioclase-andesine (Ab_{65} An_{35})	2-20%	20%
biotite	0-15%	10%
hypersthene	0-15%	5%
garnet	0-7%	3%
phlogopite	0-10%	2%
pyrite	tr-7%	1%
magnetite	tr	tr
hercynite	tr	tr
zircon	tr	tr

The texture is granoblastic seriate amoeboid. The quartz forms large (~4mm) porphyroblasts which exhibit growth mosaics, and some of the quartz is also poikiloblastic. The garnet forms anhedral rounded poikiloblasts slightly finer grained than the quartz. The quartz, plagioclase and cordierite form a mosaic (2.5-3mm) with quartz having amoeboid outlines. The cordierite which usually exhibits polysynthetic twinning (See Plate AK) has a vague tendency to be zonally (centres preferentially) altered to pinite. (See Plate AT).

Hercynite is found within the cleavage cracks of the cordierite (See Plates AJ, AK). Hypersthene is usually as smaller grains (1mm) within the mosaic and is strongly altered to antigorite. Biotite and phlogopite are seriate and found throughout the rock. The biotite is brown, except when associated with hypersthene when it is a green brown colour. The pyrite content increases markedly toward the underlying sulphide zone up to a maximum of 7% pyrite. The pyrite occurs as fine ($\leq$0.5mm) intergranular disseminations.

Unit 7. The K1 Sulphide Unit

This zone is typically felsic, with the total sulphide content varying from 15 to 75%, the predominant sulphide being pyrite. The rock is generally poorly foliated. The sulphides are present as coarse composite grains, stringers, veins and fine disseminated grains with no preferred orientation. In the more sulphide-rich zones the pyrite contains rounded ($\sim$2mm) felsic blebs (quartz, cordierite and phlogopite - identified microscopically) and sub-angular ($\sim$1-2mm) grains of a black "clayey" mineral (identified by X-ray diffraction to be thuringite).
The unit is sub-divided into two zones :

(a) Total Sulphides 15-30% and
(b) Total Sulphides 40-75%.

(a) The zone consists of the following:

	RANGE	MODE
quartz	10-40%	35%
cordierite	25-65%	25%
pyrite	10-35%	25%
biotite	0-15%	10%
sphalerite	tr-14%	3%
chalcopyrite	1-5%	1%
plagioclase	0-20%	tr

The rock has a granoblastic seriate texture with ribbon-like quartz grains dominating. The cordierite occurs as a subhedral mosaic with the grains exhibiting undulose extinction. The cordierite is typically altered to pinite

at grain boundaries. The sulphides form large (4-6mm) irregular composite grains and smaller discrete disseminated grains - with rare slight preferred orientation. The pyrite forms anhedral grains which contain anhedral blebs of sphalerite and chalcopyrite. Where sphalerite content is high the grain size is larger and encloses subhedral pyrite grains. All three sulphide minerals also occur as discrete grains.

(b) The second sub-zone consists of:

	RANGE	MODE
pyrite	25-50%	38%
quartz	15-25%	25%
phlogopite	tr-15%	10%
sphalerite	5-10%	7%
cordierite	0-15%	5%
plagioclase	0-25%	5%
orthoclase	0-5%	4%
chalcopyrite	0-15%	2%
thuringite	0-5%	2%
tourmaline	0-2%	2%
pyrrhotite	0-tr	0%
galena	0-1%	tr

The rock typically consists of rounded aggregates (~2mm) of quartz, cordierite, chlorite and phlogopite (individual grains <0.25m with a matted texture) (See Plate AL) and rounded grains of cordierite. The quartz can also form a fine grained (~1mm) interlobate mosaic with plagioclase. The tourmaline is zoned with cores of a pale green colour, with the tourmaline grain margins altering to muscovite and chlorite. The plagioclase is typically strongly saussuritized. The sulphide forms anhedral composite masses up to ~10mm across, and a highly irregular -shaped intergranular phase. Pyrite exists as two forms (i) larger anhedral intergranular grains which contain sphalerite blebs and (ii) euhedral to subhedral pyrite relatively free of inclusions but containing small blebs of chalcopyrite and traces of pyrrhotite. Chalcopyrite occurs as large anhedral grains within composite masses of pyrite and minor sphalerite. The chalcopyrite has amoeboid contacts with pyrite and also contains small irregular amoeboid grains of pyrite.

Sphalerite occurs as irregular anhedral grains intergranular between the large pyrite and chalcopyrite (See Plate AM). This relationship is reversed in the K3 area where the chalcopyrite is always the intergranular phase. The sphalerite also contains fine, rounded, exsolved blebs of chalcopyrite (See Plate AN).

Unit 8. Felsic Sillimanite Gneiss

In hand specimen this unit is a fine grained, felsic, pink rock with a poorly-defined foliation, and fine sillimanite needles.

The rock is composed of the following:

	RANGE	MODE
quartz.	48-55%	50%
plagioclase-oligoclase ($Ab_{72}An_{38}$)	28-35%	35%
orthoclase/perthite	5-10%	8%
biotite (green)	1-5%	2%
sillimanite	tr-5%	2%
sericite	0-2%	tr
pyrite	0-tr	0%

The texture is granoblastic (platy to flaser texture in places), inequigranular to seriate interlobate. The quartz and plagioclase form occasional porphyroblasts (2-3mm) with subhedral laths and interlobate grain boundaries. The perthite can form rare porphyroblasts. The ground-mass consists of fine grained mosaic (0.5mm) of quartz and feldspars. The sillimanite occurs as orientated wisps composed of minute ($\leq$0.01mm) prisms and is associated with the biotite and sericite.

In the flaser textured specimens (found in the immediate footwall of the sulphide zone) ribbons of quartz and sillimanite (up to 10mm long) define a foliation (See Pates AO, AP). The ground-mass is composed of very fine grained (0.25mm) polygonal mosaic of quartz and plagioclase. The quartz is strongly undulose. The plagioclase and orthoclase porphyroblasts are strain-free.

Unit 9. Diopside Amphibolite

This rock is a medium grained mafic amphibolite with a very vague foliation. Mesoscopically the rock is relatively consistent and is indistinguishable from the amphibolite

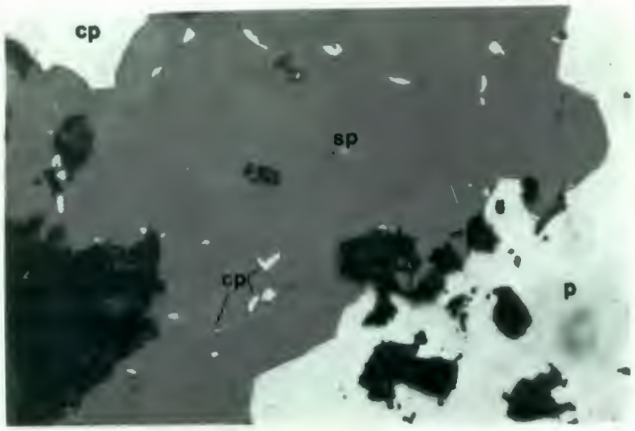

AN r

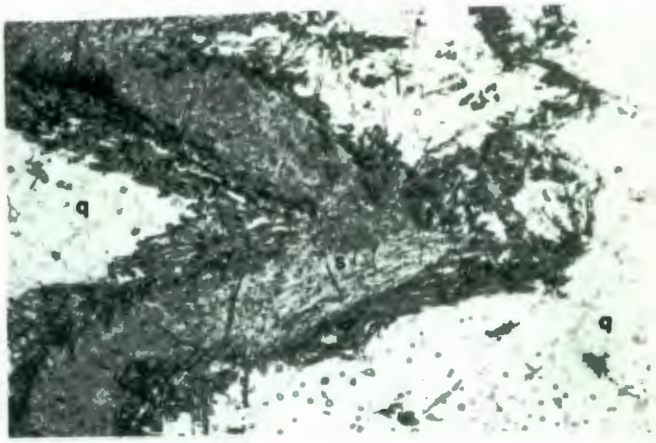

AO

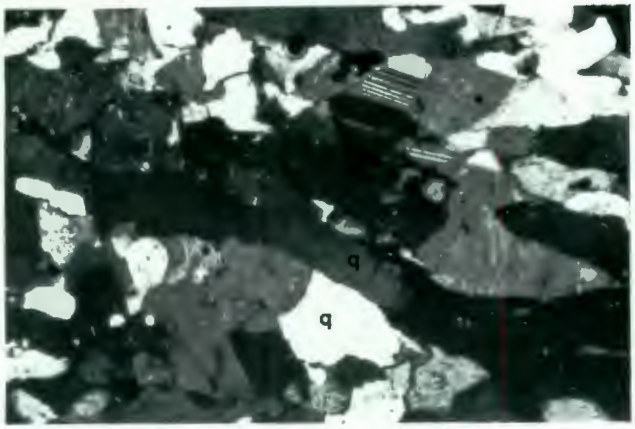

AP xn

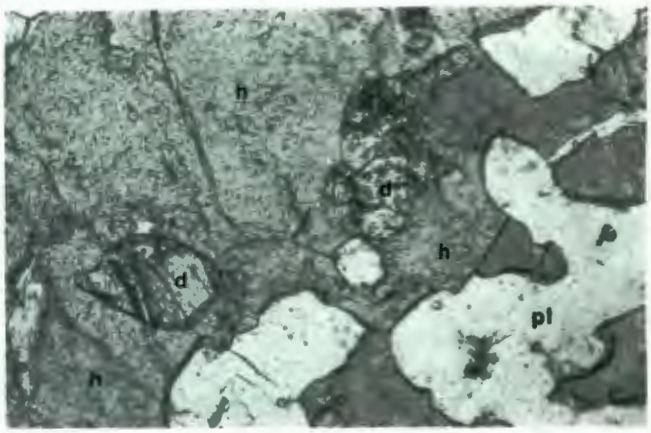

AQ

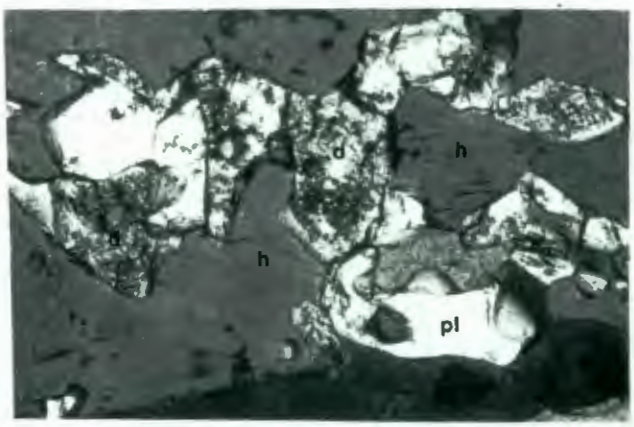

AR

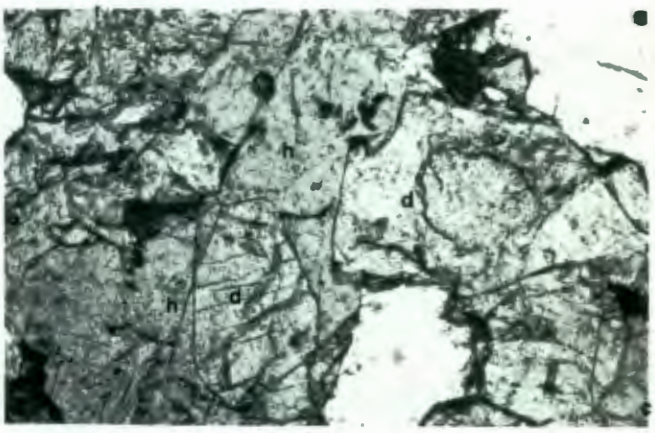

AS

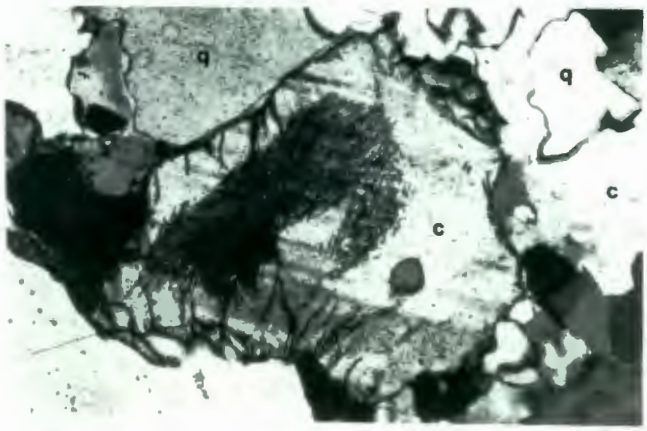

AT xn

described in unit 2, if no garnet is present in the latter. The rock is composed of:

	RANGE	MODE
hornblende (green)	40-65%	55%
plagioclase-labradorite ($Ab_{28}An_{72}$ to $Ab_{52}An_{48}$)	20-45%	35%
diopside	tr-20%	15%
quartz	0-15%	5%
pyrite	tr-1%	tr
pyrrhotite	tr	tr

The texture is granoblastic inequigranular polygonal-interlobate. The plagioclase and diopside form a fine grained (0.5mm) polygonal mosaic.
Hornblende forms large interlobate (1.5mm) grains. The diopside and plagioclase show strongly undulose extinction whereas the hornblende does not. The larger hornblende grains usually have a core of diopside, (See Plates AQ, AR, AS) and have partially replaced the pyroxene. The pyrite is found as fine anhedral grains within the hornblende and as specks (< 0.01) at the grain contacts between hornblende and plagioclase.
Quartz, when present, is usually strain-free and occurs as slightly larger grains (0.75mm) within the diopside-plagioclase mosaic.

Unit 10. Quartz-Cordierite-Garnet Gneiss

In hand specimen this is a fine grained felsic banded biotite gneiss with garnet porphyroblasts. Minor amounts of magnetite are concentrated in the layers containing biotite and other mafic minerals.
The rock is composed of:

	RANGE	MODE
quartz	40-60%	55%
cordierite	2-35%	15%
biotite	5-10%	10%
plagioclase	3-10%	5%
perthite	0-25%	5%
garnet (almandine)	1-15%	5%
hypersthene	0-4%	0%
magnetite	tr-1%	tr

The texture is granoblastic inequigranular amoeboid. The ground-mass consists of an amoeboid mosaic of quartz, cordierite and feldspar with grains varying from 0.1 to 2mm. Biotite (with hypersthene and garnet) is concentrated in layers and defines the foliation. The garnet forms "exploded" (2mm) porphyroblasts. Cordierite exhibits twinning and is zonally altered to pinite (See Plate AT).

AREA K6

Unit 1. Quartz-Feldspar Gneiss

In hand specimen the rock is a felsic, banded and foliated, fine grained gneiss.
The rock consists of:

	RANGE	MODE
quartz	35-65%	50%
orthoclase	10-40%	20%
plagioclase-oligoclase ($Ab_{75}An_{25}$)	5-20%	15%
biotite (green to green brown)	15%	15%
pyrite	0-tr	tr

Two different textures are developed within the bands, usually 10-20mm wide; (i) granoblastic fine grained ($\leq$0.4mm) interlobate equigranular. The quartz and feldspar forming a mosaic with biotite as oriented flaky grains. (ii) Seriate interlobate to amoeboid; the quartz forms poikiloblastic grains (0.8mm). The finer grained seriate matrix typically has amoeboid grain boundaries around which biotite is concentrated. Fine myrmekitic intergrowth of quartz and feldspar is common.

Unit 2. Biotite-Garnet Gneiss

In hand specimen this is a fine-grained, felsic, foliated, usually-banded, garnet gneiss. The rock can have a pale greenish colour. The fine reddish brown garnets and biotite are concentrated in bands from 2cms to 2 metres. The rock is composed of the following minerals:

	RANGE	MODE
quartz	30-70%	57%
plagioclase (andesine Ab_{60} to albite Ab_{92})	10-40%	25%
biotite (green)	10-25%	15%
garnet	1-15%	3%
magnetite	tr-1%	1%
pyrite	tr	0%
hypersthene	0-5%	0%
apatite	tr	0%
calcite	tr	0%

	RANGE	MODE
zircon	tr	0%
muscovite	tr-2%	0%
hercynite	tr	tr

The texture is fine grained (≤1.0mm) granoblastic varying from equigranular to inequigranular interlobate. The quartz and feldspar form a fine grained mosaic (0.5-0.75mm) usually interlobate but approaching polygonal in places. The quartz occasionally forms slightly larger (~1mm) poikiloblastic grains. Usually biotite is the only mineral to define a preferred orientation with fine seriate (0.1-0.5mm) wisps, however in the more deformed specimens the texture can become platy granoblastic. A mortar texture (See Plate AU) with a very fine grain is occasionally developed and magnetite grains appear boudinaged. Garnet porphyroblasts are rounded in shape and garnet also forms patches of "open" (or "exploded") grains - these poikiloblasts can be up to 4mm across. In some instances garnet fragments are concentrated in bands (See Plate AV). Magnetite and pyrite occur as subhedral fine (<0.5mm) intergranular grains.
Rare orthopyroxene is intergrown with biotite.

Unit 3. Banded Iron Formation

In hand specimen the rock is finely, regularly banded (2-6mm wide bands) with the silicate to opaque ratio variable. The magnetite-rich bands are a dark grey and the pink and green colour of the silicate bands is due to the presence of garnet and amphibole. At surface, due to hematization of magnetite and oxidation of sulphides to limonite, plus chloritization of amphibole, the rock has a different appearance to that of fresh specimens. There are two distinct mineralogical types interbedded with each other - they are as follows:

		RANGE	MODE
a)	magnetite (± hematite)	20-60%	40%
	quartz	20-25%	25%
	actinolite (manganoan)	15-20%	20%
	garnet	10-15%	15%
	biotite	0-5%	tr
	pyrite	0-8%	tr

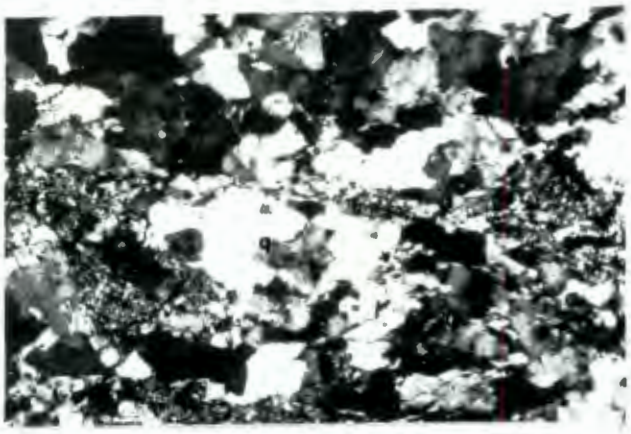

AU xn

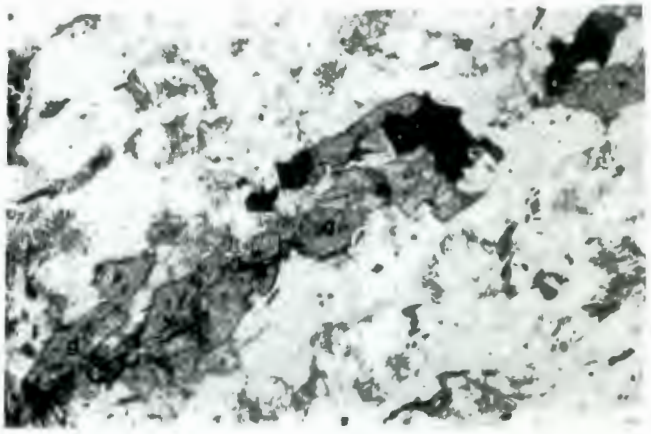

AV

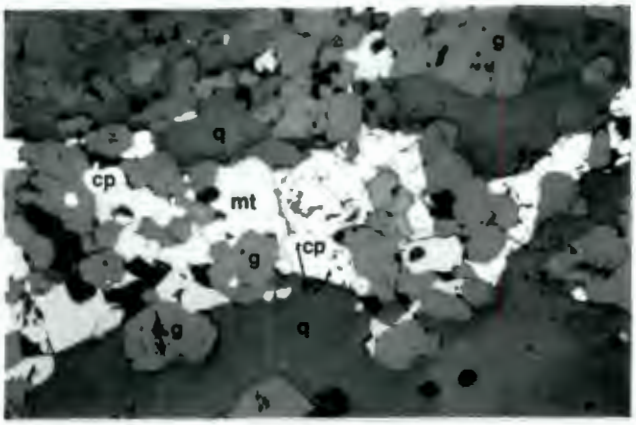

AW r

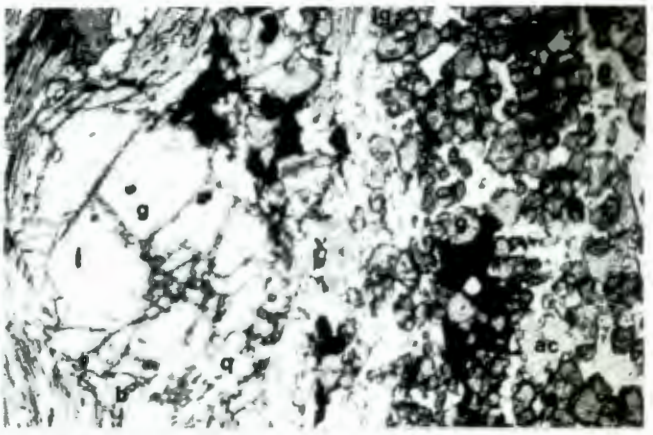

AX

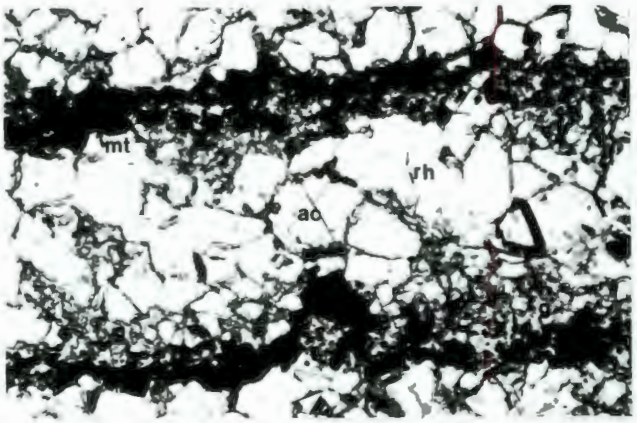

AY

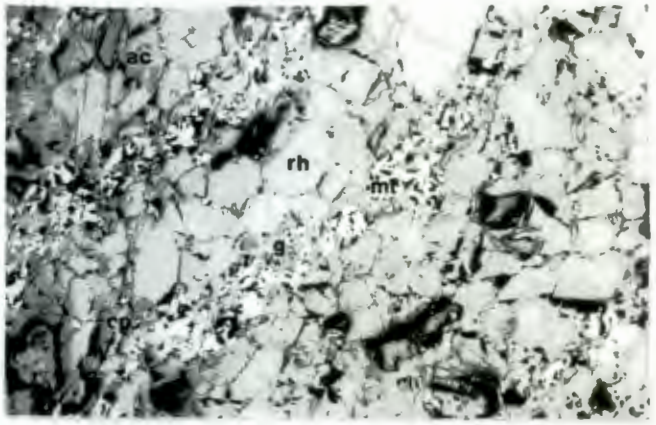

AZ r

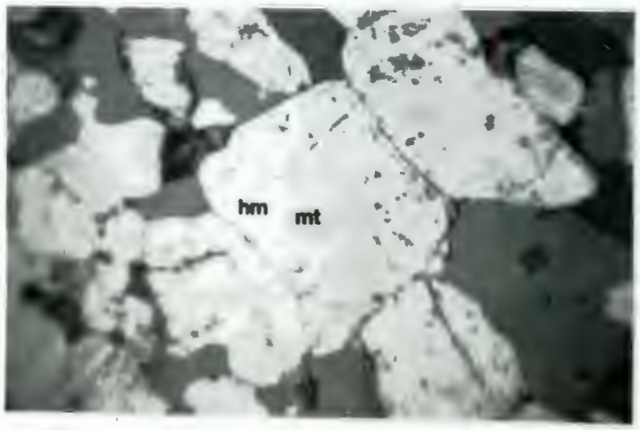

BA r

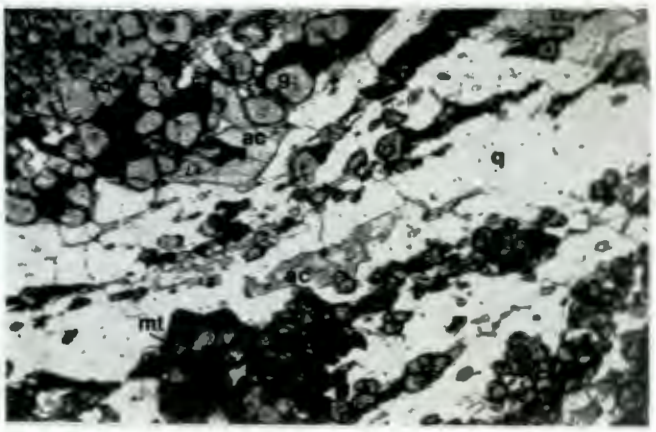

BAZ

		RANGE	MODE
a)	sphalerite	0-2%	tr
	chalcopyrite (± covellite)	0-1%	tr
b)	magnetite (± hematite)	25-50%	40%
	actinolite (manganoan)	15-30%	20%
	garnet	25-30%	25%
	rhodonite	2-25%	10%
	quartz	0-5%	2%
	chalcopyrite	tr-2%	1%
	pyrrhotite	0-tr	0%
	sphalerite	0-tr	0%
	hornblende	0-6%	0%
	calcite (veins)	tr-15%	2%

The texture is dominated by strong banding and is granoblastic equigranular polygonal to interlobate.
Bands (0.75mm wide) of quartz and minor garnet are interlayered with magnetite-garnet bands. The garnet typically forms a solid mass enclosing magnetite and other opaques. There are wider silicate rich bands (≥1cm) consisting of actinolite, rhodonite and minor garnet. The garnets in the silicate bands are fine grained (0.1mm) and zoned, with centres crowded with inclusions (See Plate AX). Rhodonite forms a fine (0.3mm) polygonal mosaic with actinolite with occasional intergranular magnetite; these mosaics form bands up to 1.5mm wide (See Plate AY).
The sulphide minerals are associated with magnetite either as discrete fine grains or as composite grains with magnetite (See Plate AW). Occasionally chalcopyrite (and pyrite) form veins cutting the silicate minerals.
Within 65m of surface the magnetite is oxidized to hematite (See Plate BA) and the sulphides altered to limonite.
Microprobe analyses of the rhodonite and actinolite were as follows:

Actinolite	Rhodonite
50.2% SiO_2	47.08% SiO_2
20.64% CaO	32.87% MnO
14.46% FeO	11.53% FeO
9.39% MnO	6.94% CaO
6.05% MgO	1.84% MgO
100.74% TOTAL	100.26% TOTAL

Unit 4. Amphibolite

In hand specimen this rock is a dark green to black, fine grained, poorly-foliated, intermediate to basic rock. Finely disseminated pyrite is sometimes present.
The rock consists of:

	RANGE	MODE
hornblende (green)	45-60%	50%
plagioclase (andesine to bytownite Ab_{60} to Ab_{26})	20-50%	45%
quartz	0-15%	5%
magnetite	0-5%	1%
calcite	0-4%	tr
pyrite	tr-2%	tr
sphene	tr	tr
biotite (brown)	0-5%	0%

The texture is granoblastic to nematoblastic inequigranular interlobate. Hornblende forms anhedral grains (0.75-1mm) which enclose finer grained (0.35mm) polygonal mosaics of quartz and plagioclase. In some instances quartz and feldspar are concentrated in fine (<2mm) layers and exist as a fine (0.35mm) polygonal mosaic.
Magnetite forms euhedral to subhedral grains usually within the quartz-feldspar mosaic, and skeletal grains within hornblende.
Calcite and pyrite are found interstitially as anhedral equigranular grains. The pyrite appears to occur preferentially with hornblende.

Unit 5. Felsic Sillimanite Gneiss

In hand specimen the felsic sillimanite gneiss is massive and fine grained. The rock, as was found in the K1 and K3 areas, grades into coarse quartz feldspar pegmatite throughout.
The rock is composed of:

	RANGE	MODE
quartz	40-50%	50%
perthite	5-20%	15%
plagioclase-andesine ($Ab_{60}An_{40}$)	10-20%	15%
cordierite	10-20%	11%
biotite (brown)	5-20%	5%

		RANGE	MODE
within 2m of massive sulphides	sillimanite	tr-5%	4%
	magnetite	tr-4%	3%
	pyrrhotite	tr-1%	1%
	chalcopyrite	tr	tr
	galena	tr	tr

The texture is granoblastic inequigranular interlobate. The quartz, feldspar and cordierite make up a fine grained (0.2mm-0.5mm) mosaic with a finer grained (<<0.1mm) mosaic between the layer grains - a mortar texture (See Plate BB). The biotite and sillimanite occur as fine (≤0.2mm) wisps between the silicate grains - the sillimanite has partially altered to sericite.

The opaques form well defined bands of composite grains of pyrrhotite and magnetite and discrete, irregular, fine, grains of chalcopyrite.

Unit 6. Amphibole Hypersthene Granulite

In hand specimen this is a strongly-foliated, coarsely-banded, intermediate hypersthene/amphibole garnet granulite, the garnet concentrated in bands. The colour is a dark green to brown with more felsic bands interlayered.

The rock is composed of:

	RANGE	MODE
plagioclase-labradorite-oligoclase ($Ab_{50} \rightarrow Ab_{70}$)	25-45%	35%
quartz	15-25%	20%
hornblende (green)	5-25%	20%
biotite (brown and green)	7-20%	15%
hypersthene	tr-20%	5%
garnet	tr-20%	4%
magnetite	tr-2%	1%
cummingtonite-grunerite	0-15%	0%
pyrite	tr	tr
apatite	tr	tr

The texture is platy granoblastic inequigranular to seriate interlobate.

The garnet and hypersthene form poikiloblastic grains up to 2mm across. The garnet, hypersthene and biotite are intimately intergrown. The quartz and feldspar form an elongated platy mosaic with grains varying 0.5 → 1.5mm. The biotite

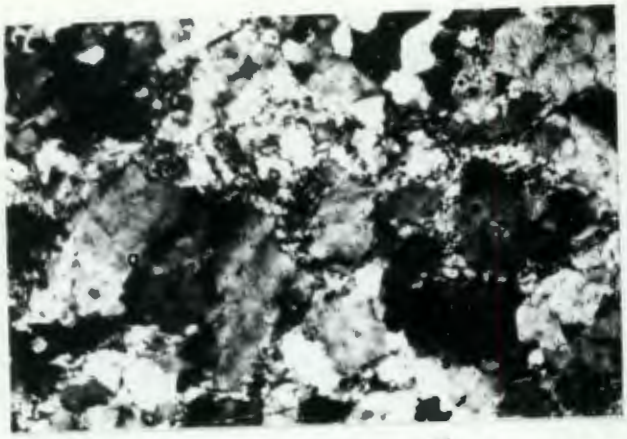

BB xn

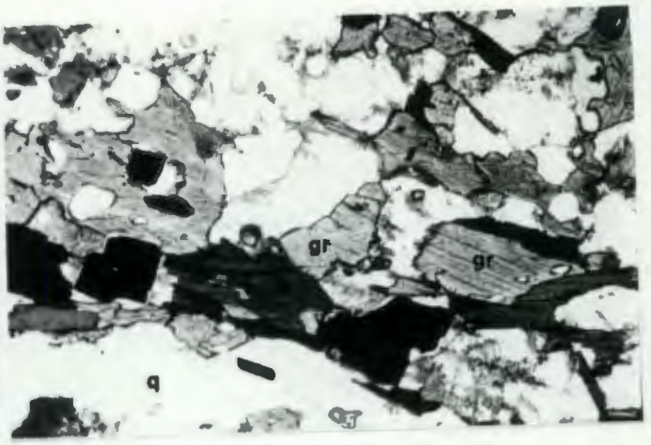

BC

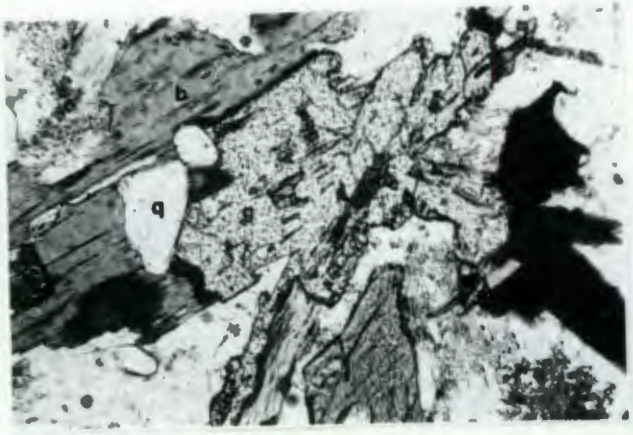

BE

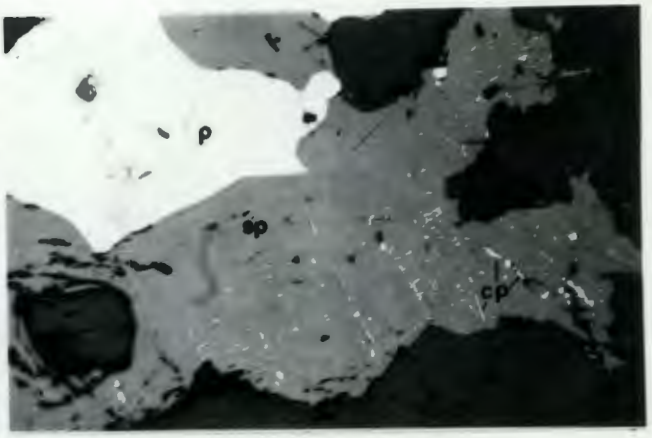

BF r

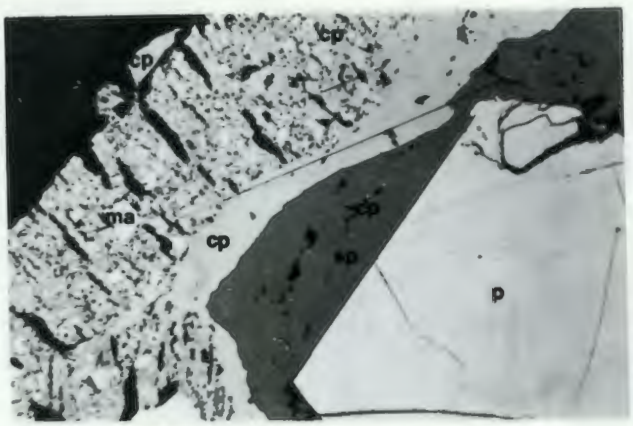

BG r

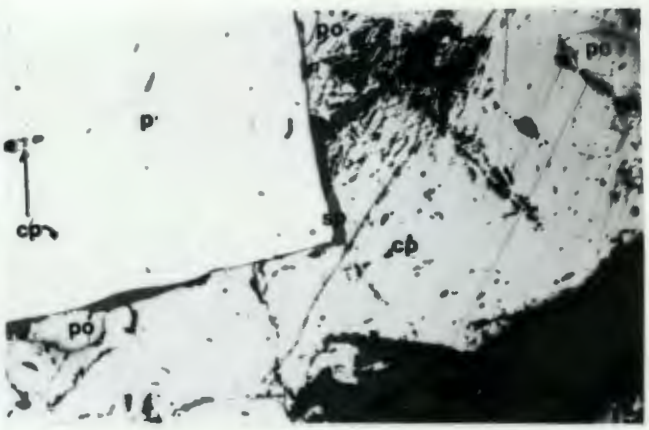

BH r

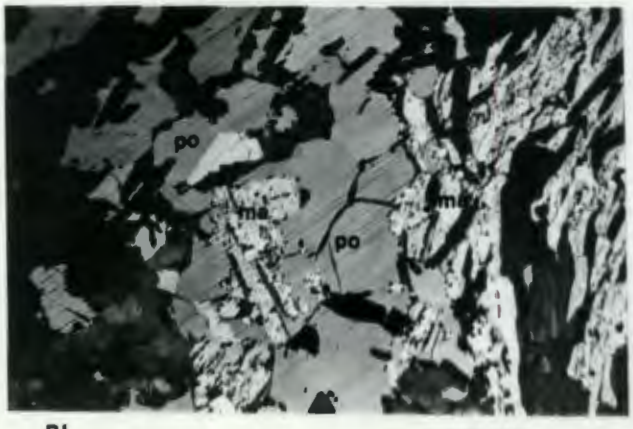

BI r ~ xn

BJ r

and amphiboles, which are intergrown, further accentuate the foliation (See Plate BC). There appears to be "microshear zones" in which biotite is concentrated with finer grained felsic minerals and fragmented garnet (See Plate BE).

Unit 7. Massive Sulphides

The massive sulphide unit consists of two distinct rock types - a) Massive sulphides i.e. sulphide $\geq$65% and
b) Semi-massive micaceous sulphide i.e. sulphide $\leq$50%.

a) The massive sulphide in hand specimen is a non-foliated coarse grained pyrite-rich rock in which the felsic gangue minerals are found as rounded (1-5mm) blebs within the coarser sulphide. Chlorite is ubiquitous throughout and gives the rock a greenish colour.
The massive sulphide unit is composed of:

	RANGE	MODE
pyrite	30-85%	50%
chlorite	10-35%	15%
quartz	5-20%	10%
sphalerite	tr-35%	10%
biotite	0-10%	5%
chalcopyrite	tr-10%	4%
pyrrhotite	tr-35%	2%
tourmaline	0-5%	0%
cordierite	0-5%	0%
galena	0-tr	0%
orthoclase	tr	0%
barite	tr	tr
sericite	tr	tr
covellite	tr	tr
plagioclase	tr	tr
hematite	tr	tr

The gangue minerals occur as rounded composite grains up to 6mm across and include:

(i) Fine grained ($\sim$0.4mm) polygonal quartz grains
(ii) Orthoclase
(iii) Composite mats of biotite, quartz and chlorite

(iv) Cordierite grains, usually with biotite and chlorite; the cordierite is shown by microprobe analyses to be an iron-poor variety (i.e. <1% FeO).

Tourmaline (dravite) is found as coarse (~3-4mm), subhedral grains which exhibit zoning. Microprobe analyses show the pleochroic green core to be slightly more iron-rich (~3% FeO) than the edge.

The pyrite occurs as coarse, anhedral and subhedral composite grains with intergranular sphalerite and chalcopyrite. Pyrite also has fine, rounded, intragranular blebs of sphalerite (up to 1mm across). The coarser grained sphalerite (i.e. that which is found intergranular to pyrite grains) always has exsolved chalcopyrite blebs (<< 0.01mm) which appear to be controlled by twin planes and polygonal grain boundaries (See Plates BF, BG).

The chalcopyrite is usually found as fine, anhedral coatings between larger and more abundant sphalerite and pyrite. This relationship is reversed where the chalcopyrite is more common than sphalerite, in which case the sphalerite becomes the intergranular phase (See Plate BG).

Pyrrhotite which rarely occurs in quantities >2% is found as (i) fine rounded blebs within pyrite (ii) fine linearly arranged blebs in sphalerite and (iii) intergranularly between pyrite and chalcopyrite (See Plate BH).

Galena occurs as relatively coarse grains with chalcopyrite or as fine, intergranular grains between other sulphides and gangue minerals. In some instances veins of quartz and galena (narrow <0.2mm) cut gangue and sulphide. Qualitative microprobe analysis shows the galena to contain variable quantities of silver. Whole rock analyses indicate silver contents to be ~0.05 to 0.15% Ag. At depths of 70 - 100m covellite is found as fine amoeboid grains edging chalcopyrite. Limonite occurs as amoeboid edges to pyrite and chalcopyrite and within the coarser grains.

b) The semi-massive micaceous sulphide is composed of:

	RANGE	MODE
phlogopite (and/or biotite)	25-70%	50%
quartz	tr-30%	20%

	RANGE	MODE
pyrite	6-30%	15%
plagioclase-oligoclase ($Ab_{74}An_{26}$)	0-25%	10%
orthoclase	0-8%	4%
sphalerite	0-8%	2%
chalcopyrite	tr-10%	2%
cordierite	0-15%	0%
hematite	tr-10%	0%
covellite	tr	0%
rutile	0-tr	0%
marcasite	tr-5%	tr
pyrrhotite	tr-4%	tr
galena	tr-1%	tr

The texture is a coarse mat of non-orientated mica (either phlogopite or biotite) with quartz and sulphides occurring as rounded, composite grains within it. Round grains composed of polygonal quartz occur within the sulphide. Cordierite forms poikiloblastic grains up to 6mm across. Plagioclase forms porphyroblastic grains.
The coarse-grained anhedral pyrite contains rounded blebs of chalcopyrite, galena and pyrrhotite. Sphalerite contains extensive blebs of chalcopyrite and pyrrhotite. Sphalerite can also be clear of any inclusions/exsolutions. Pyrrhotite is found as blebs within pyrite and chalcopyrite. Coarser grains of pyrrhotite are replaced by marcasite (See Plate BI). Marcasite also appears to have replaced chalcopyrite (See Plate BG) and pyrite.
Galena and minor chalcopyrite occur as fine specks (0.05-0.005mm) within the phlogopite mat.
In places this rock type is strongly foliated and the sulphide composite grains become elongated but have the same intergranular relationship.

Unit 8. Felsic Stringer Sulphide Zone

In hand specimen this is a coarse felsic non-foliated rock with irregular fine stringers and veinlets of pyrite and galena. The rock occasionally has a brecciated appearance. The rock is composed of:

	RANGE	MODE
quartz	5-65%	50%
plagioclase-andesine ($Ab_{60}An_{40}$)	5-50%	30%

	RANGE	MODE
perthite	0-40%	10%
sericite	0-20%	5%
pyrite	tr-20%	3%
galena	tr-4%	1%
pyrrhotite	tr-3%	1%
chalcopyrite	tr-3%	1%
marcasite	tr-5%	1%
garnet	0-2%	0%
sphalerite	0-20%	0%
chlorite	0-10%	0%
cordierite	0-15%	0%
covellite	0-tr	0%
rutile	0-tr	0%
piedmontite	0-tr	0%
hercynite	0-tr	0%
biotite	0-20%	tr

The silicate minerals have a granoblastic coarse grained (up to 4-8mm) seriate amoeboid texture. The feldspars usually occur as large poikiloblasts or porphyroblasts which are altered to sericite. In some cases the quartz forms a fine polygonal (0.75mm) mosaic with a slight preferred orientation accentuated by biotite flakes. The quartz also can exhibit mortar texture. The texture in places becomes mylonitic with ribbons of quartz and large (~4mm) augen of plagioclase. The plagioclase usually exhibits some degree of anti-perthite exsolution.

The sulphide minerals occur as intergranular anhedral aggregates which, if total sulphide content exceeds 15%, coalesce into an interlocking net texture. Around the coarser composite grains there are usually disseminations of fine (<0.1mm) sulphides (usually galena, less frequently chalcopyrite).

The more common sulphides (i.e. pyrite, chalcopyrite and marcasite) occur as composite grains. The pyrite holds blebs of chalcopyrite, although coarser chalcopyrite is also developed. Chalcopyrite also has a tendency to mantle and vein euhedral pyrite grains (See Plate BJ).

There are two generations of pyrite with chalcopyrite and within these veins euhedral cubes (See Plate BK).

Marcasite is found within pyrite/chalcopyrite aggregates

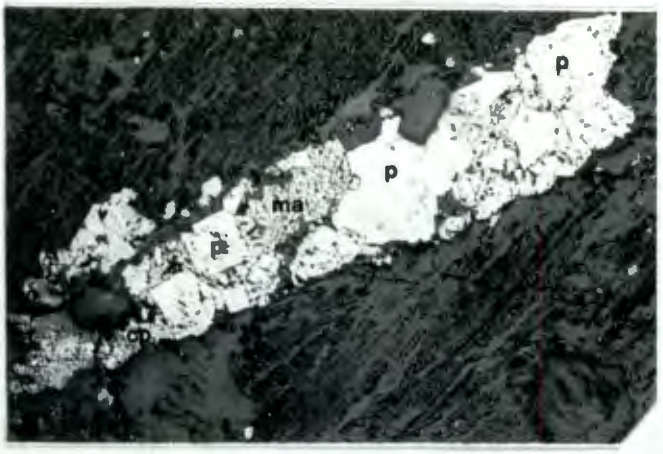

BK r

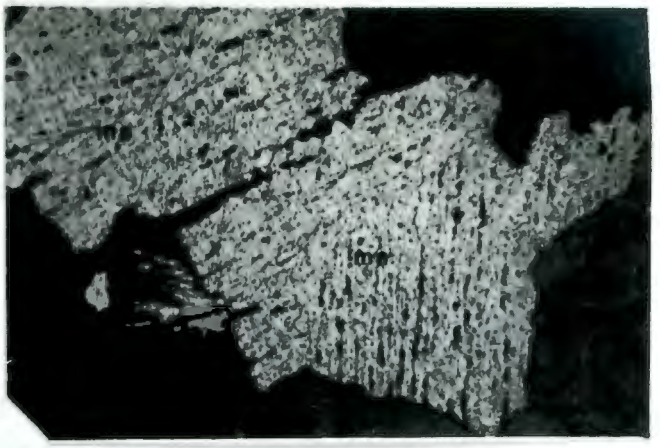

BL r

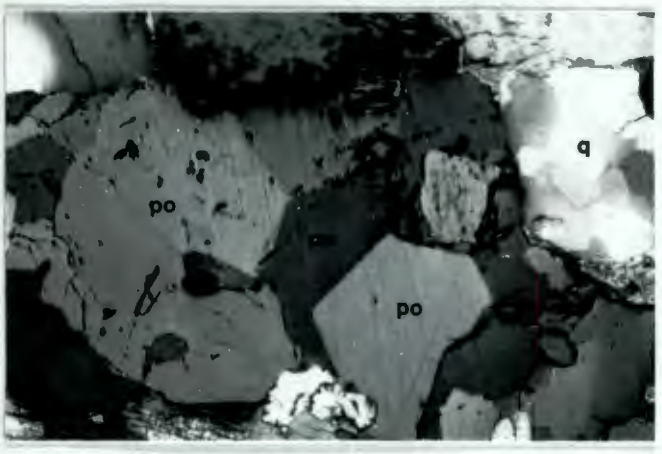

BM r - xn

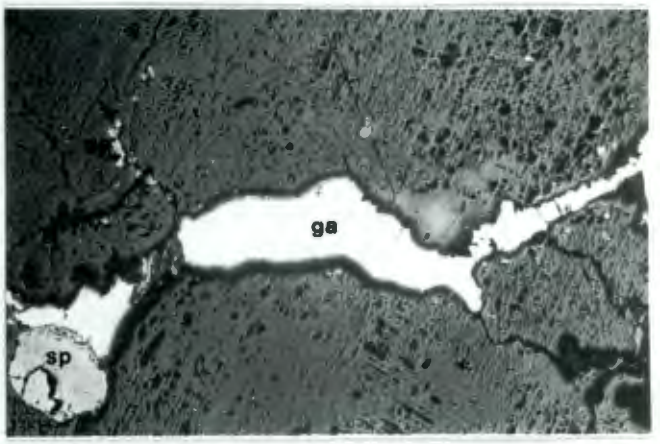

BN r

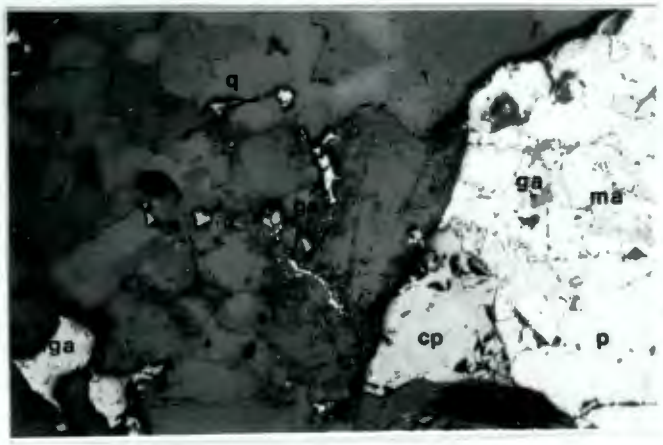

BON r

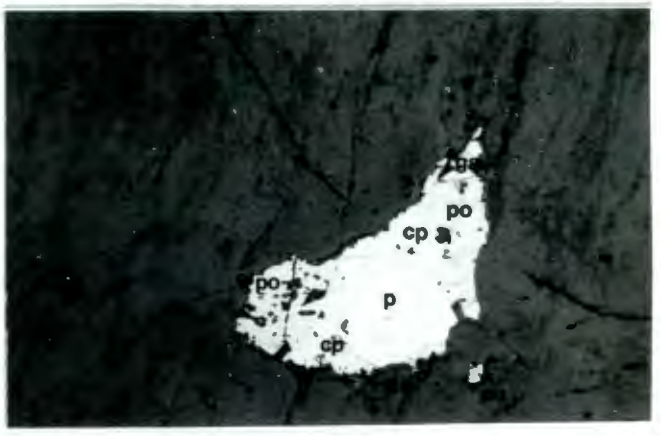

BO r

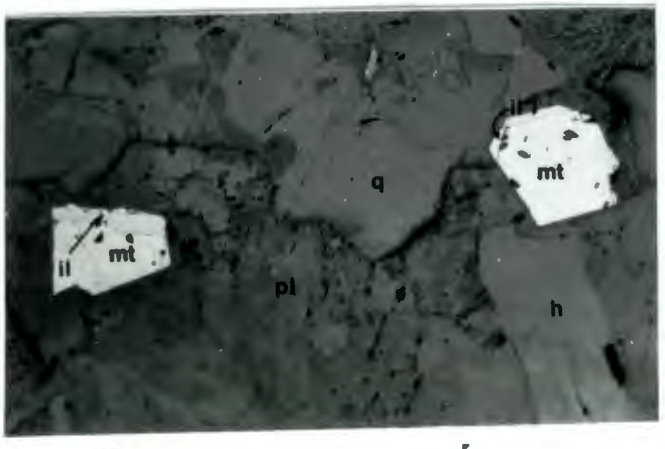

BP r

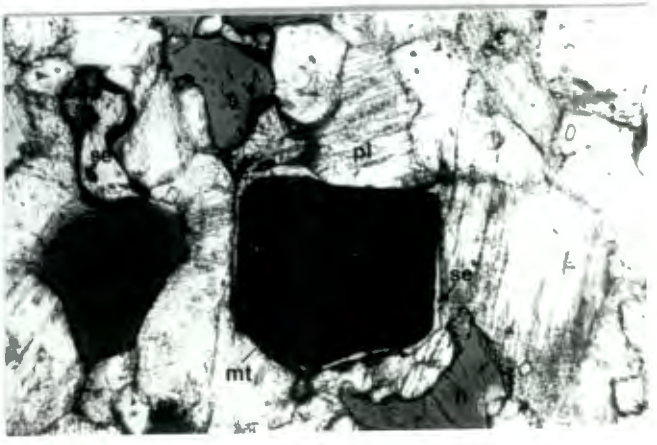

BQ

but it is not possible to determine the paragenetic sequence. Some of the larger discrete marcasite grains have extensive pits or vugs arranged linearly as if cleavage controlled (See Plate BL).
Galena is present as fine (~0.05mm), highly irregular, discrete grains within the gangue (intergranularly), usually surrounding large sulphide aggregates (See Plate BON). The latter do not necessarily carry galena. Galena is also found in veins (up to 1mm thick) together with pyrite, sphalerite and marcasite (See Plate BN). The rarer pyrrhotite and sphalerite occur as intergranular phases between the coarser pyrite and chalcopyrite. Where pyrrhotite aggregates are developed they are composed of a fine (≤0.2mm) polygonal mosaic (See Plate BM). Covellite and galena are found as edges and fine mantles to chalcopyrite and the latter also rarely as blebs within pyrite (See Plate BO). The secondary copper mineral is usually found only at a depth of <150m, except in one instance (i.e. drillhole KDH18 at 195m - vertical depth ~160m). The existence of this mineral could be due to its proximity (~40m) to a fault.

Unit 9. Magnetite (Ilmenite) Porphyritic Amphibolite

In hand specimen this is a fine grained, non-foliated, dark green amphibolite. Euhedral magnetite, occasionally with a pale halo, occurs throughout and characterize the rock. The rock is composed of:

	RANGE	MODE
plagioclase-labradorite ($Ab_{40}An_{60}$)	30-50%	40%
hornblende (green)	25-50%	35%
quartz	5-25%	10%
biotite (brown)	0-8%	5%
magnetite	3-10%	5%
ilmenite	tr-3%	2%
chalcopyrite	tr	0%
pyrite	tr-2%	tr
sphene	0-1%	tr

The texture is fine grained granoblastic inequigranular polygonal to interlobate. The hornblende, plagioclase and quartz form a fine (~0.4mm) equigranular mosaic, the hornblende in the more mafic varieties tends to coalesce into a poikiloblastic habit. There is a tendency for preferred orientation which is usually accentuated by biotite and to a lesser degree quartz.
Magnetite and ilmenite occur as euhedral grains up to 1.5mm. These can occur as composite grains or discretely. The ilmenite occurs as linear intergrowths within magnetite (See Plate BP).
Sphene mantles and appears to have replaced magnetite. The sphene has a subhedral shape, while the magnetite core is anhedral and irregular (See Plate BQ). Sphene also occurs as discrete grains when it is anhedral and intergranular. Sphene does not mantle composite magnetite and ilmenite grains. Pyrite (and traces of chalcopyrite) are found as fine intergranular grains (<0.1mm); also as fine skeletal intergrowths in plagioclase cleavage cracks.

Unit 10. Pegmatite

This rock is a felsic, coarse grained, pinkish, granitic rock with minor biotite.
The rock is composed of:

	MODE
microcline	50%
quartz	35%
biotite	15%
apatite	tr

The texture is granular seriate with interlobate grain boundaries. Microcline forms large (~4mm) subhedral porphyroblasts in a finer grained seriate ground-mass of quartz, feldspar and biotite.

THE NORTHERN GRANULITES

In hand specimen the rock is a massive, intermediate, diopside granulite with a dark green-black colour when fresh - usually has strong desert varnish on the pitted surface.

The rock consists of:

	RANGE	MODE
plagioclase-labradorite ($Ab_{40}An_{60}$)	35-45%	43%
diopside	10-40%	34%
hornblende (pargasitic)	0-35%	16%
garnet	0-25%	5%
epidote	0-10%	1%
quartz	0-5%	1%
calcite	0-7%	0%
cordierite	0-3%	0%
ilmenite	0-tr	tr
sphene	0-tr	tr

The texture is granoblastic seriate with interlobate and occasional polygonal grain boundaries. Diopside forms poikiloblastic grains up to 3mm across in a polygonal ground-mass of labradorite. The orange garnet forms large poikiloblastic ("lacy") aggregates up to 6mm across. Hornblende has replaced the diopside and these grains are rimmed by later epidote. The sphene and ilmenite are always associated as fine grained intergranular aggregates.

THE SOUTHERN GRANULITES

In hand specimen the rock is a massive, intermediate to felsic, diopside granulite, with an orange colour if garnet content is high. In outcrop the rock has a black desert varnish with a shiny pitted surface.

The rock consists of:

	RANGE	MODE
plagioclase-labradorite ($Ab_{35}An_{65}$)	20-60%	45%
diopside	5-30%	20%
quartz	0-40%	15%
hornblende (pargasitic)	0-15%	10%
garnet	0-15%	5%
carbonate	0-5%	2%

	RANGE	MODE
epidote	0-15%	1%
magnetite	0-3%	1%
sphene	0-1%	tr

The texture is usually fine grained granoblastic inequigranular polygonal to interlobate. Diopside forms larger (<4mm) poikiloblastic grains in a ground-mass of polygonal labradorite (fine grained $\leq$1mm grains). The diopside has been partially uralitized to green hornblende. Garnet, when present, forms anhedral poikiloblastic grains and has been replaced by epidote. The calcite and magnetite tend to occur together as fine grained interstitial phase. Quartz, when present, forms ribbons up to 5mm long.

APPENDIX II. BULK ROCK ANALYTICAL TECHNIQUES

Sample Preparation:

The samples (≥7.0 kg., for core specimens, and ≥ 10 kg. for surface samples) were cleaned with a stiff brush and wiped free of any drilling sludge (there was very little oil) with acetone. All the crushing and grinding equipment was wiped clean with stiff brushes and cleaned with distilled water and acetone, and precontaminated with each new specimen to be processed.

The specimens were broken down to ≤5cm pieces in a vice before crushing in a jaw crusher to <1cm pieces. Eighty grams of this coarse crushed material were further ground in a Siebtechnik swing-mill using a 100cc agate vessel (<120 mesh) and 6-8g aliquots of this fine ground (<300 mesh) in a motorized agate mortar; 4g of the <300 mesh powder was made into powder briquettes on which trace element (and Na) analyses were carried out. The rest of the <300 mesh powder was used to produce duplicate fusion discs (Norrish and Hutton, 1969). H_2O^- and L.O.I. were determined by weight loss at 110 and 1000°C respectively. Total Fe was expressed as Fe_2O_3.

Major and trace elements were analysed by XRF. Operating conditions and data reduction processes used in the Geochemistry Department at the University of Cape Town were outlined in Willis et.al(1971 and 1972). Details of more up to date procedures listed below are taken from Bristow (1980). International rock standards (USGS, N.I.M., CAAS) were used for calibration.

Major elements: were analysed on duplicate lithium tetraborate fusion discs (except Na which was done on pressed briquettes); the operating conditions and data precision are summarised below.

Major Elements:

XRF Operating Conditions: (Instrument: Siemens SRS-1)

	Fe	Mn	Ti	Ca	K	P	Si	Al	Mg	Na
Tube	W →		Cr →							
kV	60 →		50 →							
mA	50 →									
counter	flow →									

XRF Operating Conditions: (Instrument: Siemens SRS-1)

	Fe	Mn	Ti	Ca	K	P	Si	Al	Mg	Na
collimator	fine →		coarse	fine →		coarse →			fine	coarse
crystal	Lif(220) →		Lif (200)			GE	PET →		TLAP →	
counting preset time (sec)	10	40	10	10	20	100	100	100	200	200
line	$K\alpha$ →									

Estimates of precision, detection limits and average absolute error. Precision is expressed as an absolute error (20) on the given percentage oxide.

Oxide	Wt %	Precision	Accuracy	Detection Limit
Fe_2O_3	9.0	0.038	0.064	0.014
MnO	0.15	0.008	0.003	0.008
TiO_2	1.0	0.008	0.008	0.005
CaO	12.0	0.028	0.030	0.008
K_2O	0.2	0.002	0.022	0.002
P_2O_5	0.2	0.012	0.018	0.011
SiO_2	50.0	0.140	0.264	0.036
Al_2O_3	15.0	0.080	0.079	0.022
MgO	8.0	0.148	0.086	0.072
Na_2O	2.5	0.032	0.067	0.080

Trace elements: were analysed on pressed powder briquettes on a Phillips PW 1220 spectrometer (Co, Cr, V, Cu, Ni, Zn) and the Siemens SRS-1 (Y, Zr, Pb, U, Th, Nb, Sr, Rb and Mo $K\alpha$ C). Mass absorbtion coefficients were determined at Rb $K\alpha$ wavelength by measurement of the Mo $K\alpha$ Compton peak (Reynold, 1963) or were calculated from the major element data using Heinrich's values. Raw data were reduced using FORTRAN programmes written by members of the Department of Geochemistry.

The operating conditions and precision statistics are given below:

Trace Elements:

XRF OPERATING CONDITIONS:

	Sr Rb Zr Y Nb Mo $K\alpha$ Zn Cu Ni Co Cr V
Tube	Mo → W → Au → W →
kV	60 →
mA	50 →
counter	scintillation → flow →
collimator	fine →
crystal	Lif (220) →
count time (sec)(twice)	200 → 100 →
vacuum	off → on →
M.A.C. line	Rb measured → calculated → $K\alpha$ →

The absolute error and detection limits are given at 2σ and 3σ respectively.

Element	Range (ppm)	Error	Detection Limit
Zr	40-100	.9-1.4	1.4
Nb	4-150	1.0-1.2	1.8
Y	20-40	.8-1.0	1.3
Rb	2.5-90	.8-1.1	1.5
Sr	80-800	1.0-1.7	1.5
Co	18-800	1.9-2.5	4.5
Cr	25-350	1.5-2.1	2.2
Ni	10-208	2.5-3.7	4.0
V	50-350	2.4-3.7	5.5
Zr	8-150	0.9-1.7	1.4
Cu	5-90	1.8-2.1	2.9

The Niggli Values used in the text, Section 4, have been calculated from the definition given in Barth (1962), pages 62-65.

Niggli Values

The twofold way of classifying rocks—mineralogical and chemical—has been advocated and its advantages have been convincingly demonstrated by Niggli in several papers of outstanding importance to systematic petrology. In the system that Niggli has contrived to build, the chemical classification becomes identical with definition and classification of what he calls the *magma types* (see page 181).

The chemical analysis of a rock is the basis for its classification. The procedure of calculation is as follows. The figures giving the weight percentages are divided by the molecular weight of the corresponding oxide; thus we arrive at a series of relative figures—molecular numbers—which indicate the molecular proportions of the several oxides in the rock.

The molecular number for Fe_2O_3, which in terms of ferrous oxide corresponds to 2FeO, must be multiplied by 2 and then added to FeO. The remaining molecular numbers are grouped together and added in the following way:

Al_2O_3 (including Cr_2O_3 and rare earths)

+ FeO + MgO (+ MnO + CoO + NiO)

+ CaO (including BaO + SrO)

+ K_2O + Na_2O (including rare alkali earths)

The sum is recalculated to 100, and the numbers designated *al*, *fm*, *c*, and *alk*, respectively. Thus the sum $al + fm + c + alk = 100$ specifies one group of chemical substances.

The molecular numbers for SiO_2 (if desirable also for TiO_2, ZrO_2, P_2O_5, H_2O, CO_2) are recalculated according to the equation:

Molecular number for SiO_2:molecular number for $Al_2O_3 = x:al$

The resulting figure for x is called *si* (respectively, *ti*, *zr*, *p*, *h*, co_2).

The two groups, $al + fm + c + alk = 100$, and *si* (and *ti*, etc.), include the most important chemical constituents of the rock. But two additional parameters are of great value: the molecular proportion of K_2O compared to the sum of the alkalies in *alk*, and the molecular proportion of MgO compared to the sum of the divalent elements in *fm*. Separately, therefore, the following values are computed:

$$\frac{K_2O}{K_2O + Na_2O + (Li_2O)} \text{ and } \frac{MgO}{FeO + MnO + MgO}$$

and respectively designated *k* and *mg*. For many purposes in the discussion of the chemical relations in primary and metamorphic rocks, it is sufficient to set down the values *si*, *al*, *fm*, *c*, *alk*, as well as *k* and *mg*. In a general way they characterize a rock.

The *quartz index*, *qz* (Quarzzahl), is a derived quantity and is obtained as follows. The most highly silicified minerals in the rocks are feldspars and pyroxenes. In the alkali feldspars and the lime feldspars the molecular proportions are $alk:al:si = 1:1:6$ and $c:al:si = 1:1:2$, respectively. In the pyroxenes the theoretical proportions are $fm:si = 1$ and $c:si = 1$. In a rock composed of these minerals, the following relation holds:

$$si' = 6alk + 2(al - alk) + 1[c - (al - alk)] + fm \cdots \quad (1)$$

The expression $(al - alk)$ corresponds to the fraction of *c* that is bound to alumina in feldspar, provided $alk < al$; and $c - (al - alk)$ is the fraction of *c* that is associated only with *si*. If $al > alk + c$, the excess of *al* is supposed to combine with an equal amount of *si*, with formation of sillimanite.

Remembering that $al + fm + c + alk = 100$, and substituting in equation 1, we obtain:

$$si' = (100 + 4alk)$$

With $alk > al$, the excess of alkalies will usually form aegirite, and the corresponding *si*-value becomes $si' = (100 + 3al + 1alk)$.

In a rock showing a higher *si*-value than the calculated *si'*-value, free quartz will appear. If the rock shows a lower *si*-value, some minerals of low degree of silification (for example, olivine, biotite, feldspathoids, ore) are to be expected. The difference $si - si'$ is the quartz index, *qz*, which may be either positive or negative, and is a valuable indicator of the minerals to be expected.

In the table below the most important Niggli values are listed:

al from Al_2O_3	*si* from SiO_2
fm from FeO, Fe_2O_3, MnO, MgO	$k = \frac{K_2O}{K_2O + Na_2O}$
c from CaO	$mg = \frac{MgO}{FeO + MnO + MgO}$
alk from $K_2O + Na_2O$	$si' = 100 + 4alk$ (usually)
$al + fm + c + alk = 100$	$qz = si - si'$

In the example of Table III-7 the analysis of a granodiorite from California is recalculated after Niggli.

TABLE III-7

GRANODIORITE, PLACER COUNTY, CALIFORNIA

	Weight, %	Approximate Molecular Weight	Molecular Proportions × 1000		Calculations	
SiO_2	65.54	60	1092			
Al_2O_3	15.52	102	152			
Fe_2O_3	1.40	160	9 as FeO 18			
FeO	2.49	72	35			
MnO	0.06	71	1			
MgO	2.53	40	63			
CaO	4.88	56	87			
Na_2O	4.09	62	66			
K_2O	1.95	94	21			
TiO_2	0.39	80	5			
P_2O_5	0.18	142	1			
H_2O	0.71	...				
	100.74					
				152	$al = (100 \cdot 152) : 453 =$	36
				117	$fm = (100 \cdot 117) : 453 =$	26
				87	$c = (100 \cdot 87) : 453 =$	19
				87	$alk = (100 \cdot 87) : 453 =$	19
				453		100

$$ci = \frac{1092 \cdot 100}{453} = 241$$

$k = \frac{21}{87} = 0.24$

$mg = \frac{63}{117} = 0.54.$

$qz = 241 - (100 + 4 \cdot 19) = 465$

APPENDIX III MICROPROBE ANALYTICAL METHODS AND RESULTS

Microprobe analyses were obtained on polished, carbon coated, thin sections. The instrument used is a Cambridge Microscan 5 linked on line to a Varian 620L-100 minicomputer where matrix corrections and alpha factors from Albee and Ray (1970) were applied, using the methods of Bence and Albee (1968). Calibration was achieved using natural and synthetic standards (Kakanui pyrope, Kakanue hornblende, Marjalahti olivine, synthetic diopside, rutile and rhodonite. In the case of sphalerite, zinc metal and natural troilite were used as standards. Sphalerite analyses were subjected to full ZAF corrections using FORTRAN programme using TIM-1(Duncumb et.al,1969).

Microprobe Operating conditions used were:

Accelerating potential → 15 kV
Beam current ⟶ 1.5×10^{-6}A
Detectors → flow counters with Ar/CO_2 gas mixture
Analysing crystals: quartz: Fe, Mn, Ca, Ti, Cr, K
RAP : Si, Al, Mg, Na
PET : S
Lif (200): Zn, Fe
Counting time on peak (sec.): 10 (x4)

Single spot precision statistics for microprobe data are given below:

OXIDE	AVERAGE	SD(2σ)	ERROR (2σ)	DETECTION LIMIT (3σ)
SiO_2	41.97	.08	.08	.06
TiO_2	3.92	.08	.10	.07
Al_2O_3	13.51	.06	.06	.04
FeO	6.82	.15	.16	.10
MgO	16.34	.07	.10	.05
CaO	12.10	.07	.08	.05
Na_2O	2.71	.12	.14	.09
K_2O	1.18	.06	.10	.07
MnO	0.26	.01	.01	.03

(All data in wt %)

MnO data from 12 analyses of a garnet crystal (Shee, 1978). Other elements from 12 analyses of a hornblende grain (Reid, 1977).

Quantitative analyses of garnet, cordierite, biotite, hornblende, hypersthene and sphalerite are listed in Table III-I.

TABLE III-I MICROPROBE ANALYTICAL RESULTS

(i) Garnets

Element	(RKG) Sample No.											
	217/2	217/1	217/3	71/1	71/2	10/1	10/2	199/1	199/2	199/3	199/4	179/1
SiO_2	37.57	37.90	37.72	37.37	37.86	38.06	38.23	37.56	37.34	37.64	37.93	38.51
TiO_2	0.0	0.0	0.0	0.09	0.0	0.02	0.008	0.02	0.01	0.04	0.0	0.01
Al_2O_3	21.79	22.1	22.0	21.78	21.86	22.23	22.24	21.87	21.63	21.84	21.73	22.53
FeO	30.95	30.98	31.10	31.13	31.27	29.47	29.24	31.89	31.56	31.86	29.13	30.37
MnO	3.43	3.38	3.53	2.52	2.42	2.43	2.46	1.78	1.75	1.85	1.77	2.53
MgO	5.58	5.05	5.68	6.29	6.82	7.44	7.91	6.47	6.07	6.29	8.13	7.31
CaO	1.09	1.42	1.08	0.90	0.86	1.59	1.08	0.34	0.33	0.32	0.36	1.03
TOTAL	100.42	100.25	101.19	99.98	100.91	101.23	101.17	99.94	98.70	99.83	99.03	102.2

Element	(RKG) Sample No.											
	111/1	111/2	286/1	288/2	255/1	298/1	190/1	190/2	190/3	190/4	190/5	209/1
SiO_2	37.79	37.79	36.47	36.24	36.09	36.10	37.42	38.25	37.53	37.32	37.39	38.63
TiO_2	0.01	0.03	0.01	0.01	0.01	0.06	0.10	0.05	0.04	0.06	0.06	0.03
Al_2O_3	22.53	22.37	20.68	17.46	21.35	20.52	21.62	22.12	21.77	21.48	21.55	22.14
FeO	28.22	28.12	23.73	23.73	30.45	25.23	31.48	30.78	30.19	31.62	31.99	26.42
MnO	2.95	2.75	14.48	14.46	7.37	7.91	2.87	2.82	2.81	2.90	2.84	4.48
MgO	8.09	7.94	2.11	2.16	3.21	1.82	5.96	6.17	6.11	5.55	5.45	8.15
CaO	1.26	1.24	2.18	2.10	1.06	6.59	0.58	0.54	0.42	0.56	0.44	1.11
TOTAL	100.85	100.21	99.67	96.17	99.52	98.23	100.03	100.73	98.87	99.48	99.62	100.96

Element	(RKG) Sample No.				
	209/2	209/3	209/4	209/5	
SiO_2	38.27	37.72	37.69	37.58	(Garnet analyses from BIF units quoted in text)
TiO_2	0.04	0.04	0.05	0.05	
Al_2O_3	22.03	21.63	21.75	21.86	
FeO	26.41	26.43	25.34	25.87	
MnO	4.69	4.40	4.48	5.16	
MgO	7.55	7.48	7.86	6.71	
CaO	1.06	1.14	1.14	1.11	
TOTAL	100.03	98.83	98.30	98.35	

(ii) Biotites

Element	(RKG) Sample No.											
	190/1	190/2	190/3	190/4	190/5	209/1	209/2	199/1	199/2	179/1	179/2	179/3
SiO_2	36.58	37.16	36.13	36.53	34.97	36.85	36.62	37.44	35.69	37.19	37.17	37.03
TiO_2	4.08	4.39	4.36	4.12	3.16	2.63	3.06	3.49	5.11	1.23	1.68	1.91
Al_2O_3	18.11	18.21	17.54	17.68	18.66	18.84	18.71	17.55	17.83	19.37	19.75	19.24
FeO	16.44	15.24	15.48	14.21	17.16	12.70	12.87	14.12	18.84	13.62	16.19	16.52
MnO	0.06	0.05	0.05	0.06	0.11	0.06	0.08	0.02	0.08	0.01	0.05	0.09
MgO	13.02	13.56	13.26	14.83	10.92	15.87	15.27	16.28	10.58	16.20	14.92	14.23
CaO	0.00	0.01	0.02	0.02	0.04	0.01	0.02	0.02	0.02	0.02	0.03	0.02
Na_2O	0.04	0.02	0.04	0.06	0.13	0.22	0.17	0.02	0.02	0.03	0.05	0.05
K_2O	9.51	9.08	8.98	9.28	9.10	8.90	9.30	9.54	9.62	9.74	8.98	9.53
TOTAL	97.84	97.72	95.83	96.79	94.25	96.09	96.10	98.47	97.77	97.61	98.81	98.63

TABLE III-I CONT. MICROPROBE ANALYTICAL RESULTS

(ii) Biotites Cont.

Element	(RKG) Sample No.							
	111/1	111/2	217/1	217/2	71/1	71/2	10/1	10/2
SiO_2	37.36	36.39	37.46	37.95	37.18	36.68	37.07	37.30
TiO_2	3.52	3.11	1.48	1.86	3.52	3.14	5.36	4.20
Al_2O_3	17.61	18.01	18.64	18.97	17.64	17.19	16.34	16.54
FeO	13.39	12.04	15.31	15.22	16.52	15.98	14.50	14.23
MnO	0.07	0.06	0.07	0.05	0.09	0.01	0.02	0.03
MgO	16.44	16.06	15.54	15.16	13.93	14.33	14.79	15.67
CaO	0.02	0.04	0.11	0.00	0.00	0.00	0.04	0.00
Na_2O	0.08	0.08	0.34	0.46	0.11	0.12	0.06	0.04
K_2O	9.23	9.51	8.32	8.17	9.26	9.02	9.15	9.76
TOTAL	97.70	95.31	97.49	97.85	98.00	96.46	97.36	97.77

(iii) Cordierites

Element	(RKG) Sample No.									
	190/1	190/2	190/3	190/4	190/5	190/6	190/7	209/1	209/2	209/3	209/4
SiO_2	47.70	48.16	48.29	46.75	47.61	47.19	47.56	48.59	48.62	48.68	48.83
TiO_2	0.01	0.01	0.00	0.01	0.0	0.0	0.01	0.0	0.0	0.0	0.0
Al_2O_3	33.49	33.49	33.42	33.43	33.38	33.41	33.52	33.57	33.58	33.57	33.76
FeO	6.53	6.36	6.50	6.49	6.41	6.38	6.35	3.54	3.80	3.25	3.45
MnO	0.18	0.21	0.18	0.18	0.18	0.17	0.19	0.15	0.15	0.10	0.09
MgO	8.99	8.91	8.88	8.96	8.96	9.01	8.99	10.59	10.65	10.93	10.78
CaO	0.01	0.0	0.0	0.0	0.0	0.01	0.0	0.0	0.0	0.0	0.0
Na_2O	0.17	0.14	0.15	0.17	0.14	0.12	0.14	0.18	0.22	0.15	0.23
K_2O	0.0	0.0	0.0	0.0	0.015	0.01	0.01	0.00	0.00	0.01	0.0
TOTAL	97.06	97.27	97.40	95.99	96.82	96.30	96.76	96.63	97.02	96.71	97.15

Element	(RKG)Sample No.							
	209/5	209/6	209/7		211/1	211/2	313/1	313/2
SiO_2	49.13	48.34	48.60		47.70	47.69	47.82	47.65
TiO_2	0.0	0.0	0.00		0.0	0.0	0.0	0.0
Al_2O_3	34.09	33.68	33.86		33.10	33.09	33.20	33.35
FeO	3.18	4.19	3.67		0.70	0.68	1.17	1.20
MnO	0.11	0.21	0.08		0.3	0.23	0.35	0.42
MgO	11.15	10.32	10.77		13.57	11.57	13.62	12.99
CaO	0.0	0.00	0.0		0.0	0.00	0.0	0.0
Na_2O	0.21	0.23	0.18		0.86	0.01	0.75	0.69
K_2O	0.01	0.01	0.0		0.0	0.0	0.0	0.0
TOTAL	97.87	96.99	97.17		96.44	93.29	96.91	96.30

(iv) Pyroxenes (Hypersthene)

Element	(RKG) Sample No.							
	199/1	199/2	199/3	111/1	111/2	217/1	71/1	71/2
SiO_2	48.56	48.72	48.34	48.11	47.39	44.53	45.67	47.16
TiO_2	0.05	0.06	0.06	0.10	0.09	0.36	0.18	0.13
Al_2O_3	5.99	5.95	6.10	5.60	5.49	14.84	6.70	6.81
FeO	28.25	28.33	27.82	24.22	23.51	21.33	25.83	26.13
MnO	0.69	0.71	0.67	0.79	0.77	0.71	0.57	0.60
MgO	17.57	17.59	17.46	20.34	19.94	14.32	17.92	18.20
CaO	0.02	0.02	0.03	0.05	0.06	0.30	0.03	0.04
Na_2O	nd	nd	nd	nd	nd	1.60	0.06	0.03
TOTAL	101.14	101.40	100.48	99.21	97.24	98.01	96.97	99.10

TABLE III-I CONT. MICROPROBE ANALYTICAL RESULTS

(v) Amphibolites (vi) Others

Element	(RKG) Sample No.				Rhodonite	
	299/1	299/2	298/1	298/2	299/1	299/2
SiO_2	50.24	50.20	41.32	44.50	47.08	46.92
TiO_2	0.0	0.0	0.85	0.62	0.0	0.0
Al_2O_3	0.35	0.02	12.02	12.60	0.01	0.0
FeO	14.46	14.46	19.58	18.99	11.53	11.47
MnO	9.39	9.39	0.50	1.20	32.87	32.79
MgO	6.05	6.05	7.68	7.50	1.84	1.79
CaO	20.64	20.65	11.13	11.20	6.94	7.02
Na_2O	0.26	0.20	1.13	1.20	0.03	0.0
K_2O	0.02	0.0	0.86	0.52	0.0	0.0
TOTAL	101.42	100.74	95.08	98.33	100.31	100.24

(vii) Sphalerite Analyses

Element	(RKG) Sample No.											
	211/1	211/2	211/3	211/7	211/8	294/1	294/2	294/3	294/4	294/5	294/6	294/7
Zn	59.61	59.33	59.59	58.81	59.54	58.07	57.87	57.97	58.09	57.22	58.33	57.32
Fe	7.36	7.90	7.55	8.80	7.92	9.39	8.99	8.40	8.48	8.71	7.94	8.82
S	33.24	33.02	33.43	33.36	33.15	33.48	33.30	32.53	32.83	32.69	32.59	32.62
TOTAL	100.20	100.24	100.57	100.96	100.61	100.94	100.16	98.89	99.40	98.61	98.87	98.76

Element	(RKG) Sample No.											
	294/8	220/1	220/3	220/4	220/5	220/6	220/7	220/8	280/1	280/2	280/3	280/4
Zn	58.50	59.19	57.56	58.51	58.27	59.02	59.59	59.34	58.48	58.32	58.95	58.89
Fe	8.80	7.69	8.62	8.00	7.86	7.50	7.71	8.14	8.49	8.16	8.17	7.88
S	32.66	32.48	33.01	33.06	32.09	32.42	32.02	31.64	32.56	32.63	32.79	32.23
TOTAL	99.96	99.37	99.19	99.57	98.22	98.93	99.33	99.12	99.53	99.61	99.91	99.00

Element	(RKG) Sample No.											
	280/5	280/6	289/1	289/2	289/3	289/4	289/5	289/6	289/7	289/8	74/1	74/2
Zn	57.72	57.74	58.65	59.49	58.70	58.40	59.74	58.02	58.00	58.36	58.78	58.09
Fe	9.38	9.32	8.27	8.20	7.78	8.14	7.67	8.96	8.06	8.29	8.66	8.53
S	32.66	33.21	33.29	33.01	32.81	32.49	32.20	32.21	32.52	32.50	33.16	33.17
TOTAL	99.96	100.26	100.21	100.71	99.28	99.02	99.61	99.18	98.58	99.15	100.59	99.81

Element	(RKG) Sample No.											
	74/5	74/6	74/7	60/1	60/2	60/3	60/4	60/5	60/6	64/1	64/2	64/3
Zn	57.41	57.32	58.39	58.93	57.76	58.92	58.80	58.96	57.14	58.06	57.67	57.98
Fe	8.89	9.09	7.34	7.91	7.89	8.04	8.38	8.11	8.01	7.29	7.29	7.29
S	32.52	33.45	32.82	32.09	33.81	34.60	33.87	32.97	33.07	32.85	33.16	32.85
TOTAL	98.82	99.86	98.56	98.93	99.46	101.57	101.05	100.03	98.22	98.20	98.12	98.12

Element	(RKG) Sample No.											
	64/4	55/1	55/2	55/3	55/4	99/1	99/2	99/3	99/4	57/1	57/2	57/3
Zn	58.42	59.62	59.97	59.76	58.93	58.07	58.63	62.38	62.51	57.87	60.05	59.97
Fe	7.48	7.70	7.50	7.66	7.83	8.56	8.47	4.56	4.63	6.72	7.35	7.50
S	33.27	32.75	33.07	31.92	32.02	32.93	33.15	32.62	33.24	33.47	33.18	33.02
TOTAL	99.17	100.07	100.53	99.34	98.78	99.56	100.24	99.56	100.39	98.08	100.58	100.53

TABLE III-I CONT. MICROPROBE ANALYTICAL RESULTS

(vii) Sphalerite Analyses Cont.

Element	(RKG) Sample No.											
	55/5	55/6	99/1	99/2	55/7	55/8	55/9	55/10	55/11	55/12	55/13	55/14
Zn	59.76	58.93	58.07	58.63	59.37	57.56	58.06	57.67	57.98	58.07	56.37	59.61
Fe	7.66	7.83	8.56	8.46	7.26	7.32	7.29	7.29	7.29	8.56	8.38	7.24
S	31.92	32.02	32.93	33.15	33.28	32.95	32.85	33.16	32.85	32.93	33.44	33.18
TOTAL	99.34	98.78	99.56	100.24	99.92	97.83	98.20	98.12	98.12	99.56	98.18	100.03

Element	(RKG) Sample No.			
	55/15	55/16	55/17	55/18
Zn	59.61	59.62	58.42	57.98
Fe	7.24	7.70	7.49	7.29
S	33.18	32.75	33.27	32.85
TOTAL	100.03	100.07	99.17	98.12

APPENDIX IV. CHEMICAL ETCHING METHODS

Polished thin sections were chemically etched to reveal intra- and intergranular textures which were otherwise hidden in the minerals pyrite, sphalerite and galena. Pyrrhotite textures were visible under partially crossed nicols. Chalcopyrite did not respond favourably to chemical etching.

The chemicals used were: (N.B. "$KMnO_4$" is 2.5g of the crystals dissolved in 100ml of distilled water).

(i) $KMnO_4$ + H_2SO_4 (concentrated)
(1 : 1)

(ii) $KMnO_4$ + HCl (concentrated)
(1 : 1)

(iii) HCl (concentrated)

(iv) HNO_3 (concentrated) + methyl alcohol
(3 : 1)

Sphalerite textures and twinning lamellae were illustrated best when etched with reagent (ii) for 1 - 2 minutes.
Pyrite textures were revealed using reagent (i).
The time period in which the mineral was in contact with the etch liquid was critical; 55 seconds proved to be the optimum time. The critical time factor and the difficulty in obtaining uniform etching across the entire section precluded pyrite grain sizes as a quantitative measure. The difficulty in etching pyrite was also reported for Canadian ores by Rockingham and Hutchinson (1980).
Galena textures were revealed using reagent (iv).
Chalcopyrite showed some reaction with reagent (iv) but etching was markedly irregular and only useful for qualitative observation.

The microscopic identification pf monoclinic pyrrhotite from hexagonal pyrrhotite was aided by the coating of the slide with a thin layer of "magnetic colloid". The ferromagnetic monoclinic polymorph became a darker brown colour after attracting the magnetic particles out of the colloidal film. The method followed was as described by Scott (1974), who states that this

method was preferable to the older etch tests which have proved inconsistent. The magnetic colloid (after Scott, 1974) was prepared as follows:

(1) Dissolve 2gm $FeCl_2 \cdot 4H_2O$ and 5.4g $FeCl_3 \cdot 6H_2O$ in 300ml distilled water at $70^{\circ}C$.

(2) Dissolve 5gm NaOH in 50cc distilled water.

(3) Mix solutions 1 and 2 and stir vigourously. Filter black precipitate and rinse several times with distilled water and finally with 0.01N HCl. Place the black precipitate in 500ml of a 0.05% sodium oleate solution and boil for a short time to mix the soap solution and precipitate.

Sample Numbers and Locations of Specimens for Thin Section, Microprobe Analysis and Whole Rock Analysis

All specimens from the property "Gedeelte Kielder" district of Prieska, borehole locations shown on Maps 1,2 and 3 and cross-sections 1-16.

DEPT. NO.	FIELD NO.	BRIEF DESCRIPTION	LOCATION BH NO. (Prefix) (KDH)	LOCATION DEPTH (M)	COMMENTS TS - Thin Section PT/S - Polished Thin Section A - Whole Rock Analysis P - Microprobe Analysis
9828	RKG 1	Sillimanite Gneiss	2	68	TS (Type Specimens)
9829	" 2	" "	5	480	" " "
9830	" 3	" "	2	85	" " "
9831	" 4	Hypersthene Gneiss	5	425	" " "
9832	" 5	Biotite Gneiss	7	146,3	" " "
9833	" 6	Hypersthene Gneiss	5	513	" " "
9834	" 7	" "	4	238	" " "
9835	" 8	Pyroxene Granulite	4	303	" " "
9836	" 9	Hypersthene Gneiss	5	95	" " "
9837	" 10	Pyroxene Granulite	4	189	" " " P
9838	" 11	Hypersthene Gneiss	5	84	" " "
9839	" 12	Pyroxene Granulite	2	105	" " "
9840	" 13	" "	2	190	" " "
9841	" 14	Biotite Gneiss	16	78	" " "
9842	" 15	" "	5	216	" " "
9843	" 16	Sillimanite Augen Gneiss	5	119	" " "
9844	" 17	Pyroxene Granulite	2	115	" " "
9845	" 18	Diopside Granulite	2	125	" " "
9846	" 19	Amphibolite	4	152	" " "
9847	" 20	"	4	282	" " "
9848	" 21	Granodiorite	5	160	" " "
9849	" 22	"	2	150	" " "
9850	" 23	"	2	146	" " "
9851	" 24	"	5	143	" " "
9852	" 25	Garnet Gneiss	5	350	" " "
9853	" 26	Granodiorite	3	140	" " "
9854	" 27	"	5	347	" " "
9855	" 31	Hypersthene Gneiss	2	115	PT/S
9856	" 32	" "	2	117	PT/S
9857	" 33	Sulphide	2	117,5	PT/S
9858	" 34	"	2	118,5	PT/S P
9859	" 35	"	2	120,5	PT/S
9860	" 36	"	2	122,0	PT/S
9861	" 37	"	2	123,4	PT/S P
9862	" 38	Alteration Zone	2	124,5	PT/S
9863	" 40	Diopside Granulite	2	136	TS A
9864	" 41	Granodiorite	2	137	TS
9865	" 42	Garnet Gneiss	2	199	TS
9866	" 43	Sillimanite Gneiss	3	65	TS
9867	" 46	Granodiorite	3	140	TS
9868	" 48	Hypersthene Gneiss	3	157	TS
9869	" 50	" "	3	166,5	PT/S
9870	" 51	Sulphide	3	166,9	PT/S
9871	" 52	"	3	171,0	PT/S P
9872	" 53	"	3	172,4	PT/S P
9873	" 54	"	3	175,00	PT/S
9874	" 55	"	3	179,5	PT/S P
9875	" 56	"	3	180	"
9876	" 57	"	3	181,4	" P
9877	" 58	"	3	183,0	" P
9878	" 59	"	3	184,00	"
9879	" 60	"	3	185,9	" P
9880	" 61	Siliceous Zone	3	186,0	"
9881	" 62	Diopside Granulite	3	186,8	TS
9882	" 64	Sulphide	3	191	PT/S P
9883	" 65	Diopside Granulite	3	194	TS
9884	" 66	Biotite Gneiss	3	210	TS
9885	" 68	" "	3	260	TS
9886	" 69	" "	4	75	TS
9887	" 71	" "	4	210	" A P
9888	" 72	Hypersthene Gneiss	4	227	PT/S
9889	" 73	Sulphide	4	236	"
9890	" 74	"	4	239	" P
9891	" 76	"	4	243	" P
9892	" 77	"	4	244	"
9893	" 78	"	4	245	"
9844	" 79	Siliceous Zone	4	247	"
9895	" 80	Sulphide	4	248,6	"
9896	" 81	Breccia	4	251,0	TS
9897	" 82	Granite	4	260,0	TS
9898	" 83	Diopside Granulite	4	283	"
9899	" 85	Garnet Gneiss	4	300	"
9900	" 87	" "	4	450	"
9901	" 88	Granodiorite	2	136,4	"
9902	" 89	"	2	182,0	"

DEPT. NO.	FIELD NO.	BRIEF DESCRIPTION	LOCATION BH NO. (prefix) (KDH)	DEPTH (M)	COMMENTS TS- Thin Section PT/S - Polished Thin Section A - Whole Rock Analysis P - Microprobe Analysis
9903	RKG 90	Hypersthene Gneiss	5	420	TS
9904	" 92	" "	5	510	TS A
9905	" 94	" "	5	544	PT/S P
9906	" 95	Sulphide	5	548	PT/S
9907	" 96	"	5	550	"
9908	" 97	"	5	552	"
9909	" 98	Hypersthene Gneiss	5	555	TS
9910	" 99	Sulphide	5	557	PT/S P
9911	" 100	Hypersthene Gneiss	5	565	TS
9912	" 101	Diopside Granulite	5	572	TS
9913	" 102	" "	5	575	"
9914	" 104	Biotite Gneiss	5	595	"
9915	" 105	Sillimanite Gneiss	8	34	"
9916	" 106	Garnet Gneiss	8	44	"
9917	" 107	Amphibolite	8	105	"
9918	" 108	Biotite Gneiss	8	115	"
9919	" 109	" "	8	135	"
9920	" 111	" "	8	145	PT/S P
9921	" 112	Sulphide	8	151	"
9922	" 113	Sillimanite Gneiss	8	160	"
9923	" 114	Diopside Granulite	8	167	TS
9924	" 116	Biotite Gneiss	9	58	"
9925	" 117	Amphibolite	9	81	" A
9926	" 119	Biotite Gneiss	9	137	"
9927	" 120	Hypersthene Gneiss	9	143	PT/S
9928	" 121	" "	9	144	PT/S
9929	" 122	Sulphide	9	148	PT/S
9930	" 123	Biotite Gneiss	9	171	TS
9931	" 124	Diopside Granulite	9	191	TS
9932	" 127	Biotite Gneiss	9	220	TS
9933	" 131	Hypersthene Gneiss	7	80	TS
1934	" 132	" "	7	101	TS
9935	" 133	Sulphide	7	105	PT/S
9936	" 134	"	7	106	"
9937	" 136	Biotite Gneiss	7	116	TS
9938	" 137	Diopside Granulite	7	118,5	TS
9939	" 138	Biotite Gneiss	7	148	TS
9940	" 139	" "	16	45	TS
9941	" 140	Amphibolite	16	80	"
9942	" 143	Biotite Gneiss	16	117	"
9943	" 144	" "	16	120	PT/S
9944	" 145	Sulphide	16	142	PT/S
9945	" 146	Sillimanite Gneiss	16	146	TS
9946	" 147	Sulphide	16	149	PT/S
9947	" 148	Biotite Gneiss	16	160	TS
9948	" 149	Sillimanite Gneiss	16	185	TS
9949	" 150	Sulphide	16	207	PT/S
9950	" 152	Granodiorite	16	211	TS
9951	" 153	Biotite Gneiss	16	220	"
9952	" 154	" "	29	54	"
9953	" 155	Sillimanite Gneiss	29	79	"
9954	" 156	Biotite Gneiss	29	128	"
9955	" 157	Sulphide	29	147,3	PT/S
9956	" 158	"	29	154,7	"
9957	" 159	Biotite Gneiss	29	166,5	TS
9958	" 168	" "	5	70	PT/S
9959	" 169	Hypersthene Gneiss	5	83	PT/S
9960	" 170	" "	5	105	"
9961	" 171	Augen Gneiss	5	110	"
9962	" 172	Pyritic Gneiss	5	121	"
9963	" 173	" "	5	130	"
9964	" 176	Biotite Gneiss	12	53	TS
9965	" 177	" "	12	55	TS
9966	" 178	Amphibole Gneiss	12	75	"
9967	" 179	" "	12	101	" P
9968	" 180	Hypersthene Gneiss	12	103	"
9969	" 181	Sulphide	12	105	PT/S P
9970	" 182	"	12	107,5	" P
9971	" 183	Sillimanite Gneiss	12	108,7	TS
9972	" 184	" "	12	130	TS
9973	" 185	Amphibolite	12	145	TS A
9974	" 186	"	12	165	TS
9975	" 187	"	12	192	TS
9976	" 188	"	12	215	TS
9977	" 189	"	12	250	TS A
9978	" 190	Biotite Gneiss	12	275	TS P
9979	" 191	Amphibolite	12	298	TS
9980	" 192	Diopside Granulite	14	60	TS A
9981	" 193	Biotite Gneiss	14	65	TS
9982	" 194	" "	14	78	TS
9983	" 195	" "	14	84.5	TS

DEPT. NO.	FIELD NO.	BRIEF DESCRIPTION	LOCATION BH NO. (Prefix) (KDH)	DEPTH (M)	COMMENTS TS - Thin Section PT/S - Polished Thin Section A - Whole Rock Analysis P - Microprobe Analysis		
9984	RKG 196	Sulphide	14	85.5	PT/S		P
9985	" 198	Amphibolite	14	99	TS	A	
9986	" 199	Biotite Gneiss	14	105	TS		P
9987	" 200	Amphibolite	14	128	TS	A	
9988	" 202	Biotite Gneiss	22	49	TS		
9989	" 203	Amphibolite	22	86	TS		
8890	" 204	"	22	95	TS	A	
9991	" 205	Biotite Gneiss	22	110	"		
9992	" 206	Diopside Granulite	24	83.5	"	A	
9993	" 207	Biotite Gneiss	24	166	"		
9994	" 208	" "	24	186	"		
9995	" 209	Sulphide	24	198	PT/S		P
9996	" 210	"	24	199.5	"		
9997	" 211	"	24	201	"		P
9998	" 212	"	24	204.8	"		
9999	" 213	Sillimanite Gneiss	24	210	TS		
10000	" 214	Biotite Gneiss	15	50	TS		
10001	" 215	Amphibolite	15	63	TS		
10002	" 216	Sillimanite Gneiss	15	75	TS		
10003	" 217	Amphibole Gneiss	15	95	TS		P
10004	" 219	Sulphide	15	117	PT/S		
10005	" 220	"	15	119	"		P
10006	" 221	"	15	120	"		
10007	" 222	"	15	122	"		P
10008	" 223	"	15	121.5	"		
10009	" 224	Diopside Granulite	15	132	PT/S		
10010	" 225	Biotite Gneiss	15	173	TS		
10011	" 227	Amphibolite	17	55	TS		
10012	" 228	Biotite Gneiss	17	68	"		
10013	" 229	Pegmatite	17	92	"		
10014	" 230	Diopside Granulite	17	95	"		
10015	" 231	Biotite Gneiss	17	110	"		
10016	" 232	Diopside Granulite	17	115	"		
10017	" 233	Sulphide	17	120.5	PT/S		P
10018	" 234	"	17	121.0	"		
10019	" 235	Magnetite Porphyry	17	122	"		
10020	" 236	Biotite Gneiss	17	124.0	TS		
10021	" 237	" "	17	140	"		
10022	" 238	" "	17	170	"		
10023	" 239	" "	18	50	"		
10024	" 240	Banded Iron Formation	18	57	PT/S		P
10025	" 241	Gneiss	18	95	TS		
10026	" 242	Amphibolite	18	110	TS	A	
10027	" 243	Gneiss	18	124	TS		
10028	" 244	"	18	145	TS		
10029	" 245	"	18	180	TS		
10030	" 246	Sulphide	18	184.9	PT/S		
10031	" 247	"	18	186.3	"		
10031	" 248	"	18	187.6	"		
10033	" 249	Magnetite Porphyry	18	189.0	"		P
10034	" 250	Sulphide	18	195.0	"		P
10035	" 251	Biotite Gneiss	18	209	TS		
10036	" 252	" "	18	230	TS		
10037	" 253	" "	19	53	TS		
10038	" 254	Amphibolite	19	85	TS	A	
10039	" 255	Biotite Gneiss	19	135	TS		P
10040	" 256	Sulphide	19	145.5	PT/S		P
10041	" 257	"	19	146	"		
10042	" 258	Biotite Gneiss	19	147.5	TS		
10043	" 259	" "	19	185	TS		
10044	" 260	" "	20	50	TS		
10045	" 261	Banded Iron Formation	20	65.5	PT/S		
10046	" 262	" " "	20	67.0	"		
10047	" 263	Amphibolite	20	110	TS		
10048	" 264	"	20	140	TS	A	
10049	" 265	Biotite Gneiss	20	165	TS		
10050	" 266	" "	20	180	TS		
10051	" 267	Sulphide	20	193	PT/S		P
10052	" 268	"	20	194.75	"		
10053	" 269	"	20	195.75	"		
10054	" 270	Biotite Gneiss	20	198	TS		
10055	" 272	Amphibolite	20	213	TS		
10056	" 273	Biotite Gneiss	20	230	TS		
10057	" 274	" "	25	53	TS		
10058	" 275	Banded Iron Formation	25	63	PT/S		
10059	" 276	Amphibolite	25	125.6	TS		
10060	" 277	Biotite Gneiss	25	206	TS		
10061	" 278	Sulphide	25	229.5	PT/S		
10062	" 279	"	25	230	PT/S		P
10063	" 280	"	25	232	PT/S		P
10064	" 281	"	25	232.5	PT/S		
10065	" 282	Biotite Gneiss	25	240	TS		

DEPT NO.	FIELD NO.	BRIEF DESCRIPTION	LOCATION BH NO. (Prefix) (KDH)	DEPTH (M)	COMMENTS TS - Thin Section PT/S - Polished Thin Section A - Whole Rock Analysis P - Microprobe Analysis		
10066	RKG 283	Amphibolite	25	245	TS		
10067	" 284	Biotite Gneiss	26	92	TS		
10068	" 285	Banded Iron Formation	26	118.8	PT/S		P
10069	" 286	Amphibolite	26	155	TS		
10070	" 287	Biotite Gneiss	26	223	TS		
10071	" 288	Sulphide	26	241.8	PT/S		P
10072	" 289	"	26	244	PT/S		P
10075	" 290	"	26	245	"		
10076	" 291	"	26	246	"		
10077	" 292	"	26	247	"		
10078	" 293	"	26	248	"		
10079	" 294	"	26	249	"		P
10080	" 295	"	26	250	"		P
10081	" 296	Amphibolite	26	253	"		
10082	" 297	"	26	263	TS		
10083	" 298	Biotite Gneiss	26	275	TS		P
10084	" 299	Banded Iron Formation	27	122	PT/S		P
10085	" 300	Amphibolite	27	170	TS		
10086	" 301	Biotite Gneiss	27	256	TS		
10087	" 302	Sulphide	27	280	PT/S		
10088	" 303	"	27	280.9	PT/S		
10089	" 304	Gneiss	27	300	TS		
10090	" 306	Gneiss	28	45	TS		
10091	" 308	Amphibolite	28	260	TS		
10092	" 309	Gneiss	28	330	TS		
10093	" 310	Sulphide	28	339.4	PT/S		
10094	" 311	"	28	339.5	PT/S		P
10095	" 312	Gneiss	28	345	TS		
10096	" 313	Sulphide	28	353.5	PT/S		
10097	" 314	Gneiss	28	357	TS		
	SURFACE SAMPLES (CO-ORDINATES SEE MAP 4)						
10099	" 316	Banded Iron Formation	32E/13.5S		PT/S		
10100	" 317	" " "	32E/13.5S		PT/S		
10101	" 318	Granulite	28E/22S		TS		
10102	" 319	"	24E/20.5S		TS	A	
10103	" 320	"	20E/18S		TS		
10104	" 321	"	8E/15.8S		TS	A	
10105	" 322	"	48E/29S		TS		
10106	" 323	"	16W/2S		TS	A	
10107	" 324	"	26E/11N		TS	A	
10108	" 326	"	35E/1.5S		TS		
10109	" 327	"	40E/0.0N		TS	A	
10110	" 328	"	12W/8N		TS		
10111	" 329	"	12W/8N		TS		
10112	" 330	"	33E/6S		TS	A	
10113	" 331	Granulite	55E/2.2N		TS		

APPENDIX VI. X-RAY DIFFRACTION METHODS

Qualitative X-ray diffraction was carried out to help in the identification of unknown minerals which occurred in sufficient quantities to allow mechanical separation and preparation.

The mineral requiring identification was identified in the original core specimen from which the thin section had been cut and a small piece of the core separated and crushed.

Initial crushing was done in a manually operated steel crusher, followed by pulverising to < 300 mesh in an agate mortar. This powder was mounted on a glass slide with rubber-based gum, and placed into the X-ray chamber.

The instrument used is a Philips Automatic X-ray powder diffractometer with PW1350 - PW1394.

The X-ray diffraction operating conditions used were;

kV	...	40
mA	...	20
diverging, receiving and anti-scatter slits	...	$\frac{1}{2}^{o}$, $\frac{1}{2}^{o}$, 1^{o}.
scanning speed	...	2^{o} 2θ/min.
count rate	...	10^{3}
time constant	...	1
chart drive speed	...	2cm/min.
tube	...	Cu

The peaks were identified using ASTM cards, the Fink Inorganic index (1966) and Selected Powder diffraction data for minerals (published 1974, Joint Committee on powder diffractometry standards).

Pyrrhotite polymorph identification followed a different procedure (after Arnold (1966) and Graham (1969)). The presence and grain size of pyrrhotite was established initially using polished thin sections and normal qualitative X-ray diffraction scans as described above.

The sample to be used for pyrrhotite polymorph identification was crushed and ground carefully to avoid overgrinding and

overheating in an agate vessel with acetone. The <300 mesh finely ground powder was placed in an aluminium sample tray and subjected to pressure approximately 20lbs., the excess sample scraped away using a glass slide.

The sample was then subjected to X-rays under the following instrument conditions:

kV	...	40
mA	...	20
slits	...	$\frac{1}{2}^{o}$, $\frac{1}{2}^{o}$, 1^{o}.
scanning speed	...	$1/4^{o}$ 2θ/min.
count rate	...	10^{3}
time constant	...	4
chart drive speed	...	1cm/min.
tube	...	Cu
range scanning	...	42.5 - 44.5 $^{o}2\theta$

The ferromagnetic monoclinic pyrrhotite polymorph gives a doublet at about d= 2.051 Å and d= 2.064 Å. These two peaks, the monoclinic $(20\bar{2})$ and monoclinic (202) are approximately of the same intensity. Consequently a presence of monoclinic polymorph gives a symetrical doublet.

The paramagnetic hexagonal pyrrhotite polymorph gives a sharp single peak at d_{102} = 2.065, which overlaps with the 202 peak of the monoclinic variety. Consequently a mixture of hexagonal and monoclinic pyrrhotite polymorphs gives an asymetrical doublet. The degree of asymetry giving an approximation of the amount of hexagonal pyrrhotite.

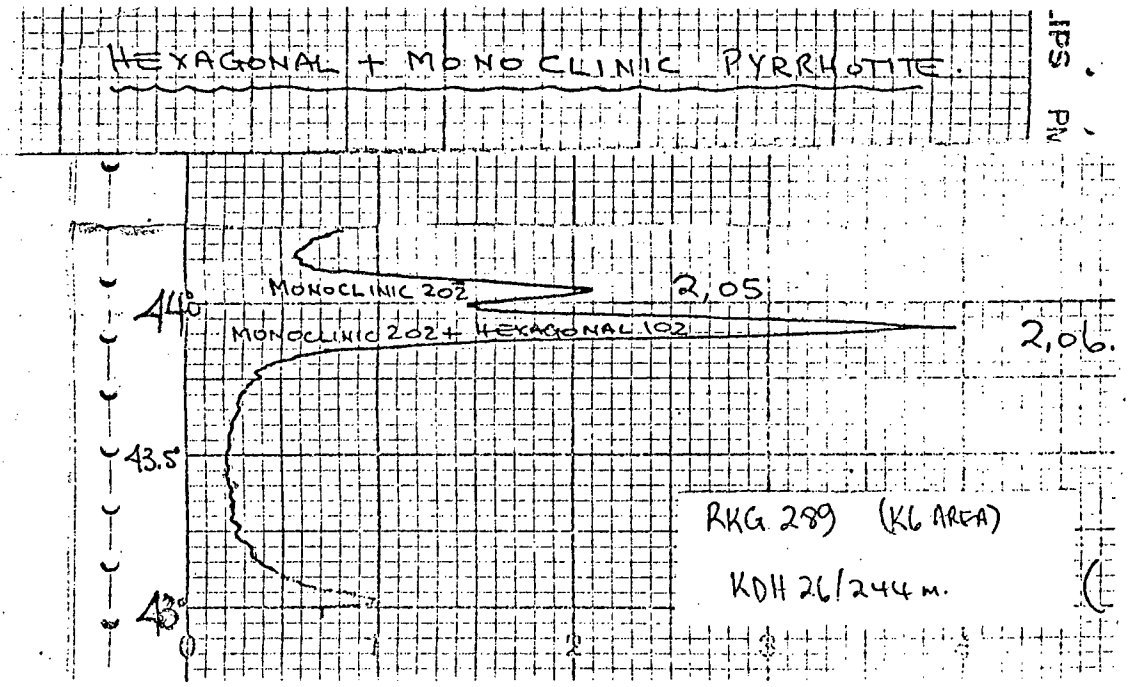

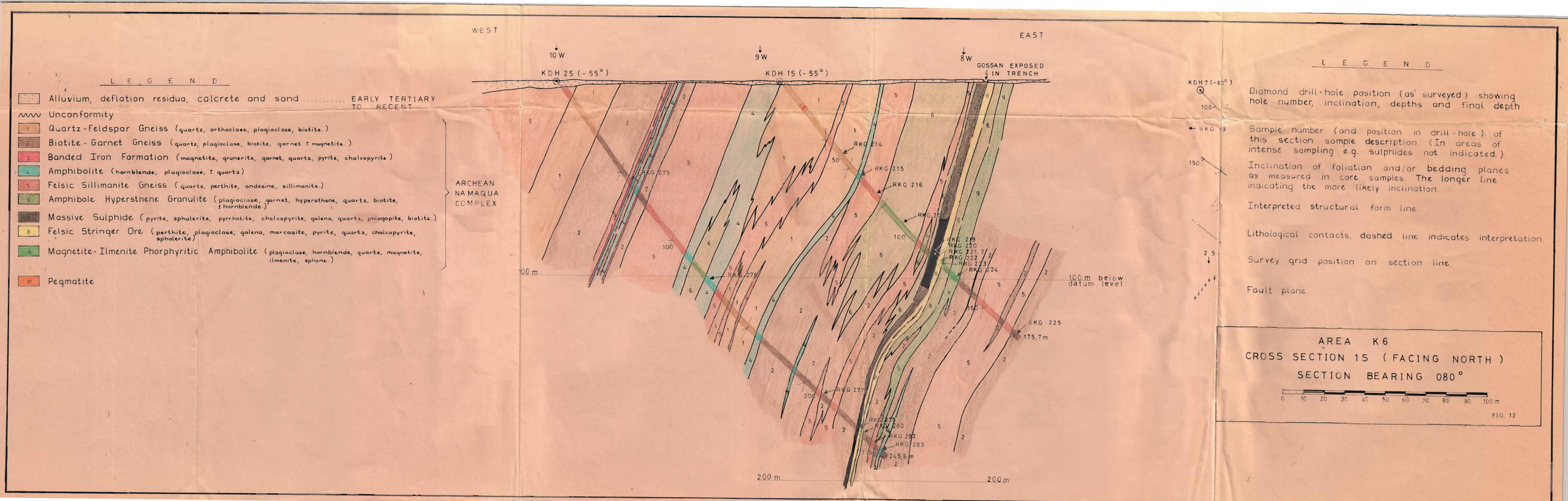

L E G E N D

- Alluvium, deflation residua, calcrete and sand ..... EARLY TERTIARY TO RECENT
- Unconformity

ARCHEAN NAMAQUA COMPLEX

1. Quartz-Feldspar Gneiss (quartz, orthoclase, plagioclase, biotite.)
2. Biotite-Garnet Gneiss (quartz, plagioclase, biotite, garnet ± magnetite.)
3. Banded Iron Formation (magnetite, grunerite, garnet, quartz, pyrite, chalcopyrite)
4. Amphibolite (hornblende, plagioclase, ± quartz)
5. Felsic Sillimanite Gneiss (quartz, perthite, andesine, sillimanite.)
6. Amphibole Hypersthene Granulite (plagioclase, garnet, hypersthene, quartz, biotite, ± hornblende.)
7. Massive Sulphide (pyrite, sphalerite, pyrrhotite, chalcopyrite, galena, quartz, phlogopite, biotite.)
8. Felsic Stringer Ore (perthite, plagioclase, galena, marcasite, pyrite, quartz, chalcopyrite, sphalerite)
9. Magnetite-Ilmenite Phorphyritic Amphibolite (plagioclase, hornblende, quartz, magnetite, ilmenite, sphene.)

P. Pegmatite

L E G E N D

- Diamond drill-hole position (as surveyed) showing hole number, inclination, depths and final depth
- Sample number (and position in drill-hole) of this section sample description (In areas of intense sampling e.g. sulphides not indicated.)
- Inclination of foliation and/or bedding planes as measured in core samples. The longer line indicating the more likely inclination.
- Interpreted structural form line.
- Lithological contacts, dashed line indicates interpretation.
- Survey grid position on section line.
- Fault plane.

AREA K6
CROSS SECTION 1S (FACING NORTH)
SECTION BEARING 080°

0 10 20 30 40 50 60 70 80 90 100 m

FIG. 12

B.S. SEPT. 1980

REGIONAL GEOLOGICAL MAP OF THE KIELDER PROPERTIES.

MAP 4

KIELDER

GEDEELTE KIELDER

KIELDER CAMP

SAND

SAND OVER CALCRETE

CALCRETE

DWYKA ERRATICS

DWYKA TILLITE

TILLITE

KLIP GOSSAN

BASE LINE

MAINTAINED GRAVEL ROAD

1:20,000

0 500 1000 1500 m

LEGEND

- Sand, Calcrete, Alluvium, Dwyka rubble
- Dwyka Group tillite with BIF Lava, Dolomite, Gneiss and Quartzite erratics
- Quartz veins (qv) and pegmatites (pg)
- Diopside - Granulite
- Gossan
- Amphibolite
- Banded iron formation, Strongly Banded Quartz, Magnetite and Hematite
- Quartz-feldspar gneiss garnetiferous and pegmatitic in places
- Quartz-plagioclase - diopside Granulite
- Red sericitic quartz feldspar rock
- Hornblende Granulite-gneiss
- Amphibole gneiss
- Drainage with flow direction
- Pan, Topographic depression
- Telephone pole
- Prospecting trenches + pits
- RKG 324 Chip buttk sample location number
- Stock fence
- Boundary fence
- Farm track
- Windpump Trees Dam
- WH Water Hole
- Main road
- Gate
- House (H) barn
- Bearing (B) and plunge of lineation
- Strike and dip of foliation
- Strike and vertical foliation
- Geological contact
- Outcrop boundary
- Assumed strike stratigraphic horizons
- Trig survey Beacon with number and height in metres above sea level

L E G E N D

- Alluvium, deflation residua, calcrete and sand ..... EARLY TERTIARY TO RECENT
- Unconformity

ARCHEAN NAMAQUA COMPLEX

- 1 Quartz - Feldspar Gneiss (quartz, orthoclase, plagioclase, biotite.)
- 2 Biotite Garnet Gneiss (quartz, plagioclase, biotite, garnet ± magnetite.)
- 4 Amphibolite (hornblende, plagioclase, ± quartz.)
- 5 Felsic Sillimanite Gneiss (quartz, perthite, andesine, sillimanite.)
- 6 Amphibole Hypersthene Granulite (plagioclase, garnet, hypersthene, quartz, biotite, ± hornblende.)
- 7 Massive Sulphide (pyrite, sphalerite, pyrrhotite, chalcopyrite, galena, quartz, phlogopite, biotite.)
- 9 Magnetite - Ilmenite Phorphyritic Amphibolite (plagioclase, hornblende, quartz, magnetite, ilmenite, sphene.)

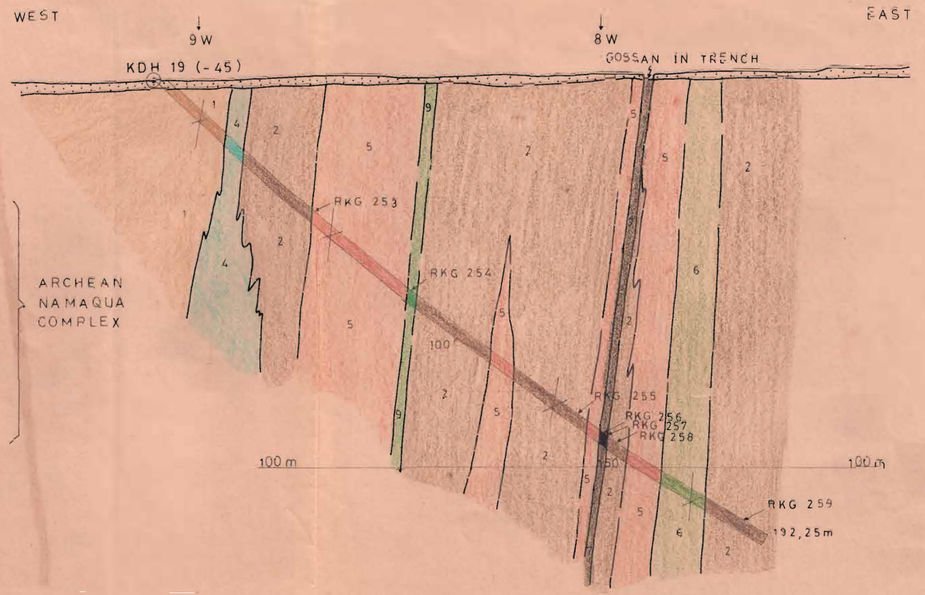

L E G E N D

- KDH 7 (-60°) / 100 — Diamond drill-hole position (as surveyed) showing hole number, inclination, depths and final depth.
- ← RKG 85 — Sample number (and position in drill-hole) of this section sample description. (In areas of intense sampling e.g. sulphides not indicated.)
- 150 — Inclination of foliation and/or bedding planes as measured in core samples. The longer line indicating the more likely inclination.
- Interpreted structural form line.
- Lithological contacts, dashed line indicates interpretation.
- 2.6 — Survey grid position on section line.
- Fault plane.

AREA K6

CROSS SECTION 00 (FACING NORTH)

SECTION BEARING 080°

0 10 20 30 40 50 60 70 80 90 100m

FIG. 15

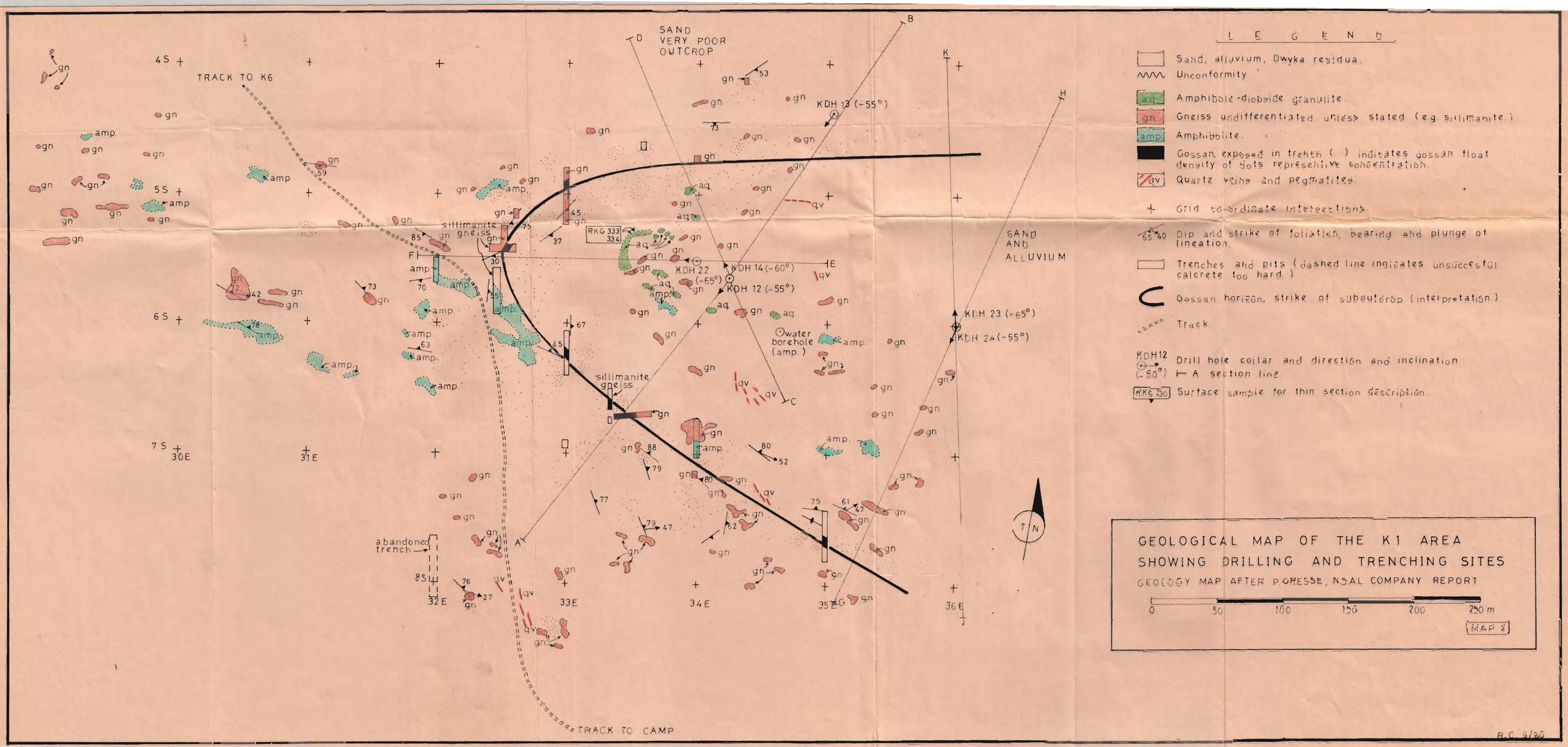

L E G E N D

- Sand, alluvium, Dwyka residua.
- Unconformity
- aq. Amphibole-diopside granulite.
- gn. Gneiss undifferentiated unless stated (e.g. sillimanite.)
- amp. Amphibolite.
- Gossan exposed in trench ( ) indicates gossan float density of dots representive concentration.
- qv Quartz veins and pegmatites.
- \+ Grid co-ordinate intersections.
- 65/40 Dip and strike of foliation, bearing and plunge of lineation.
- Trenches and pits (dashed line indicates unsuccesful calcrete too hard.)
- Gossan horizon, strike of subcrop (interpretation.)
- Track.
- KDH12 (-60°) Drill hole collar and direction and inclination
- ⊢ A section line.
- RKG 330 Surface sample for thin section description.

GEOLOGICAL MAP OF THE K1 AREA SHOWING DRILLING AND TRENCHING SITES

GEOLOGY MAP AFTER PORESSE, NSAL COMPANY REPORT

0 50 100 150 200 250 m

MAP 2

B.C. 9/30

L E G E N D

- Alluvium, deflation residua, calcrete and sand ..... EARLY TERTIARY TO RECENT
- Unconformity

- 4 Banded Biotite Gneiss (quartz, oligoclase, orthoclase, biotite, ± hypersthene)
- 5 Felsic Sillimanite Gneiss (Upper Unit) (quartz, perthite, andesine, sillimanite ± biotite, ± sericite)
- 6 Hypersthene - Quartz - Garnet Granulite (quartz, hypersthene, andesine, biotite, orthoclase, garnet, magnetite.)
- 7 Amphibolite (hornblende, labradorite, hypersthene, diopside, biotite.)
- 8 Porphyroblastic Hypersthene - Biotite Granulite (hypersthene, quartz, plagioclase, biotite, orthoclase, magnetite.)
- 10 Quartz - Cordierite - Sillimanite Granulite (cordierite, quartz, biotite, sillimanite, pyrrhotite, pyrite, magnetite.)
- 13 Massive Sulphides and Intercalated Siliceous Zone (pyrrhotite, pyrite, sphalerite, chlorite, barite, chalcopyrite, quartz.)
- 12 Diopside Plagioclase Granulite (diopside, labradorite, hornblende, hypersthene, magnetite, biotite.)
- 13 Banded Hypersthene Granulite (quartz, hypersthene, andesine, biotite, magnetite ± pyrite, pyrrhotite (±).)
- 14 Felsic Sillimanite Gneiss (Lower Unit) (quartz, perthite, andesine, sillimanite ± biotite ± sericite.)
- 15 Banded Biotite - Garnet Gneiss (quartz, andesine, hypersthene, biotite, garnet, magnetite.)

ARCHEAN NAMAQUA COMPLEX

— Intrusive Rocks —

- 18 Granodiorite (quartz, andesine, microcline, biotite.) ..... LATE TECTONIC INTRUSIVE

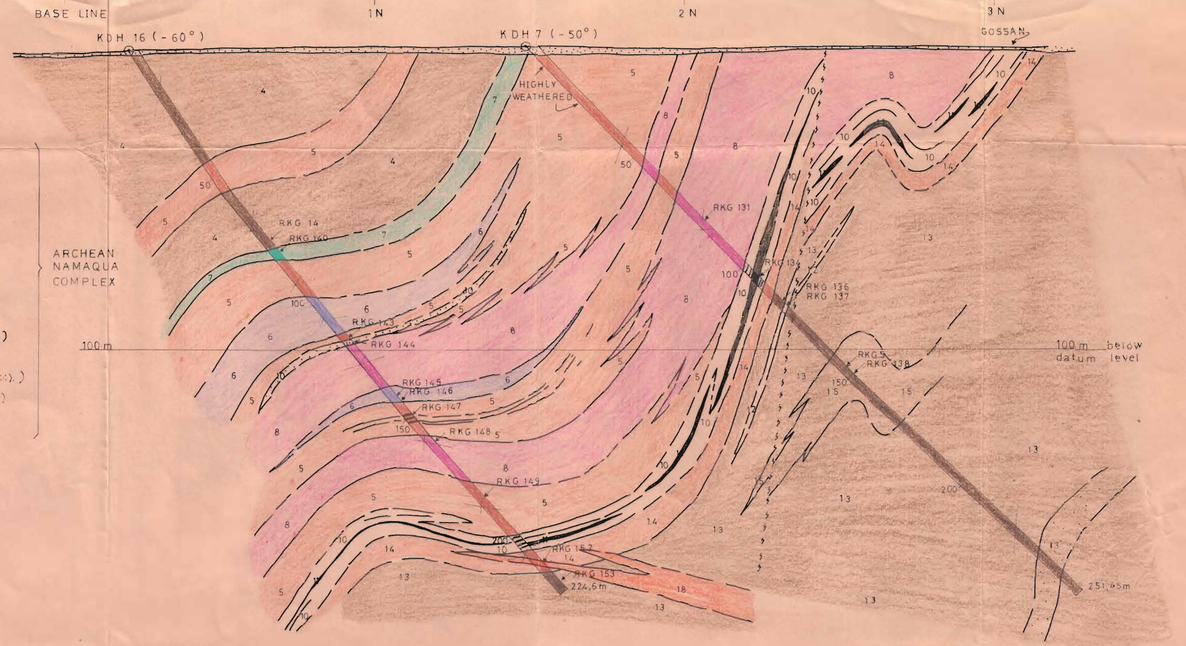

L E G E N D

KDH7 (-60°) 100 — Diamond drill-hole position (as surveyed) showing hole number, inclination, depths and final depth.

RKG 59 — Sample number (and position in drill-hole) of this section sample description. (In areas of intense sampling (e.g. sulphides not indicated.)

150 — Inclination of foliation and/or bedding planes as measured in core samples. The longer line indicating the more likely inclination.

Interpreted structural form line.

Lithological contacts, dashed line indicates interpretation.

2.5 — Survey grid positions on section line.

Fault plane

AREA K3
CROSS SECTION 56E (FACING WEST)
SECTION BEARING 349°

0 10 20 30 40 50 60 70 80 90 100 m

FIG. 5

R.G. AUG. 1980

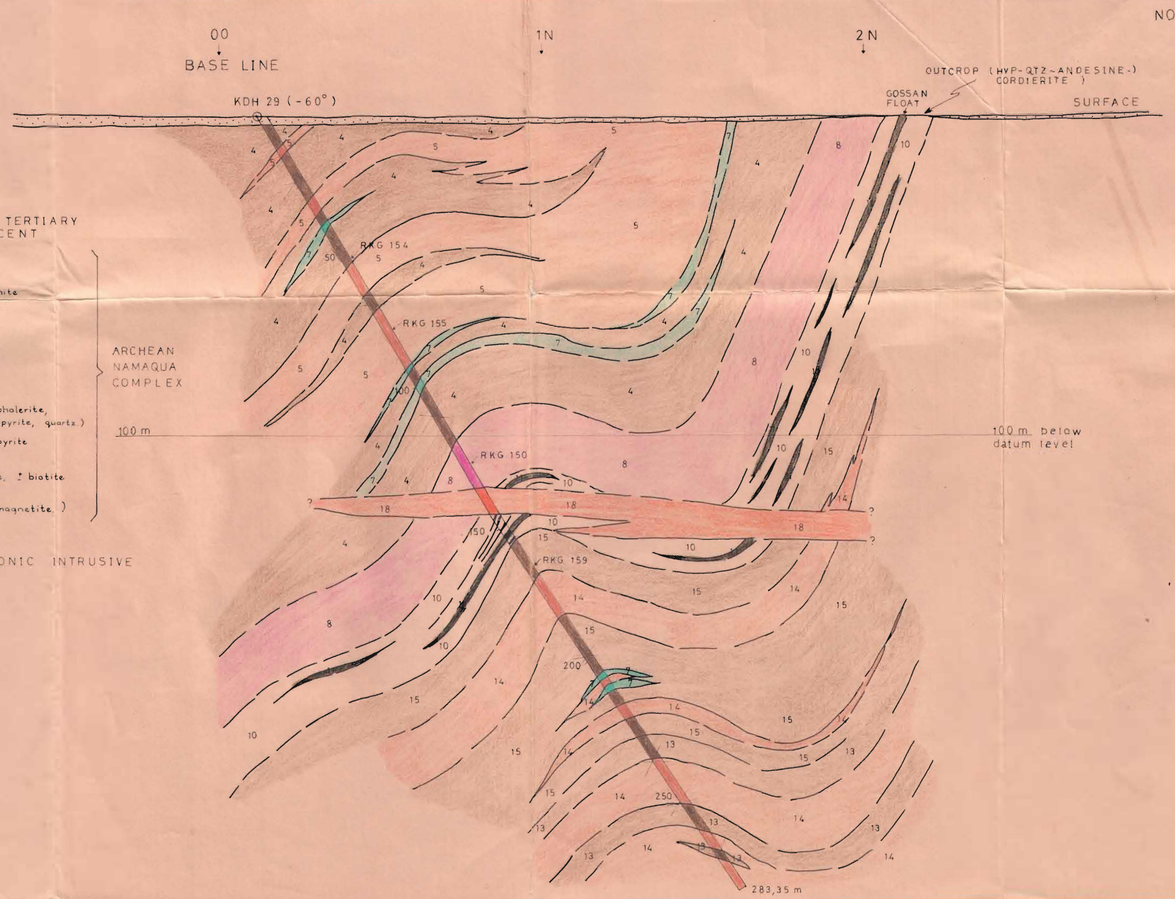

L E G E N D

- Alluvium, deflation residua, calcrete and sand ..... EARLY TERTIARY TO RECENT
- Unconformity

ARCHEAN NAMAQUA COMPLEX

- 4 Banded Biotite Gneiss (quartz, oligoclase, orthoclase, biotite : hypersthene.)
- 5 Felsic Sillimanite Gneiss (Upper Unit) (quartz, perthite, andesine, sillimanite : biotite : sericite)
- 7 Amphibolite (hornblende, labradorite, hypersthene, diopside, biotite)
- 8 Porphyroblastic Hypersthene - Biotite Granulite (hypersthene, quartz, plagioclase, biotite, orthoclase, magnetite.)
- 10 Quartz - Cordierite - Sillimanite Granulite (cordierite, quartz, biotite, sillimanite, pyrrhotite, pyrite, magnetite)
- 11 Massive Sulphides and Intercalated Siliceous Zone (pyrrhotite, pyrite, sphalerite, chlorite, barite, chalcopyrite, quartz.)
- 13 Banded Hypersthene Granulite (quartz, hypersthene, andesine, biotite, magnetite, : pyrite pyrrhotite (trace))
- 14 Felsic Sillimanite Gneiss (Lower Unit) (quartz, perthite, andesine, sillimanite, : biotite : sericite.)
- 15 Banded Biotite - Garnet Gneiss (quartz, andesine, hypersthene, biotite, garnet, magnetite.)

— Intrusive Rocks —

- 18 Granodiorite (quartz, andesine, microcline, biotite.) ..... LATE TECTONIC INTRUSIVE

L E G E N D

KDH 7 (-60°) / 100 — Diamond drill-hole position (as surveyed) showing hole number, inclination, depths and final depth.

← RKG 69 — Sample number (and position in drill-hole) of this section sample description. (In areas of intense sampling (e.g. sulphides not indicated.)

150 — Inclination of foliation and/or bedding planes as measured in core samples. The longer line indicating the more likely inclination.

Interpreted structural form line.

Lithological contacts, dashed line indicates interpretation.

2S — Survey grid positions on section line.

Fault plane.

AREA K3

CROSS SECTION 55E (FACING WEST)

SECTION BEARING 349°

0 10 20 30 40 50 60 70 80 90 100 m

FIG. 4

— GEOLOGICAL MAP OF K6 AREA —

SHOWING DRILLING AND TRENCHING SITES

Scale 1:2000

MAP N°3

B.H. 9/80

KDH 21 (-45°)
KDH 19 (-45°)
KDH 25 (-55°)
KDH 15 (-55°)
KDH 18° (-65°)
KDH 17° (-55°)
KDH 28° (-65°)
KDH 26 (-55°)
KDH 20 (-55°)
KDH 27 (-65°)

Track to Kielder
Track to K1 & K3
(Base Line) 00
gossan
BIF (abandoned)

4N 3N 2N 1N 00 1S 2S 3S 4S 5S
10W 9W 8W 7W 6W 5W 4W 3W 2W 1W

T N

0 10 20 30 40 50 100 150 200 250
metres

— L E G E N D —

- Alluvium, deflation residua, calcrete.
- fq — Undifferentiated quartz feldspar gneiss.
- dg — Diopside granulite
- amp — Amphibolite
- Gossan in situ and float
- BIF — Banded Iron Formation
- + Grid co-ordinate intersections.
- 65/40 Dip and strike of foliation bearing and plunge of lineation.
- Trenches and pits (showing gossan intersection)
- KDH7 (-55°) Drill hole collar and direction and inclination.
- Track

SOUTH 3S | 2S | 1S | 00 (BASE LINE) | 1N | 2N | NORTH 3N

KDH 5 (-70°) | KDH 4 (-70°) | KDH 3 (-60°) | KDH 2 (-65°) | KDH 1 (-55°)

GOSSAN SUBCROP

95,06 m ABANDONED

100m | 200m | 300m | 400m | 500m

RKG 16B | RKG 11 | RKG 169 | RKG 9 | RKG 170 | RKG 171 | RKG 16 | RKG 172 | RKG 173 | RKG 24 | RKG 21 | RKG 15 | RKG 25 | RKG 19 | RKG 10 | RKG 20 | RKG 83 | RKG 85 | RKG 8 | RKG 80 | RKG 81 | RKG 2 | RKG 92 | RKG 6 | RKG 100 | RKG 101 | RKG 102 | RKG 26 | RKG 62 | RKG 65 | RKG 66 | RKG 87 | RKG 1 | RKG 3 | RKG 12 | RKG 37 | RKG 38 | RKG 18 | RKG 40 | RKG 88 | RKG 23 | RKG 22 | RKG 89 | RKG 13 | RKG 18 | RKG 69

KDH 7 (-60°) | RKG 69

159,08 m | 274,5 m | 491,01 m | 596,75 m

LEGEND

- Alluvium, deflation residua, calcrete and sand . . . . . EARLY TERTIARY TO RECENT
- Varved shales, siltstones with occasional pebbles . . . . DWYKA FORMATION KARROO SUPERGROUP
- Unconformity

ARCHEAN NAMAQUA COMPLEX

1. Felsic Pyritic Gneiss (quartz, oligoclase, perthite, biotite, sericite, pyrite)
2. Hypersthene Cordierite Pyritic Granulite (hypersthene, cordierite, andesine, quartz, biotite, pyrite, pyrrhotite, magnetite)
3. Sillimanite - augen Pyritic Quartzite (quartz, sillimanite, pyrrhotite, pyrite, sericite, ± sphalerite)
4. Banded Biotite Gneiss (quartz, oligoclase, orthoclase, biotite ± hypersthene)
5. Felsic Sillimanite Gneiss (Upper Unit) (quartz, perthite, andesine, sillimanite ± biotite ± sericite)
6. Hypersthene - Quartz - Garnet Granulite (quartz, hypersthene, andesine, biotite, orthoclase, garnet, magnetite)
7. Amphibolite (hornblende, labradorite, hypersthene, diopside, biotite)
8. Porphyroblastic Hypersthene - Biotite Granulite (hypersthene, quartz, plagioclase, biotite, orthoclase, magnetite)
9. Cordierite - Hypersthene - Quartz Granulite (cordierite, quartz, biotite, hypersthene, orthoclase, pyrite, pyrrhotite, magnetite)
10. Quartz - Cordierite - Sillimanite Granulite (cordierite, quartz, biotite, sillimanite, pyrrhotite, pyrite, magnetite)
11. Massive Sulphides and intercalated siliceous zone (pyrrhotite, pyrite, sphalerite, chlorite, barite chalcopyrite, quartz)
12. Diopside Plagioclase Granulite (diopside, labradorite, hornblende, hypersthene, magnetite, biotite)
13. Banded Hypersthene Granulite (quartz, hypersthene, andesine, biotite, magnetite, ±pyrite, pyrrhotite (±))
14. Felsic Sillimanite Gneiss (Lower Unit) (quartz, perthite, andesine, sillimanite, ± biotite ± sericite)
15. Banded Biotite - Garnet Gneiss (quartz, andesine, hypersthene, biotite, garnet, magnetite)

— Intrusive Rocks —

POST TECTONIC INTRUSIVES

- P. Pegmatite (quartz, orthoclase, biotite)
- 17. Coarse - grained Granite (perthite, quartz, oligoclase)

LATE TECTONIC INTRUSIVE

- 18. Granodiorite (quartz, andesine, microcline, biotite)

SOUTH | 2S | 1S | BASE LINE | NORTH

KDH 30 (-60°)

100m below datum level

100m

200m

200m

300m

300m

405, 35m

L E G E N D

- Alluvium, deflation residua, calcrete and sand..... EARLY TERTIARY TO RECENT
- Varved shales, siltstones with occasional pebbles ... DWYKA FORMATION KARROO SUPERGROUP
- Unconformity
- Banded Biotite Gneiss (quartz, oligoclase, orthoclase, biotite ± hypersthene)
- 5 Felsic Sillimanite Gneiss (Upper Unit) (quartz, perthite, andesine, sillimanite ± biotite ± sericite)
- 6 Hypersthene - Quartz - Garnet Granulite (quartz, hypersthene, andesine, biotite, orthoclase, garnet, magnetite)
- 7 Amphibolite (hornblende, labradorite, hypersthene, diopside, biotite)
- 8 Porphyroblastic - Hypersthene - Quartz Granulite (hypersthene, quartz, plagioclase, biotite, orthoclase, magnetite)
- 9 Cordierite - Hypersthene - Quartz Granulite (cordierite, quartz, biotite, hypersthene, orthoclase, pyrite, pyrrhotite, magnetite)
- 11 Massive Sulphides and intercalated siliceous zone (pyrrhotite, pyrite, sphalerite, chlorite, barite, chalcopyrite, quartz)
- 12 Diopside Plagioclase Granulite (diopside, labradorite, hornblende, hypersthene, magnetite, biotite)
- 13 Banded Hypersthene Granulite (quartz, hypersthene, andesine, biotite, magnetite, ± pyrite, pyrrhotite (...))
- 14 Felsic Sillimanite Gneiss (Lower Unit) (quartz, perthite, andesine, sillimanite, ± biotite ± sericite)

ARCHEAN NAMAQUA COMPLEX

KDH 76 (-60°)

Diamond number

RKG69 Sample sample sulphide

Inclina in core likely

Interpr

Litholog

Survey

Fault

CROSS

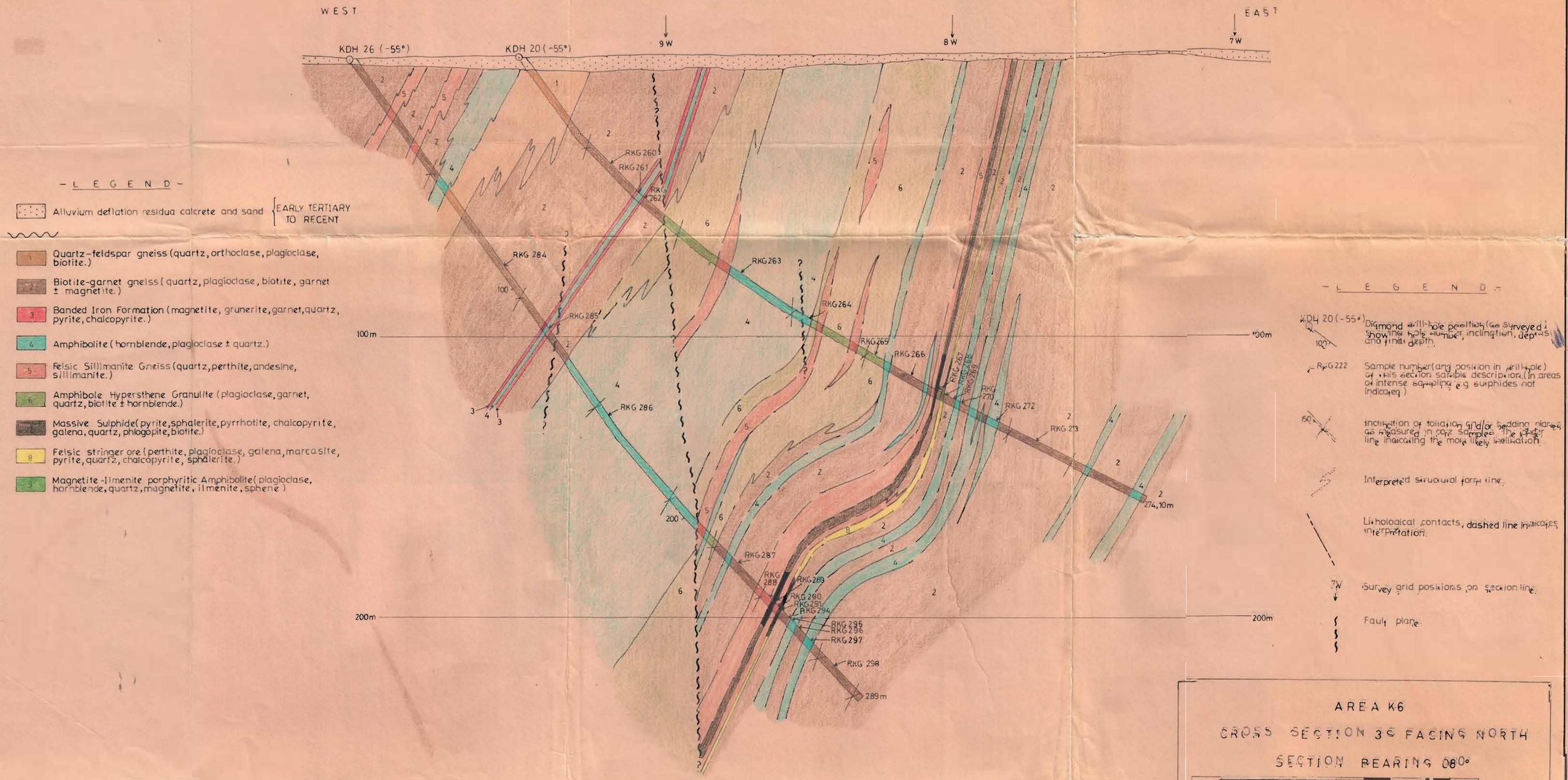
WEST
EAST
KDH 26 (-55°)
KDH 20 (-55°)
9W
8W
7W
RKG 260
RKG 261
RKG 262
RKG 263
RKG 264
RKG 265
RKG 266
RKG 267
RKG 268
RKG 269
RKG 270
RKG 272
RKG 273
RKG 274,10m
RKG 284
RKG 285
RKG 286
RKG 287
RKG 288
RKG 289
RKG 290
RKG 291
RKG 294
RKG 295
RKG 296
RKG 297
RKG 298
289m
100m
200m
- L E G E N D -
Alluvium deflation residua calcrete and sand
EARLY TERTIARY TO RECENT
1 Quartz-feldspar gneiss (quartz, orthoclase, plagioclase, biotite.)
2 Biotite-garnet gneiss (quartz, plagioclase, biotite, garnet ± magnetite.)
3 Banded Iron Formation (magnetite, grunerite, garnet, quartz, pyrite, chalcopyrite.)
4 Amphibolite (hornblende, plagioclase ± quartz.)
5 Felsic Sillimanite Gneiss (quartz, perthite, andesine, sillimanite.)
6 Amphibole Hypersthene Granulite (plagioclase, garnet, quartz, biotite ± hornblende.)
7 Massive Sulphide (pyrite, sphalerite, pyrrhotite, chalcopyrite, galena, quartz, phlogopite, biotite.)
8 Felsic stringer ore (perthite, plagioclase, galena, marcasite, pyrite, quartz, chalcopyrite, sphalerite.)
9 Magnetite-Ilmenite porphyritic Amphibolite (plagioclase, hornblende, quartz, magnetite, ilmenite, sphene)
- L E G E N D -
KDH 20 (-55°) Diamond drill-hole position (as surveyed) showing hole number, inclination, depth and final depth.
RKG 222 Sample number (and position in drill-hole) of this section sample description. (In areas of intense sampling e.g. sulphides not indicated)
50 Inclination of foliation and/or bedding planes as measured in core samples. The longer line indicating the more likely inclination.
Interpreted structural form line.
Lithological contacts, dashed line indicates interpretation.
7W Survey grid positions on section line.
Fault plane.
AREA K6
CROSS SECTION 3S FACING NORTH
SECTION BEARING 080°
0 10 20 30 40 50 60 70 80 90 100m
FIG 13
BH. 9/30

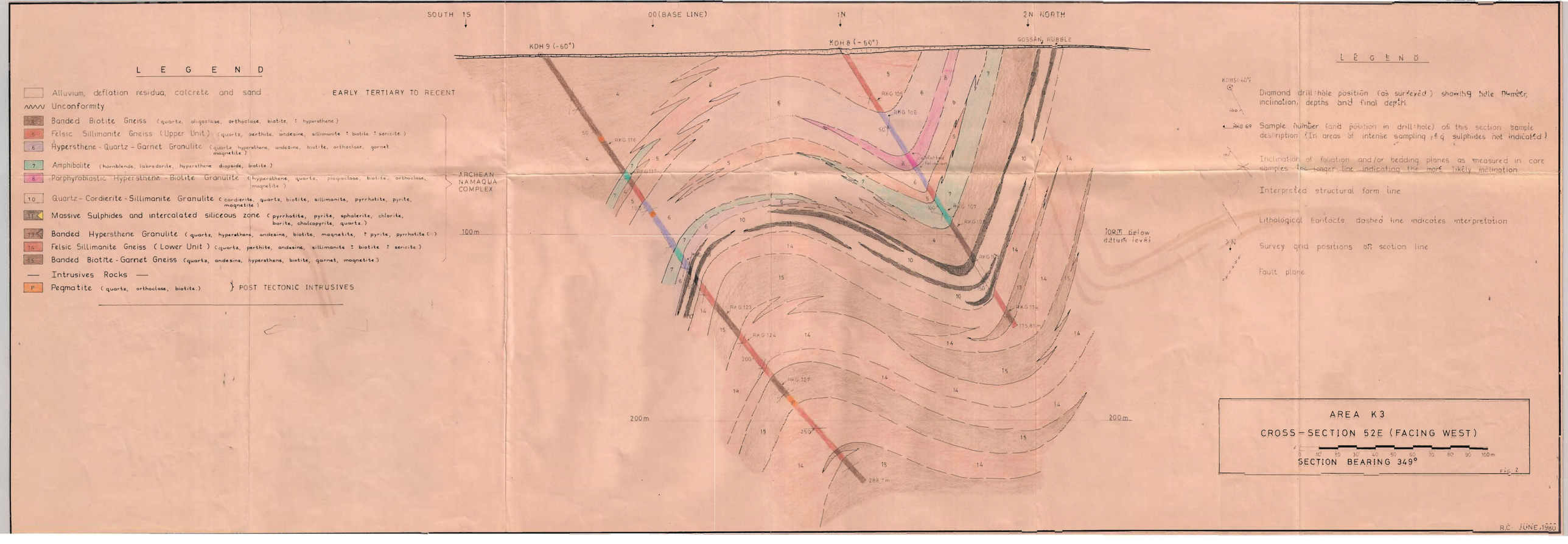
SOUTH 1S
00 (BASE LINE)
1N
2N NORTH
KDH 9 (-60°)
KDH 8 (-60°)
GOSSAN RUBBLE
RKG 105
RKG 106
RKG 107
RKG 108
RKG 109
RKG 110
RKG 111
RKG 112
RKG 113
RKG 114
RKG 116
RKG 123
RKG 124
RKG 127
Controlled foliation
175.81m
288.7m
100m below datum level
100m
200m
200m
50°
100°
200°
250°
L E G E N D
Alluvium, deflation residua, calcrete and sand
EARLY TERTIARY TO RECENT
Unconformity
Banded Biotite Gneiss (quartz, oligoclase, orthoclase, biotite, ± hypersthene)
Felsic Sillimanite Gneiss (Upper Unit) (quartz, perthite, andesine, sillimanite ± biotite ± sericite)
Hypersthene - Quartz - Garnet Granulite (quartz hypersthene, andesine, biotite, orthoclase, garnet magnetite)
Amphibolite (hornblende, labradorite, hypersthene diopside, biotite)
Porphyroblastic Hypersthene - Biotite Granulite (hypersthene, quartz, plagioclase, biotite, orthoclase, magnetite)
Quartz - Cordierite - Sillimanite Granulite (cordierite, quartz, biotite, sillimanite, pyrrhotite, pyrite, magnetite)
Massive Sulphides and intercalated siliceous zone (pyrrhotite, pyrite, sphalerite, chlorite, barite, chalcopyrite, quartz)
Banded Hypersthene Granulite (quartz, hypersthene, andesine, biotite, magnetite, ± pyrite, pyrrhotite (-))
Felsic Sillimanite Gneiss (Lower Unit) (quartz, perthite, andesine, sillimanite ± biotite ± sericite)
Banded Biotite - Garnet Gneiss (quartz, andesine, hypersthene, biotite, garnet, magnetite)
ARCHEAN NAMAQUA COMPLEX
Intrusives Rocks
Pegmatite (quartz, orthoclase, biotite.)
POST TECTONIC INTRUSIVES
L E G E N D
KDH 5 60°
Diamond drill hole position (as surveyed) showing hole number, inclination, depths and final depth
RKG 69
Sample number (and position in drill hole) of this section. Sample description (In areas of intense sampling e.g. sulphides not indicated)
Inclination of foliation and/or bedding planes as measured in core samples. The longer line indicating the more likely inclination
Interpreted structural form line
Lithological contacts, dashed line indicates interpretation
2N
Survey grid positions on section line
Fault plane
AREA K3
CROSS - SECTION 52E (FACING WEST)
0 10 20 30 40 50 60 70 80 90 100m
SECTION BEARING 349°
FIG. 2
R.C. JUNE, 1980

LEGEND

- Alluvium, deflation residua, calcrete and sand ..... EARLY TERTIARY TO RECENT
- Unconformity
- 1 Banded Biotite Gneiss (quarts, plagioclase, orthoclase, biotite.)
- 2 Amphibole – Quartz Granulite (edenite, hornblende, quartz, labradorite, garnet, diopside.)
- 3 Quartz - Biotite Gneiss (occasional garnet) (quartz, labradorite, biotite, hypersthene, garnet.)
- 4 Hypersthene - Cordierite - Biotite Gneiss (hypersthene, cordierite, biotite, quartz, plagioclase.)
- 5 Quartz - Plagioclase - Garnet Gneiss (quartz, plagioclase, biotite, garnet.)
- 6 Quartz - Cordierite Granulite (quartz, cordierite, plagioclase, hypersthene.)
- 7 Semi - Massive Sulphide (pyrite, chalcopyrite, sphalerite) in quartz, plagioclase, scapolite, phlogopite and thuringite.
- 8 Felsic Sillimanite Gneiss (quartz, plagioclase, orthoclase, biotite, sillimanite.)
- 9 Diopside Amphibolite (hornblende, labradorite, diopside, quartz.)
- 10 Quartz - Cordierite - Garnet Gneiss (quartz, cordierite, plagioclase, perthite, garnet, biotite.)

ARCHEAN NAMAQUA COMPLEX

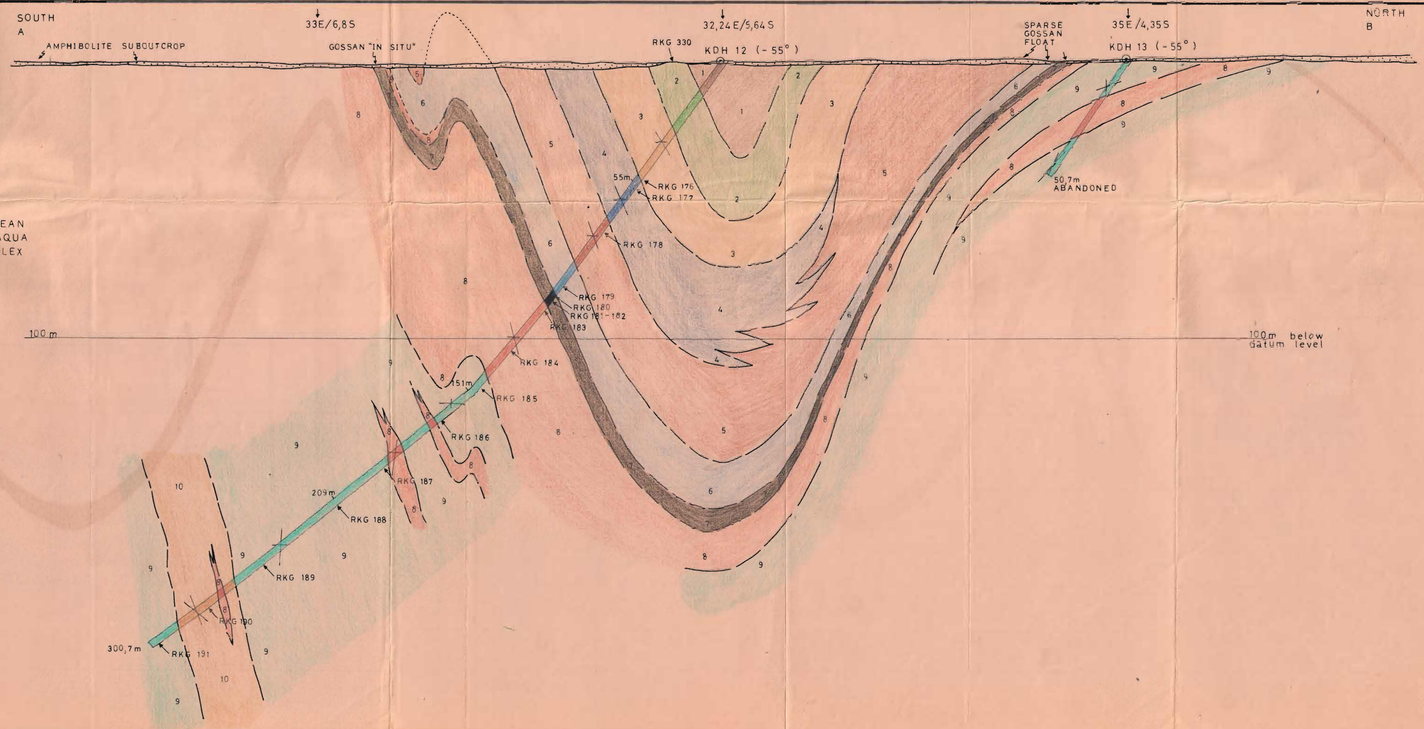

LEGEND

- KDH 7 (-60°) / 100 — Diamond drill-hole position (as surveyed) showing hole number, inclination, depths and final depth.
- ← RKG 69 — Sample number (and position in drill-hole) of this section sample description. (In areas of intense sampling (e.g. sulphides) not indicated.)
- 150 — Inclination of foliation and/or bedding planes as measured in core samples. The longer line indicating the more likely inclination.
- Interpreted structural form line.
- Lithological contacts, dashed line indicates interpretation.
- 2 S — Survey grid positions on section line.
- Fault plane.

AREA K1
CROSS SECTION AB (FACING WEST)
SECTION BEARING 200°

0 10 20 30 40 50 60 70 80 90 100 m

FIG. 6

H.C. AHO. 1970

L E G E N D

- Alluvium, deflation residua, calcrete and sand ..... EARLY TERTIARY TO RECENT
- Unconformity

ARCHEAN NAMAQUA COMPLEX

1. Banded Biotite Gneiss (quartz, plagioclase, orthoclase, biotite.)
2. Amphibole - Quartz Granulite (edenite, hornblende, quartz, labradorite, garnet, diopside.)
3. Quartz - Biotite Gneiss (occasional garnet) (quartz, labradorite, biotite, hypersthene, garnet.)
4. Hypersthene - Cordierite - Biotite Gneiss (hypersthene, cordierite, biotite, quartz, plagioclase.)
5. Quartz - Plagioclase - Garnet Gneiss (quartz, plagioclase, biotite, garnet.)
6. Semi - Massive Sulphide (pyrite, chalcopyrite, sphalerite) in quartz, plagioclase, scapolite, phlogopite and thuringite
7. Felsic Sillimanite Gneiss (quartz, plagioclase, orthoclase, biotite, sillimonite.)
8. Diopside Amphibolite (hornblende, labradorite, diopside, quartz.)
9. Quartz - Cordierite - Garnet Gneiss (quartz, cordierite, plagioclase, perthite, garnet, biotite.)

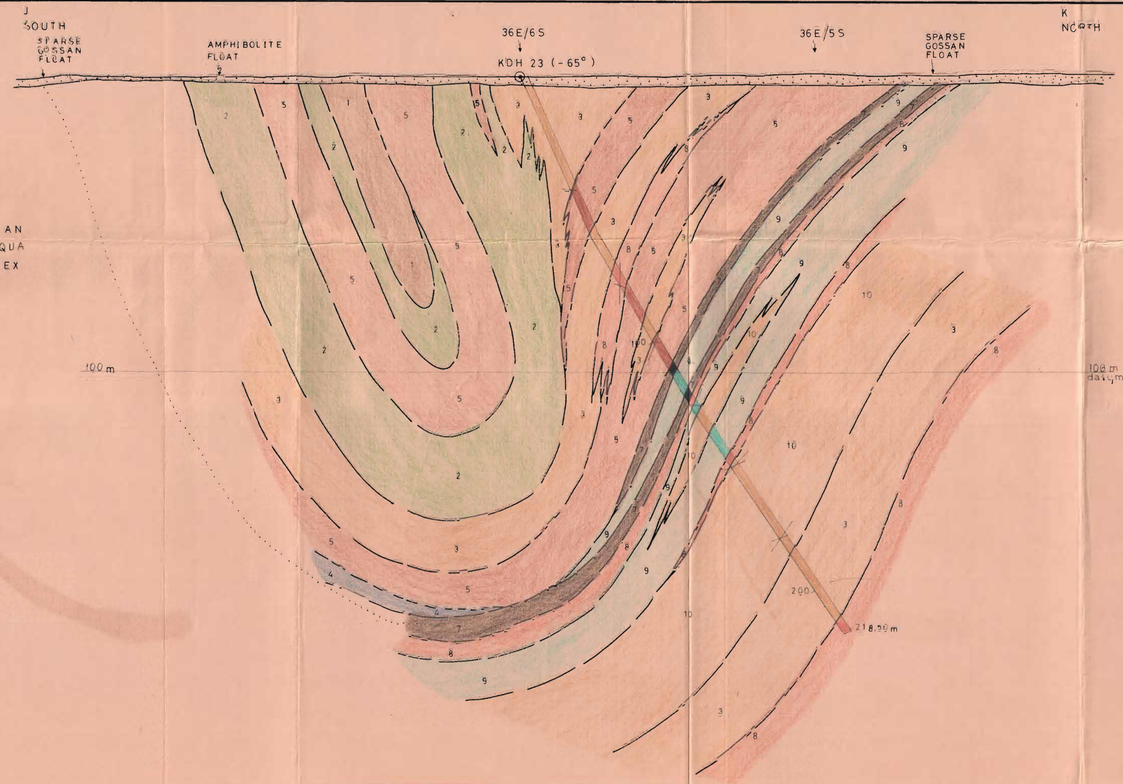

L E G E N D

- KDH 7 (-60°) / 120 — Diamond drill-hole position (as surveyed) showing hole number, inclination, depth and final depth.
- ← RKe 69 — Sample number (and position in drill-hole) of this section sample description. (In areas of intense sampling (eg sulphides) not indicated.)
- 150 — Inclination of foliation and/or bedding planes as measured in core samples. The longer line indicating the more likely inclination.
- Interpreted structural form line.
- Lithological contacts, dashed line indicates interpretation.
- 2, S — Survey grid positions on section line.
- Fault plane.

AREA K1
CROSS SECTION JK (FACING WEST)
SECTION BEARING 349°

0 10 20 30 40 50 60 70 80 90 100m

FIG 10

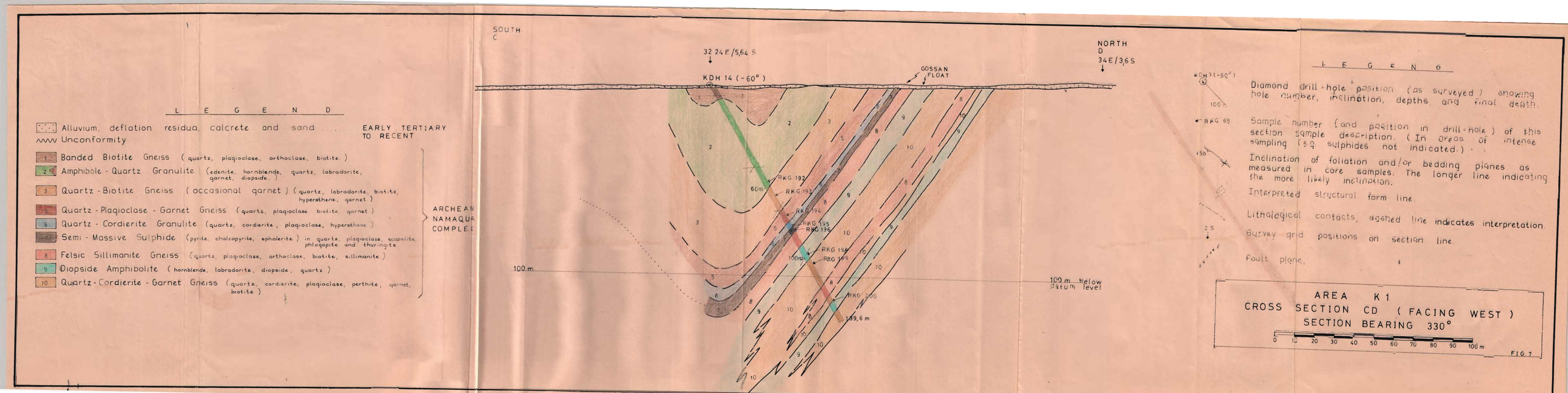
SOUTH
C
NORTH
D
32 24 E/5,64 S
34E/3,6S
KDH 14 (-60°)
GOSSAN FLOAT
RKG 192
RKG 193
RKG 194
RKG 195
RKG 196
RKG 198
RKG 199
RKG 200
60m
150m
100 m
139,6 m
100 m below datum level
L E G E N D
Alluvium, deflation residua, calcrete and sand . . . . EARLY TERTIARY TO RECENT
Unconformity
1 Banded Biotite Gneiss (quartz, plagioclase, orthoclase, biotite)
2 Amphibole - Quartz Granulite (edenite, hornblende, quartz, labradorite, garnet, diopside.)
3 Quartz - Biotite Gneiss (occasional garnet) (quartz, labradorite, biotite, hypersthene, garnet)
4 Quartz - Plagioclase - Garnet Gneiss (quartz, plagioclase, biotite, garnet)
5 Quartz - Cordierite Granulite (quartz, cordierite, plagioclase, hypersthene)
6 Semi - Massive Sulphide (pyrite, chalcopyrite, sphalerite) in quartz, plagioclase, scapolite, phlogopite and thuringite
7 Felsic Sillimanite Gneiss (quartz, plagioclase, orthoclase, biotite, sillimanite)
8 Diopside Amphibolite (hornblende, labradorite, diopside, quartz)
10 Quartz - Cordierite - Garnet Gneiss (quartz, cordierite, plagioclase, perthite, garnet, biotite)
ARCHEAN NAMAQUA COMPLEX
L E G E N D
KDH 7 (-50°)
100 m
RKG 69
150 m
2 S
Diamond drill-hole position (as surveyed) showing hole number, inclination, depths and final depth.
Sample number (and position in drill-hole) of this section sample description. (In areas of intense sampling (e.g. sulphides not indicated.)
Inclination of foliation and/or bedding planes as measured in core samples. The longer line indicating the more likely inclination.
Interpreted structural form line.
Lithological contacts, dashed line indicates interpretation.
Survey grid positions on section line.
Fault plane.
AREA K1
CROSS SECTION CD (FACING WEST)
SECTION BEARING 330°
0 10 20 30 40 50 60 70 80 90 100 m
FIG 7
R.C. AUG 1980

LEGEND

Alluvium, deflation residue, calcrete and sand ..... EARLY TERTIARY TO RECENT

Unconformity

ARCHEAN NAMAQUA COMPLEX

1. Banded Biotite Gneiss (quartz, plagioclase, orthoclase, biotite)
2. Amphibole - Quartz Granulite (diopside, hornblende, quartz, labradorite, garnet, diopside)
3. Quartz - Biotite Gneiss (occasional garnet) (quartz, labradorite, biotite, hypersthene, garnet)
5. Quartz - Plagioclase - Garnet Gneiss (quartz, plagioclase, biotite, garnet)
6. Semi - Massive Sulphide (pyrite, chalcopyrite, sphalerite) (+ quartz, plagioclase, scapolite, phlogopite and tourmaline)
8. Felsic Sillimanite Gneiss (quartz, plagioclase, orthoclase, biotite, sillimanite)
9. Diopside Amphibolite (hornblende, labradorite, diopside, quartz)
10. Quartz - Cordierite - Garnet Gneiss (quartz, cordierite, plagioclase, perthite, garnet, biotite)

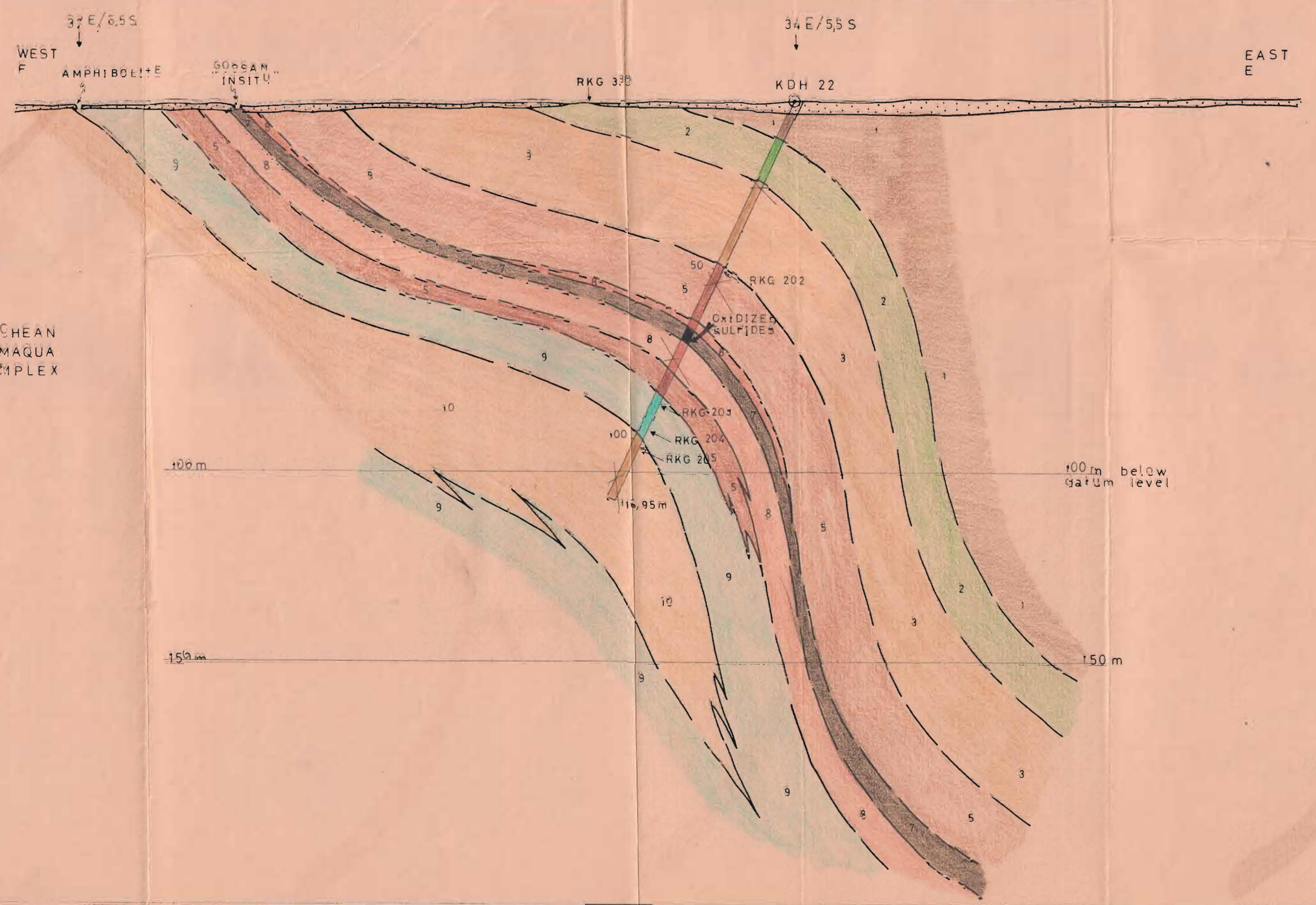

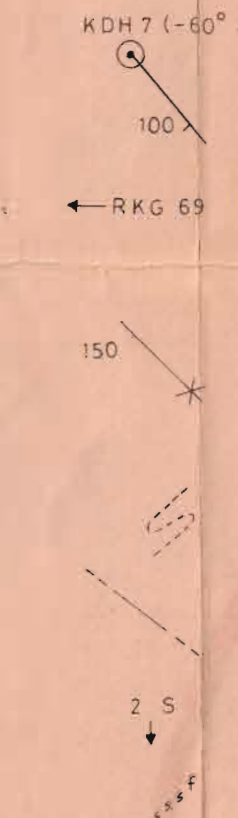

LEGEND

Diamond drill-hole position (as surveyed) showing hole number, inclination, depths and final depth.

Sample number (and position in drill-hole) of this section sample description. (In areas of intense sampling (e.g. sulphides not indicated.)

Inclination of foliation and/or bedding planes as measured in core samples. The longer line indicating the more likely inclination.

Interpreted structural form line.

Lithological contacts, dashed line indicates interpretation.

Survey grid position on section line.

Fault plane.

AREA K1
CROSS SECTION EF (FACING NORTH)
SECTION BEARING 264°

0 10 20 30 40 50 60 70 80 90 100 m

FIG. 8

R.C. AUG 1980

L E G E N D

- Alluvium, deflation residue, calcrete and sand ..... EARLY TERTIARY TO RECENT
- Unconformity
- 1 Banded Biotite Gneiss (quartz, plagioclase, orthoclase, biotite.)
- 2 Amphibole - Quartz Granulite (edenite, hornblende, quartz, labradorite, garnet, diopside)
- 3 Quartz - Biotite Gneiss (occasional garnet) (quartz, labradorite, biotite, hypersthene, garnet)
- 4 Hypersthene - Cordierite - Biotite Gneiss (hypersthene, cordierite, biotite, quartz, plagioclase)
- 5 Quartz - Plagioclase - Garnet Gneiss (quartz, plagioclase, biotite, garnet)
- 6 Quartz - Cordierite Granulite (quartz, cordierite, plagioclase, hypersthene)
- 7 Semi - Massive Sulphide (pyrite, chalcopyrite, sphalerite) in quartz, plagioclase, aplite, phlogopite and tourmaline
- 8 Felsic Sillimanite Gneiss (quartz, plagioclase, orthoclase, biotite, sillimanite)

ARCHEAN NAMAQUA COMPLEX

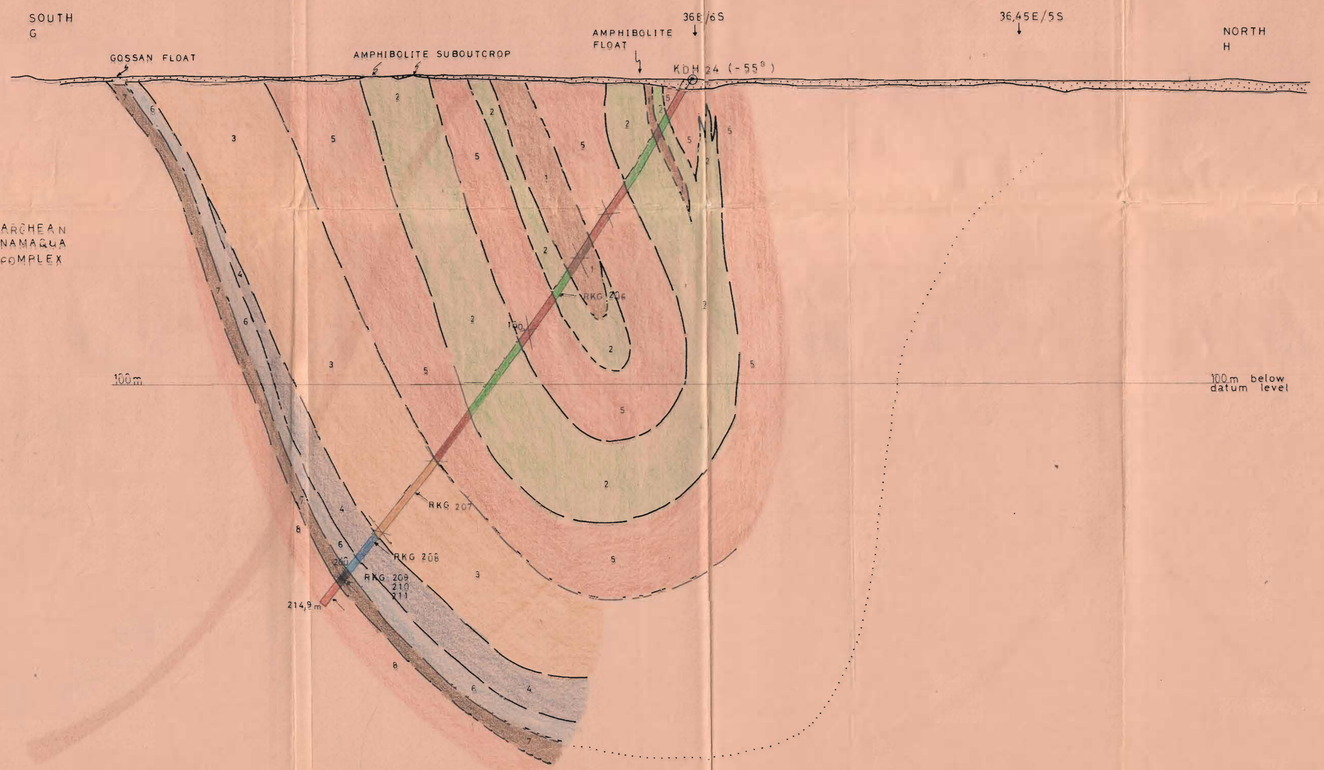

L E G E N D

- KDH 7 (-60°) / 100 — Diamond drill-hole position (as surveyed) showing hole number, inclination, depths and final depth.
- ← RKG 69 — Sample number (and position in drill-hole) of this section sample description. (In areas of intense sampling (e.g. sulphides not indicated.)
- 150 — Inclination of foliation and/or bedding planes as measured in core samples. The longer line indicating the more likely inclination.
- Interpreted structural form line.
- Lithological contacts, dashed line indicates interpretation.
- 2 S — Survey grid positions on section line.
- Fault plane

AREA K1
CROSS SECTION GH (FACING WEST)
SECTION BEARING 192°

0 10 20 30 40 50 60 70 80 90 100 m

FIG. 9

R.C. AUG. 1980

CAMP SITE

TRACK TO MAIN ROAD

T N

KDH 1 (-55°)

KDH 2 (-70°)

KDH 3 (-60°)

KDH 4 (-70°)

KDH 5 (-70°)

KDH 7 (-60°)

KDH 8 (-60°)

KDH 9 (-60°)

KDH 10 (-60°)

KDH 29 (-60°)

KDH 30 (-60°)

RKG 337
336

RKG 335
RKG 336

RKG 332

4N

3N

2N

1N

BASE LINE

1S

2S

3S

50E

51E

52E

53E

54E

55E

56E

TRACK

TRACK

TRACK

TRACK TO K1

BROAD DRAINAGE FLAT

L E G E N D

- Sand, alluvium, Dwyka residue.
- Subcropping Dwyka shale.
- Unconformity
- pg — Pyroxene granulite (hypersthene, quartz, biotite, plagioclase ± garnet ± cordierite.)
- gn — Gneiss, undifferentiated
- fq — Feldspathic quartzite (quartz, oligoclase, microcline.)
- Gossan exposed only in trenches, float indicated by dots (.) density indicating relative concentration
- qv — Quartz veins and pegmatites.
- \+ Grid co-ordinate intersections.
- 65 20 — Dip and strike of foliation, bearing and plunge of lineation.
- Trenches and pits (showing gossan intersection.)
- KDH 8 (-70°) — Drill hole collar and direction and inclination
- RKG 275 — Sample taken for thin section study.
- Farm track
- Farm fence.
- Fault plane (interpretation.)
- Direction of drainage.

GEOLOGICAL MAP OF THE K3 AREA SHOWING DRILLING AND TRENCHING SITES

(GEOLOGY AFTER P. GRESSE, N.S.A.L. COMPANY REPORT)

0 50 100 150 200 250 m

MAP 1

B.C. 9/80

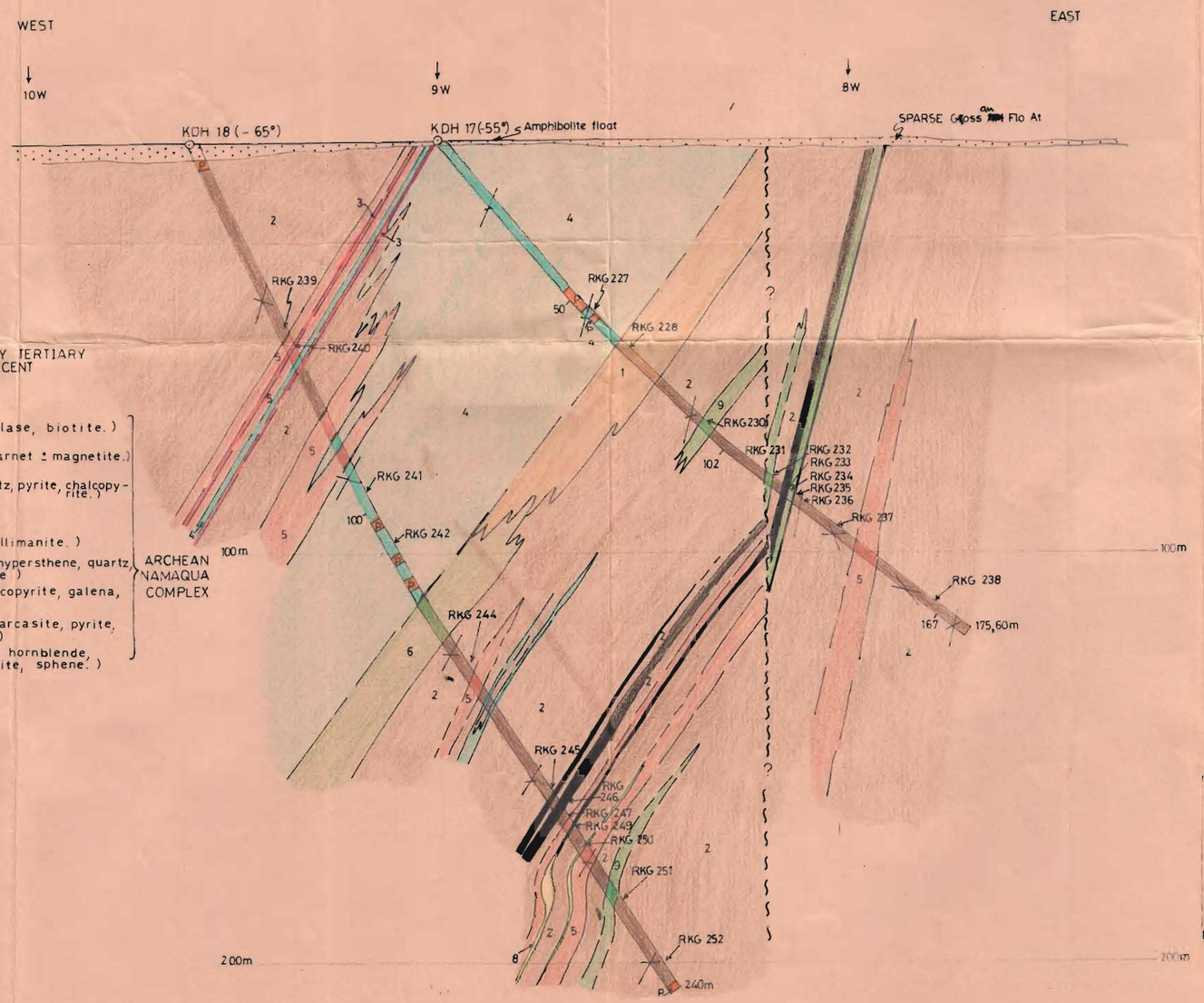

- L E G E N D -

- Alluvium, deflation residua, calcrete and sand ..... EARLY TERTIARY TO RECENT
- Unconformity
- 1 Quartz-feldspar gneiss (quartz, orthoclase, plagioclase, biotite.)
- 2 Biotite-garnet gneiss (quartz, plagioclase, biotite, garnet ± magnetite.)
- 3 Banded Iron Formation (magnetite grunerite, garnet, quartz, pyrite, chalcopyrite.)
- 4 Amphibolite (hornblende, plagioclase ± quartz)
- 5 Felsic Sillimanite Gneiss (quartz, perthite, andesine, sillimanite.)
- 6 Amphibole Hypersthene Granulite (plagioclase, garnet, hypersthene, quartz, biotite ± hornblende)
- 7 Massive Sulphide (pyrite, sphalerite, pyrrhotite, chalcopyrite, galena, quartz, phlogopite, biotite.)
- 8 Felsic Stringer Ore (perthite, plagioclase, galena, marcasite, pyrite, quartz, chalcopyrite, sphalerite.)
- 9 Magnetite-Ilmenite Porphyritic Amphibole (plagioclase, hornblende, quartz, magnetite, ilmenite, sphene.)
- P Pegmatite.

- L E G E N D -

- KDH 17 (-55°) Q 100m — Diamond drill hole position (as surveyed) showing hole number, inclination, depths and final depth.
- ← RKG 233 — Sample number (and position in drill hole) of this section sample description. (In areas of intense sampling e.g. sulphides not indicated).
- 150° — Inclination of foliation and/or bedding planes as measured in core samples. The longer line indicating the more likely inclination.
- Interpreted structural form line.
- Lithological contacts, dashed line indicates interpretation.
- 2 S ↓ — Survey grid position on section line.
- Fault plane.

AREA K6

CROSS SECTION 2S (FACING NORTH)

SECTION BEARING 080°

0 10 20 30 40 50 60 70 80 90 100m FIG 11

B.H. 9/80

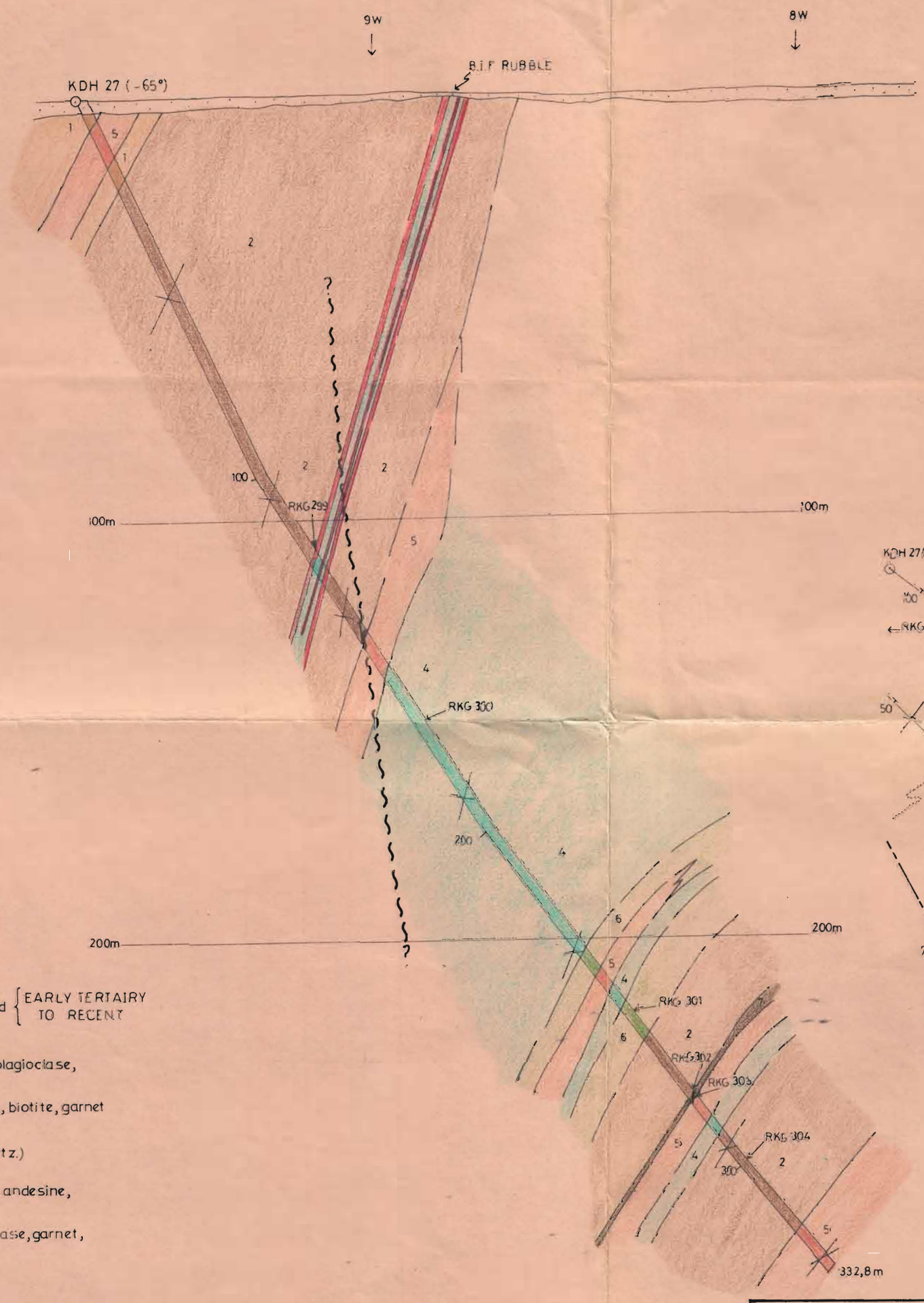

— L E G E N D —

Alluvium deflation residua calcrete and sand { EARLY TERTAIRY TO RECENT

1 Quartz-feldspar gneiss (quartz, orthoclase, plagioclase, biotite.)

2 Biotite garnet gneiss (quartz, plagioclase, biotite, garnet ± magnetite.)

4 Amphibolite (hornblende, plagioclase, ±quartz.)

5 Felsic Sillimanite Gneiss (quartz, perthite, andesine, sillimanite.)

6 Amphibole Hypersthene Granulite (plagioclase, garnet, quartz, biotite ± hornblende.)

— L E G E N D —

KDH 27 (-65°) / 300 Diamond drill-hole position (as surveyed) showing hole number, inclination, depths and final depth.

←RKG 299 Sample number (and position in drill-hole) of this section sample description (In areas of intense sampling e.g. sulphides not indicated.)

50 Inclination of foliation and/or bedding planes as measured in core samples. The longer line indicating the more likely inclination.

Interpreted structural form line.

Lithological contacts dashed line indicates interpretation.

7W Survey grid positions on section line.

Fault plane.

AREA K6

CROSS SECTION 4S FACING NORTH

SECTION BEARING 080°

FIG 14

0 10 20 30 40 50 60 70 80 90 100m

BH 9/80